

DISSERTATION

Stability of Coupled Adaptive Filters

in part fulfilment of the requirements for the degree of
Doktor der technischen Wissenschaften

submitted to the TU Wien,
Faculty of Electrical Engineering and Information Technology

by
Dipl.-Ing. Robert Dallinger

Advisor and First Examiner:
Univ.-Prof. Dipl.-Ing. Dr.techn.
Markus Rupp
Institute of Telecommunications
TU Wien
Austria

Second Examiner:
Prof. Dr.
Vítor Heloiz Nascimento
Signal Processing Laboratory
University of São Paulo
Brasil

Vienna, December 2015

Author's Signature

This thesis has been assessed by:

1. Univ.-Prof. Dipl.-Ing. Dr.techn. Markus Rupp

Institute of Telecommunications
TU Wien
Austria

2. Prof. Dr. Vítor Heloiz Nascimento

Signal Processing Laboratory
University of São Paulo
Brasil

This document exactly coincides with the approved version of this thesis, which is available in printed form at the TU Wien University Library. However, it is augmented by the following contents

- the lines on this page,
- one sheet after page viii which contains acknowledgements,
- an errata section at the end of this document, and
- marginalia that identify those parts of the text that are addressed in the errata section.

All content that does not exist in the originally approved version is type set in a different color. Added pages are annotated by a comment in their footer.

Vienna, 8 March 2016

I certify that the work reported in this thesis is my own, and the work done by other authors is appropriately cited. This thesis itself, as well as related scientific work, has been conducted, in all conscience, complying with the “Code of Conduct” of the TU Wien [TUW07].

Vienna, December 2015

Robert Dallinger

Abstract

Nowadays, many disciplines in science and engineering deal with problems for which a solution relies on knowledge about the characteristics of one or more given systems that can only be ascertained based on restricted observations. This requires the fitting of an adequately chosen model, such that it “best” conforms to a set of measured data. Depending on the context, this fitting procedure may resort to a huge amount of recorded data and abundant numerical power, or contrarily, to only a few streams of samples, which have to be processed on the fly at low computational cost. This thesis, exclusively focuses on the latter scenario. It specifically studies unexpected behaviour and reliability of the widely spread and computationally highly efficient class of gradient type algorithms. Additionally, special attention is paid to systems that combine several of them.

Chapter 3 is dedicated to so called asymmetric algorithms. These are gradient type algorithms that do *not* employ the (commonly used) unaltered input vector for regression. In a first step, it is shown that for such algorithms, the mapping matrix of the underlying homogeneous recursion has one singular value that is larger than one. This entails the risk of parameter divergence. Restricting to the most prominent subclass of asymmetric algorithms, the least-mean-squares (LMS) algorithm with matrix step-size, simulation experiments demonstrate that such divergence does not occur for all step-size matrices, even under worst case conditions. Motivated by this observation, the first part of this chapter dissects this phenomenon based on geometric arguments and comes to the novel insight that persistently changing eigenspaces of the step-size matrix are at the core of this worst case parameter divergence. In the second part, analytic as well as numeric methods are derived that allow to intentionally provoke this type of divergence, in order to assess specific algorithms.

A combination of arbitrarily many symmetric algorithms, i.e., conventional LMS algorithms, is addressed in Chapter 4. It considers a structure of such algorithms that mutually interfere with each other via a linear memoryless coupling among their individual a priori errors. Conditions for ℓ_2 -stability as well as boundedness of the parameter error are derived. The primer are obtained by the solution of a linear system of inequalities, resorting to the theory of M -matrices. The latter are compactly stated by means of the Khatri-Rao matrix product. Finally, a practically relevant case of coupling is analysed, where all of the individual adaptive schemes employ the same update error. This situation is found to be equivalent to an LMS algorithm with matrix step-size, making it accessible to the findings of Chapter 3.

The such obtained theoretic apparatus is applied in Chapter 5 to types of adaptive systems that are encountered in real life. First, for an adaptive Wiener model in a configuration that is typically used in digital pre-distortion of microwave power amplifiers, consisting of a linear filter followed by a memoryless non-linearity, a condition for ℓ_2 -stability and boundedness of its parameter error is identified. Resorting to the knowledge gained about asymmetric algorithms, this boundedness is then found to be extendible to less restrictive and practically more feasible constraints. Then, the multichannel filtered- x LMS is studied in context of active noise control, leading to sufficient bounds for ℓ_2 -stability and boundedness of its parameter error. Finally, the theory of Chapters 3 and 4 is harnessed to confirm that parameter convergence of an arbitrarily sized multilayer perceptron trained by the backpropagation algorithm can barely be ensured and strongly depends on the quality of its parameter initialisation.

Kurzfassung

Die Lösung vieler Problemstellungen im naturwissenschaftlichen und technischen Bereich beruht auf Kenntnis eines Systems, das nur teilweise durch Beobachtungen erfasst werden kann. Typischerweise wird in solchen Fällen ein passendes Modell gewählt, das einem Satz von gemessenen Daten hinreichend gut angepasst werden kann. In manchen Fällen sind diese Daten sehr umfangreich und es kann auf entsprechend leistungsstarke numerische Mittel zurückgegriffen werden. In anderen Fällen, handelt es sich bei diesen Daten um einige wenige Ströme von Messwerten, die gleich nach ihrem Eintreffen mit geringem Rechenaufwand verarbeitet werden müssen. Diese Arbeit beschäftigt sich ausschließlich mit letzterer Situation und betrachtet speziell das Verhalten sowie die Verlässlichkeit von Gradientenverfahren, sowie von Strukturen die mehrere von diesen kombinieren.

Kapitel 3 widmet sich sogenannten asymmetrischen Algorithmen. Dies sind Gradientenverfahren, bei denen die Regressionsrichtung *nicht* wie sonst üblich der Richtung des Eingangsvektors entspricht. In einem ersten Schritt wird gezeigt, dass die korrespondierende homogene Rekursion potentiell divergieren kann, da deren Koeffizientenmatrix einen Singulärwert größer eins besitzt. Simulationsexperimente für eine der wichtigsten Teilklassen asymmetrischer Algorithmen, den Least-Mean-Squares (LMS) Algorithmus mit Matrixschrittweite, eröffnen jedoch die Einsicht, dass diese Divergenz selbst unter widrigsten Umständen in einigen Fällen *nicht* zutage tritt. Eine anschließende detaillierte Analyse dieses Phänomens basierend auf geometrischen Argumenten führt zu der Erkenntnis, dass nur dann Divergenz auftreten kann, wenn sich die Eigenräume der Schrittweitenmatrix unaufhörlich verändern. Der zweite Teil dieses Kapitels präsentiert zwei Methoden, mit deren Hilfe konkrete Algorithmen auf die Existenz eines solchen Verhaltens getestet werden können. Beide Methoden erlauben die Generierung ungünstiger Anregungsfolgen, wobei in einem Fall analytische Mittel, im anderen Fall eine numerische Suche für deren Erzeugung eingesetzt wird.

Das vierte Kapitel konzentriert sich auf konventionelle Gradientenverfahren, hier auch als symmetrische Algorithmen bezeichnet. Es wird allerdings nicht nur *ein* solcher Algorithmus isoliert betrachtet, sondern eine spezielle Struktur, die mehrere von diesen kombiniert, indem deren individuelle a priori Fehler gegenseitig linear und ohne Gedächtnis interferieren. Für diese Struktur werden einerseits Bedingungen für ℓ_2 -Stabilität hergeleitet, basierend auf der Lösung von Systemen linearer Ungleichungen in Kombination mit der Theorie zu M -Matrizen. Andererseits erfolgt eine Analyse auf Basis der Inhalte von Kapitel 3. Mit Hilfe des Khatri-Rao Matrixprodukt lassen sich so kompakte Schranken angeben, die einen endlichen Grenzwert des Parameterfehlers garantieren. Schließlich wird der für die Praxis relevante Spezialfall behandelt, bei dem alle einzelnen Gradientenverfahren denselben Fehler benutzen um deren Parameter zu adaptieren. Es zeigt sich, dass das Verhalten einer solchen Struktur durch einen LMS Algorithmus mit Matrixschrittweite beschrieben werden kann, wodurch sämtliche Erkenntnisse aus Kapitel 3 zur Anwendung gebracht werden können.

Kapitel 5 wendet die zuvor entwickelte Theorie auf praktisch eingesetzte adaptive Systeme an. Dies erlaubt für das, in der digitalen Vorverzerrung von Leistungsverstärkern eingesetzte, adaptive Wiener Modell, bestehend aus einem linearen Filter gefolgt von einer gedächtnislosen Nichtlinearität, Bedingungen für ℓ_2 -Stabilität und für einen begrenzten Parameterfehler anzugeben. Äquivalente Ergebnisse werden auch für den mehrkanaligen LMS Algorithmus mit gefiltertem Eingangssignal (MC-FXLMS), verwendet in der aktiven Rauschunterdrückung, hergeleitet. Abschließend wird ein künstliches neuronales Netz (ein mehrlagiges Perzeptron) betrachtet, das mittels Fehlerrückführung trainiert wird. Das Resultat für ein solches Netz beliebiger Größe zeigt, dass Parameterkonvergenz kaum garantiert werden kann und wesentlich von der Qualität der Initialisierung abhängt.

Acknowledgements

Foremost, I thank my advisor and first examiner, Markus Rupp, for sharing his vast experience and introducing me to the numerous fascinating facets of adaptive signal processing. Beyond that, I am deeply indebted to him, for his continuous and encouraging support during all the years of my doctoral studies.

Deepest gratitude goes to Vítor H. Nascimento, for travelling around half of the globe, from São Paulo to Vienna, in order to act as my second examiner. Our fruitful discussions three days before my defence impressively demonstrated how thoroughly he went through my thesis. Some of the errata included at the end of this extended version are a direct consequence of these discussions.

For providing necessary facilities and funding for my research, I thank the the Institute of Telecommunications, the TU Wien, the Austrian Science Fund (FWF), and Emerson Network Power.

I am fortunate that I had the chance to pursue my doctoral degree at the Institute of Telecommunications, the former Institute of Communications and Radio-Frequency Engineering. It stands out due to its high quality of research and teaching, as well as its lively, inspiring, and cooperative working environment among a highly motivated team of colleagues from all over the world. I especially thank my former colleagues who populated the legendary Sixth Floor with its familiar atmosphere, where beside from mature technical discussions many other topics were dissected at a considerably high level of expertise, such as latest trends in bicycle technology, details about Hammond organs and Leslie speakers, ancient radio frequency equipment, work flows for appealing figures in \LaTeX documents, bread baking etc.

Exceptionally indebted, I am to Gregor Lasser, Robert Langwieser, Stefan Schwandter, and Florian Xaver, who beside from being valued colleagues, all became trusted friends, as well as, nerd level competitor, mentor, highly respected musician, and counterpart for profound mathematical discussions, respectively.

Special thanks go to those who participated in the institute's band - some only for few rehearsals, others regularly over all the years since 2008. Thank you for spending hours of your spare time in our acoustic laboratory, allowing for a relaxed and joyful contrast program after hard working days.

Indeed, university and work is only half of the picture. In my private live, a multitude of absolutely unique individuals deserve my deepest gratitude, as without them, this work would have never become reality. Expressing this gratitude in words would probably double the page count of this work, thus, I keep it simple by saying thank you – to my parents, to my whole family, to all my truthful friends, for all their encouragement, support, advice, patience, motivation, and for the countless moments of fun, laughing and even for those of crying together! Beyond that, thank you Karolina for your love, for your abundance of patience, and for keeping faith with me!

Thank you very much¹,

Alux, Arrate A., Bastian K., Brigitte R., Carolina R., Christian M., Christian T., Christoph A., Christoph J., Christoph M., Cynthia C., Emilia & Lisa R., Ernst B., Eva F., Franz H., Gerald M., Gerhard D., Gerhard S., Günther K., Hannelore D., Helga D., Henri R., Julia S., Kunibert R.v.S., Laura B., Lukas M., Lukas P., Marco T., Markus L., Martin H., mfi, Michael F., Norbert G., Ondrej S., Peter F., Philipp G., Philipp H., Qi W., Stefan Z., Ulrich H., Valentin S., Veronika S., Werner D., Wolfgang V. B., Wolfgang K., Wolfgang M.

... and many others more – apologies to those who seek their name above in vain!

¹ The names are (almost) in alphabetical order and do not reflect any ranking.

I am also much obliged to a multitude of people, most of which I do not even know by name. They made my scientific live a lot easier by sharing their helpful and laboriously gained experience in situations when I was desperately straying amidst a forest of cryptic error messages, by providing the tweaks that allowed me to tackle seemingly intractable problems of typesetting, and by actively participating in the open source community yielding very helpful and technically mature tools – special thanks go to all the programmers who contribute to the $\text{T}_{\text{E}}\text{X}$ / $\text{L}^{\text{A}}\text{T}_{\text{E}}\text{X}$ / $\text{L}^{\text{u}}\text{a}\text{T}_{\text{E}}\text{X}$ projects, to $\text{T}_{\text{E}}\text{X}$ lipse and $\text{T}_{\text{E}}\text{X}$ studio, as well as to the operators and the big actively participating crowd which enables the existence of platforms like WIKIPEDIA and **stackoverflow**.

Finally, regretful apologies go to my little chilli plant. It produced incredibly many pods, survived severe diseases, but in the end, had to die of thirst, when I was out of office for two weeks and logistic irregularities in its water supply occurred.

Vienna, 8 March 2016

Robert Dallinger

Contents

1	Introduction	1
1.1	Motivation	2
1.2	Original Contributions and Scope of this Work	3
1.2.1	Contributions in Detail	4
1.2.2	Related Publications	5
1.3	Brief Outline	6
1.4	Notation	7
1.5	Comment on the Graphical Representation of Simulation Results	9
2	Preliminaries	11
2.1	System Identification using Gradient Type Algorithms	11
2.2	Excitation Sequences	14
2.2.1	Interpretation of Excitation Vectors	14
2.2.1.1	Linear Combiner	15
2.2.1.2	Finite Impulse Response Filter	15
2.2.1.3	Non-linear Basis Expansion	15
2.2.1.4	Truncated Volterra Series	16
2.2.2	Persistent Excitation	16
2.3	Homogeneous First-Order System of Linear Difference Equations	17
2.3.1	Eigenvalues and Singular Values of Mapping Matrix \mathbf{B}_k	17
2.3.2	Mapping Behaviour of Autonomous Recursions	18
2.3.3	Mapping Behaviour of Nonautonomous Recursions	19
2.3.4	Implications to the Nonhomogeneous Case	20
2.4	Stability and Convergence	21
2.4.1	Uniform Stability	22
2.4.2	Input-Output Stability	22
3	Asymmetric Gradient Type Algorithms	27
3.1	Motivation	28
3.2	Related Work	31
3.2.1	Condition Ensuring ℓ_2 -Stability	31
3.2.2	Lyapunov Based Convergence Condition	32
3.2.3	Divergence Caused by Non-Persistent Excitation	34
3.2.4	Further Related Methods and Results	38
3.3	Mapping Matrix \mathbf{B}_k of Asymmetric Algorithms	40
3.3.1	Eigenvalues of Mapping Matrix \mathbf{B}_k	41
3.3.2	Singular Value Decomposition of \mathbf{B}_k	41
3.3.3	Meaning of the Worst Case	44

3.4	Mapping Analysis of Asymmetric Algorithms	45
3.4.1	Independent Regression Vector	46
3.4.2	Normal Step-Size Matrix	49
3.4.3	Positive Definite Diagonal Step-Size Matrices	52
3.4.4	Impact of Matrix Step-Sizes to the Convergence Behaviour	55
3.5	Worst Case Excitation – Analytic Approach	57
3.5.1	Identification of Worst Case Excitation Vectors	58
3.5.2	Influence of Orthogonal Components of the Excitation Vector	62
3.6	Worst Case Excitation – Numeric Search	66
3.6.1	General Step-Size Matrix	66
3.6.2	Normal Step-Size Matrix	67
4	Coupled Adaptive Filters	69
4.1	General Coupled Adaptive Structure	70
4.2	Systems of Inequalities Involving Z -Matrices	72
4.3	The Khatri-Rao Product	74
4.4	ℓ_2 -Stability of Coupled Adaptive Filters	78
4.4.1	Energy Relations for Coupled Adaptive Filters	78
4.4.2	ℓ_2 -Stability in Terms of Absolute Energies	80
4.4.3	ℓ_2 -Stability in Terms of Weighted Energies	82
4.5	Mapping Analysis of Coupled Adaptive Filters	85
4.6	Identical Error Case	89
5	Examples and Applications	93
5.1	Special Case of Two Coupled Adaptive Filters	93
5.1.1	ℓ_2 -Stability of Two Coupled Adaptive Gradient Type Algorithms	94
5.1.2	Convergence Behaviour of Two Coupled Gradient Type Algorithms	95
5.1.3	Two Illustrative Examples with Strong Symmetries	96
5.1.3.1	Symmetric Cross Coupling	96
5.1.3.2	Identical Error Case	99
5.2	The (Simplified) Wiener Model	101
5.3	Multichannel Filtered- x LMS Algorithm	106
5.3.1	The Single Input Multiple Output Case	110
5.3.2	The Multiple Input Single Output Case	112
5.3.3	The Multiple Input Multiple Output Case	114
5.4	Multilayer Perceptrons Trained by the Backpropagation Algorithm	117
6	Conclusions	125
6.1	Summary of Key Results	125
6.2	Critical Discussion, Open Issues, and Outlook	126
6.2.1	Considerations with Respect to Asymmetric Algorithms in Chapter 3	126
6.2.2	Considerations with Respect to the Coupled Structure in Chapter 4	127
6.3	Conclusion	128

A Singular Values of Mapping Matrix \mathbf{B}_k	129
A.1 Derivation of the Non-Unit Singular Values of \mathbf{B}_k	129
A.2 Analysis of the two Non-Unit Singular Values of \mathbf{B}_k	130
A.2.1 Dependency with respect to the Magnitude of the Effective Step-Size	131
A.2.2 Dependency with respect to the Magnitude of the Correlation Coefficient	132
A.2.2.1 Details for the First Singular Value	133
A.2.2.2 Details for the Second Singular Value	134
A.2.3 Dependency with respect to the Phase Offset	135
A.3 Bounds on the Singular Values of \mathbf{B}_k	136
B Complement to Section 3.5	139
B.1 Semi-Minors and Semi-Majors of the Ellipse	139
B.2 Parametrisation of the Ellipse	140
B.3 Maximum of Product $a_1 a_2$	141
B.4 Intersecting the Ellipse with a Hyperbola	142
C Mathematical Supplement	145
C.1 Operator Trigonometry	145
C.2 M -Matrices	146
C.3 Submatrices and Minors	147
D Proofs	149
D.1 Proofs for Chapter 3	149
D.1.1 Proof of Lemma 3.4	149
D.1.2 Proof of Lemma 3.5	150
D.1.3 Proof of Lemma 3.6	150
D.1.4 Proof of Lemma 3.8	151
D.1.5 Proof of Lemma 3.9	151
D.1.6 Proof of Lemma 3.12	152
D.1.7 Proof of Lemma 3.13	153
D.1.8 Proof of Lemma 3.14	153
D.1.9 Proof of Lemma 3.15	154
D.2 Proofs for Chapter 4	154
D.2.1 Proof of Lemma 4.1	154
D.2.2 Proof of Lemma 4.2	154
D.2.3 Proof of Lemma 4.3	155
D.2.4 Proof of Lemma 4.4	155
D.2.5 Proof of Lemma 4.5	156
D.2.6 Proof of Lemma 4.6	156
D.2.7 Partial Proof of Conjecture 4.1	156
D.3 Proofs for Chapter 5	157
D.3.1 Proof of Corollary 5.1	157
D.3.2 Proof of Lemma 5.1	159

D.3.3	Proof of Lemma 5.2	159
D.3.4	Proof of Lemma 5.3	160
	Bibliography	161
	Frequently used Symbols	177
	Acronyms	183
	Index	185
	Errata	E.1

Chapter 1

Introduction

A frequently encountered problem in science and engineering, is the necessity of obtaining a quantitative description for the behaviour of some system that is only partially known or even completely unknown. The underlying process to solve such a problem is usually referred to by the term “system identification” [Zad56; Lju10]. In this work, the (partially) unknown system will be denoted as *reference system*, its corresponding quantitative description as *system model*. A common example for a system identification problem is found in the daily weather forecast. Here, the aim is to prognosticate meteorological figures of merit, such as air temperature, atmospheric humidity, sky cover, wind speed, and probability of precipitation. To accomplish this, a description of weather dynamics, i.e., the system model, is required that allows to predict future weather conditions based on observations of their past development [Cah15]. Here, the reference system coincides with the terrestrial climate system in all of its facets.

The weather forecast employs system identification for prediction. However, it is also applied in system analysis, extraction of simulation models, and controller design [SS89a]. A virtually countless number of applications for system identification can be found in numerous disciplines [GS01], such as, electrical engineering and communications [SS89a; Lju99; Hay02; Say03], biology and biomedicine [e.g., FS12], in automotive applications [e.g., AHdR12], in aviation [e.g., Lju99; KM06], as well as, in economics, and chemistry [Lju10]. This high importance of system identification is concisely expressed by Lennart Ljung in [Lju10, p. 1]:

System identification is the art and science of building mathematical models of dynamic systems from observed input-output data. It can be seen as the interface between the real world of applications and the mathematical world of control theory and model abstractions. As such, it is an ubiquitous necessity for successful applications.

A typical approach in system identification, is to first choose a system model which exhibits sufficient degrees of freedom, in order to be later fitted to the behaviour of the reference system. Two sources of information about the latter can be used to choose such a system model, (i) prior knowledge and (ii) expectations deduced from observations.

Observations made through experiments are also the basis for the subsequent fitting process that takes place as soon as an adequate model has been selected. In this second phase, the goal is to “tune” the system model within the range that is reachable by its degrees of freedom, such that it “best” approximates the real behaviour of the reference system. Here, the two quoted terms inherently manifest the need for (i) a method that systematically modifies the system model, i.e., a training scheme, and (ii) some criteria that allow to evaluate the accuracy of the system model, i.e., a metric or a cost function. The just described procedure is not necessarily executed only once, instead, it may be iterated several times until the desired performance is reached [SS89a; Lju99; Hay02; Lju10].

1.1 Motivation

Due to the vast range of applications, the variants of used models and corresponding identification algorithms are similarly manifold. The analyses presented in this work are restricted to a certain class of system identification algorithms. Nevertheless, this class is of high relevance, as it covers a multitude of parametrised adaptive schemes that are based on gradient descent. It specifically includes the renowned and due to its robustness and computational simplicity widely used LMS algorithm, as well as many of its generalisations [Hay02; Say03]. The here developed theory provides deep insight to the internal mechanisms that decide on their convergence or divergence. Moreover, it enables a closed representation and investigation of a structure that combines arbitrarily many interacting gradient type algorithms.

The special interest which eventually lead to this work was initiated by the desire to design robust methods for adaptive digital pre-distortion (DPD) of the microwave power amplifiers that are employed in the transmitters of wireless communication systems. Briefly, the goal of DPD is to virtually extend the linear operating area of the power amplifier towards higher input powers. This is achieved by inserting a controller, i.e., the pre-distorter, which compensates the distortions introduced by the power amplifier [EP97; ZD07]. As a result higher output powers can be achieved which in turn improves the overall power efficiency of the transmitter. Hence, the power consumed by the required auxiliary hardware is crucial for the applicability of a DPD scheme [Cri02; GH09]. Consequently, stringent restrictions with respect to computational complexity have to be met during implementation. In terms of system identification, these algorithms have to comprise of the system model, as well as the mechanism that accomplishes the fitting to the reference system, i.e., in context of DPD, the inverse of the baseband model that corresponds to the power amplifier. Typically, the fitting mechanism has to be able to track variations of the power amplifier characteristics.

For small bandwidths of the transmit signal, usually a memoryless pre-distorter can be used. However, the increase in bandwidth [VRM01; Vuo01] which goes hand in hand with the evolution in mobile networks [HT11], as well as new technologies, such as envelope tracking power amplifiers, necessitate pre-distorters that additionally allow to compensate dispersive effects [ZDH+08; GZ11; AEF12]. Cascade structures consisting of one linear dynamic block and one static non-linear block are amongst the simplest models that are able to comply with this requirement. If such an approach is adopted, typically, the system model of the power amplifier has the structure of a so called (simplified)¹ Wiener model, i.e., the linear dynamic block precedes the non-linear block [CCM+98; RZV05; AR05; Asc05; Sil07; SOGG09]. With respect to low computational complexity, gradient type algorithms are the most adequate update scheme.

For the such obtained adaptive Wiener model, in literature first and second order moments stability analyses have been published [BCV00; CBV00; CBV01]. However, they rely on strong statistical assumptions that may not be met in realistic scenarios. In contrast, the advantage of deterministic stability and convergence analyses is that they do not necessitate to impose such constraints. This in turn leads to often more conservative, yet more trustful stability bounds [SR96; RS96a]. With the aim to perform such a deterministic analysis for the adaptive Wiener model, I found that this can be systematically achieved by mapping it to an equivalent structure, consisting of two coupled gradient type algorithms. Complementary, an alternative interpretation revealed the Wiener model with gradient update to behave equivalent to an LMS algorithm with matrix step-size. As a side effect, I observed for the latter class of algorithms the less known behaviour that under unfortunate but possible circumstances, they can surprisingly diverge notwithstanding the use of a

¹ In the context of power amplifier modelling and DPD, such a two-block cascade structure is simply called a Wiener model. This convention is also (mostly) adopted in this work. The additional term “*simplified*” is included here, in order to emphasise that the original Wiener model dating back to [Wie58] has a more general structure.

(supposedly) correctly chosen step-size. These two insights, i.e., the equivalent coupled structure and the surprising divergence effects of the LMS with matrix step-size, initiated the thorough analyses presented in this work. They are introduced from a general point of view and detached from any specific application. The afore described relation to the Wiener model is also included in more detail in Section 5.2.

1.2 Original Contributions and Scope of this Work

The focus of this work lies exclusively on a deterministic analyses of gradient type algorithms in the context of system identification. The contributions can be roughly separated into three main lines.

The first one, investigates *hidden divergence* of so called *asymmetric algorithms*. They are characterised by a regression vector which has a different direction than the excitation vector. Such algorithms are shown to bare an inherent risk of divergence in terms of their parameter vector. For the LMS algorithm with matrix step-size, a rigorous geometric analysis of the mapping mechanisms is provided. It reveals that permanently changing eigenspaces of the step-size matrix are the main reason for potential parameter divergence. The such obtained clear picture extends previous results in literature and allows to deduce constructive guidelines for the choice of “safe” matrix step-sizes. As the here focussed divergence only occurs under adverse excitation situations, an analytical method is derived for synthesis of test sequences – in the sequel referred to by the term worst case (w.c.) sequences – that systematically allow to provoke such a malign scenario. On some occasions, if the domain space of the excitation sequences is restricted, this analytical method may not be applicable. For such cases, additionally, efficient numerical search schemes are proposed.

The second line of contributions is concerned with a specific structure of *gradient type algorithms* that interact with each other via a linear memoryless *coupling among their individual a priori errors*. Conditions for boundedness of the parameter vector as well as ℓ_2 -stability bounds are derived. Ties to the first line of contributions are established by a special and practically important case of coupling that causes all individual gradient type algorithms to be updated by the same error. This *identical error case* is identified to correspond to an LMS algorithm with matrix step-size. Knowing about the drawbacks of asymmetric algorithm, guidelines are stated that ensure equivalence of this identical error case with a symmetric algorithm, i.e., a gradient type algorithm with a regression vector that is in parallel with the excitation vector.

Finally, the third line of contributions is formed by *application of the afore obtained results* to practical scenarios. Specifically, it is shown that the widely used adaptive Wiener model that consists of a finite impulse response (FIR) filter followed by a memoryless non-linearity, can be mapped to the above mentioned identical error case of the coupled structure. By this, conditions for ℓ_2 -stability and boundedness of the parameter error vector are obtained. As second application, the multichannel filtered- x LMS (MC-FXLMS) algorithm, typically deployed in active noise control (ANC), is mapped to the coupled structure, again leading to rules and bounds for ℓ_2 -stability and boundedness of the parameter error vector. Finally, a multilayer perceptron of arbitrary size, trained by the backpropagation algorithm, is expressed in terms of this coupled structure. The obtained results disclose that convergence of the parameter error vector is hard to guarantee and that a well chosen parameter initialisation is of crucial importance. It augments results from literature that either require assumptions regarding the separability of input data, or restrict themselves to one single layer.

1.2.1 Contributions in Detail

After the afore provided brief overview of the contributions presented in this thesis, this section goes more into detail. Below, our relevant publications are included by their bibliographic keys, at the end of each heading. For convenience, their complete entries are enclosed in Section 1.2.2. References to the work of other authors are excluded for the sake of brevity. A detailed discussion of related literature is contained directly in the corresponding sections.

Hidden Divergence of Asymmetric Algorithms [DR09a; DR10; DRWR10; DR13]

Gradient type algorithms that use a regression vector that does not have the same direction as the excitation vector are in this work referred to by the term *asymmetric algorithms*. Chapter 3 is dedicated to their analysis, where emphasis is given to the special class of LMS algorithms with matrix step-size. The first observation in Section 3.3 is that the mapping matrix occurring in the homogeneous recursive part of such algorithms, always – except from degenerate or trivial cases – has one singular value larger than one. The evoked speculation that this fact inherently entails a permanent risk of divergence is refuted by counterexamples, such as the LMS algorithm with *constant* matrix step-size, which is known to converge for adequately scaled step-sizes. That this also holds in some cases of varying step-size matrices is illustrated by the comparison of two² simulation examples in Section 3.1. A detailed review of existing literature, in Section 3.2, demonstrates that none of the available results is able to classify the considered matrix step-size with respect to their w.c. convergence behaviour.

Based on this motivation, Section 3.4 presents a rigorous geometric dissection of the mapping mechanisms that underlie such algorithms. The main result is achieved in Section 3.4.4, which clarifies that persistent variations of the eigenspaces of the step-size matrix are necessary for divergence under w.c. excitation. Additionally, it provides a novel perspective to the reason why the LMS algorithm with *fixed* matrix step-size is ensured to remain bounded.

Resorting to operator trigonometry, Section 3.5 derives an analytical method to synthesise excitation sequences that provoke diverging trajectories – if they exist for a given algorithm. As an alternative, purely numeric search schemes are proposed that can be resorted to, if the analytic methods are inapplicable. This may be the case if the excitation vectors have to obey some additional constraints, such as a shift dependency (cf. Section 2.2), or if the domain of their elements is non-continuous.

Gradient Type Algorithms with Linearly Coupled Update Errors [DR09b; DR15]

In Chapter 4, a novel structure is investigated that contains arbitrarily many gradient type algorithms, which interfere with each other via a linear memoryless coupling of their individual a priori errors. Conditions for ℓ_2 -stability are derived in Section 4.4, based on the theory of M -matrices and their application to the solution of linear systems of inequalities (cf. Section 4.2). Two different versions of ℓ_2 -stability are considered, one with respect to absolute, the other with respect to weighted energies. Moreover, motivated by the mapping analysis of asymmetric algorithm in Chapter 3, the mapping behaviour in terms of the combined parameter error vector is analysed in Section 4.5. Employing the Khatri-Rao product, which is a generalisation of the Hadamard product to block matrices, conditions for a bounded parameter error vector are derived. Finally, in Section 4.6, the practically important situation is analysed, where all individual gradient type algorithms use the same update error. As in this case, the behaviour of the adaptive coupled structure coincides with an asymmetric algorithm, all results from Chapter 3 become applicable here. Specifically, the insight that symmetric algorithms do not share the potential risk of divergence with asymmetric algorithms, leads to criteria that ensure a bounded parameter error vector, as well as to ℓ_2 -stability bounds.

² In fact, Section 3.1 compares three examples. However, one of them is the LMS algorithm with constant matrix step-size.

Parameter Convergence of the Adaptive Wiener Model [DR10; DR11; DR12]

In Section 5.2, the adaptive Wiener model already mentioned in Section 1.1, is analysed by mapping it to the coupled structure from Chapter 4. The criteria obtained for the identical error case in Section 4.6 ensuring parameter convergence and ℓ_2 -stability, directly apply in this case. Although, the obtained condition is hard to enforce in practical situations, it still gives a guide on how to foster stability. Moreover, it very compactly reveals that the risk of divergence reduces with increasing quality of the estimated system model. Due to its practical relevance to non-linear dispersive problems, the adaptive Wiener model has received considerable attention in literature. Yet deterministic analysis are rare and to the knowledge of the author, the here obtained results are in their form novel.

Stability and Convergence of the Multichannel Filtered- x LMS Algorithm

The filtered- x LMS (FXLMS) algorithm is known for decades. Several stochastic as well as deterministic stability analyses have been conducted in literature. In the context of ANC, an extension to multiple inputs and multiple outputs, the MC-FXLMS, has been introduced more recently. Applying the results obtained for asymmetric algorithms (Chapter 3) and for the coupled structure of gradient type algorithms (Chapter 4), in Section 5.3, novel conditions for boundedness of the parameter error vector as well as ℓ_2 -stability, are derived for the MC-FXLMS, under the assumption of perfect knowledge of the secondary path. This is done step wise, starting with the single input multiple output (SIMO) case in Section 5.3.1, continuing with the multiple input single output (MISO) case in Section 5.3.2, and ending up at the most general multiple input multiple output (MIMO) case in Section 5.3.3.

Convergence of a Multilayer Perceptron Trained by the Backpropagation Algorithm

In pattern recognition, a common training scheme of multilayer perceptrons is the backpropagation algorithm. Although the latter dates back to the late sixties, a comprehensive picture of its convergence behaviour is not available yet. In Section 5.4, the scheme is analysed by mapping it to the structure of coupled gradient type algorithms from Chapter 4. The obtained result indicates that convergence of the parameter error vector is strongly depending on the quality of the initial state, and in fact almost impossible to ensure. The main novelty is found in the chosen approach, as well as, in the result, which does not require the restriction to one single layer or the assumption of linearly separable training classes.

1.2.2 Related Publications

- [DR09b] R. Dallinger and M. Rupp, "On robustness of coupled adaptive filters," in *Proceedings of the IEEE International Conference on Acoustics, Speech and Signal Processing*, Taipei, Taiwan, Apr. 2009, pp. 3085–3088.
- [DR09a] R. Dallinger and M. Rupp, "A strict stability limit for adaptive gradient type algorithms," in *Conference Record of the 43rd Asilomar Conference on Circuits, Systems and Computers*, Pacific Grove, CA, USA, Nov. 2009, pp. 1370–1374.
- [DR10] R. Dallinger and M. Rupp, "Stability analysis of an adaptive Wiener structure," in *Proceedings of the IEEE International Conference on Acoustics, Speech and Signal Processing*, Dallas, TX, USA, Mar. 2010, pp. 3718–3721.

- [DRWR10] R. Dallinger, H. Ruotsalainen, R. Wichman, and M. Rupp, “Adaptive pre-distortion techniques based on orthogonal polynomials,” in *Conference Record of the 44th Asilomar Conference on Circuits, Systems and Computers*, Pacific Grove, CA, USA, Nov. 2010, pp. 1945–1950.
- [DR11] R. Dallinger and M. Rupp, *Adaptive digital pre-distortion based on two-block models*, IEEE Forum on Signal Processing for Radio Frequency Systems, Vienna, Austria, Mar. 2011.
- [DR12] R. Dallinger and M. Rupp, “Improved robustness and accelerated power amplifier identification with adaptive Wiener models in the complex domain,” in *Conference Record of the 46th Asilomar Conference on Circuits, Systems and Computers*, Pacific Grove, CA, USA, Nov. 2012, pp. 787–791.
- [DR13] R. Dallinger and M. Rupp, “On the robustness of LMS algorithms with time-variant diagonal matrix step-size,” in *Proceedings of the IEEE International Conference on Acoustics, Speech and Signal Processing*, Vancouver, BC, Canada, May 2013, pp. 5691–5695.
- [DR15] R. Dallinger and M. Rupp, “Stability of adaptive filters with linearly interfering update errors,” in *Proceedings of the 23rd European Signal Processing Conference*, Nice, France, Sep. 2015, pp. 2731–2735.

1.3 Brief Outline

As a complement to Section 1.2.1, this section provides a rough overview of this thesis.

Chapter 2 (Preliminaries) provides the most important background information that is required for the following chapters. It is kept rather concise and by far not exhaustive. Nevertheless, it is also intended to provide an overview of selected references which quickly enable the reader to clarify unclear points. The chapter first introduces the adaptive algorithm that is at the core of all of the algorithms considered in this work. After a short discussion regarding possible interpretations of the input sequences, it introduces the methods and definitions that are required for the following analyses of stability and convergence.

Chapter 3 (Asymmetric Gradient Type Algorithms) focuses on parameter convergence of one single gradient type algorithms with matrix step-size. Such algorithms are called asymmetric throughout this work. An introducing simulation experiment reveals that diverging behaviour can occur, even if conventional stability bounds are safely fulfilled. It raises the question under which conditions such an effect can be observed. After a review of the findings available from existing literature, Section 3.3 returns to the original question and answers it on the basis of a detailed theoretic dissection of the underlying mapping mechanisms. The remainder of Chapter 3 then presents methods that allow to synthesise excitation sequences in order to provoke possible diverging modes for a given algorithm. Such sequences are also referred to by the term w.c. sequences in this work. First, Section 3.5 takes an analytic synthesis approach which applies if the excitation sequences can be chosen rather arbitrarily. In situations where they are subject to stronger restrictions, Section 3.6 provides a numeric alternative.

Chapter 4 (Coupled Adaptive Filters) starts by introducing a structure consisting of arbitrary many gradient type algorithms that are linearly coupled via their individual update errors. In Section 4.4 conditions for ℓ_2 -stability are derived based on the solution of a specific kind of system of inequalities. These results are complemented in Section 4.5 by a mapping analysis which applies the same idea that underlies the theory in Chapter 3. Finally, a tight relation to Chapter 3 is established in Section 4.6, which treats the coupled structure in the special case, when some or all of the gradient type algorithms use the same error to adapt their parameters.

Chapter 5 (Examples and Applications) finally connects the theoretic results from the foregoing chapters with applications. Section 5.1 discusses two idealised cases of coupled adaptive filters which allow for a clear comparison of the two methods developed in this work. The following Section 5.2 gives more details on the adaptive Wiener model that has already been briefly addressed in Section 1.1. For the MC-FXLMS, in the context of ANC, Section 5.3 derives bounds that ensure a bounded parameter error vector, respectively, ℓ_2 -stability. Finally, in Section 5.4, the general coupled structure from Chapter 4 is applied to a neural network that is trained by the backpropagation algorithm. The result illustrates convergence problems that are faced for such schemes.

Chapter 6 (Conclusions) summarises the novel results presented in this thesis. The newly obtained insights that are critically discussed. Moreover, open questions and ideas for future research are pointed out.

Appendix A (Singular Values of Mapping Matrix \mathbf{B}_k) contains the derivations for the two non-unit singular values that occur in the mapping matrix of asymmetric algorithms, discussed in Chapter 3.

Appendix B (Complement to Section 3.5) collects complementary calculations that are required for the analytical design of w.c. sequences in Section 3.5.

Appendix C (Mathematical Supplement) is a conglomeration of several brief paragraphs on mathematical topics that are used in this thesis. It covers operator trigonometry, M -matrices, and details about submatrices.

Appendix D (Proofs) contains the proofs for Chapters 3 to 5.

1.4 Notation

In this section, notational conventions are introduced that apply to the whole thesis. A detailed list of frequently used mathematical symbols can be found subsequently to the appendix, starting on page 177. The latter list is complemented by Table 4.1, Table 5.2, and Table 5.3, which summarise the symbols describing the coupled structure in Chapter 4, the MC-FXLMS in Section 5.3, and the multilayer perceptron in Section 5.4, respectively.

Scalars, Vectors, and Matrices: Scalars are typeset in the standard mathematical slanted font, e.g., k . Vectors are indicated by small letters, matrices by capital letters, both in upright boldface characters, e.g., \mathbf{u} and \mathbf{U} . Scalars typically enclose their arguments in brackets, e.g., $\mu(k)$. Arguments of vector- or matrix-valued entities are mostly attached as a subscript, e.g., \mathbf{u}_k and \mathbf{U}_k . However, few exceptions exist. For example, mixing of both kinds of notation occurs in Section 5.2, where non-linear function $h_{\mathbf{w}_2}(y(k))$ is parametrised by vector \mathbf{w}_2 and additionally depends on scalar input $y(k)$.

Iteration Index k : The integer k denotes the index of the instantaneous iteration. It represents the independent variable throughout this work. Value $k = -1$ indicates initialisation, the first actual calculation is executed at $k = 0$. In general, the number of iterations is unbounded, meaning that in theory, k is incremented by 1 up to infinity.

Symbols with Caret ($\hat{\cdot}$): As this thesis adopts the perspective of system identification, in almost all cases, a reference system has to be identified by an adaptively modified system model. One of the main assumptions made later on (cf. Section 2.1) that applies to the complete work, is that both of these systems have the same structure. Thus, both of them have almost the same mathematical description. To reflect this fact, the symbols corresponding to the adaptive system model are identical to those used for the reference system, augmented by a Caret, e.g., \mathbf{w} denotes the parameter vector of the reference system, $\hat{\mathbf{w}}_k$ the parameter vector of the system model.

Symbols with Tilde ($\tilde{\cdot}$): The tilde symbol has two different meanings in this work. On the one hand, it denotes the difference among the parameter vectors of the reference system and the system model. Hence, if the primer is denoted by \mathbf{w} and the latter by $\hat{\mathbf{w}}_k$, the parameter error vector is given by $\tilde{\mathbf{w}}_k = \mathbf{w} - \hat{\mathbf{w}}_k$ (cf. (2.10)). On the other hand, it indicates that a symbol refers to a noisy entity, e.g., throughout this work, $\tilde{d}(k)$ refers to the output of the reference system in presence of noise, the symbols of the noiseless version is $d(k)$.

Implicit Extension to all k : In statements like $\mu(k) \in \mathbb{R}_{0+}$, it is implicitly assumed that they apply to all $k \geq 0$.

Meaning of the Phrase “for all k ”: In some statements, the phrase “for all k ” is used. In most cases, it can actually be replaced by “for *almost* all k ”, in the sense that a finite number of exceptions may be acceptable. Although the latter formulation would be formally more general, the primer is used in this thesis for simplicity reasons.

Suppression of Iteration Index k : On some occasions, the dependency on iteration index k , is inherently clear and does not contribute essential information to the context. Then, for reasons of readability the corresponding argument is consistently suppressed for all symbols in the scope. The suppression will be indicated by a light grey bar in the outer page margin, usually accompanied by an introducing comment such as “*Below, iteration index k is suppressed.*”. In these cases, symbols that refer to the preceding iteration $k - 1$ are underlined, e.g., $\tilde{\mathbf{w}}$ is then synonymous for $\tilde{\mathbf{w}}_{k-1}$.

Omitting Trivial Indices: On a few occasions, specifically in Section 5.3, special cases are considered for which the range of one, or more, indices reduces to one single value. Then, the corresponding trivial subscripts are collapsed. For example, symbol $\tilde{e}_{i,j,l}(k)$, modifies to $\tilde{e}_{i,j}(k)$ if $l \equiv 1$, or similarly, vector $\hat{\mathbf{w}}_{i,j,k}$ reduced to $\hat{\mathbf{w}}_{i,k}$, if $j \equiv 1$. Although, this convention is not completely unambiguous, the context should make the meaning clear.

Skipping of Argument \mathbf{B}_k for Symbols that refer to Mapping Matrix \mathbf{B}_k : In this work, eigenvalues $\lambda_i(k)$, eigenvectors $\mathbf{q}_{i,k}$, singular values $\sigma_i(k)$, and singular vectors, $\mathbf{r}_{i,k}$ and $\mathbf{t}_{i,k}$, refer to the mapping matrix \mathbf{B}_k . Otherwise, the corresponding symbols include the addressed matrix in form of an argument, e.g., $\lambda_i(\mathbf{D})$, $\mathbf{q}_i(\mathbf{D})$.

Index ranges: If an operator, e.g., \sum or \prod , is applied to a whole sequence of arguments, identified by an index $i \in \{i_{\text{start}}, \dots, i_{\text{stop}}\}$, this may be equivalently written as

$$\operatorname{operator} \dots, \quad \text{or,} \quad \operatorname{operator} \dots \quad (1.1)$$

$$i=i_{\text{start}} \qquad \qquad \qquad i \in \{i_{\text{start}}, \dots, i_{\text{stop}}\}$$

Open, Half-Open, and Closed Intervals: Intervals on the real axis are represented by a pair of values in brackets. If the interval boundaries are given by real numbers a and b , (a, b) denotes the open interval, $[a, b]$ the closed interval, and either $(a, b]$, or $[a, b)$, the left- or right-open interval, respectively. Note that the order of the limits is not required to fulfil $a \leq b$.

Norms, Sequences, and Pairs: Throughout this work, the symbol $\|\cdot\|$ denotes the Euclidean norm. A sequence is indicated by braces, enclosing the symbol that denotes one specific sample, e.g., $\{u(k)\}$ refers to the sequence of all excitation samples $u(k)$, here typically, $k \geq -1$. A pair of values is indicated by angle brackets, e.g., $\langle a, b \rangle$.

Symbols with a Prime ('): The prime (') is not used consistently throughout this work. In most cases, it indicates a relation among – except from the prime – identical symbols. However, in Sections 5.2 and 5.4 it also denotes the first order derivative. On rare occasions, such as in Section 3.4.2, more than one prime is required, i.e., $'$ and $''$. Yet, their meaning is analogous to the single prime.

1.5 Comment on the Graphical Representation of Simulation Results

In this work, plots with a large number of data points have been sampled down in order to reduce the file size of this document. This downsampling is not done in an equidistant way, but instead, it uses the (Ramer-)Douglas-Peucker algorithm [Ram72; DP73]. By this, for common scaling and adequate settings of the allowed deviation error, the shape of the processed graphs is perceived identical to their original shape. The processing was performed with the C++ implementation of the algorithm that is included in the Open Source Computer Vision Library (OpenCV) [OCV14] (version 2.4.11), in conjunction with a MATLAB interface based on mexopencv (version 2.4.5) [Yam14]³. Below the affected figures are listed:

- Figure 3.1,
- Figure 3.2,
- Figure 3.4,
- Figure 3.5,
- Figure 3.6,
- Figure 3.11,
- Figure 3.12,
- Figure 5.3,
- Figure 5.4.

Confidence intervals are all estimated by function `bootci` provided by MATLAB. Their estimation is based on 1000 bootstrap samples of the ensemble data, obtained by the performed Monte Carlo simulations. For calculation, the “bias corrected and accelerated percentile method” was used [ZB98; ZI07].

³ OpenCV and mexopencv are both available under a Berkeley Software Distribution (BSD) license.

Chapter 2

Preliminaries

The purpose of this chapter is to concisely present a conglomeration of already known and well established methods, schemes, and notions. They are considered fundamental for the following chapters. Clearly, their selection has to incorporate space limitations, and is based on a subjective decision. Hence, related topics may require further reading.

Section 2.1 briefly describes gradient type algorithms which are at the core of all algorithms throughout this work. As the input sequences that are used for excitation of such algorithms, play an important role, Section 2.2 discusses some common interpretations of their meaning, and in which situations these are encountered. Additionally, the notion of persistent excitation (PE) – in a deterministic regime – is introduced, up to the extend that is necessary here. Some basic facts about homogeneous recursions and a first motivation for Chapter 3 are provided in Section 2.3; complemented by a very short excursus to the impact of nonhomogeneous portions. Finally, the theoretic framework for the here used notions of stability is established by Section 2.4.

2.1 System Identification using Gradient Type Algorithms

This thesis focuses on the problem of adaptive system identification¹, which aims to iteratively adjust a tunable system – also referred to by the term *system model* – such that it best resembles the behaviour of some unknown *reference system*. Here, such an iterative adjustment is assumed to be done by some sort of gradient type algorithm that is intended to traverse the surface of a cost function down to its global minimum [Lju99; Hay02; Say03]. The following assumptions are valid for the whole scope of this work:

1. The reference system is described by a time-invariant vector of parameters, e.g., \mathbf{w} , of known length, e.g., M .
2. The reference system has the same number of parameters as the (adaptive) system model. The latter is described by a parameter vector, e.g., $\hat{\mathbf{w}}_k$, that is adapted from iteration to iteration.
3. The excitation of both systems may be scalar or vector-valued. Their responses are in any case scalar.
4. For each iteration k , the output of both, the reference system, as well as the adaptive system model, is linear in the corresponding parameter vector.
5. The reference system, the excitation sequences, the noise sequences, and the initial states of

¹ System identification schemes are also often referred to by the term “model reference techniques” [BA80a; LS85; ÅW95].

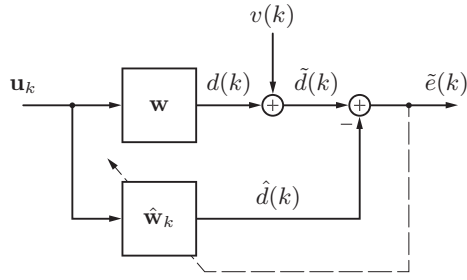


Figure 2.1: Basic structure of adaptive system identification.

the system models are bounded².

6. The reference system and the system model operate perfectly synchronous, and are excited by the same excitation sequence.
7. The response of the reference system may be contaminated by (unknown) additive noise.

Figure 2.1 depicts the basic structure of a system identification setting. For each iteration k , the reference system and the system model, given by

$$\mathbf{w} = [w_1 \quad w_2 \quad \cdots \quad w_M]^T \in \mathbb{C}^M, \quad (2.1)$$

and

$$\hat{\mathbf{w}}_{k-1} = [\hat{w}_1(k-1) \quad \hat{w}_2(k-1) \quad \cdots \quad \hat{w}_M(k-1)]^T \in \mathbb{C}^M, \quad (2.2)$$

respectively, are excited by excitation vector $\mathbf{u}_k \in \mathbb{C}^M$. Response $\hat{d}(k)$ of the system model is computed and compared to response $\tilde{d}(k)$ of the reference system. Based on the observed error

$$\tilde{e}(k) = \tilde{d}(k) - \hat{d}(k), \quad (2.3)$$

the system model is updated at the end of each iteration. It is common practice [BA80a; And82; Set92; BKS93; Hay02; Say03] to subsume inaccurate modelling, variations of the reference system, and measurement noise in (unknown) additive noise $v(k)$. Here, in agreement with the convention pointed out in Section 1.4, the symbol $\tilde{d}(k)$ reflects the fact that it is a noisy variant of the actual system output $d(k)$. The same applies in an analogous way to errors $\tilde{e}(k)$ and $e(k)$.

The actual update mechanism which maps old estimate $\hat{\mathbf{w}}_{k-1}$ to new vector $\hat{\mathbf{w}}_k$, depends on the metric that is introduced in order to assess the quality of the adapted system model. If a gradient type algorithm is employed that does not (explicitly) depend on more than one previous iteration, the update equation has the form [Men73; LS85; Hay02; Say03; Kre09]

$$\hat{\mathbf{w}}_k = \hat{\mathbf{w}}_{k-1} - \mu(k) \mathbf{M}_k \left(\left. \frac{\partial J(\hat{\mathbf{w}})}{\partial \hat{\mathbf{w}}} \right|_{\hat{\mathbf{w}}=\hat{\mathbf{w}}_{k-1}} \right)^H, \quad (2.4)$$

² Note that for most of the simulations performed in this work, Gaussian distributed random variables are used as basis for excitation sequences and noise sequences. Hence, they are formally unbounded. However, they are in fact only quasi-Gaussian, as numeric precision forces their domain to be limited. Similarly, in applications, signals have to undergo analogue-to-digital and digital-to-analogue conversion, which inherently enforces a restriction of their range of values to a finite interval.

where $\mu(k)$ is a positive step-size, \mathbf{M}_k is a positive definite step-size matrix, and $J(\cdot)$ is a cost function. The for its simplicity and robustness renowned LMS algorithm that dates back to [WH60], is obtained for

$$\mathbf{M}_k = \mathbf{I}, \quad (2.5)$$

and

$$J_{\text{LMS}}(\hat{\mathbf{w}}) = \text{E} \left\{ |\tilde{e}(k)|^2 \right\} \Rightarrow \left(\frac{\partial J(\hat{\mathbf{w}})}{\partial \hat{\mathbf{w}}} \Big|_{\hat{\mathbf{w}}=\hat{\mathbf{w}}_{k-1}} \right)^{\text{H}} = -\text{E} \{ \mathbf{u}_k^* \tilde{e}(k) \}, \quad (2.6)$$

if the expectation is replaced by the instantaneous (and noisy) approximation [Say03, pp. 214f.]

$$\text{E} \{ \mathbf{u}_k^* \tilde{e}(k) \} \approx \mathbf{u}_k^* \tilde{e}(k). \quad (2.7)$$

Cost function (2.6), together with approximation (2.7), is adopted for this whole thesis. However, the special step-size matrix in (2.5) only applies to Chapter 4. In contrast, the goal of Chapter 3 is to carve out subtle implications for algorithms with $\mathbf{M}_k \neq \mathbf{I}$. In fact, all of the gradient type algorithms this work focuses on, are basically of the form

$$\hat{\mathbf{w}}_k = \hat{\mathbf{w}}_{k-1} + \mu(k) \mathbf{M}_k \mathbf{u}_k^* \tilde{e}(k). \quad (2.8)$$

The actual definition of the update error $\tilde{e}(k)$ varies, but it is always given by (2.3) or a linear combination of several errors of this type. In the latter case, the symbol $\tilde{e}(k)$ is replaced by $\tilde{\varepsilon}_i(k)$ (cf. (4.2)). Defining regression vector

$$\mathbf{x}_k \triangleq \mathbf{M}_k^* \mathbf{u}_k, \quad (2.9)$$

and introducing parameter error vector

$$\tilde{\mathbf{w}}_k \triangleq \mathbf{w} - \hat{\mathbf{w}}_k, \quad (2.10)$$

(2.8) can be equivalently written as

$$\tilde{\mathbf{w}}_k = \tilde{\mathbf{w}}_{k-1} - \mu(k) \mathbf{x}_k^* \tilde{e}(k). \quad (2.11)$$

With the a priori error expressed in terms of $\tilde{\mathbf{w}}_{k-1}$, i.e.,

$$\tilde{e}(k) = \mathbf{w}^{\text{T}} \mathbf{u}_k - \hat{\mathbf{w}}_{k-1}^{\text{T}} \mathbf{u}_k + v(k) = \mathbf{u}_k^{\text{T}} \tilde{\mathbf{w}}_{k-1} + v(k), \quad (2.12)$$

eventually, update equation (2.8) is obtained in terms of the parameter error vector as

$$\tilde{\mathbf{w}}_k = \tilde{\mathbf{w}}_{k-1} - \mu(k) \mathbf{x}_k^* \mathbf{u}_k^{\text{T}} \tilde{\mathbf{w}}_{k-1} - \mu(k) \mathbf{x}_k^* v(k) \quad (2.13)$$

$$= [\mathbf{I} - \mu(k) \mathbf{x}_k^* \mathbf{u}_k^{\text{T}}] \tilde{\mathbf{w}}_{k-1} - \mu(k) \mathbf{x}_k^* v(k). \quad (2.14)$$

$$= \mathbf{B}_k \tilde{\mathbf{w}}_{k-1} - \mu(k) \mathbf{x}_k^* v(k), \quad (2.15)$$

with mapping matrix

$$\mathbf{B}_k \triangleq \mathbf{I} - \mu(k) \mathbf{x}_k^* \mathbf{u}_k^{\text{T}}. \quad (2.16)$$

Equation (2.15) is a nonhomogeneous first-order system of linear difference equations that is

nonautonomous, since \mathbf{B}_k varies with iteration index k [Aga92; Ela99]. In the noiseless case, i.e., $v(k) \equiv 0$, it reduces to the homogeneous recursion

$$\tilde{\mathbf{w}}_k = [\mathbf{I} - \mu(k)\mathbf{x}_k^*\mathbf{u}_k^\top] \tilde{\mathbf{w}}_{k-1} \quad (2.17)$$

$$= \mathbf{B}_k \tilde{\mathbf{w}}_{k-1}, \quad (2.18)$$

which is of central importance for this thesis.

Algorithms of structure (2.8), with $\mathbf{M}_k \neq \mathbf{I}$, are addressed by different names, such as second-order gradient algorithm [Men73, p. 200], generalised gradient descent algorithm [Kre09, p. 53], or simply LMS with matrix step-size [RC00]. From (2.9), it can be seen that $\mathbf{M}_k \neq \mathbf{I}$ leads to a regression vector that has a different direction than the excitation vector, causing matrix $\mathbf{x}_k^*\mathbf{u}_k^\top$ in (2.16), and consequently, also mapping matrix \mathbf{B}_k , to be nonsymmetric. Accordingly, in this work, this type of algorithms is coined by the term *asymmetric algorithm*. If contrarily, $\mathbf{M}_k \equiv \mathbf{I}$, the description *symmetric algorithm* is used to emphasise this difference.

Since the behaviour of the parameter error vector defined in (2.10) is at the core of all analyses pursued in this work, the performance metric used in the simulations will be the parameter mismatch, denoted by $m(k)$. It is defined as

$$m(k) \triangleq \mathbb{E} \left\{ \frac{\|\tilde{\mathbf{w}}_k\|^2}{\|\tilde{\mathbf{w}}_{-1}\|^2} \right\}, \quad (2.19)$$

with $\tilde{\mathbf{w}}_{-1}$ being the parameter error vector at algorithm initialisation. As the actual expectation cannot be captured by simulations, the ensemble average, together with its 95 %-confidence intervals, as well, as the extremal range over the whole ensemble, will be used for evaluation.

2.2 Excitation Sequences

The system model in Figure 2.1 is assumed to have a vector-valued input of adequate dimension, but the nature of its individual entries has not further been discussed, yet. Section 2.2.1 makes up for that and describes four different common interpretations, which cover a wide range of applications. Then, Section 2.2.2 goes one step beyond by considering the whole sequence of input vectors. It introduces the notion of persistent excitation, which plays an important role in the context of parameter convergence.

2.2.1 Interpretation of Excitation Vectors

The meaning of the excitation vector \mathbf{u}_k at the input of the structure in Figure 2.1 strongly depends on the actual physical background of the reference system, and is tightly related to the chosen system model. In any case, forgetting about additive noise $v(k)$ in Figure 2.1, for each iteration k , the output of both systems is obtained by summing up over the M entries in \mathbf{u}_k , weighted by the respective parameter vector, i.e.,

$$d(k) = \mathbf{w}^\top \mathbf{u}_k, \quad \text{and} \quad \hat{d}(k) = \hat{\mathbf{w}}_{k-1}^\top \mathbf{u}_k. \quad (2.20)$$

In Sections 2.2.1.1 to 2.2.1.4, four different interpretations of excitation vector \mathbf{u}_k are presented which also clarify the related meaning of its entries.

2.2.1.1 Linear Combiner

The most general situation is obtained, if both systems in Figure 2.1 are assumed to be linear combiners. This means that at each iteration step, one completely new excitation vector arrives at their input. Although the individual entries of the excitation vector may depend on each other, this is not structurally reflected by this type of model. Typically, systems with multidimensional input data lead to this situation. Then, the input vectors may represent, e.g., arbitrary patterns or feature vectors [WH60; WL90; Hay94]. Of course, also the cases described in the following sections can be considered as a linear combiner case, however, with additional constraints adhering to the elements of the excitation vector.

Especially, statistical analyses often rely on the assumption that the elements of the excitation vector are independent or uncorrelated [Gar84; FW85; TF88; Hay02; Say03]. Such a simplification can also be interpreted as a fictive replacement of the actual model structure, e.g., an FIR filter (cf. Section 2.2.1.2) by a linear combiner.

2.2.1.2 Finite Impulse Response Filter

In adaptive filtering, the two blocks in Figure 2.1 frequently represent linear dispersive single input single output (SISO) systems, described by FIR filters [WH60; Ung72; Hay02; Say03]. Then, both of them are excited by the same *scalar* input sequence $\{u(k)\}$. Whereas, the actual excitation vector at iteration k consists of the M most recent input samples, i.e.,

$$\mathbf{u}_k = [u(k) \quad u(k-1) \quad \cdots \quad u(k-M+1)]^T. \quad (2.21)$$

In this case, the two parameter vectors in (2.20) correspond to the tap weights of the individual FIR filters, the vector \mathbf{u}_k to the state of the delay line at iteration k .

2.2.1.3 Non-linear Basis Expansion

If the reference system is an (unknown) memoryless non-linearity, one approach in system identification is to pre-select a set of non-linear basis functions, and adaptively find the “best” set of expansion coefficients. Assuming that the scalar input at iteration k is given by $u(k)$, the set of non-linear basis functions $\psi_m(\cdot)$, $m \in \{1, \dots, M\}$, evaluated at $u(k)$, can be composed into the corresponding excitation vector [MS00a], according to

$$\mathbf{u}_k = [\psi_1(u(k)) \quad \psi_2(u(k)) \quad \cdots \quad \psi_M(u(k))]^T. \quad (2.22)$$

Then, (2.20) resembles the two non-linear models

$$d(k) = \sum_{m=1}^M w_m \psi_m(u(k)) \quad \text{and} \quad \hat{d}(k) = \sum_{m=1}^M \hat{w}_m(k-1) \psi_m(u(k)). \quad (2.23)$$

The actual choice of basis functions strongly depends on the expected behaviour of the reference system and the statistical properties of the excitation sequence $\{u(k)\}$. As an example, for smooth functions with rather low order of non-linearity, a monomial basis may be adequate [MS00a], i.e., in the simplest case, for $u(k) \in \mathbb{R}$,

$$\psi_m(u(k)) = u^{m-1}(k). \quad (2.24)$$

If the probability density function (pdf) of the excitation sequence is known a priori, the use of a polynomial basis may allow to achieve probabilistic orthogonality among the individual basis functions [RZ04; RQZ04; Abr72], which leads to improved convergence of the employed gradient type algorithm [DRWR10]. In order to reduce the computational complexity, piecewise linear functions can be used as an alternative basis [CWB+12; Che14].

2.2.1.4 Volterra Series

Out of the four here presented approaches, the by far widest range of functions can be covered by truncated Volterra Series. They combine the non-linear basis expansion in Section 2.2.1.3 with the linear dynamic system in Section 2.2.1.2 [Sch80; MS00a]. In the real valued case, a system of non-linearity order $P \geq 0$ can be described by a (discrete-time truncated) Volterra Series of the form

$$\begin{aligned}
 d(k) = h_0 + \sum_{l_1=0}^{M_1-1} h_1(l_1)u(k-l_1) + \sum_{l_1=0}^{M_2-1} \sum_{l_2=0}^{M_2-1} h_2(l_1, l_2)u(k-l_1)u(k-l_2) + \dots \\
 + \underbrace{\sum_{l_1=0}^{M_P-1} \dots \sum_{l_P=0}^{M_P-1}}_{P \text{ sums}} h_P(l_1, \dots, l_P) \underbrace{u(k-l_1) \dots u(k-l_P)}_{P \text{ factors}}, \tag{2.25}
 \end{aligned}$$

with Volterra kernels $h_p : \mathbb{N}_0^p \mapsto \mathbb{R}$ and memory lengths $M_p \geq 0$, $p \in \{0, \dots, P\}$. Again, (2.25) can be brought into the vector product form in (2.20). This is basically done by stacking all products of $u(\cdot)$ that occur in (2.25) into an excitation vector, and by associating the parameter vector with a stacked version of all discrete Volterra weights. For further details on this process, see, e.g., [EP97; MS00a; Asc05; Dal07]. The advantage of this method is that the resulting models are still linear in parameters, and thus, suited for adaptation by a gradient type algorithm. The disadvantage is the tremendous number of parameters that is obtained even for low non-linearity orders and short memory lengths. As a consequence, in literature many works propose methods to smartly reduce the number of parameters [KK01; ZPB06; ZDH+08; AZF+11; AZF+13].

2.2.2 Persistent Excitation

Section 2.2.1 presents several possible interpretations of the nature underlying the excitation vectors \mathbf{u}_k . While the analyses presented in Chapters 3 and 4 do not directly rely on the source of excitation, they *do depend* on the space that is spanned by the excitation sequence $\{\mathbf{u}_k\}$. This insight is not new and a wide range of literature studies this issue of PE (also referred to as mixing condition [WM79], or sufficient richness condition [BS83]) from several points of view. For further reading, [Bit84] is recommended as starting point, as it allows for smooth yet concise access to this topic. Moreover, it contains a multitude of additional references [amongst others, WM79; AJ82]. A more system theoretic perspective is found in [SK95; Lju99]. With respect to gradient type algorithms, the works [SMA+88; SAJ89; Set92] are of special interest. Specifically, the latter two are tightly related to Chapter 3, and their gist is applied in Section 3.2.

Here, the notion of PE is presented briefly, in a deterministic context, which should still give enough insight for the scope of this work. The following definition combines the corresponding statements in [Bit84, p. 185; SMA+88, p. 615; SAJ89, p. 391; Set92, p. 2202].

Definition 2.1: Persistent Excitation (in a deterministic sense)

The sequence of excitation vectors $\{\mathbf{u}_k\}$ is persistently exciting for the gradient type algorithm in (2.8), if for all iterations k , a constant and finite $K \geq M$ can be found such that all, i.e., $i \in \{1, \dots, M\}$, eigenvalues $\lambda_i(\mathbf{U}_{M,k}^{(K)})$ of the accumulated excitation matrix

$$\mathbf{U}_{M,k}^{(K)} \triangleq \sum_{j=k-K+1}^k \mathbf{M}_j \mathbf{u}_j^* \mathbf{u}_j^T, \quad (2.26)$$

satisfy

$$\operatorname{Re} \left\{ \lambda_i \left(\mathbf{U}_{M,k}^{(K)} \right) \right\} \geq A > 0. \quad (2.27)$$

From Definition 2.1, it becomes clear that even though the actual source of excitation is not of direct importance, it of course inherently influences the behaviour of the gradient type algorithms.

2.3 Homogeneous First-Order System of Linear Difference Equations

Recursions of the form (2.18) play a central role in this thesis. This section reviews some important facts about their mapping behaviour. At this point, no special structure of mapping matrix \mathbf{B}_k is presumed. Hence, (2.16) is temporarily discarded until the end of this section. Accordingly, the here obtained insights are of general validity and not restricted to algorithms of the kind in (2.17). Before focus is brought to the central homogeneous recursion (2.18), Section 2.3.1 provides few prerequisites and conventions. After that the autonomous case, i.e., $\mathbf{B}_k \equiv \mathbf{B}$, is considered in Section 2.3.2. The more general nonautonomous case that corresponds to a variant mapping matrix is addressed in Section 2.3.3.

2.3.1 Eigenvalues and Singular Values of Mapping Matrix \mathbf{B}_k

The important facts introduced in this section are not restricted to a special mapping matrix \mathbf{B}_k , they are valid for any square matrix belonging to $\mathbb{C}^{M \times M}$. Without loss of generality (wo.l.o.g.), \mathbf{B}_k is diagonalised by the singular value decomposition (SVD) [see, e.g., HJ13, Theorem 2.6.3], i.e.,

$$\begin{aligned} \mathbf{B}_k &= \mathbf{R}_k \boldsymbol{\Sigma}_k \mathbf{T}_k^H, \\ \mathbf{R}_k &\triangleq [\mathbf{r}_{1,k}, \dots, \mathbf{r}_{M,k}], \\ \mathbf{T}_k &\triangleq [\mathbf{t}_{1,k}, \dots, \mathbf{t}_{M,k}], \\ \boldsymbol{\Sigma}_k &\triangleq \operatorname{diag}\{\sigma_i(k)\}_{i=1}^M, \end{aligned} \quad (2.28)$$

where \mathbf{R}_k and \mathbf{T}_k are unitary square matrices of dimension $M \times M$, i.e., $\mathbf{R}_k \mathbf{R}_k^H = \mathbf{R}_k^H \mathbf{R}_k = \mathbf{I}$, $\mathbf{T}_k \mathbf{T}_k^H = \mathbf{T}_k^H \mathbf{T}_k = \mathbf{I}$, and where $\sigma_i(k) \in \mathbb{R}_{0+}$ are the singular values of \mathbf{B}_k , such that

$$\sigma_{\max}(\mathbf{B}_k) = \sigma_1(k) \geq \sigma_2(k) \geq \dots \geq \sigma_M(k) = \sigma_{\min}(\mathbf{B}_k). \quad (2.29)$$

The squared singular values $\sigma_i^2(k)$ are identical to the eigenvalues of the Gramian matrix $\mathbf{B}_k^H \mathbf{B}_k$, or its conjugate transpose $\mathbf{B}_k \mathbf{B}_k^H$. The left-sided singular vectors $\mathbf{r}_{i,k}$ are the eigenvectors of $\mathbf{B}_k \mathbf{B}_k^H$,

the right-sided singular vectors $\mathbf{t}_{i,k}$ are the eigenvectors of $\mathbf{B}_k^H \mathbf{B}_k$. Moreover, let $\lambda_i(k) \in \mathbb{C}$ be the eigenvalues of \mathbf{B}_k [HJ13, Definition 1.1.2]. Analogous to the singular values, w.o.l.o.g., they are assumed to be sorted such that

$$S(\mathbf{B}_k) = |\lambda_{\max}(\mathbf{B}_k)| = |\lambda_1(k)| \geq |\lambda_2(k)| \geq \dots \geq |\lambda_M(k)| = |\lambda_{\min}(\mathbf{B}_k)|, \quad (2.30)$$

where $S(\mathbf{B}_k) \in \mathbb{R}_{0+}$ denotes the spectral radius of \mathbf{B}_k , which by definition is identical to the modulus of its maximum eigenvalue [HJ13, Definition 1.2.9]. An important relation between the eigenvalues in (2.30) and the singular values (2.29) is given by [Wey49; Hor54; MOA11, p. 317],

$$\begin{aligned} \prod_{i=1}^m |\lambda_i(k)| &\leq \prod_{i=1}^m \sigma_i(k); \quad m = 1, \dots, M-1, \\ \prod_{i=1}^M |\lambda_i(k)| &= \prod_{i=1}^M \sigma_i(k). \end{aligned} \quad (2.31)$$

A direct consequence of (2.31) is

$$\sigma_1(k) \geq S(\mathbf{B}_k) = |\lambda_1(k)| \geq |\lambda_M(k)| \geq \sigma_M(k). \quad (2.32)$$

2.3.2 Mapping Behaviour of Autonomous Recursions

The autonomous case, i.e., $\mathbf{B}_k = \mathbf{B}$, of recursion (2.18) is well studied [Var62, pp. 6ff.; Men73, p. 24; HY81, p. 8; GV96, p. 509; MS00b, p. 701; Hig02, p. 339; HJ13, Corollary 5.6.14]. Accordingly, with initial state $\tilde{\mathbf{w}}_{-1}$, the solution of (2.18) is found as

$$\tilde{\mathbf{w}}_k = \mathbf{B}^{k+1} \tilde{\mathbf{w}}_{-1}, \quad k \geq 0, \quad (2.33)$$

for which $\lim_{k \rightarrow \infty} \tilde{\mathbf{w}}_k = \mathbf{0}$ is ensured for all $\tilde{\mathbf{w}}_{-1}$, if and only if (iff)

$$S(\mathbf{B}) < 1. \quad (2.34)$$

With the latter condition satisfied, a subtle fact that is less widely known concerns the upper bound

$$\sup_{k \geq 0} \{\|\tilde{\mathbf{w}}_k\|\}, \quad (2.35)$$

reached by parameter error distance $\|\tilde{\mathbf{w}}_k\|$ in (2.33). While for Hermitian matrices, it is easy to see that supremum (2.35) coincides with $S(\mathbf{B}) \|\tilde{\mathbf{w}}_{-1}\|$ (for $k = 0$), as pointed out in [Hig02, pp. 340ff.], for non-Hermitian matrices, the exact value of (2.35) can be arbitrarily high, and is in most cases only accessibly via approximate bounds. The reason for the existence of this behaviour can be explained by (2.32), as it shows that with (2.34) satisfied, it is still possible that at least one singular value is strictly larger than one. Contemplate, e.g., the case [Hig02, pp. 340ff.]

$$\mathbf{B} = \begin{bmatrix} a & b \\ 0 & a \end{bmatrix}, \quad (2.36)$$

with $0 < a < 1$, $b \in \mathbb{R}$. This matrix has the eigenvalues $\lambda_1 = \lambda_2 = a$, however, its maximum singular value is given by

$$\sigma_1 = b \sqrt{\frac{1}{2} + \left(\frac{a}{b}\right)^2} + \sqrt{\frac{1}{4} + \left(\frac{a}{b}\right)^2}, \quad (2.37)$$

which even if $a \ll 1$, can be made arbitrarily large just by choosing a sufficiently large value for b .

Even more extreme is the situation in the case of nilpotent matrices. For these, all eigenvalues can be shown to be zero [HJ13; Gra13, p. 61]. Nevertheless, their largest singular value can be essentially greater than zero. Consider, e.g., the following nilpotent (6×6) -matrix \mathbf{B} found in [Bee12, Subsection NLT]

$$\mathbf{B} = \begin{bmatrix} -3 & 3 & -2 & 5 & 0 & -5 \\ -3 & 5 & -3 & 4 & 3 & -9 \\ -3 & 4 & -2 & 6 & -4 & -3 \\ -3 & 3 & -2 & 5 & 0 & -5 \\ -3 & 3 & -2 & 4 & 2 & -6 \\ -2 & 3 & -2 & 2 & 4 & -7 \end{bmatrix}. \quad (2.38)$$

It can be verified that $\mathbf{B}^4 = \mathbf{0}$, that all eigenvalues of \mathbf{B} are zero, and that the maximum singular value evaluates to $\sigma_1 = 21.970\,458\dots$

In summary, (2.34) ensures convergence in the limit but for non-Hermitian matrices \mathbf{B} , it does not allow to conclude that the sequence $\{\|\tilde{\mathbf{w}}_k\|\}$ is monotonously decreasing.

2.3.3 Mapping Behaviour of Nonautonomous Recursions

For nonautonomous recursions, i.e., if the mapping matrix in recursion (2.18) varies with iteration index k , the decision on convergence is an involved problem, and a condition similarly compact as (2.34) is far out of reach [Men73, p. 193; BBC+94, p. 14; Kah13, p. 13]. To see the insufficiency of (2.34), consider a recursion such as in (2.18), where for all $k > -1$, (2.34) is satisfied, but where at least one singular value is strictly larger than one, i.e., $\sigma_1(k) \geq 1 + \delta_\sigma$ with some $\delta_\sigma > 1$. Then, in the unlikely but possible situation that for each iteration, the a priori parameter error vector $\tilde{\mathbf{w}}_{k-1}$ is in parallel with $\mathbf{t}_{1,k}$ in (2.28),

$$\tilde{\mathbf{w}}_k = \sigma_1(k) \tilde{\mathbf{w}}_{k-1} \geq (1 + \delta_\sigma) \tilde{\mathbf{w}}_{k-1} \geq (1 + \delta_\sigma)^{k+1} \tilde{\mathbf{w}}_{-1} \geq (1 + k\delta_\sigma) \tilde{\mathbf{w}}_{-1}, \quad (2.39)$$

which clearly grows unbounded with increasing k . The assumption $\tilde{\mathbf{w}}_{k-1} \parallel \mathbf{t}_{1,k}$, for all k , which is equivalent to $\mathbf{r}_{1,k-1} = \pm \mathbf{t}_{1,k}$, imposes very strong restrictions on \mathbf{B}_k . However, as it will be seen in Section 3.4.1 (specifically, Lemma 3.4), it actually occurs for the algorithmic structure in (2.17). Moreover, a more detailed look shows that slight deviations from $\tilde{\mathbf{w}}_{k-1} \parallel \mathbf{t}_{1,k}$ still lead to a growth. To see this, first assume, w.o.l.o.g., that the singular values can be separated into three groups,

$$\begin{aligned} \text{Group 1: } & \sigma_i(k) > 1, \quad \text{for } 1 \leq i \leq \hat{i}_+, \\ \text{Group 2: } & \sigma_i(k) = 1, \quad \text{for } \hat{i}_+ < i < \hat{i}_-, \\ \text{Group 3: } & \sigma_i(k) < 1, \quad \text{for } \hat{i}_- \leq i \leq M, \end{aligned}$$

with adequate indices \hat{i}_+ and \hat{i}_- that satisfy $\hat{i}_+ \leq \hat{i}_-$, where equality occurs if no unit singular value exists. Then, with the parameter error vector transformed to the space spanned by the right-sided

singular vectors,

$$\tilde{\mathbf{w}}'_{k-1} = [\tilde{w}'_1(k-1) \ \cdots \ \tilde{w}'_M(k-1)]^\top \triangleq \mathbf{T}_k \tilde{\mathbf{w}}_{k-1}, \quad (2.40)$$

since \mathbf{R}_k and \mathbf{T}_k are unitary, the parameter error increment defined as

$$W(k) \triangleq \|\tilde{\mathbf{w}}_k\|^2 - \|\tilde{\mathbf{w}}_{k-1}\|^2, \quad (2.41)$$

satisfies [DR09a]

$$\begin{aligned} W(k) &= \|\mathbf{B}_k \tilde{\mathbf{w}}_{k-1}\|^2 - \|\tilde{\mathbf{w}}_{k-1}\|^2 = \left\| \mathbf{R}_k \boldsymbol{\Sigma}_k \mathbf{T}_k^\text{H} \tilde{\mathbf{w}}_{k-1} \right\|^2 - \|\tilde{\mathbf{w}}_{k-1}\|^2 \\ &= \left\| \boldsymbol{\Sigma}_k \mathbf{T}_k^\text{H} \tilde{\mathbf{w}}_{k-1} \right\|^2 - \left\| \mathbf{T}_k^\text{H} \tilde{\mathbf{w}}_{k-1} \right\|^2 = \tilde{\mathbf{w}}_{k-1}^\text{H} \mathbf{T}_k (\boldsymbol{\Sigma}_k^2 - \mathbf{I}) \mathbf{T}_k^\text{H} \tilde{\mathbf{w}}_{k-1} \\ &= \sum_{i=1}^{\hat{i}_+} [\sigma_i^2(k) - 1] \left| \tilde{w}'_i(k-1) \right|^2 - \sum_{i=\hat{i}_-}^M [1 - \sigma_i^2(k)] \left| \tilde{w}'_i(k-1) \right|^2 > 0, \end{aligned} \quad (2.42)$$

as long as

$$\sum_{i=1}^{\hat{i}_+} [\sigma_i^2(k) - 1] \left| \tilde{w}'_i(k-1) \right|^2 > \sum_{i=\hat{i}_-}^M [1 - \sigma_i^2(k)] \left| \tilde{w}'_i(k-1) \right|^2. \quad (2.43)$$

Obviously, for a given set of singular values at iteration k , the squared magnitudes $|\tilde{w}'_i(k-1)|^2$ act as weighting factors in (2.43). While the afore considered case $\tilde{\mathbf{w}}_{k-1} \parallel \mathbf{t}_{1,k}$ leads to the maximum increase of $\|\tilde{\mathbf{w}}_k\|$ in iteration k , in general, a whole subspace is described by (2.43) that causes the parameter error vector to elongate. Throughout this work, this space is often addressed as worst case, or briefly as w.c., subspace (cf. Section 3.3.3). The crucial difference to the autonomous case in Section 2.3.2 is that the unitary matrices \mathbf{R}_k and \mathbf{T}_k change from iteration to iteration. By this, an alignment can occur such that (2.43) is satisfied for all k .

2.3.4 Implications to the Nonhomogeneous Case

Although, the mapping analyses in this work exclusively consider homogeneous recursions, in almost all practical situations, an external driving force exists that introduces an additional nonhomogeneous component. This section briefly discusses the implications that can be deduced for the nonhomogeneous case, based on the insights obtained for the homogeneous case.

In this work, the nonhomogeneous component originates from additive noise. One possibility to assess the influence of noise is to conduct a separate analysis. This is done for the coupled structure in Chapter 4. There, on the one hand, results are obtained for the mapping behaviour of the homogeneous system. On the other hand, rather independently from the mapping analysis, ℓ_2 -stability is considered, which focuses on stability in the presence of noise with bounded energy.

For the asymmetric algorithms discussed in Chapter 3 – and also for the general identical error case of the coupled structure in Section 4.6 – the here adopted method that is used to study ℓ_2 -stability fails. Yet, it has to be noted that for specific asymmetric algorithms, ℓ_2 -stability has been shown [SR96; Rup11a]. Nevertheless, also based on the mapping behaviour of the homogeneous recursion, some instructive insights can be gained. A brief look to the results that are available for the conventional LMS algorithm gives some orientation. Besides from the multitude of statistical analyses [see, e.g., Bit84; Hay02; Say03], in the deterministic regime, ℓ_2 -stability [e.g., SR96], as

well as, total stability in conjunction with PE have proven valuable [Bit84; Set92, p. 2201]. As pointed out afore, ℓ_2 -stability seems to be hard to establish in general for asymmetric algorithms. Similarly, the total stability theorem relies on exponential stability of the homogeneous recursion, which appears unlikely to be true for asymmetric algorithms in general. However, one class of results for the conventional LMS, is found to be considerably instructive. Accordingly, the violation of PE in the presence of noise, bears the risk of an unbounded drift of the parameter error vector [SLJB86; Nas99]. Anticipating the findings of Chapter 3, asymmetric algorithms are susceptible to hidden diverging modes. Taking this into account, even in specific situations, where such modes cannot be excited, it has to be expected that the phenomenon of parameter drift also exists for asymmetric algorithm. This becomes even more plausible in the following way. For the general asymmetric algorithm, accumulating (2.15) from the initial iteration $k = 0$ up to some certain iteration $K \geq 0$, leads to

$$\tilde{\mathbf{w}}_K = \left(\prod_{l=0}^K \mathbf{B}_l \right) \tilde{\mathbf{w}}_{-1} - \sum_{l=1}^K \mu(l)v(l) \left(\prod_{n=l+1}^K \mathbf{B}_n \right) \mathbf{u}_l^*. \quad (2.44)$$

Taking the squared Euclidean norm and applying the triangle inequality [MS00b, p. 72], gives

$$\|\tilde{\mathbf{w}}_K\|^2 \leq \left\| \left(\prod_{l=0}^K \mathbf{B}_l \right) \tilde{\mathbf{w}}_{-1} \right\|^2 + \sum_{l=1}^{K-1} |\mu(l)|^2 |v(l)|^2 \left\| \left(\prod_{n=l+1}^K \mathbf{B}_n \right) \mathbf{u}_l^* \right\|^2 + |\mu(K)|^2 |v(K)|^2 \|\mathbf{u}_K\|^2. \quad (2.45)$$

The first term on the right-hand side corresponds to the homogeneous part. As the bound provided by the triangle inequality is indeed reachable, it becomes clear that even if the homogeneous part converges towards zero – which is not necessarily guaranteed for asymmetric algorithms – the second term on the right-hand side of (2.45) can still cause an unbounded drift of the parameter error distance $\|\tilde{\mathbf{w}}_k\|^2$. Hence, these algorithms cannot be expected to behave more benign with respect to a potential parameter drift than the conventional LMS algorithm.

2.4 Stability and Convergence

This section briefly introduces different notions of stability that are of relevance for this work. As the topic stability is a vast area, literature is similarly vast. Comprehensive access to this topic is provided by [Kha02; ZDG96]. The book [Vid02] is an extensive reference and considerably condensed. For a general introduction to adaptive control, [LLM98; ÅW95] are suggested. Last but not least, the well known reference books [Hay02; Say03] are recommended, if a focus on adaptive filters is desired.

The approach pursued by the analyses in this work is purely deterministic and barely requires any a priori knowledge about the involved signals and systems. Two notions of stability are of special relevance for the corresponding problems. The first one, uniform stability, is introduced in Section 2.4.1. It basically allows to investigate the convergence behaviour of the parameter error vector. The second one, ℓ_p -stability, is described in Section 2.4.2. It focuses on the energy of the update error with respect to the disturbance energies.

2.4.1 Uniform Stability

In the optimal case, the parameter vector estimated by a system identification algorithm, should unconditionally converge towards the unknown reference vector. In terms of parameter error vector $\tilde{\mathbf{w}}_k$ introduced in (2.10), this means

$$k \rightarrow \infty \Rightarrow \tilde{\mathbf{w}}_k \rightarrow \mathbf{0}. \quad (2.46)$$

Contemplating homogeneous recursion (2.18), $\tilde{\mathbf{w}}_{k-1} = \mathbf{0}$ is an equilibrium, as $\mathbf{B}_k \tilde{\mathbf{w}}_{k-1} = \mathbf{B}_k \mathbf{0} = \mathbf{0}$. However, whether this equilibrium is actually attracting – and thus stable – depends on the sequence of matrices $\{\mathbf{B}_k\}$. Moreover, the question remains open whether this equilibrium is unique.

To answer the above posed questions, many approaches have been proposed in literature. They are reviewed in more detail in Section 3.2. As done in [Men73], one notion of stability is based on Lyapunov theory [Vid02]. Starting point is the assumption that the sequence $\{\mathbf{B}_k\}$ is given a priori. Furthermore, it is assumed that iteration index k is always transformed such that initialisation takes place at $k = -1$, and the first actual calculation is performed at $k = 0$. Then, a so called motion vector $\mathbf{s}_k(\tilde{\mathbf{w}}_{-1})$ can be introduced, which describes the unique solution of (2.18) for all $k \geq 0$, given an initial state $\tilde{\mathbf{w}}_{-1}$. With this at hand, based on [Men73, pp. 193ff.; Vid02, pp. 136f.], the following notion of stability can be introduced.

Definition 2.2: Uniform Stability

An equilibrium state $\tilde{\mathbf{w}}_e \in \mathbb{C}^M$ of recursion (2.18) is said to be uniformly stable, if for any real number $\varepsilon > 0$, a positive $\delta(\varepsilon)$ can be found, for all $k \geq -1$, such that the trajectory $\mathbf{s}_k(\tilde{\mathbf{w}}_{-1})$ that is unique for a given initial state $\tilde{\mathbf{w}}_{-1}$, satisfies

$$\|\tilde{\mathbf{w}}_{-1} - \tilde{\mathbf{w}}_e\| \leq \delta(\varepsilon) \Rightarrow \|\mathbf{s}_k(\tilde{\mathbf{w}}_{-1}) - \tilde{\mathbf{w}}_e\| \leq \varepsilon. \quad (2.47)$$

Thus, a uniformly stable equilibrium $\tilde{\mathbf{w}}_e$ ensures that for any initial state $\tilde{\mathbf{w}}_{-1}$, with a distance to $\tilde{\mathbf{w}}_e$ that is not larger than ε , trajectory $\mathbf{s}_k(\tilde{\mathbf{w}}_{-1})$ remains bounded within a ball with finite radius $\delta(\varepsilon)$. As a consequence, neither does uniform stability give any insight to the speed of convergence, nor does it – except from boundedness – entail any quantitative restriction to the radius $\delta(\varepsilon)$. Obviously, even if the origin is found to be an equilibrium that satisfies Definition 2.2, the aforementioned desired behaviour of (2.46) is by far not ensured³. However, if by contrast $\mathbf{0}$ – or any other equilibrium – can be found that violates Definition 2.2, it is ensured that under no circumstance (2.46) is unconditionally true. This is of importance for the line of argumentation that is adopted in Chapter 3, where the potentially unstable behaviour of asymmetric algorithms is revealed.

2.4.2 Input-Output Stability

In situations where assumptions about statistical properties of the involved signals and systems are not justified or, due to lack of knowledge impossible, different approaches are required in order to assess the stability of a control system [RS96a; HSK99]. One famous candidate out of these alternative approaches is input-output stability which dates back to Sandberg and Zames [Zam66] in the 1960s [Vid02]. It is a purely deterministic framework and basically analyses the image space that is obtained if a system is fed by functions or sequences from a given domain space. In continuous time, domain and image space are described by function spaces, in discrete time, they are represented

³ In order to ensure an unconditional satisfaction of (2.46), equilibrium $\mathbf{0}$ would need to be uniformly asymptotically stable in the large [Men73, p. 196].

by sequence spaces. The sequel of this section briefly introduces those parts of this theory that will be required in Section 4.4. They can be found in more detail in [Vid02; Kha02; vdS00; DV75], out of which especially [DV75] is almost exclusively dedicated to the introduction of this theory.

Definition 2.3: ℓ_p -Space of Scalar Sequences

The ℓ_p -space, with $p \in [1, \infty)$, contains all sequences $\{z_k\}$, with $k \geq 0$, for which

$$\sum_{k=0}^{\infty} |z_k|^p < \infty, \quad (2.48)$$

where the elements z_k can be taken from some arbitrary field (in the algebraic sense). By endowing ℓ_p with the norm for all $\{z_k\} \in \ell_p$

$$\|z_k\|_{\ell_p} \triangleq \sqrt[p]{\sum_{k=0}^{\infty} |z_k|^p}, \quad (2.49)$$

the space becomes a Banach space.

In this work, the field from which sequence elements z_k are taken, is typically the set of complex numbers, i.e., $z_k \in \mathbb{C}$, or the set of real numbers $z_k \in \mathbb{R}$. Note that for reasons of readability the brackets $\{\cdot\}$ (indicating a sequence) are omitted on the left-hand side of (2.49). On the right-hand side however, the symbol z_k actually refers to the individual elements of the sequence $\{z_k\}$.

Definition 2.4: ℓ_p^M -Space of Vector Valued Sequences

The ℓ_p^M -space, with $M \in \mathbb{N}$ and $p \in [1, \infty)$, contains all sequences $\{\mathbf{z}_k\}$, with $k \geq 0$, for which

$$\sum_{k=0}^{\infty} \|\mathbf{z}_k\|_p^p < \infty, \quad (2.50)$$

where the vector valued elements \mathbf{z}_k can be taken from some arbitrary field (in the algebraic sense) with dimension M . By endowing ℓ_p^M with the norm for all $\{\mathbf{z}_k\} \in \ell_p^M$

$$\|\mathbf{z}_k\|_{\ell_p} \triangleq \sqrt[p]{\sum_{k=0}^{\infty} \|\mathbf{z}_k\|_p^p}, \quad (2.51)$$

the space becomes a Banach space.

Note that the field from which the vectors \mathbf{z}_k are taken, is in most cases the set of complex-valued vectors of some dimension M , i.e., $\mathbf{z}_k \in \mathbb{C}^M$. Moreover, accepting a slight inaccuracy in notation, the norm in (2.51), uses the same symbol as in (2.49). This is done as the different typefaces of scalars and vectors, as well as, the context should make clear which norm is addressed. Finally, it is mentioned that according to [Kha02, p. 196] in (2.51), the used vector norm does not necessarily have to be the p -norm. However, this is the way how the ℓ_p -norm for vector valued sequences is commonly defined.

Sequences contained in one of the spaces defined by Definitions 2.3 and 2.4 can be considered

as finite energy sequences. The notion of input-output stability is based on this interpretation, as it defines a system as stable, if it always responds with an energy limited sequence, as long as the input sequence has finite energy. The following definition renders this more precisely⁴.

Definition 2.5: ℓ_p -Stability (with Finite Gain)

A system described by a mapping H , with image space contained in ℓ_p , is ℓ_p -stable, as long as its domain space also belongs to ℓ_p , i.e.,

$$H : \ell_p \mapsto \ell_p. \quad (2.52)$$

If moreover, for any input sequence $\{z_k\} \in \ell_p$, output sequence $\{\zeta_k\}$ satisfies

$$\|\zeta_k\|_{\ell_p} \leq g_p \|z_k\|_{\ell_p} + b_p, \quad (2.53)$$

with finite constants $g_p \in \mathbb{R}_{0+}$ and $b_p \in \mathbb{R}_{0+}$, the system is called ℓ_p -stable with finite gain. For an ℓ_p -stable system H , the smallest possible value for g_p is called the ℓ_p -gain of H . It is defined as

$$g_p(H) \triangleq \arg \inf_{\forall \{z_k\} \in \ell_p} \left\{ \|\zeta_k\|_{\ell_p} \leq g_p \|z_k\|_{\ell_p} + b_p \right\}. \quad (2.54)$$

Definition 2.5 analogously applies to the case of input and/or output sequences with vector-valued elements.

To see, how this theory is put into practice, results from [SR95b; RS96a; SR96] that address ℓ_2 -stability of the conventional LMS algorithm (see Section 2.1), are briefly repeated in the remainder of this section. Starting point is update equation (2.8), with identity step-size matrix, i.e., (2.5). Taking the squared Euclidean norm on both sides of (2.8) gives

$$\|\tilde{\mathbf{w}}_k\|^2 = \|\tilde{\mathbf{w}}_{k-1}\|^2 + \mu^2(k) \|\mathbf{u}_k\|^2 |\tilde{e}(k)|^2 - 2\mu(k) \operatorname{Re} \{ \tilde{e}(k) e(k)^* \}. \quad (2.55)$$

Substituting the noisy error $\tilde{e}(k)$ with (2.12), expanding by $\mu(k) |v(k)|^2 - \mu(k) |v(k)|^2$ on the right-hand side, rearranging terms, and finally reinserting $\tilde{e}(k)$ leads to

$$\|\tilde{\mathbf{w}}_k\|^2 + \mu(k) |e(k)|^2 = \|\tilde{\mathbf{w}}_{k-1}\|^2 + \mu(k) |v(k)|^2 + \mu(k) |\tilde{e}(k)|^2 \left(\mu(k) \|\mathbf{u}_k\|^2 - 1 \right). \quad (2.56)$$

With the well known step-size bounds⁵

$$0 \leq \mu(k) \|\mathbf{u}_k\|^2 \leq 1, \quad (2.57)$$

(2.56) satisfies a local passivity relation of the form

$$\|\tilde{\mathbf{w}}_k\|^2 + \mu(k) |e(k)|^2 \leq \|\tilde{\mathbf{w}}_{k-1}\|^2 + \mu(k) |v(k)|^2. \quad (2.58)$$

⁴ Note that the definition is almost equivalent to the definition of ℓ_p -stability in [Vid02, p. 365]. As in this thesis, all systems can be described by an actual mapping $H : \ell_p \mapsto \ell_p$, the further abstraction introduced in [Vid02, p. 277] that describes a system more generally as a binary mapping, is skipped here. Instead, the interpretation of [Kha02, p. 197] is adopted, taking into account that in discrete time the separate use of extended sequence spaces is not required, as pointed out in [Vid02, p. 365].

⁵ Note that upper bound 1, on the right-hand side of (2.57), is replaced by 2, if common independence assumptions are adopted, and stability in the mean-square sense is addressed instead [Hay02; Say03].

To obtain a global statement, (2.58) is summed up on both sides from 0 to some certain iteration $K \geq 0$ and bounded based on the Minkowsky inequality [MS00b, p. 871], yielding

$$\sqrt{\sum_{k=0}^K \mu(k) |e(k)|^2} \leq \|\tilde{\mathbf{w}}_{-1}\| + \sqrt{\sum_{k=0}^K \mu(k) |v(k)|^2}. \quad (2.59)$$

Comparing this result with (2.53) shows that (2.57) establishes ℓ_2 -stability for the LMS, in the sense that bounded energy of the weighted noise sequence $\{\sqrt{\mu(k)}v(k)\}$ ensures bounded energy of the sequence of weighted a priori errors $\{\sqrt{\mu(k)}e(k)\}$.

Chapter 3

Asymmetric Gradient Type Algorithms

In adaptive system identification, based on stochastic gradient search, in many situations, matrix step-sizes are used to improve convergence speed. For example, [MKK93] proposes a constant diagonal step-size matrix with exponentially decaying entries in order to speed up identification of a room impulse response. Here, the exponential decay constant has to be determined separately in advance. This requirement is overcome by other approaches which employ a time-varying matrix step-size. Out of these, one prominent example is the proportionate normalised LMS (PNLMS) algorithm [Dut00]. The PNLMS algorithm has been designed to accelerate convergence of echo cancellation algorithms in analogue landline telephone networks, which show long but rather sparse impulse responses. Several modifications have been proposed, e.g., [Gay98; BG02; dSTSM09; dSTSM10].

Moreover, other iterative minimisation methods, which aim to increase adaptation speed by use of a more accurate direction of the stochastic gradient, can be considered as gradient type algorithm with matrix step-size. For example, the recursive-least-squares (RLS) algorithm and the Gauß-Newton algorithm (for a quadratic cost function) rely on an iteratively improved estimate of the inverse autocorrelation matrix in lieu of the step-size matrix [RS95; RS96c; Say03, pp. 245ff.]. Similarly, the pseudo affine projection (PAP) algorithm – a predecessor of the well known affine projection algorithm (APA) [OU84] – and its variant in [Rup98; BSC99] are of that kind.

Also in the case of an adaptive system model that employs a basis of non-linear functions (cf. Section 2.2.1.3), the derivation of the corresponding gradient type algorithm introduces a matrix step-size which contains the first derivatives of the basis functions [e.g., MS00a; RZ04; RQZ04; CWB+12; Che14].

All of these algorithms share the property that their regression vector has a different direction than their excitation vector. Hence, as motivated in Section 2.1, they belong to the class of asymmetric algorithms. An example for an asymmetric algorithm that does *not* rely on an explicit matrix step-size is the signed regressor LMS (SR-LMS) [Luc65, p. 557; Say03], which performs regression based on a computationally efficient regression vector that contains the elements of the excitation vector, reduced to their signs.

Asymmetric algorithms are at the focus of this chapter. More specifically, their convergence and divergence behaviour under w.c. conditions, is the main concern, here. One of the major goals pursued, is to reveal unbounded growth of the parameter vector, and find explanations for scenarios where the latter remains bounded. It has to be emphasised that, as a consequence, most of the following investigations take a rather unconventional perspective. *Typically, the aim is to prove convergence, here, in contrast, more attention is paid to the contrary case.* The reader is asked to keep this in mind in the sequel, as otherwise, the line of arguments may in some points appear counter-intuitive.

Why in this thesis – entitled to deal with coupled adaptive filters – the chapter with the largest extent deals with asymmetric algorithm, has the following reason. The actual coupled structure, considered in Chapter 4, is found in Section 4.6 to have a practically important mode of operation – the so called identical error case – that can be described by an LMS algorithm with matrix step-size. The just mentioned practical relevance is established in Chapter 5, where the adaptive Wiener model and the MC-FXLMS are analysed by mapping them to such a coupled adaptive structure that operates exactly in this mode. Beyond these examples, many other combinations of gradient type algorithms, such as cascaded structures, can be analysed in this way.

This chapter is organised as follows. Comparison of three simulation experiments with LMS algorithm with matrix step-size in Section 3.1, demonstrates the problem of hidden divergence and poses three questions which motivate the following analyses. As the here considered algorithms are known for decades, a wide range of related literature can be found. In Section 3.2, an overview about existing results is given. Out of these, the three most relevant are applied to the simulation experiments from Section 3.1, in order to demonstrate that they do not allow for a conclusive interpretation of the observed behaviour. As an introductory step, Section 3.3 determines the eigenvalues and singular values of the underlying mapping matrix. It is found that the latter has (almost) always one singular value that is larger than one. Hence, resorting to the arguments of Section 2.3.2, the corresponding homogeneous recursion may lead to an increase of the parameter error distance. Knowing about this inevitable risk, Section 3.4 aims to answer the questions that are motivated by the simulation experiments in Section 3.1. This is achieved by a detailed investigation of the geometric mechanisms that happen during one iteration of the homogeneous recursion. First, Section 3.4.1 studies general mapping characteristics of asymmetric algorithms that are independent from any matrix step-size. The existence of a matrix step-size is then covered in Sections 3.4.2 and 3.4.3. Section 3.4.4, finally brings all the afore obtained results together and carves out the important properties that decide on convergence and divergence. With all the obtained insights to hidden divergence, the remaining two sections engage in the synthesis of excitation sequences that provoke this phenomenon. In a first step, this is approached analytically in Section 3.5. In situations of excitation sequences with restricted domain, these analytical methods may not be applicable. Hence, a numerical alternative is provided by Section 3.6, which derives efficient search algorithms in order to synthesise w.c. sequences.

3.1 Motivation

In order to motivate the extensive mapping analysis presented in this chapter, this section starts with simulation experiments which extend those presented in [DR09a]. Let us consider a stochastic gradient algorithm of the type (2.8) with a positive definite diagonal matrix step-size, i.e.,

$$\mathbf{M}_k = \mathbf{D}_k = \text{diag} \{d_i(k)\}_{i=1}^M, \quad \text{with} \quad d_i(k) > 0, \quad i \in \{1, \dots, M\}. \quad (3.1)$$

In order to normalise the excitation power, the scalar step-size $\mu(k) > 0$ is chosen according to

$$\mu(k) = \frac{\bar{\mu}}{\mathbf{u}_k^H \mathbf{D}_k \mathbf{u}_k} = \frac{\bar{\mu}}{\|\mathbf{u}_k\|_{\mathbf{D}_k}^2}, \quad (3.2)$$

with the normalised step-size $\bar{\mu} \in (0, 2)$. The fixed reference system and the system model are represented by linear combiners (cf. Section 2.2.1.1) of length M with parameter vectors $\mathbf{w} \in \mathbb{C}^M$ and $\hat{\mathbf{w}}_k \in \mathbb{C}^M$, respectively. Real and imaginary parts of the entries in \mathbf{w} are all independently drawn

from a uniform distribution over interval $(0, 1]$. Then, the vectors are scaled such that $\|\mathbf{w}\| = 1$. No additive noise is added at the output of the reference system. All simulations in the following two sections use normalised step-sizes selected from

$$\bar{\mu} \in \{0.05, 0.5\}. \quad (3.3)$$

By this, it is possible to observe that the investigated effects are only affected in their intensity by the (normalised) step-size but not their existence, as long as

$$0 < \bar{\mu} < 2. \quad (3.4)$$

The justification for this bound is given further down in Lemma 3.1. If the step-size matrix simplifies to identity, the here considered algorithm coincides with the normalised least-mean-squares (NLMS) algorithm. Then, (3.4) resembles the corresponding well known step-size bound that ensures stability in several senses, depending on the perspective of analysis and chosen ancillary assumptions [NN67; BA80a; BA80b; Abu82; Ber86; TF88; Hay02; Say03]. Moreover, (3.4) agrees with the step-size bounds for LMS algorithm with matrix step-sizes stated in [Men73, Theorem 4-4; MKK93; Dut00; BG02]. Finally, as choice (3.3) guarantees $\bar{\mu} < 1$, also the local passivity relations in [SR96] and the ℓ_2 -stability condition in [RC00] are satisfied.

By numerical experiments, three versions of the algorithm (2.8) with (3.2) are investigated in the sequel. The three variants are addressed by the superscripts (I) to (III), where

Algorithm I uses a constant step-size matrix $\mathbf{D}^{(I)}$, which contains random diagonal entries, drawn from a uniform distribution on the interval $(0, 1]$.

Algorithm II uses a varying diagonal step-size matrix $\mathbf{D}_k^{(II)}$, which only slightly differs from the identity matrix. For each iteration, its entries are independently chosen from a uniform distribution on the interval $(0.9, 1]$.

Algorithm III also employs a varying step-size matrix. Here, for each iteration k , M independent random values are generated from a constant pdf over the interval $(0, 1]$. They are then brought in descending order and used as diagonal elements of the corresponding step-size matrix $\mathbf{D}_k^{(III)}$. Thus, $d_1^{(III)}(k) \geq d_2^{(III)}(k) \geq \dots \geq d_M^{(III)}(k)$.

All of the involved systems have length $M = 10$. For the three algorithms, two sets of Monte Carlo simulations are performed, with $N_{\text{avg}} = 100$ runs each. For the first set, the systems are simply excited by complex-valued random vectors that are drawn from $\mathcal{N}_{\mathbb{C}}^M(\mathbf{0}, \mathbf{I})$ [MS00b]. For the second set of simulations, for each iteration k , the excitation vector is generated by a w.c. search, i.e., \mathbf{u}_k is chosen from a set of $N_{\text{w.c.}} = 10\,000$ random realisations such that parameter error distance $\|\tilde{\mathbf{w}}_k\|$ is maximised. This is a straightforward approach to approximatively maximise the parameter error increment $W(k)$ in (2.41). Further details on this procedure are described in Section 3.6. Figure 3.1 shows the results in terms of the estimated parameter mismatch (cf. (2.19)). On the left-hand side, the behaviour with purely random excitation is depicted. Clearly, all of the graphs show converging behaviour. A steady state is reached due to the limited precision of computation, as *no* noise $v(k)$ is added. On the first glance it may irritate that Algorithm I, in Figure 3.1(a), converges in the mean with a rather poor rate. However, this is not surprising as in the long run, the latter is dictated by the smallest entry in $\mathbf{D}^{(I)}$. Since the M diagonal elements $d_i^{(I)}$ are randomly drawn from interval $(0, 1]$, it is not surprising that the minimal value is likely to be considerably low in magnitude. Note that especially for the larger step-size, the variance is much larger compared to the other two algorithms. This is due to the stronger variations of the step-size matrix with respect to the whole ensemble.

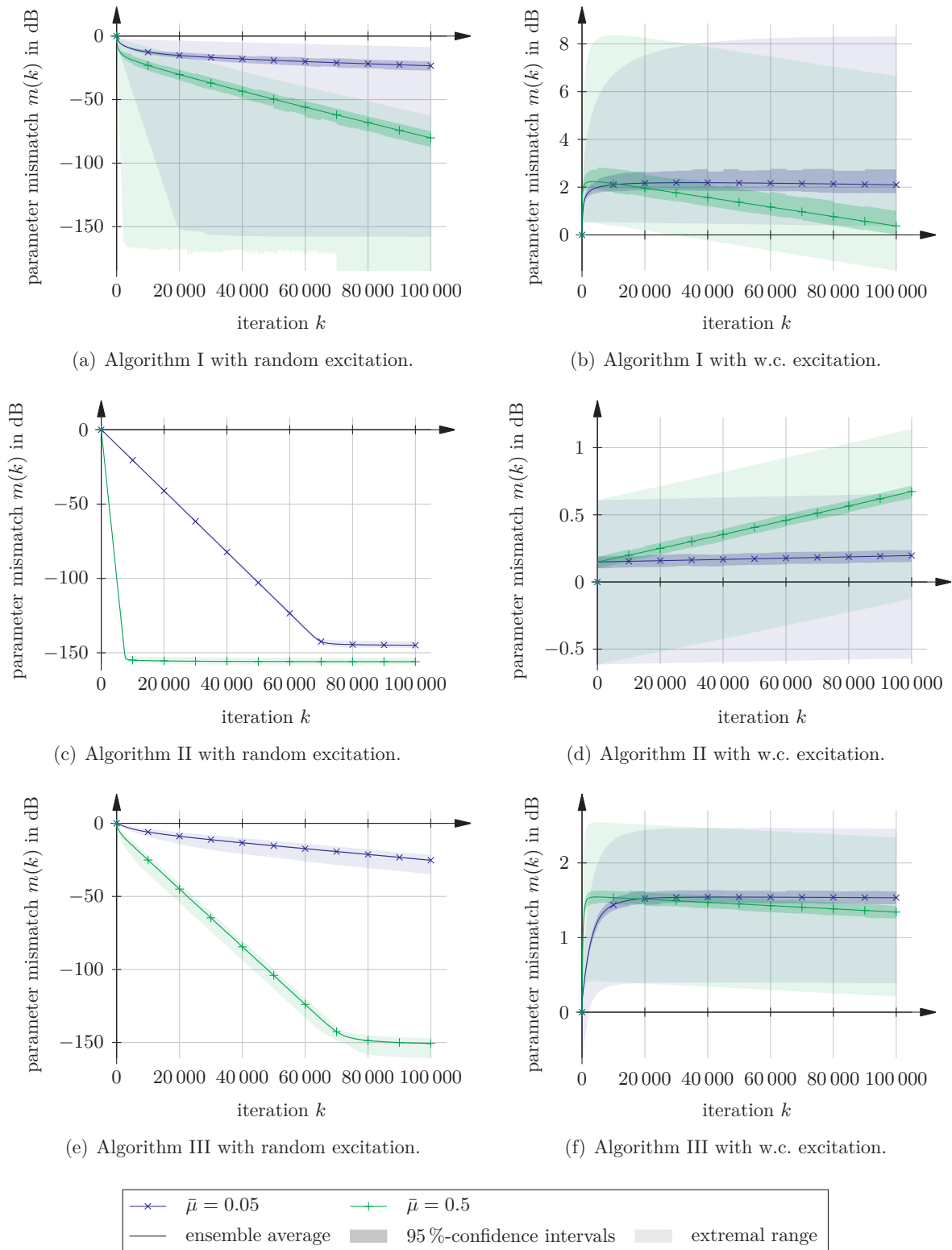


Figure 3.1: Learning behaviour of the three algorithms in terms of their estimated parameter mismatch $m(k)$ (cf. (2.19)), for the two step-size values in (3.3). The estimates for mean, confidence intervals, and extrema originate from simulations with 100 Monte Carlo runs.

Yet, the extrema show that some – or at least one – of the randomly chosen step-size matrices lead to a learning performance that even outperforms Algorithm II in Figure 3.1(c). The latter has a step-size matrix similar to identity, and thus, performs comparable to an NLMS algorithm. Finally, for random excitation, Algorithm III, in Figure 3.1(e), shows an average convergence rate between Algorithms I and II. As mentioned for Algorithm I, on the long run, the speed of convergence is dictated by the smallest entry of the step-size matrix. Since the latter is varying over all iterations, on average it appears to be effectively larger than for Algorithm I.

Let us now move our attention to the right column of Figure 3.1, i.e., the results for the three algorithms with w.c. excitation. Algorithm I, and III, in Figure 3.1(b) and Figure 3.1(f), respectively, seem to ensure boundedness, if not even some kind of convergence for the parameter error vector. Striking is the fact, that Algorithm II – the scheme which for random excitation lead to the best average convergence rates and a behaviour similar to the NLMS algorithm – now, gives reason to suspect some kind of diverging behaviour.

Supposing that the w.c. search leads to reliable insight regarding convergence, respectively, divergence, of the parameter error vector, the intriguing question is what property of the step-size matrix is the reason for the different behaviours. Comparing Algorithm I and II may tempt to blame the time-varying nature of $\mathbf{D}_k^{(\text{II})}$. However, as the step-size matrix of Algorithm III also varies with time, and indeed shows considerably stronger fluctuations of its elements than Algorithm II, the answer cannot be that simple. In fact, it can be observed – though not presented here – that under w.c. excitation, the increasing parameter mismatch of Algorithm II persists, even if the fluctuations of the step-size matrix are further reduced. A glimpse to the solution is given by the remaining difference between $\mathbf{D}_k^{(\text{II})}$ and $\mathbf{D}_k^{(\text{III})}$, which is that the latter keeps its elements in sorted order over all iterations k .

Summarising, the presented simulation results pose the questions:

1. Does Algorithm II in fact diverge under w.c. excitation?
2. Does the parameter error vector of the other two algorithms actually remain bounded?
3. What exactly makes the difference which decides on boundedness or divergence?

These questions are approached by Sections 3.2 to 3.4. First, Section 3.2 reviews results existing in literature. Out of these, it consults the three most relevant approaches, in order to find explanations for the behaviour observed in the afore simulation experiment. Then, Sections 3.3 and 3.4 follow a novel path to extend insight. By this, the three questions, can be revisited again in Section 3.4.4.

3.2 Related Work

Since gradient type algorithms have been studied for decades now, a wide range of literature is available on this topic. This section provides a detailed discussion of results relevant to this work. First, Sections 3.2.1 to 3.2.3 review three tightly related methods and applies them to the simulation experiment in Section 3.1. After that, Section 3.2.4 gives an overview of works that consider similar topics.

3.2.1 Condition Ensuring ℓ_2 -Stability

Gradient type algorithms with positive definite matrix step-size \mathbf{M}_k that use update rule (2.8), are considered in [RC00]. As a first step, it is shown that for a constant step-size matrix, the algorithm can be mapped to a conventional LMS algorithm. For the general case of varying step-size matrices,

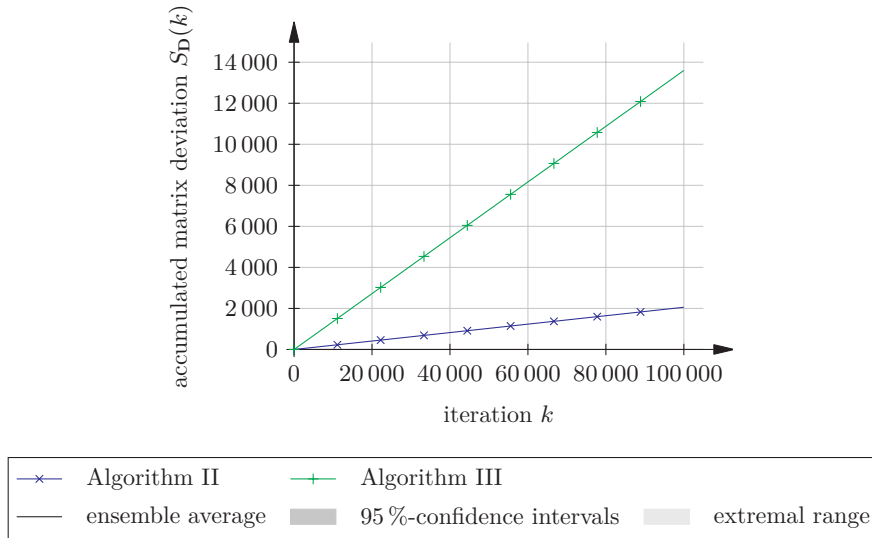


Figure 3.2: Accumulated matrix deviation $S_{\mathbf{D}}(k)$ (cf. (3.5)) for Algorithms II and III. Algorithm I is omitted, as here, the deviation trivially coincides with zero. Note that the graphs do *not* depend on the step-size, and are thus valid for both cases $\bar{\mu} \in \{0.05, 0.5\}$. Extrema and confidence intervals are included, however, they are too narrow to be distinguished from the average.

boundedness of the parameter error vector $\tilde{\mathbf{w}}_k$ and convergence of the update error $\tilde{e}(k)$ is basically tied to finite noise energy and convergence of the accumulated matrix deviation,

$$S_{\mathbf{M}}(k) = \sum_{l=0}^k \left\| \mathbf{M}_l^{\frac{1}{2}} - \mathbf{M}_{l+1}^{\frac{1}{2}} \right\|, \quad (3.5)$$

to a finite limit for $k \rightarrow \infty$. Alternatively, [SR96] derives corresponding local passivity relations and shows ℓ_2 -stability for constant step-size matrices. An extension to algorithms with non-Hermitian fixed step-size matrices is provided in [Rup11a].

Let us see what the just reviewed approach tells us about the algorithms from the simulation experiment in Section 3.1. Accordingly, Algorithm I is ensured to be ℓ_2 -stable which – as no noise at all is added – also implies boundedness of the parameter error vector. For PE (cf. Section 2.2.2), even convergence can be concluded. Clearly, as step-size matrix $\mathbf{D}^{(I)}$ is fixed, the accumulated matrix deviation in (3.5) is identical to zero. For Algorithms II and III, the situation is completely different. Both, $\mathbf{D}_k^{(II)}$ and $\mathbf{D}_k^{(III)}$, keep changing over all iterations. Not very surprising is the evaluation of $S_{\mathbf{D}^{(II)}}(k)$ and $S_{\mathbf{D}^{(III)}}(k)$, depicted in Figure 3.2. Obviously, in either case, it grows unbounded, entailing that based on this theory, no conclusive statement regarding convergence or stability can be achieved for Algorithms II and III.

3.2.2 Lyapunov Based Convergence Condition

Stability and convergence of algorithms belonging to the class that here addressed by the term “asymmetric algorithms”, specifically, for the LMS algorithm with matrix step-size, has been investigated for decades. One early work with a strong focus on this topic is [Men73]¹. Especially, the deterministic analysis of uniform (asymptotic) stability in the large, respectively, convergence of

¹ In [Men73, pp. 199f.], algorithms of the form (2.8) with a step-size matrix different from identity, are referred to as second-order gradient algorithms instead of the here used term asymmetric algorithms.

the parameter error vector, presented in Chapter 4 [ibid.] – and specifically Section 4.4.5 [ibid.] – are closely related to the contents of this chapter. Accordingly, based on the “Second Method of Lyapunov”, convergence of the parameter error vector towards $\mathbf{0}$ is ensured almost always², for a step-size normalised according to (3.2) and obeying (3.4), if the step-size matrix

- is diagonal, i.e., of the structure in (3.1),
- is positive definite, i.e., $d_i(k) > 0$ for $i \in \{1, \dots, M\}$, and $k \geq 0$,
- contains at least one main diagonal element $d_{\hat{j}}(k)$, with index $\hat{j} \in \{1, \dots, M\}$, that shows for all $k \geq 0$, smaller relative fluctuations than the remaining elements, i.e., for $i \in \{1, \dots, M\} \setminus \{\hat{j}\}$,

$$\frac{d_{\hat{j}}(k+1) - d_{\hat{j}}(k)}{d_{\hat{j}}(k)} \leq \frac{d_i(k+1) - d_i(k)}{d_i(k)} \quad \Leftrightarrow \quad \frac{d_{\hat{j}}(k+1)}{d_{\hat{j}}(k)} \leq \frac{d_i(k+1)}{d_i(k)}. \quad (3.6)$$

From the right-hand side of (3.6), since all the diagonal elements are positive, a direct consequence is that for any $K > 0$,

$$\prod_{k=0}^{K-1} \frac{d_{\hat{j}}(k+1)}{d_{\hat{j}}(k)} \leq \prod_{k=0}^{K-1} \frac{d_i(k+1)}{d_i(k)} \quad \Rightarrow \quad \frac{d_{\hat{j}}(K)}{d_{\hat{j}}(0)} \leq \frac{d_i(K)}{d_i(0)}. \quad (3.7)$$

Hence, also globally, the relative fluctuations of $d_{\hat{j}}(k)$ have to be smaller than those of the remaining $d_i(k)$.

Again, an interesting point is, what insight this theory provides to the three algorithms in Section 3.1. As the step-size matrix of Algorithm I is diagonal, positive definite, and constant, it is trivially found to satisfy all of the above required conditions. Hence, almost always convergence of its parameter error vector can be concluded. For Algorithm II and III, the step-size matrices are also diagonal and positive definite. The implications of the third of the above requirement, however, are not that obvious. For assessment, the data that were collected in the simulation experiments conducted for Section 3.1, are consulted again. In fact, only one of the two considered normalised step-sizes $\bar{\mu}$ (cf. (3.2)) has to be taken into account, as both of them satisfy (3.4), and do not further affect (3.6). The evaluation is done in two steps. First, for each of the 100 Monte Carlo runs and for each iteration k , index \hat{j} is detected that locally satisfies (3.6). Moreover, for each Monte Carlo run, the number of consecutive iterations is determined, for which \hat{j} does not change – in the sequel abbreviated by the term *run length*. As an extension, the whole range of iterations is split up into 10 blocks of the same length 10 000, in order to roughly monitor whether the observed behaviour changes with progress of iterations. Stacking the individual results for all of these 10 blocks on top of each other, the histograms depicted in Figure 3.3 are obtained. The height of the histogram bars shows, in % of all iterations and all Monte Carlo runs, how often each of the dimensions $\{1, \dots, M\}$ coincides with \hat{j} . As the separate Monte Carlo runs are not distinguished, this information implicitly averages over the whole ensemble and is thus, on its own, only of restricted value. For this reason, also the maximum run lengths for each of the blocks is shown – and encoded by different colours and hatching. As a consequence, it is revealed that for Algorithm II, the index \hat{j} changes at least after every second iteration, and for Algorithm III, at least after every fifth iteration. Accordingly, both of them do not satisfy (3.6), which inhibits a conclusive answer regarding their convergence.

² The additional phrase “almost always” addresses here the fact that permanent orthogonality among the parameter error vector and the excitation vector causes the algorithm to remain in the same state. In this work, such a situation is later on precluded by assuming non-stalling adaptation (cf. Assumption 3.1).

Only a hint may be found by the different statistics that are approximately revealed by the differing shapes of the two histograms.

3.2.3 Divergence Caused by Non-Persistent Excitation

Of similarly high relevance for the analyses in this chapter is [Set92], which investigates local exponential stability of gradient type algorithms with memoryless, sign preserving non-linear modifications of the regression vector and/or the update error. The idea therein is to consider an auxiliary algorithm that uses recursion (2.18), however, with the mapping matrix \mathbf{B}_k replaced by a sliding average. Accordingly, if the such obtained autonomous algorithm is exponentially stable, based on the slow time variation lemma [SAJ89, Lemma 3], exponential stability of the original nonautonomous algorithm can be concluded. In analogy to w.c. excitation considered in this work (cf. Section 3.3.3), for a non-linear memoryless map among the excitation vector and the regression vector, the existence of excitation sequences that lead to an increase of the parameter error distance is stated [Set92, Lemma 4]. This is shown, based on the fact that then, it is always possible to find excitation sequences that cause the sliding average of the excitation matrix $\mathbf{U}_{\mathbf{M},k}^{(K)}$ in (2.26) to have at least one eigenvalue with negative real part. As a complement to the results on gradient type algorithms with memoryless non-linearities, [SAJ89] considers the case of modifications imposed to the regression vector and/or the update error that are linear but introduce memory.

The rest of this section, studies the insights that this approach provides to Algorithms I–III from Section 3.1. The evaluation is based on the corresponding simulation data and resorts to the brief description of PE, presented in Section 2.2.2. Accordingly, special attention has to be given to the real parts of the eigenvalues of excitation matrix $\mathbf{U}_{\mathbf{D},k}^{(K)}$. For convenience, the definition of the latter, found in (2.26), is repeated below³,

$$\mathbf{U}_{\mathbf{D},k}^{(K)} = \sum_{j=k-K+1}^k \mathbf{D}_j \mathbf{u}_j^* \mathbf{u}_j^T, \quad (3.8)$$

where depending on the considered algorithm, the step-size matrix is selected from (cf. Section 3.1)

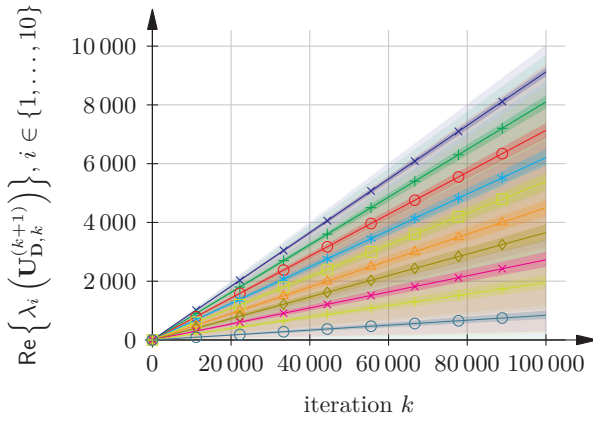
$$\mathbf{D}_k \in \left\{ \mathbf{D}^{(\text{I})}, \mathbf{D}_k^{(\text{II})}, \mathbf{D}_k^{(\text{III})} \right\}. \quad (3.9)$$

In a first step, scope K of the running average in (3.8) is chosen, such that it grows with iteration step k , i.e., $K = k + 1$. By this, for each iteration step, the average over the whole iteration history is taken into account. This obviously, does not comply with Definition 2.1, as there, scope K is required to be constant. Nevertheless, without knowledge of an adequate choice, this seems reasonable for a first approach. Figure 3.4 depicts the corresponding results, for all of the three algorithms and for both types of excitation – random and w.c. excitation. However, for reasons of visual clarity, only step-size $\bar{\mu} = 0.5$ is included, for the other step-size value, the results do not show any qualitatively important difference. The individual graphs represent the real parts of the eigenvalues of excitation matrix $\mathbf{U}_{\mathbf{D},k}^{(K)}$, sorted such that

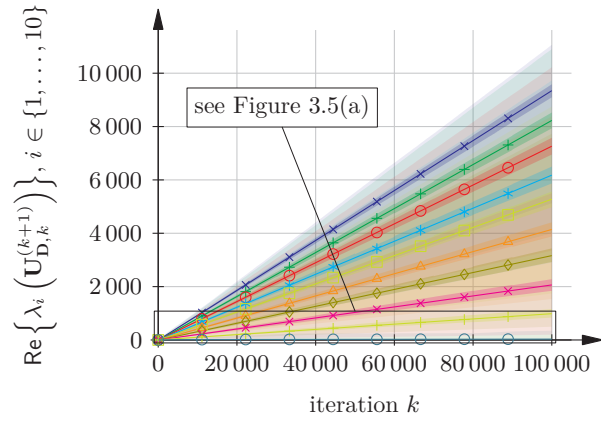
$$\operatorname{Re} \left\{ \lambda_1 \left(\mathbf{U}_{\mathbf{D},k}^{(K)} \right) \right\} \geq \operatorname{Re} \left\{ \lambda_2 \left(\mathbf{U}_{\mathbf{D},k}^{(K)} \right) \right\} \geq \dots \geq \operatorname{Re} \left\{ \lambda_M \left(\mathbf{U}_{\mathbf{D},k}^{(K)} \right) \right\}. \quad (3.10)$$

In the left column of Figure 3.4, representing the case of random excitation, all such real parts

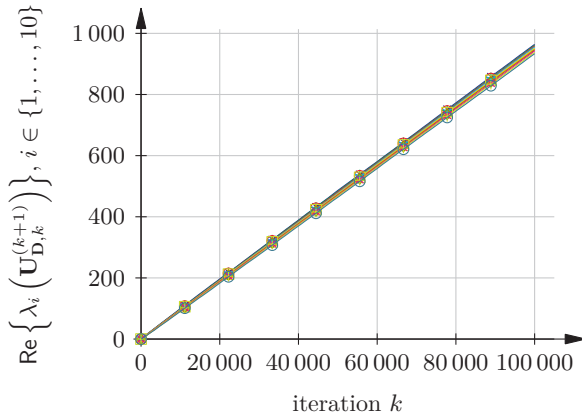
³ In contrast to (2.26), the step-size matrix in (3.8) is denoted by \mathbf{D}_k , as in this context, the latter is known to be of diagonal structure.



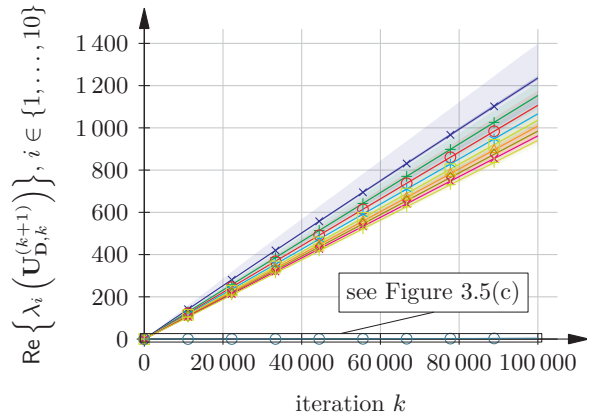
(a) Algorithm I with random excitation.



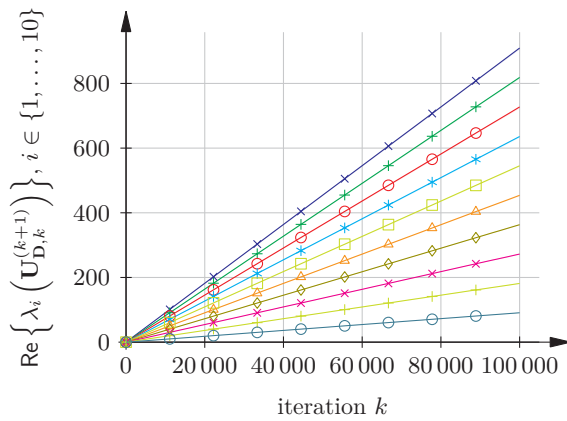
(b) Algorithm I with w.c. excitation.



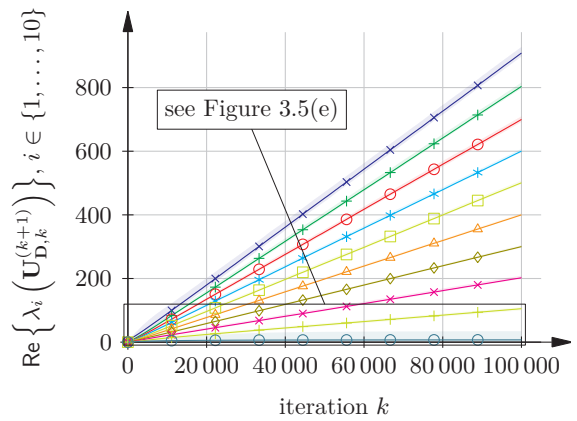
(c) Algorithm II with random excitation.



(d) Algorithm II with w.c. excitation.



(e) Algorithm III with random excitation.



(f) Algorithm III with w.c. excitation.

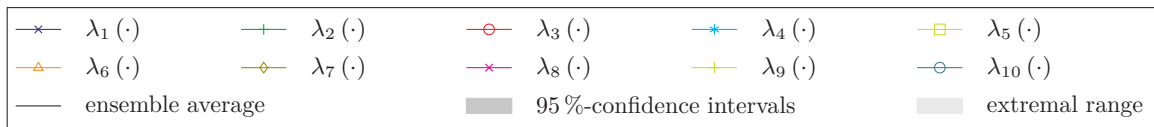
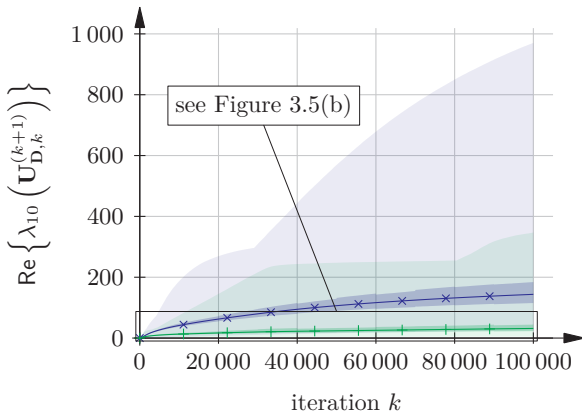
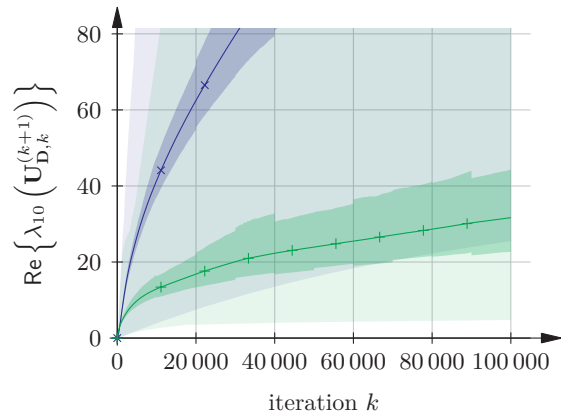


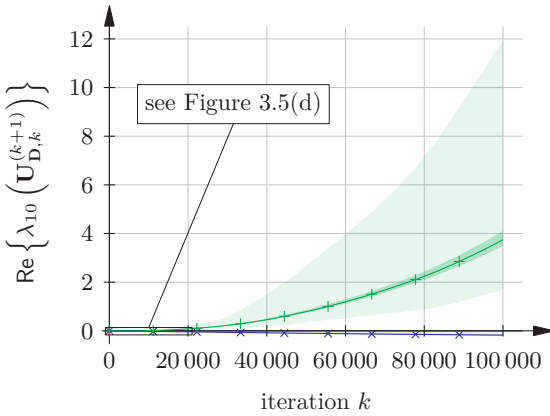
Figure 3.4: Real part of the eigenvalues of excitation matrix $\mathbf{U}_{D,k}^{r(k+1)}$ defined in (2.26). Since the superscript grows with iteration k , the matrix actually incorporates the whole history of excitation, instead of only a restricted moving average. For reasons of clarity, only the results for $\bar{\mu} = 0.5$ are depicted.



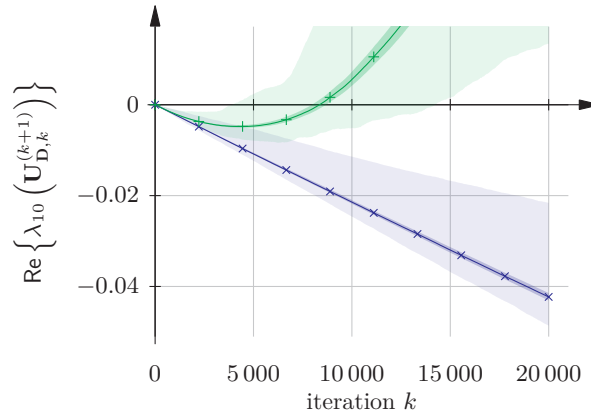
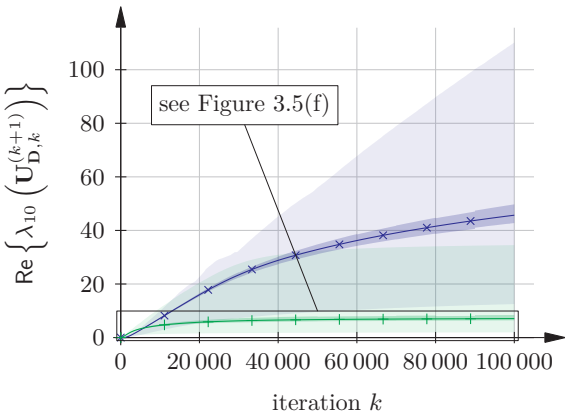
(a) Algorithm I with w.c. excitation – zoom level 1.



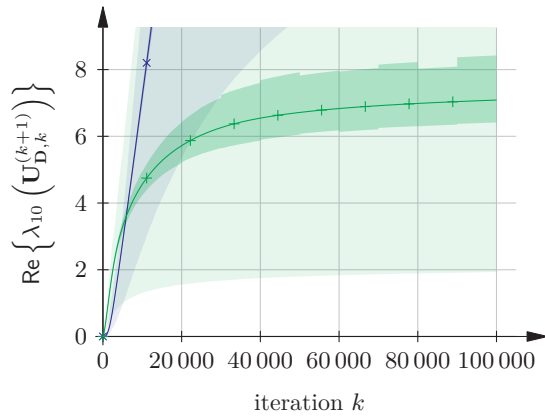
(b) Algorithm I with w.c. excitation – zoom level 2.



(c) Algorithm II with w.c. excitation – zoom level 1.

(d) Algorithm II with w.c. excitation – zoom level 2. *Differently scaled abscissa!*

(e) Algorithm III with w.c. excitation – zoom level 1.



(f) Algorithm III with w.c. excitation – zoom level 2.

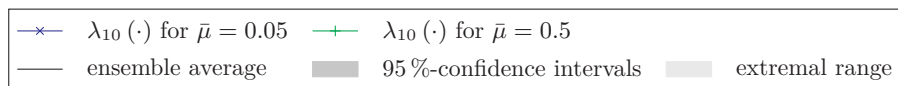


Figure 3.5: Minimum real part of the eigenvalues of excitation matrix $\mathbf{U}_{\mathbf{D},k}^{(k+1)}$ defined in (2.26). The graphs show two different levels of magnification, omitting all eigenvalues with a real part larger than that of $\lambda_{10}(\mathbf{U}_{\mathbf{D},k}^{(K)})$. Here, both step-sizes, $\bar{\mu} \in \{0.05, 0.5\}$, are considered again.

of Algorithm II and III are inevitably positive. Hence, PE is ensured. For Algorithm I, this is visually hard to decide, however, anticipating the observation found in Figure 3.5 further down, the corresponding real parts are also verified to be larger than zero. The right-hand side, which contains the results for w.c. excitation, reveals that all but the last eigenvalues have positive real parts. In order to decide on the remaining eigenvalues $\lambda_{10}(\mathbf{U}_{\mathbf{D},k}^{(K)})$, for all algorithms a more detailed look is required.

Figure 3.5 presents two scales of magnification. As now the number of depicted graphs has reduced noteworthy, the second step-size, $\bar{\mu} = 0.05$, is temporarily included again for reference. The right column finally reveals the desired insight. As anticipated before, for Algorithm I all of the respective eigenvalues are in the right complex half-plane. The same applies to Algorithm III. Hence, both of them are persistently excited. For Algorithm II, for the larger step-size, clearly, a negative real part occurs. In case of the larger step-size, however, after a short period of approximately 14 000 iterations, for all Monte Carlo runs, the real parts have turned from negative to positive, and seem to proceed with this trend of growth. This observation hints us with a possible choice of a constant value for scope K , in order to evaluate the actual running average in (3.8). Hence, as a final step of evaluation, the latter expression is calculated for three different values of K , i.e., $K \in \{10\,000, 15\,000, 20\,000\}$. Figure 3.6⁴ shows the results with w.c. excitation and normalised step-size $\bar{\mu} = 0.5$. For reference, it additionally includes the results obtained for Algorithm III. Accordingly, it can be identified that for all Monte Carlo runs, Algorithm II is persistently excited for $K \geq 20\,000$. For Algorithm III this holds for all three values of K .

This evaluation reveals that the diverging effect observed for Algorithm II under w.c. excitation, observable in Figure 3.1(d), is for step-size $\bar{\mu} = 0.5$ *not* caused by insufficient persistency of excitation. For the second step-size $\bar{\mu} = 0.05$, the graphs are not that conclusive. However, it is expected that the same behaviour occurs. Yet, due to the smaller step-size, with a considerably lower rate of progress.

3.2.4 Further Related Methods and Results

The SR-LMS [Luc65, p. 557; Mos70; CM80] uses a regression vector that only contains $\{\pm 1\}$, as its elements are obtained by reducing the individual entries of the excitation vector to their signs. This algorithm is a well known and conceptually simple member out of the class of the here considered asymmetric algorithms. Due to its low computational complexity, it has been focus of several works that also point out the existence of excitation sequences that provoke divergence of the parameter error vector. Specifically, [CM81] briefly mentions geometric arguments that are related to the ones visualised in Figure 3.8 further down. [SMA+88, Theorem 2] confirms this insight based on the theory of persistence of excitation from a deterministic as well as from a stochastic point of view. In his correspondence to [CM81], [Ber85] argues that in a Gaussian regime convergence of the parameter error vector is ensured. [BKS93] extends the stochastic analysis by considering the impact of the pdf that underlies the excitation process.

A problem that is also closely related to the considerations in this chapter is the stability of discrete-time switched linear systems [Ant00; Mar06; LA09]. In this context, again a recursion of the form in (2.18) is studied. Then, $\tilde{\mathbf{w}}_k$ does not refer to a parameter error vector but instead, it has the meaning of a state vector. Mapping matrix \mathbf{B}_k varies with iteration index k , however, it can only assume one out of a finite set of discrete modes. The mapping of each of these modes to the respective iteration instant, i.e., the selection of the active mode, is determined by a switching signal.

⁴ Note that in both subfigures, visualisation of the maxima is suppressed. This is done in order not to overload them and since the maxima are not relevant in this context.

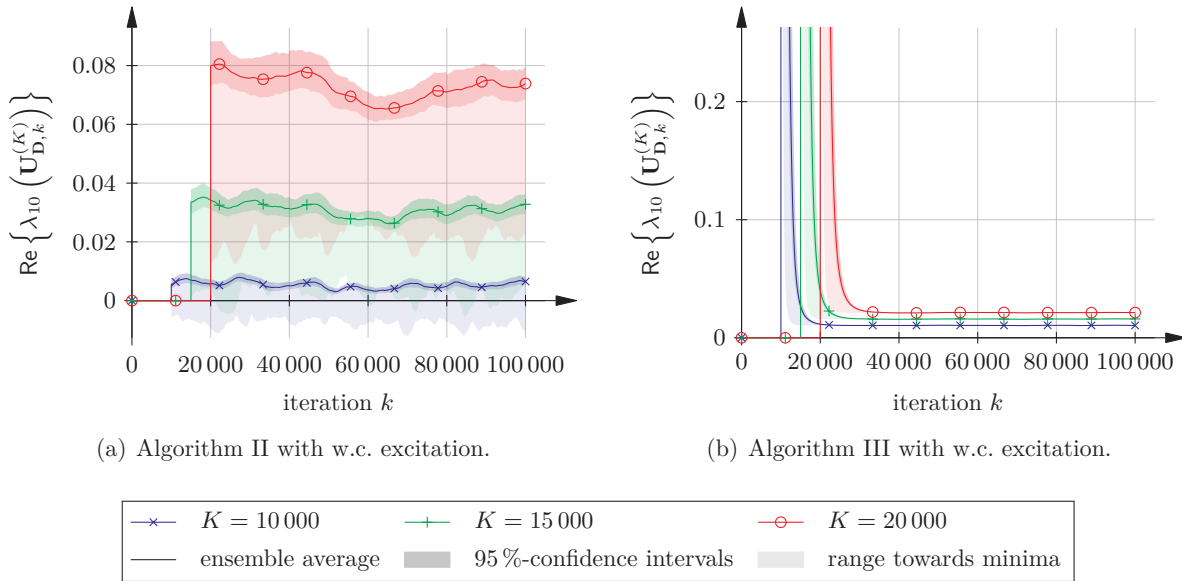


Figure 3.6: Graphical evaluation of persistency of excitation under w.c. excitation, for Algorithms II and III of the simulation experiments in Section 3.1. Depicted is the eigenvalue of excitation matrix $\mathbf{U}_{\mathbf{D},k}^{(K)}$ (cf. (3.8)) with smallest real part, for the three scopes $K \in \{10\,000, 15\,000, 20\,000\}$. In all cases, the step-size is set to $\bar{\mu} = 0.5$. *In contrast to other figures, here, only the ensemble minima are included. Maxima are excluded, for reasons of visual clarity, and since they do not provide any further insight with respect to PE.*

As pointed out in [LA09], also in this situation, divergence of the state vector may occur, even if all autonomous recursions that correspond to the individual modes of \mathbf{B}_k are exponentially stable. In this context, one approach of stability analysis investigates the spectral radius of all possible matrix products that can be composed by selecting a certain number of modes [LA05; LA09]. Another method considers a modified recursion, where the mapping matrix can assume any value out of the convex hull that contains all of the original discrete modes. Either of these stability analysis does not seem applicable to the algorithms that are focussed in this chapter, as here, infinite many non-discrete modes exist.

For specific algorithms, belonging to the class of asymmetric algorithms, several studies on convergence have been pursued. Most of them are based on statistical considerations, e.g., [MKK93; Dut00] for the PNLMS algorithm with fixed and varying step-size matrix, respectively, and [dBBC05; dBB09] for the PAP algorithm. A deterministic analysis of the latter, in terms of ℓ_2 -stability, can be found in [Rup11b]. Moreover, [RS95; RS96c] investigate the Gauß-Newton algorithm, respectively, the RLS algorithm, and derive conditions for ℓ_2 -stability based on the small gain theorem.

A topic that is related to expanding, respectively, diverging behaviour of the parameter error vector, studied in this chapter, is addressed in literature by the term “parameter drift” [GMW82; Cio87; SLJB86; LSR93; Nas99, pp. 211ff.; Say03, p. 428]. For the LMS algorithm – without matrix step-size – this phenomenon is observed only for specific excitation sequences and may be caused due to several reasons,

1. finite precision and related bias due to non-odd quantiser functions [GMW82; Cio87; Nas99],
2. dynamics of the reference system that are not covered by the system model [RVAS81; IK84],
3. positive feedback in the error path, e.g., if the system model is an infinite impulse response (IIR) filter and the feedback filter component does not satisfy the strict positive realness (SPR) condition [LSR93; see, e.g., SK95, for details on SPR],

4. the existence of biased additive noise [Nas99], or even unbiased and finite energy noise, if the excitation sequence contains certain components that decay faster than the noise sequence [SLJB86].

What is remarkable and pointed out by [GMW82, p. 1818; SLJB86, p. 874; LSR93, p. 585], is the fact that even if parameter drift occurs and tends towards infinity, this is *not* necessarily observable in the a priori error, which in fact still may converge towards zero, respectively, a steady state power that agrees with the present noise level.

The expanding behaviour of the parameter error vector for asymmetric algorithms show some distinguishing differences to the above listed phenomena that are observed in the context of parameter drift:

- ad 1. As the derivations in this chapter are all obtained analytically, effects caused by finite precision effects can be neglected. The obtained statements are in fact independent from any numerical representation.
- ad 2. One of the strong assumptions adopted in this work, is that the structure of the chosen system model perfectly agrees with the actual structure of the reference system (cf. Section 2.1). Thus, the existence of unmodelled dynamics can be discarded.
- ad 3. The here analysed gradient type algorithms are all assumed to operate on systems that do not introduce any feedback. Hence, e.g., adaptive IIR filters based on either the equation error method, or the output error method [Hay02] are not covered. This entails that here, a positive feedback in the error path cannot occur.
- ad 4. Most of the here obtained results assume the absence of any noise. Note that also the simulation experiments in Section 3.1 exclude any disturbances. Consequently, parameter drift phenomena that are caused by noise cannot arise.

It is emphasised that at the time of this being written, it is not completely resolved how agreement can be established among the divergence behaviour observed in this chapter and the conditions on PE in [SLJB86; Set92]. Yet there is evidence that insufficient excitation – or any of the other applicable parameter drift mechanism described above – cannot completely explain the occurrence of the here studied effects. This becomes clear as here, the parameter error distance is found to grow exponentially (cf., e.g., Figure 3.1(d)), whereas parameter drift due to insufficient excitation or additive noise, typically leads to increase rates that are much lower [SLJB86; Nas99].

3.3 Mapping Matrix \mathbf{B}_k of Asymmetric Algorithms

This section, investigates the eigenvalues, the singular values, and the singular vectors of mapping matrix $\mathbf{B}_k \in \mathbb{C}^{M \times M}$ in (2.16) that is specific for asymmetric algorithms. This establishes the basis for the rest of this chapter, which thoroughly investigates internal divergence provoking mechanisms of asymmetric algorithms, based on geometric considerations. At this point, no specific relation among the excitation vector and the regression vector is assumed. It is emphasised that the obtained findings *do not* depend on any step-size matrix as introduced in (2.9), and as it is the case in Section 3.1. Existence of a step-size matrix will be taken into account from Section 3.4.2 on.

Initially, for reasons of convenience, effective step-size $\alpha(k) \in \mathbb{C}$ and correlation coefficient $\rho(k) \in \mathbb{C}$, $0 \leq |\rho(k)| \leq 1$ are introduced according to

$$\alpha(k) \triangleq \mu(k) \|\mathbf{u}_k\| \|\mathbf{x}_k\|, \quad (3.11)$$

$$\rho(k) \triangleq \frac{\mathbf{x}_k^\top \mathbf{u}_k^*}{\|\mathbf{u}_k\| \|\mathbf{x}_k\|}, \quad (3.12)$$

together with the complex argument amongst them,

$$\varphi_{\alpha\rho^*}(k) \triangleq \arg(\alpha(k)\rho^*(k)) = \arg\left(\frac{\alpha(k)}{\rho(k)}\right). \quad (3.13)$$

3.3.1 Eigenvalues of Mapping Matrix \mathbf{B}_k

From (2.16) it can be directly verified that one eigenvector $\mathbf{q}_{1,k}$ of mapping matrix \mathbf{B}_k is given by the direction of \mathbf{x}_k^* , corresponding to the eigenvalue

$$\lambda_1(k) = 1 - \mu(k) \mathbf{u}_k^\top \mathbf{x}_k^* = 1 - \alpha(k) \rho^*(k). \quad (3.14)$$

The remaining $M - 1$ eigenvectors $\mathbf{q}_{i,k} \perp \mathbf{x}_k^*$, $i = 2, \dots, M$ span the eigenspace belonging to eigenvalue $\lambda_2(k) = 1$ that has (algebraic and geometric) multiplicity $M - 1$ [Bit84]. Hence, due to the structure of \mathbf{B}_k , for $M > 1$, its spectral radius can never be smaller than one. However, as given in the following lemma, it can at least be ensured not to exceed a value of one.

Lemma 3.1: Condition for a Unit Spectral Radius, i.e., $S(\mathbf{B}_k) = 1$

For $M > 1$, the spectral radius of mapping matrix \mathbf{B}_k in (2.16) is equal to one, iff

$$|\varphi_{\alpha\rho^*}(k)| \leq \frac{\pi}{2}, \quad \text{and} \quad |\alpha(k)| |\rho(k)| \leq 2 \cos(\varphi_{\alpha\rho^*}(k)). \quad (3.15)$$

Proof. Since all eigenvalues of \mathbf{B}_k are equal to one except from $\lambda_1(k)$, bounding its magnitude by one is necessary and sufficient for a spectral radius of one. The conditions in (3.15) are obtained from $|\lambda_1(k)| = |1 - \alpha(k)\rho^*(k)| \leq 1$. \square

As discussed in Section 2.3.2, under the assumption of a constant mapping matrix, i.e., $\mathbf{B}_k \equiv \mathbf{B}$, Lemma 3.1 does not ensure convergence but it at least excludes the possibility of an unbounded growth of the parameter error vector in (2.18). Note that the conditions in (3.15) cause product $\alpha(k)\rho^*(k)$ to be contained inside, or on, a circle in the complex plane, with radius 2, centred at $1 + j0$. Specifically, in the common case of a real-valued positive step-size, this entails that the correlation coefficient has to be non-negative, or equivalently – from a geometric perspective – that the angle enclosed by the excitation vector and the regression vector is required to be non-obtuse.

Note that Lemma 3.1 is assumed to be satisfied throughout the whole chapter. This makes sense, as the goal here is the investigation of hidden diverging behaviour. This in turn would be a trivial task if Lemma 3.1 is violated, as then, divergence is guaranteed.

3.3.2 Singular Value Decomposition of \mathbf{B}_k

This section resembles and extends the findings of [DR09a]. Below, the notation introduced in Section 2.3.1, and especially, (2.28), is adopted. Moreover, for the sake of readability, *iteration*

index k is suppressed. The general structure of the mapping matrix for asymmetric algorithm in (2.16) leads to the following expressions for the Gramian of \mathbf{B} , respectively its Hermitian,

$$\mathbf{B}^H \mathbf{B} = \mathbf{I} + |\mu|^2 \|\mathbf{x}\|^2 \mathbf{u}^* \mathbf{u}^T - (\mu^* \mathbf{u}^* \mathbf{x}^T + \mu \mathbf{x}^* \mathbf{u}^T), \quad (3.16)$$

$$\mathbf{B} \mathbf{B}^H = \mathbf{I} + |\mu|^2 \|\mathbf{u}\|^2 \mathbf{x}^* \mathbf{x}^T - (\mu^* \mathbf{u}^* \mathbf{x}^T + \mu \mathbf{x}^* \mathbf{u}^T). \quad (3.17)$$

Obviously, any vector \mathbf{v} orthogonal to the hyperplane spanned by the two vectors \mathbf{x}^* and \mathbf{u}^* , i.e.,

$$\mathbf{v} \perp \mathcal{S}_{\mathbf{u}^*, \mathbf{x}^*}, \quad \text{with } \mathcal{S}_{\mathbf{u}^*, \mathbf{x}^*} \triangleq \text{span} \{\mathbf{x}^*, \mathbf{u}^*\}, \quad (3.18)$$

leads to

$$\mathbf{B}^H \mathbf{B} \mathbf{v} = \mathbf{B} \mathbf{B}^H \mathbf{v} = \mathbf{v}, \quad (3.19)$$

which entails that 1 is singular value of \mathbf{B} . More precisely, since the orthogonal complement $\mathcal{S}_{\mathbf{u}^*, \mathbf{x}^*}^\perp$ of $\mathcal{S}_{\mathbf{u}^*, \mathbf{x}^*}$ has dimension $M - 2$, it is always possible to identify $M - 2$ mutually orthogonal vectors $\mathbf{v}_i \in \mathcal{S}_{\mathbf{u}^*, \mathbf{x}^*}^\perp$ that satisfy (3.19). Obviously, such a set of vectors forms an orthonormal basis for $\mathcal{S}_{\mathbf{u}^*, \mathbf{x}^*}^\perp$. From (3.19), it also becomes clear that if \mathbf{v} is a right-sided singular vector of \mathbf{B} , it is identical to the corresponding left-sided singular vector of \mathbf{B} , and vice versa. Consequently, matrix \mathbf{B} has one unit singular value with multiplicity $M - 2$ and singular vectors – both, left and right-sided – contained in $\mathcal{S}_{\mathbf{u}^*, \mathbf{x}^*}^\perp$, i.e.,

$$\sigma_i = 1, \quad \mathbf{r}_i = \mathbf{t}_i \in \mathcal{S}_{\mathbf{u}^*, \mathbf{x}^*}^\perp \perp \mathcal{S}_{\mathbf{u}^*, \mathbf{x}^*}, \quad i \in \{3, \dots, M\}, \quad (3.20)$$

where, w.o.l.o.g., it is assumed that the corresponding indices cover the last $M - 2$ values of the whole index range. Note that further down, in the context of (3.30), this assumption is found to slightly violate the convention introduced in (2.29). However, as the latter is not of central importance in this section, the level of confusion should be tolerable.

The two remaining singular vectors, \mathbf{r}_1 and \mathbf{r}_2 , respectively, \mathbf{t}_1 and \mathbf{t}_2 , corresponding to singular values σ_1 and σ_2 , are all completely contained in $\mathcal{S}_{\mathbf{u}^*, \mathbf{x}^*}$. Thus, they can be expressed as a linear combination of unit vectors $\mathbf{e}_{\mathbf{u}}$ and $\mathbf{e}_{\mathbf{x}}$, having the direction as \mathbf{u} and \mathbf{x} , respectively, i.e.,

$$\mathbf{r}_i = a_i \mathbf{e}_{\mathbf{u}}^* + b_i \mathbf{e}_{\mathbf{x}}^*, \quad \mathbf{t}_i = b_i^* \mathbf{e}_{\mathbf{u}}^* + a_i^* \mathbf{e}_{\mathbf{x}}^*, \quad (3.21)$$

with $i \in \{1, 2\}$, and the complex-valued coefficients a_i, b_i that typically both depend on the here suppressed iteration index k . The similar structure of the left and right-sided singular vectors in (3.21), is a direct consequence of the fact that (3.17) can be obtained from (3.16) by simply swapping \mathbf{u} and \mathbf{x} , and vice versa. Since $\mathbf{B} \mathbf{B}^H \mathbf{r}_i = \sigma_i^2 \mathbf{r}_i$ has to be true for arbitrary \mathbf{u} and \mathbf{x} , and since $\|\mathbf{r}_i\| \triangleq 1$ – ensuring $\mathbf{r}_i \neq \mathbf{0}$ – with (3.16), a comparison of coefficients yields

$$\sigma_i^2 = 1 + \frac{|\alpha|^2}{2} - \text{Re} \{ \alpha \rho^* \} + (-1)^{i-1} \sqrt{\left(\frac{|\alpha|^2}{2} - \text{Re} \{ \alpha \rho^* \} \right)^2 + |\alpha|^2 (1 - |\rho|^2)}, \quad (3.22)$$

$$a_i = \frac{|\alpha| \exp \left(j \frac{1}{2} \text{arc} (c_i) \right)}{\sqrt{(1 - \sigma_i^2)^2 + |\alpha|^2 (1 - |\rho|^2)}}, \quad (3.23)$$

$$b_i = a_i c_i, \quad (3.24)$$

with

$$c_i \triangleq \frac{1 - \sigma_i^2}{\alpha^*} - \rho. \quad (3.25)$$

In the real-valued case, the term $\frac{1}{2} \arccos(c_i)$ in (3.23) assumes either⁵ 0 or $\frac{\pi}{2}$. Hence, in the latter case, the above expressions would result in complex-valued singular vectors. This can be circumvented, if for $c_i < 0$, the singular vectors are properly phase-compensated according to (note that in any case, $|c_i| = \sigma_i$)

$$\mathbf{r}_i = |a_i| (\mathbf{e}_{\mathbf{u}}^* - \sigma_i \mathbf{e}_{\mathbf{x}}^*), \quad \mathbf{t}_i = |a_i| (\sigma_i \mathbf{e}_{\mathbf{u}}^* - \mathbf{e}_{\mathbf{x}}^*). \quad (3.27)$$

The justification for this modification is based on the general structure of the SVD in (2.28). As with a diagonal matrix of the form

$$\mathbf{\Psi} \triangleq \text{diag} \left\{ \exp(j\psi_i) \right\}_{i=1}^M, \quad (3.28)$$

containing arbitrary angles $\psi_i \in (-\pi, \pi]$ – which may depend on the here suppressed iteration index k – the SVD in (2.28) leads to [HJ13]

$$\mathbf{B} = \mathbf{R}\mathbf{\Sigma}\mathbf{T}^H = \mathbf{R} \underbrace{\mathbf{\Psi}\mathbf{\Psi}^H}_{\mathbf{I}} \mathbf{\Sigma}\mathbf{T}^H = \mathbf{R}\mathbf{\Psi}\mathbf{\Sigma}\mathbf{\Psi}^H\mathbf{T}^H = \underbrace{\mathbf{R}\mathbf{\Psi}}_{\mathbf{R}'} \mathbf{\Sigma} \underbrace{(\mathbf{T}\mathbf{\Psi})^H}_{\mathbf{T}'}. \quad (3.29)$$

Thus, the phase-rotated unitary matrices \mathbf{R}' and \mathbf{T}' are also adequate modal matrices for the SVD.

Note that, w.o.l.o.g., (3.22) defines the singular values, σ_1 and σ_2 , to be obtained by the positive and the negative square-root, respectively. It can easily be verified that this entails

$$\sigma_1 \geq \sigma_j = 1 \geq \sigma_2, \quad \text{with } j = 3, \dots, M, \quad (3.30)$$

which allows to identify that σ_1 and σ_2 coincide with the maximum and the minimum singular value, respectively, i.e., $\sigma_{\max} = \sigma_1$ and $\sigma_{\min} = \sigma_2$. As already pointed out afore, this violates the index ordering introduced in (2.29). However, $\sigma_1 \geq \sigma_2$ still holds and as in the sequel, the unit singular values are only of peripheral interest, the here chosen indexing sacrifices consistency in favour of readability.

The dependency of the two non-unit singular values, given by (3.22), with respect to the effective step-size, the correlation coefficient, and complex argument $\varphi_{\alpha\rho^*}(k)$ is discussed in Appendix A. Here, the results are condensed in the following two statements, Theorem 3.1 and Lemma 3.2, which specify their overall extremal ratings and their dependency on the complex argument $\varphi_{\alpha\rho^*}(k)$.

⁵ It can be verified that for $\alpha \in \mathbb{R}_{0+}$ and $\rho \in [-1, 1]$, $c_1 = -\sigma_1 \leq 0$, and

$$c_2 = \begin{cases} \sigma_2 \geq 0; & \text{for } \alpha\rho \leq 1 \\ -\sigma_2 \leq 0; & \text{for } \alpha\rho > 1 \end{cases}. \quad (3.26)$$

Theorem 3.1: Bounds for the two Non-Unit Singular Values of B_k

With the magnitude of correlation coefficient $\rho(k)$ in (3.12), (inherently) bounded by $0 \leq |\rho(k)| \leq 1$, and an arbitrary effective step-size $\alpha(k) \in \mathbb{C}$, the two non-unit singular values, $\sigma_1(k)$ and $\sigma_2(k)$, specified by (3.22) are in any case bounded from above by

$$\hat{\sigma}_1(k) \triangleq \max_{\substack{|\rho(k)| \in [0,1], \\ \varphi_{\alpha\rho^*}(k) \in [-\pi,\pi]}} \{\sigma_1(k)\} = \sigma_1(k) \Big|_{|\rho(k)|=1, \varphi_{\alpha\rho^*}(k)=\pi} = 1 + |\alpha(k)|, \quad (3.31)$$

$$\hat{\sigma}_2(k) \triangleq \max_{\substack{|\rho(k)| \in [0,1], \\ \varphi_{\alpha\rho^*}(k) \in [-\pi,\pi]}} \{\sigma_2(k)\} = \sigma_2(k) \Big|_{|\rho(k)|=1, \varphi_{\alpha\rho^*}(k)=\pi} = 1, \quad (3.32)$$

and bounded from below by

$$\check{\sigma}_1(k) \triangleq \min_{\substack{|\rho(k)| \in [0,1], \\ \varphi_{\alpha\rho^*}(k) \in [-\pi,\pi]}} \{\sigma_1(k)\} = \sigma_1(k) \Big|_{|\rho(k)|=1, \varphi_{\alpha\rho^*}(k)=0} = \begin{cases} 1; & |\alpha(k)| \leq 2 \\ |\alpha(k)| - 1; & |\alpha(k)| > 2 \end{cases}, \quad (3.33)$$

$$\check{\sigma}_2(k) \triangleq \min_{\substack{|\rho(k)| \in [0,1], \\ \varphi_{\alpha\rho^*}(k) \in [-\pi,\pi]}} \{\sigma_2(k)\} = \begin{cases} \sigma_2(k) \Big|_{|\rho(k)|=1, \varphi_{\alpha\rho^*}(k)=0} = 1 - |\alpha(k)|; & |\alpha(k)| \leq 1 \\ \sigma_2(k) \Big|_{|\rho(k)|=\frac{1}{|\alpha(k)|}, \varphi_{\alpha\rho^*}(k)=0} = 0; & |\alpha(k)| > 1 \end{cases}, \quad (3.34)$$

with complex argument $\varphi_{\alpha\rho^*}(k)$ defined in (3.13).

Proof. See Appendix A.3 for a sketched proof. □

Lemma 3.2: Dependency of the two Non-Unit Singular Values on $\varphi_{\alpha\rho^*}(k)$

Assuming that the two non-unit singular values, $\sigma_i(k)$, $i \in \{1, 2\}$, are given for a certain pair $\langle \alpha(k), \rho(k) \rangle$ of the effective step-size and the correlation coefficient. Then, for an alternative pair $\langle \alpha'(k), \rho'(k) \rangle$, which preserves magnitudes, i.e., $|\alpha'(k)| = |\alpha(k)|$ and $|\rho'(k)| = |\rho(k)|$, but leads to a complex argument $\varphi_{\alpha'\rho'^*}(k)$ according to (3.13) that is larger in magnitude, i.e., $0 \leq |\varphi_{\alpha\rho^*}(k)| < |\varphi_{\alpha'\rho'^*}(k)| \leq \pi$, the corresponding alternative singular values satisfy

$$\sigma'_i(k) > \sigma_i(k). \quad (3.35)$$

Proof. The proof is given in Appendix A.2.3. □

3.3.3 Meaning of the Worst Case

In Section 2.3.3, (2.42), respectively, (2.43), state the condition which has to hold in order to obtain an increasing parameter error distance. In this work, such a situation is briefly referred to as *worst case (w.c.)*. The aim of this section is to take a more detailed look at this situation, and to clarify the meaning of the term “worst case”. Adopting the notion of [Mar06], the situation of a w.c. can be compared with *the* recursion – out of all recursions of type (2.18) that can be generated given certain domains for the excitation sequence and the sequence of regression vectors – that follows

the worst trajectory in terms of the parameter error vector, given an initial value $\tilde{\mathbf{w}}_{-1}$. With the results achieved for the SVD of the mapping matrix in Section 3.3.2, it is clear that for asymmetric algorithms, (2.43) simplifies to [DR09a]

$$(\sigma_1^2(k) - 1) \left| \mathbf{t}_{1,k}^H \tilde{\mathbf{w}}_{k-1} \right|^2 > (1 - \sigma_2^2(k)) \left| \mathbf{t}_{2,k}^H \tilde{\mathbf{w}}_{k-1} \right|^2, \quad (3.36)$$

where the relevant $\tilde{w}_i'(k) = \mathbf{t}_{i,k}^H \tilde{\mathbf{w}}_{k-1}$ have been reinserted. Clearly, for given $\sigma_1(k)$ and $\sigma_2(k)$, the absolute w.c., in the sense that parameter error increment $W(k)$ in (2.42), respectively, (3.36), is maximised, occurs if $\tilde{\mathbf{w}}_{k-1} \parallel \mathbf{t}_{1,k}$. Note however, that the non-unit singular values, as well as their corresponding singular vectors, are a function of the excitation and the regression vector. In a practical situation, typically, an a priori parameter error vector $\tilde{\mathbf{w}}_{k-1}$ is given as result of the previous iteration. Then, in the context of a w.c. analysis, the goal is to find the combination of \mathbf{u}_k and \mathbf{x}_k that maximises (2.42). Of course, contrarily one may also be interested in showing that no such pair exists. Especially, in the common case of a regression vector that is related to the excitation vector by a step-size matrix as it is given in (2.9), i.e., $\mathbf{x}_k = \mathbf{M}_k^* \mathbf{u}_k$, the singular values and vectors depend on \mathbf{u}_k in a strongly non-linear way. Consequently, finding the \mathbf{u}_k that actually maximises (3.36) for a given $\tilde{\mathbf{w}}_{k-1}$, is rather involved and in general only accessible to numerical methods. For this reason, the term w.c. is here used in a looser meaning, as it refers to any situation for which (2.42), respectively, (2.43), is satisfied. Section 3.5 develops methods that allow to analytically identify such w.c. excitation vectors. Section 3.6 in turn approaches this problem numerically and proposes efficient search algorithms in order to find them.

3.4 Mapping Analysis of Asymmetric Algorithms

After raising the question about the reasons for hidden divergence that can be observed in the simulation experiments of Section 3.1, the discussion of existing literature in Section 3.2 indicated that still only a partial understanding of the observed effects is available. Then, Section 3.3 studied the characteristics of the mapping matrix of asymmetric algorithms and revealed that this matrix seems to inherently introduce the risk of an increasing parameter error distance. As a consequence, this section continues with the aim to develop novel theoretical insights in order to extend the knowledge about the convergence behaviour of asymmetric algorithms. First, a brief overview, in conjunction with Figure 3.7, is provided facilitate orientation.

Section 3.4.1 starts with an investigation of the mapping mechanisms that can be observed for asymmetric algorithms under w.c. excitation. This is done from the most general point of view, meaning that the excitation vector and the regression vector are assumed to be completely independent. After this, we will know about certain directions of the parameter error vector that are ensured to be increased in length by mapping matrix \mathbf{B} (cf. Lemma 3.4), as well as about situations which inhibit any growth of the parameter error distance (cf. Lemma 3.6). Also a first insight to the direction of change is achieved (cf. Lemma 3.5).

As the point of view adopted by Section 3.4.1, which assumes the regression vector to be completely independent from the excitation vector, is hardly the case in practice, Section 3.4.2 takes the next step and considers the typical case of a step-size matrix that imposes a linear dependence among the latter two vectors. The first two formal statements (Lemmas 3.7 and 3.8) establish a relation among (rather) general step-size matrices and more specific positive definite diagonal step-size matrices. By this it is clarified if, and how, results valid for the latter case, can be applied to gain insight for the primer. Additionally, Lemma 3.9 points a very general mapping behaviour that holds for any normal matrix. This will be important in Section 3.4.3 to analyse the trajectory of the parameter

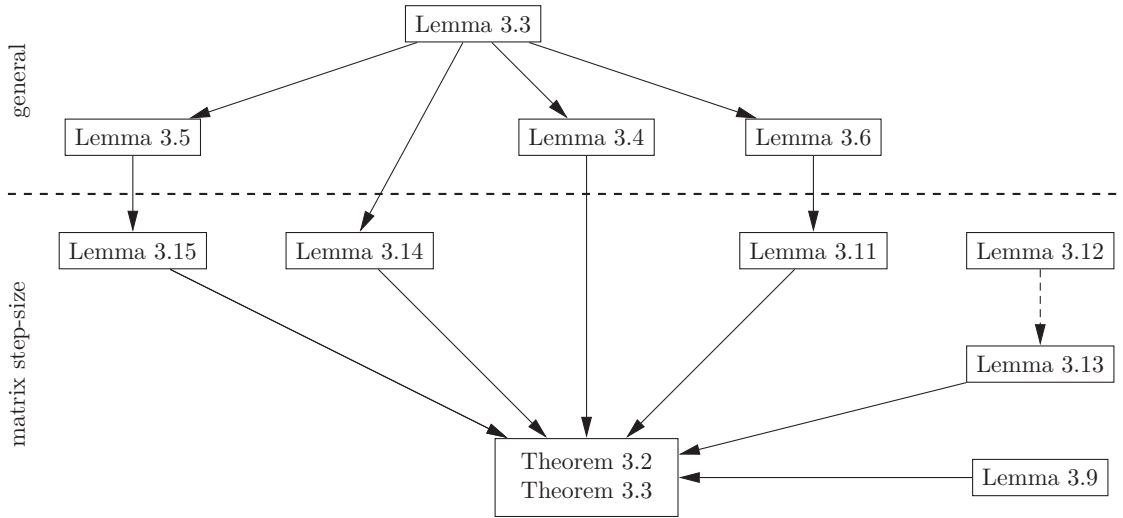


Figure 3.7: Overview over the statements derived in this Section 3.3, together with their dependencies.

error vector for an algorithm under w.c. excitation.

Section 3.4.2 paves the way to justify the assumption of a positive definite diagonal step-size matrix. This in turn gives access to a set of conclusive insights that altogether lead to Theorems 3.2 and 3.3 in Section 3.4.4. In brief, Lemma 3.11 shows in which cases, a growth of the parameter error distance is impossible. It can be considered as a specialised version of Lemma 3.6. Lemmas 3.12 and 3.13 are important to assess the trajectory that is under w.c. conditions, followed by the parameter error vector. Lemma 3.14 and Theorem 3.2 identify those directions of the parameter error vector, for which an increase of the parameter error distance can occur.

Finally, the results from Sections 3.4.1 to 3.4.3 are condensed in Section 3.4.4. There, Theorem 3.2 comes to the conclusion that a fixed matrix step-size prohibits the existence of hidden convergence. This result is already known [SR96; RC00], yet to the knowledge of the author, the presented approach is new and provides further understanding of gradient type algorithms with matrix step-size. In contrast, no comparable results seem to exist with respect to Theorem 3.3. The latter provides a necessary condition for the existence of hidden divergence, which additionally gives insight what characteristics practical step-size matrices should *not* have. By this, eventually, the crucial differences among the three algorithms considered in Section 3.1 can be carved out.

3.4.1 Independent Regression Vector

In this section, a detailed analysis of the local convergence behaviour for the gradient type algorithm in (2.17) is presented. At this point, no specific assumptions regarding the relation among the excitation vector and the regression vector are made. Contrarily, they are assumed to be completely independent. Restrictions induced by a step-size matrix are deferred to Section 3.4.2. Nevertheless, in both sections, argumentation is based on the geometric mapping mechanisms happening inside the M -dimensional space – or an orthogonal projections of it – that contains the parameter error vector. The analysis is tightly related to the condition for local growth (2.43) in Section 2.3.3. Thus, let us start with the parameter error increment $W(k)$ defined in (2.41), tailored to the specific form of the noiseless update equation (2.17),

$$W(k) = |\mu_k|^2 \|\mathbf{x}_k\|^2 |\tilde{\mathbf{w}}_{k-1}^\top \mathbf{u}_k|^2 - 2\text{Re} \left\{ \mu_k (\tilde{\mathbf{w}}_{k-1}^\top \mathbf{x}_k)^* (\tilde{\mathbf{w}}_{k-1}^\top \mathbf{u}_k) \right\}. \quad (3.37)$$

With effective step-size $\alpha(k)$ from (3.11), and unit vectors, $\mathbf{e}_{\mathbf{u}_k}$ and $\mathbf{e}_{\mathbf{x}_k}$, that correspond to excitation vector \mathbf{u}_k and regression vector \mathbf{x}_k , respectively, (3.37) is equivalent to

$$W(k) = |\alpha(k)|^2 |\tilde{\mathbf{w}}_{k-1}^\top \mathbf{e}_{\mathbf{u}_k}|^2 - 2\text{Re} \left\{ \alpha(k) (\tilde{\mathbf{w}}_{k-1}^\top \mathbf{e}_{\mathbf{x}_k})^* (\tilde{\mathbf{w}}_{k-1}^\top \mathbf{e}_{\mathbf{u}_k}) \right\}. \quad (3.38)$$

Clearly, for $\alpha(k) = 0$ or $\tilde{\mathbf{w}}_{k-1}^\top \mathbf{e}_{\mathbf{u}_k} = 0$, $W(k) = 0$. Therefore, we continue with the constraint of non-stalling adaptation given in the following assumption.

Assumption 3.1: Non-Stalling Update Conditions

If the effective step-size is different from zero, and the excitation vector is not perfectly aligned with the parameter error vector, i.e.,

$$\alpha(k) \neq 0, \quad \text{and} \quad \tilde{\mathbf{w}}_{k-1}^\top \mathbf{e}_{\mathbf{u}_k} \neq 0, \quad (3.39)$$

parameter error increment $W(k)$ in (3.37) and (3.38), does not trivially vanish.

Under these restrictions, (3.38) can be rewritten as

$$W(k) = |\alpha(k)|^2 |\tilde{\mathbf{w}}_{k-1}^\top \mathbf{e}_{\mathbf{u}_k}|^2 \left[1 - 2\text{Re} \left\{ \frac{\tilde{\mathbf{w}}_{k-1}^\top \mathbf{e}_{\mathbf{x}_k}}{\alpha(k) \tilde{\mathbf{w}}_{k-1}^\top \mathbf{e}_{\mathbf{u}_k}} \right\} \right], \quad (3.40)$$

and the following lemma can be formulated, which is of central importance throughout this section.

Lemma 3.3: Condition for Expanding Worst Case Behaviour

The mapping in (2.17) leads to an increase of parameter error distance $\|\tilde{\mathbf{w}}_k\|$ iff

$$W(k) = |\alpha(k)|^2 |\tilde{\mathbf{w}}_{k-1}^\top \mathbf{e}_{\mathbf{u}_k}|^2 - 2\text{Re} \left\{ \alpha(k) (\tilde{\mathbf{w}}_{k-1}^\top \mathbf{e}_{\mathbf{u}_k}) (\tilde{\mathbf{w}}_{k-1}^\top \mathbf{e}_{\mathbf{x}_k})^* \right\} > 0, \quad (3.41)$$

or equivalently, for non-stalling adaptation (cf. Assumption 3.1), if

$$\text{Re} \left\{ \frac{\tilde{\mathbf{w}}_{k-1}^\top \mathbf{e}_{\mathbf{x}_k}}{\alpha(k) \tilde{\mathbf{w}}_{k-1}^\top \mathbf{e}_{\mathbf{u}_k}} \right\} < \frac{1}{2}. \quad (3.42)$$

Section 3.3.2 shows that mapping matrix \mathbf{B}_k for the here considered gradient type algorithm in (2.16), has exactly one singular value $\sigma_1(k) \geq 1$, one singular value $\sigma_2(k) \leq 1$, and $M - 2$ unit singular values. Let us assume that the algorithm arrived at iteration k and that the current a priori parameter error vector is in a certain but arbitrary state $\tilde{\mathbf{w}}_{k-1}$. Knowing that for (3.39), the maximum singular value is always larger than one, the question is whether in any case, a pair \mathbf{u}_k and \mathbf{x}_k can be found such that the condition in Lemma 3.3 is satisfied. Before a rigorous statement of existence is given in Lemma 3.4, a less formal thought experiment is presented.

Contemplate, an excitation vector and a regression vector,

$$\mathbf{u}'_k = \mathbf{V}_k \mathbf{u}_k, \quad \mathbf{x}'_k = \mathbf{V}_k \mathbf{x}_k, \quad (3.43)$$

which are both arbitrary up to the not yet justified fact that they are related to \mathbf{u}_k and \mathbf{x}_k by some unitary matrix $\mathbf{V}_k \in \mathbb{C}^{M \times M}$. Due to unitary invariance of the Euclidean norm [HJ13, Sec. 5.2], with (3.11) and (3.12), the corresponding effective step-size $\alpha'(k)$ and correlation coefficient $\rho'(k)$,

are obtained as

$$\alpha'(k) = \mu(k) \|\mathbf{u}'_k\| \|\mathbf{x}'_k\| = \mu(k) \|\mathbf{V}_k \mathbf{u}_k\| \|\mathbf{V}_k \mathbf{x}_k\| = \mu(k) \|\mathbf{u}_k\| \|\mathbf{x}_k\| = \alpha(k) \quad (3.44)$$

$$\rho'(k) = \frac{\mathbf{x}'_k{}^\top \mathbf{u}'_k{}^*}{\|\mathbf{u}'_k\| \|\mathbf{x}'_k\|} = \frac{\mathbf{x}_k^\top \mathbf{V}_k^\top \mathbf{V}_k^* \mathbf{u}_k^*}{\|\mathbf{V}_k \mathbf{u}_k\| \|\mathbf{V}_k \mathbf{x}_k\|} = \frac{\mathbf{x}_k^\top \mathbf{u}_k^*}{\|\mathbf{u}_k\| \|\mathbf{x}_k\|} = \rho(k). \quad (3.45)$$

As found in Section 3.3.2, the singular values – and also the eigenvalues – of \mathbf{B}_k are completely determined by $\rho(k)$ and $\alpha(k)$. Hence, (3.44) and (3.45) show their invariance with respect to a rotation of \mathbf{u}_k and \mathbf{x}_k by an arbitrary unitary matrix \mathbf{V}_k . Furthermore,

$$\mathbf{B}'_k = \mathbf{I} - \mu(k) \mathbf{x}'_k{}^* \mathbf{u}'_k{}^\top = \mathbf{I} - \mu(k) \mathbf{V}_k^* \mathbf{x}_k^* \mathbf{u}_k^\top \mathbf{V}_k^\top = \mathbf{V}_k^* [\mathbf{I} - \mu(k) \mathbf{x}_k^* \mathbf{u}_k^\top] \mathbf{V}_k^\top = \mathbf{V}_k^* \mathbf{B}_k \mathbf{V}_k^\top, \quad (3.46)$$

and with (2.28), the SVD of \mathbf{B}'_k is identified as

$$\mathbf{B}'_k = \mathbf{R}'_k \boldsymbol{\Sigma}_k \mathbf{T}'_k{}^H = \mathbf{V}_k^* \mathbf{R}_k \boldsymbol{\Sigma}_k \mathbf{T}_k^H \mathbf{V}_k^\top \Rightarrow \mathbf{R}_k = \mathbf{V}_k^\top \mathbf{R}'_k, \quad \mathbf{T}_k = \mathbf{V}_k^\top \mathbf{T}'_k. \quad (3.47)$$

Thus, starting with some vectors \mathbf{u}'_k and \mathbf{x}'_k an intermediate mapping matrix \mathbf{B}'_k can be obtained. Performing the SVD, yields matrix \mathbf{T}'_k of its right-sided singular vectors. If then, a unitary matrix \mathbf{V}_k is chosen such that its first column coincides with the complex conjugate of the singular vector $\mathbf{t}'_{1,k}$, then

$$\mathbf{T}'_k{}^H \mathbf{V}_k^* \tilde{\mathbf{w}}_{k-1} = \|\tilde{\mathbf{w}}_{k-1}\| \mathbf{e}_1 \Rightarrow \mathbf{V}_k^* \tilde{\mathbf{w}}_{k-1} = \|\tilde{\mathbf{w}}_{k-1}\| \mathbf{t}'_{1,k}, \quad (3.48)$$

where \mathbf{e}_1 is the first basis vector of the underlying Cartesian coordinate system. Hence, under constraint (3.39) which ensures $\sigma_1(k) > 1$ (cf. Section 3.3.2), mapping matrix \mathbf{B}_k obtained for the original vectors $\mathbf{u}_k = \mathbf{V}_k^H \mathbf{u}'_k$ and $\mathbf{x}_k = \mathbf{V}_k^H \mathbf{x}'_k$ in (3.43), leads to

$$\|\tilde{\mathbf{w}}_k\| = \|\mathbf{B}_k \tilde{\mathbf{w}}_{k-1}\| = \sigma_1(k) \|\tilde{\mathbf{w}}_{k-1}\| > \|\tilde{\mathbf{w}}_{k-1}\| \Rightarrow W(k) > 0. \quad (3.49)$$

As it is always possible to choose \mathbf{V}_k according to (3.48), the above derivation allows to conclude that if the regression vector can be independently chosen from the excitation vector, $W(k) > 0$ is always achievable.

In practical settings, such a complete independence will never be the case. Then, (3.48) may barely be achievable. However, as Section 3.3 has shown, \mathbf{B}_k has only one singular value, $\sigma_2(k)$, that is less than one. Accordingly, $W(k) > 0$ still holds as long, as $\tilde{\mathbf{w}}_{k-1} \not\perp \mathbf{t}_{1,k}$ and $\tilde{\mathbf{w}}_{k-1} \perp \mathbf{t}_{2,k}$. With this objective, (3.48) modifies to the more relaxed requirements

$$\mathbf{t}'_{1,k}{}^H \mathbf{V}_k^* \tilde{\mathbf{w}}_{k-1} \neq 0, \quad \text{and} \quad \mathbf{t}'_{2,k}{}^H \mathbf{V}_k^* \tilde{\mathbf{w}}_{k-1} = 0. \quad (3.50)$$

For practical gradient type algorithms, (3.50) is much more likely to occur than (3.48). Finally, it should be noted that (3.50) still does not allow to derive *all* pairs $\langle \mathbf{u}_k, \mathbf{x}_k \rangle$ that satisfy condition (2.43) for a positive parameter error increment. This further extension is skipped here, as it does not provide any further understanding of the underlying mechanisms. Instead, the just found insights are condensed in the following lemma.

Lemma 3.4: Expanding Behaviour for Unconstrained $\mathbf{u}_k \not\parallel \mathbf{x}_k$

Assuming non-stalling adaptation (cf. Assumption 3.1), then, inequalities (3.41) and (3.42) have at least one solution, if \mathbf{u}_k and \mathbf{x}_k are not in parallel and can be chosen independently.

Proof. See Appendix D.1.1. □

If the parameter error increment $W(k)$ is positive, i.e., Lemma 3.3 holds, it is additionally possible to gain insight how the mapping by \mathbf{B}_k influences the direction of the parameter error vector. This knowledge is expressed in the next lemma, which will prove useful further down, as it tells us in simple terms that under w.c. excitation, the parameter error vector is attracted by the regression vector and repelled by the excitation vector.

Lemma 3.5: Direction of Expansion of the Parameter Error Vector

If the conditions required by Lemmas 3.1 and 3.3 are satisfied, then, the (expanding) mapping $\tilde{\mathbf{w}}_k = \mathbf{B}_k \tilde{\mathbf{w}}_{k-1}$ turns the parameter error vector $\tilde{\mathbf{w}}_{k-1}$ away from the complex conjugate \mathbf{u}_k^ of the excitation vector and towards the complex conjugate \mathbf{x}_k^* of the regression vector.*

Proof. See Appendix D.1.2. □

Similarly important to the statement of Lemma 3.5, is the fact that parallelism of the excitation vector and the regression vector renders the conditions of Lemma 3.3 unreachable. Hence, it inhibits a growth of the parameter error vector, which is the gist of the following lemma.

Lemma 3.6: Non-Expanding Behaviour for $\mathbf{u}_k \parallel \mathbf{x}_k$, i.e., $|\rho(k)| = 1$

For $|\rho(k)| = 1$, the parameter error distance can never increase if (3.15) is satisfied.

Proof. See Appendix D.1.3. □

3.4.2 Normal Step-Size Matrix

The investigations in the previous section, focussed on the case that the regression vector is completely independent from the excitation vector. This section, in contrast, assumes a linear dependency by a possibly time-varying matrix step-size. Specifically, inserting regression vector (2.9) into the homogeneous recursion in (2.17), modifies the latter to

$$\tilde{\mathbf{w}}_k = [\mathbf{I} - \mu(k)\mathbf{M}_k\mathbf{u}_k^*\mathbf{u}_k^T] \tilde{\mathbf{w}}_{k-1}, \quad (3.51)$$

with step-size matrix $\mathbf{M}_k \in \mathbb{C}^{M \times M}$. In order to simplify the following investigations, a further assumption is being made.

Assumption 3.2: Real-Valued Step-Size and Positive Definite Step-Size Matrix

1. Step-size $\mu(k)$, and thus, the effective step-size $\alpha(k)$ as well, are real-valued and non-negative.
2. Step-size matrix \mathbf{M}_k is (Hermitian and) positive definite.

Point 1 in Assumption 3.2 does not pose any actual restriction as, w.o.l.o.g., any phase rotation arc ($\mu(k)$) introduced by the step-size can be incorporated into a modified step-size matrix \mathbf{M}'_k ,

$$\mu(k)\mathbf{M}_k = \underbrace{|\mu(k)|}_{\mu'(k)} \underbrace{\exp(j \arccos(\mu(k)))\mathbf{M}_k}_{\mathbf{M}'_k}. \quad (3.52)$$

The second assumption is of course restrictive and needs further justification:

- a. Due to Lemma 3.1, in order to ensure a spectral radius bounded by one – and thus, the possibility for convergence – the numerical range [GR97] of the step-size matrix has to be contained within the right complex half-plane (including the imaginary axis). Accordingly, Hermitian step-size matrices are not allowed to be negative definite or indefinite. Hence, the motivation to assume positive definiteness.
- b. Gradient type algorithms with matrix step-size do not require the latter to be Hermitian. Not even the analysis presented in the sequel is bonded to such an assumption. In fact, it is at least applicable to step-size matrices that belong to the class of normal matrices, which in turn contains Hermitian matrices as a subclass [HJ13, Sec. 2.5]. However, as Lemma 3.8 shows below, the singular value spread of mapping matrix \mathbf{B}_k is minimised if all eigenvalues of \mathbf{M}_k are real-valued and positive. Accordingly, if the step-size matrix would actually be normal but not Hermitian, the analysis of an equivalent algorithm that uses its nearest positive definite equivalent, i.e., the matrix that is obtained by replacing the eigenvalues by their magnitudes, may still result in conclusive results. Specifically, if an asymmetric algorithm based on the nearest positive definite equivalent is found to diverge, the algorithm that employs the original normal matrix cannot be expected to qualitatively behave differently. Of course, in the case of convergence such a deduction is in general not allowed. However, as this work prioritises the unmasking of hidden divergence, it seems justified to restrict to Hermitian (and positive definite) matrices for the sake of clarity.
- c. Most gradient type algorithms are found to utilise a positive definite diagonal step-size matrix [MKK93; Gay98; Dut00; BG02; dSTSM09; dSTSM10], which is more than covered by Assumption 3.2. Hence, Point 2 of Assumption 3.2 is again justified from a practical point of view.

The first and the last of the above justifications are rather evident or self-contained. The second one, requires further examination. Before this is done, a very important simplification that is accessible for any normal step-size matrix, is presented below in Lemma 3.7.

Lemma 3.7: Equivalence of Normal and Diagonal Step-Size Matrix

If step-size matrix $\mathbf{M}_k \in \mathbb{C}^{M \times M}$ is normal, with eigendecomposition [HJ13, Theorem 2.5.3]

$$\mathbf{M}_k = \mathbf{Q}_{\mathbf{M},k} \mathbf{\Lambda}_{\mathbf{M},k} \mathbf{Q}_{\mathbf{M},k}^H, \quad \mathbf{\Lambda}_{\mathbf{M},k} \triangleq \text{diag} \{ \lambda_i(\mathbf{M}_k) \}_{i=1}^M, \quad (3.53)$$

and $\mathbf{Q}_{\mathbf{M},k}$ being unitary, by introducing the rotated vectors

$$\mathbf{u}'_k \triangleq \mathbf{Q}_{\mathbf{M},k}^T \mathbf{u}_k, \quad \tilde{\mathbf{w}}'_k \triangleq \mathbf{Q}_{\mathbf{M},k}^H \tilde{\mathbf{w}}_k, \quad \text{and} \quad \tilde{\mathbf{w}}''_{k-1} \triangleq \mathbf{Q}_{\mathbf{M},k}^H \tilde{\mathbf{w}}_{k-1}, \quad (3.54)$$

for each iteration step k , (3.51) can be mapped to

$$\tilde{\mathbf{w}}'_k = [\mathbf{I} - \mu(k) \mathbf{\Lambda}_{\mathbf{M},k} \mathbf{u}'_k \mathbf{u}'_k{}^T] \tilde{\mathbf{w}}''_{k-1}. \quad (3.55)$$

The proof of Lemma 3.7 is straightforward and skipped here. A very similar reasoning was used for positive definite matrices in [SR96; RC00]. The latter references, however, do not employ a length and angle preserving rotation as it is done in Lemma 3.7 due to $\mathbf{Q}_{\mathbf{M},k}$ being unitary. There, instead an orthogonal coordinate transform is applied, based on a Cholesky factorisation of the step-size matrix [HJ13, Corollary 7.2.9]. The reason why here, the eigendecomposition is preferred to the

Cholesky factorisation, is the length preserving property [HJ13, Sec. 5.2] of $\mathbf{Q}_{\mathbf{M},k}$, entailing

$$\|\mathbf{u}'_k\| = \|\mathbf{u}_k\|, \quad \text{and} \quad \|\tilde{\mathbf{w}}''_k\| = \|\tilde{\mathbf{w}}'_k\| = \|\tilde{\mathbf{w}}_k\|. \quad (3.56)$$

Hence, as crucial consequence,

$$\|\tilde{\mathbf{w}}'_k\|^2 - \|\tilde{\mathbf{w}}''_{k-1}\|^2 = \|\tilde{\mathbf{w}}_k\|^2 - \|\tilde{\mathbf{w}}_{k-1}\|^2 = W(k), \quad (3.57)$$

which shows that in terms of the Euclidean norm, with the scope of one single iteration, the mapping behaviour of (3.55), is equivalent to the mapping behaviour of the original homogeneous recursion in (3.51). Based on this insight, Lemma 3.7 provides the key to extend the results of Section 3.4.3 – that are restricted to positive definite diagonal step-size matrices – to non-diagonal normal matrices.

Yet, it is important to notice that for modal matrices $\mathbf{Q}_{\mathbf{M},k}$ that depend on iteration step k , Lemma 3.7 does *not* allow to conclude that the algorithm can completely be replaced by its equivalent with diagonal step-size matrix. This is, because $\tilde{\mathbf{w}}'_k$ calculated during iteration k is not identical to $\tilde{\mathbf{w}}''_k$, which represents the a priori parameter error vector of iteration $k + 1$. Only if the sequence $\{\mathbf{M}_k\}$ has a constant modal space, the unitary matrices do not depend on k , i.e., $\mathbf{Q}_{\mathbf{M},k} = \mathbf{Q}_{\mathbf{M}}$, and $\tilde{\mathbf{w}}'_k = \mathbf{Q}_{\mathbf{M}}^H \tilde{\mathbf{w}}_k = \tilde{\mathbf{w}}''_k$.

After this excursus about usability and limitations of results obtained for diagonal step-size matrices, let us turn our focus back to the justification of Point 2 in Assumption 3.2.

Lemma 3.8: Minimum Singular Value Spread for Real-Valued Eigenvalues

If for an arbitrary iteration step k the asymmetric algorithm in (3.51) has a real-valued non-negative step-size $\mu(k)$ and a normal step-size matrix \mathbf{M}_k , then, for given magnitudes $|\lambda_i(\mathbf{M}_k)|$ of the eigenvalues in (3.53), the maximum (minimum) singular value of the corresponding mapping matrix \mathbf{B}_k in homogeneous recursion (2.16) is minimised (maximised), if all entries satisfy $\lambda_i(\mathbf{M}_k) \in \mathbb{R}_{0+}$, i.e., if $\mathbf{\Lambda}_{\mathbf{M},k} \geq \mathbf{0}$.

Proof. See Appendix D.1.4. □

Lemma 3.8 shows that a detailed analysis of gradient type algorithms with positive definite step-size matrix allows to deduce statements for algorithms with more general step-size matrices. Accordingly, Point 2 in Assumption 3.2 is indeed reasonable.

Finally, before moving on to the next section which is dedicated to a detailed analysis of gradient type algorithms with positive definite diagonal step-size matrix, another important property of normal step-size matrices is investigated. Formulated in a general way, it gives insight to the changes of direction that are introduced by a normal step-size matrix, during the mapping of an excitation vector to the corresponding regression vector. In conjunction with Lemma 3.5 that is concerned with the direction of $\tilde{\mathbf{w}}_k$ in the case of a positive parameter error increment, i.e., $W(k) > 0$, the following Lemma 3.9 will be of central importance in Section 3.4.4.

Lemma 3.9: Amplifying and Attenuating Eigenspaces

For an arbitrary normal matrix $\mathbf{A} \in \mathbb{C}^{M \times M}$, with eigenvalues $\lambda_i(\mathbf{A})$, $i \in \{1, \dots, M\}$, and some non-zero vector $\mathbf{x} \in \mathbb{C}^M$, the relative growth imposed by the mapping $\mathbf{A}\mathbf{x}$ to the component contained in the eigenspace $\mathcal{E}(\lambda_i(\mathbf{A}))$ is given by $|\lambda_i(\mathbf{A})| - 1$.

Proof. See Appendix D.1.5. □

3.4.3 Positive Definite Diagonal Step-Size Matrices

Lemmas 3.7 and 3.8 show that gradient type algorithms with positive definite diagonal step-size matrix allow to infer insight to the behaviour of algorithms with more general step-size matrix. For this reason, this section essentially extends the findings in [DR13], and presents a concise analysis of the mapping mechanisms that can be observed for a step-size matrix that is diagonal and positive definite. Note however, that the wording of the below given statements only requires positive definiteness, as the extension to non-diagonal step-size matrices is ensured by Lemma 3.7. Moreover, for the same reason, I will also stick to the more general notion of eigenvalues and eigenvectors (as well as eigenspaces), although for diagonal step-size matrices the primer coincide with their diagonal entries, the latter with the basis vectors.

Accordingly, the here considered algorithms use the general update equation of asymmetric algorithms, given in (2.17), with the regression vector and its unit vector given by (cf. (2.9))

$$\mathbf{x}_k = \mathbf{D}_k \mathbf{u}_k, \quad \mathbf{e}_{\mathbf{x}_k} = \frac{\mathbf{D}_k \mathbf{e}_{\mathbf{u}_k}}{\|\mathbf{D}_k \mathbf{e}_{\mathbf{u}_k}\|}, \quad (3.58)$$

where $\mathbf{e}_{\mathbf{u}_k}$ denotes the unit vector with direction of excitation vector \mathbf{u}_k , and a diagonal step-size matrix

$$\mathbf{D}_k \triangleq \text{diag}_{i=1}^M \{d_i(k)\}, \quad \text{with} \quad d_i(k) \in \mathbb{R}_+, i \in \{1, \dots, M\}. \quad (3.59)$$

Thus, the effective step-size and the correlation coefficient in (3.11) and (3.12), respectively, modify to

$$\alpha(k) = \mu(k) \|\mathbf{u}_k\| \|\mathbf{D}_k \mathbf{u}_k\| = \mu(k) \|\mathbf{u}_k\|^2 \|\mathbf{D}_k \mathbf{e}_{\mathbf{u}_k}\|, \quad (3.60)$$

$$\rho(k) = \frac{\mathbf{u}_k^\top \mathbf{D}_k \mathbf{u}_k^*}{\|\mathbf{u}_k\| \|\mathbf{D}_k \mathbf{u}_k\|} = \frac{\mathbf{e}_{\mathbf{u}_k}^\top \mathbf{D}_k \mathbf{e}_{\mathbf{u}_k}^*}{\|\mathbf{D}_k \mathbf{e}_{\mathbf{u}_k}\|} = \mathbf{e}_{\mathbf{x}_k}^\top \mathbf{e}_{\mathbf{u}_k}^*, \quad (3.61)$$

and since $\alpha(k) \in \mathbb{R}_{0+}$, the complex argument in (3.13) becomes

$$\varphi_{\alpha\rho^*}(k) = \arccos(\alpha(k)\rho^*(k)) = \arccos(\rho^*(k)) = -\arccos(\rho(k)). \quad (3.62)$$

Hence, the mapping matrix from (2.16) can be expressed as

$$\mathbf{B}_k = \mathbf{I} - \mu(k) \mathbf{x}_k^* \mathbf{u}_k^\top = \mathbf{I} - \mu(k) \mathbf{D}_k \mathbf{u}_k^* \mathbf{u}_k^\top \quad (3.63)$$

$$= \mathbf{I} - \mu(k) \|\mathbf{u}_k\| \|\mathbf{D}_k \mathbf{u}_k\| \frac{\mathbf{D}_k \mathbf{e}_{\mathbf{u}_k}^*}{\|\mathbf{D}_k \mathbf{e}_{\mathbf{u}_k}\|} \mathbf{e}_{\mathbf{u}_k}^\top = \mathbf{I} - \alpha(k) \mathbf{e}_{\mathbf{x}_k}^* \mathbf{e}_{\mathbf{u}_k}^\top. \quad (3.64)$$

The correlation coefficient in (3.61) looks similar to a Rayleigh quotient (cf. (C.1)) [Theorem 4.2.2 HJ13], but it is not identical. In fact, it is a function that is well studied in context of operator trigonometry [Gus00; Rao05; GR97], and gives access to the notion of antieigenvalues and antieigenvectors. Appendix C.1 provides further details about this topic, which can be directly applied to prove the following lemma.

Lemma 3.10: Minima and Maxima of Correlation Coefficient $\rho(k)$

With a positive definite step-size matrix \mathbf{D}_k , the correlation coefficient in (3.61) is real-valued and positive. It assumes its maximum value

$$\rho_{\max}(k) \triangleq \max_{\mathbf{u}_k \in \mathbb{C}^M} \{\rho(k)\} = 1, \quad (3.65)$$

if the excitation vector \mathbf{u}_k is in parallel with one of the M eigenvectors of \mathbf{D}_k , i.e., one of the elementary basis vectors. Its minimum is given by

$$\rho_{\min}(k) \triangleq \min_{\mathbf{u}_k \in \mathbb{C}^M} \{\rho(k)\} = \frac{2\sqrt{d_{\min}(k)d_{\max}(k)}}{d_{\min}(k) + d_{\max}(k)}, \quad (3.66)$$

with

$$d_{\min}(k) \triangleq \min_{i=1}^M \{d_i(k)\}, \quad d_{\max}(k) \triangleq \max_{i=1}^M \{d_i(k)\}. \quad (3.67)$$

The correlation coefficient reaches its minimum, if \mathbf{u}_k is in parallel with one of the first antieigenvectors of \mathbf{D}_k .

Erratum 4

Proof. Since $\rho(k)$ in (3.61) obeys the Kantorovich inequality (cf. (C.6)), its minimum is by definition identical to the first antieigenvalue of step-size matrix \mathbf{D}_k (cf. (C.3)). Consequently, this minimum is achieved if the excitation vector coincides with one of the first antieigenvectors of \mathbf{D}_k (cf. (C.5)). \square

A first consequence of (3.61) is the following lemma which directly allows to apply Lemma 3.6 to the matrix step-size case.

Lemma 3.11: $|\rho(k)| = 1$ and Non-Expanding Behaviour for $\mathbf{u}_k \in \mathcal{E}(d_i(k))$

For a positive definite step-size matrix, the parameter error distance can never increase, if step-size condition (3.15) is satisfied, and if excitation vector \mathbf{u}_k is completely contained in eigenspace $\mathcal{E}(d_i(k))$ of eigenvalue $d_i(k)$ of step-size matrix \mathbf{D}_k .

Proof. That $|\rho(k)| = 1$ is equivalent to $\mathbf{u}_k \in \mathcal{E}(d_i(k))$ is a direct consequence of Lemma 3.10. From $|\rho(k)| = 1$, in turn, with (3.15) being satisfied, Lemma 3.6 allows to conclude that the parameter error increment does not increase. \square

Lemma 3.11 provides a statement about the overall energy contained in the parameter error vector, and is only valid for special directions of the excitation vector. The next lemma, in contrast, is concerned with the energies in the individual dimensions of the parameter error vector. The statement is true for all iterations that satisfy step-size condition (3.15). Moreover, it has to be pointed out that Point 1 in Assumption 3.2 is not required for Lemma 3.12, as it holds for any complex-valued effective step-size.

Lemma 3.12: Non-Increasing Element of the Parameter Error Vector

If at iteration step k , step-size condition (3.15) is satisfied and the step-size matrix \mathbf{D}_k is positive definite, then, for $\alpha(k) \in \mathbb{C}$, at least one element $\tilde{w}_i(k)$ of the parameter error vector $\tilde{\mathbf{w}}_k$ can be found that does not increase, i.e.,

$$\exists i \in \{1, \dots, M\} : |\tilde{w}_i(k)| \leq |\tilde{w}_i(k-1)|. \quad (3.68)$$

Proof. See Appendix D.1.6. □

Based on Lemma 3.12, a further interesting behaviour of the algorithm can be discovered. It can be considered as complement to Lemma 3.10, as it investigates the mechanisms that operate if the parameter error vector is contained in one of the eigenspaces of the step-size matrix. Its statement is an important key to geometrically understand, why algorithms with constant step-size matrix at some point *have to* converge, as long as step-size condition (3.15) is fulfilled. Similar to Lemma 3.12, also Lemma 3.13 ignores Point 1 in Assumption 3.2 and allows the effective step-sizes to be complex-valued.

Lemma 3.13: Parameter Error Leakage for $\tilde{\mathbf{w}}_{k-1} \in \mathcal{E}(d_i(k))$

If step-size condition (3.15) is satisfied for any $\alpha(k) \in \mathbb{C}$, and step-size matrix \mathbf{D}_k is positive definite, a parameter error vector that is completely contained in the eigenspace of one of the eigenvalues of the step-size matrix, i.e., $\tilde{\mathbf{w}}_{k-1} \in \mathcal{E}(d_i(k))$, leads to a leakage of the parameter error power from $\mathcal{E}(d_i(k))$ into the orthogonal complement of $\mathcal{E}(d_i(k))$, i.e.,

$$|\tilde{w}_j(k)|^2 - |\tilde{w}_j(k-1)|^2 \begin{cases} \leq 0; & \mathbf{e}_j \in \mathcal{E}(d_i(k)) \\ \geq 0; & \mathbf{e}_j \notin \mathcal{E}(d_i(k)) \end{cases}. \quad (3.69)$$

Proof. See Appendix D.1.7. □

Lemma 3.13 does not give any insight how the described leakage affects the parameter error increment $W(k)$. Under which conditions the latter can be positive despite the existence of leakage, is covered by Lemma 3.14, which again does not depend on Point 1 in Assumption 3.2.

Lemma 3.14: Increasing Parameter Error Distance with $\tilde{\mathbf{w}}_{k-1} \in \mathcal{E}(d_i(k))$

Assuming non-stalling adaptation (cf. Assumption 3.1), if step-size condition (3.41) is satisfied for any $\alpha(k) \in \mathbb{C}$, and if $\tilde{\mathbf{w}}_{k-1} \in \mathcal{E}(d_i(k))$, an excitation vector can be found such that the parameter error increment $W(k)$ is positive iff

$$\frac{|\alpha(k)|}{\cos(\arccos(\alpha(k)))} > 2 \frac{d_i(k)}{d_{\max}(k)}. \quad (3.70)$$

Specifically, for i such that $d_i(k) = d_{\max}$, (3.70) can never be satisfied.

Proof. See Appendix D.1.8. □

The final piece that is required before the questions posed by the simulation example in Section 3.1 can be answered, concerns the existence of an excitation vector such that the parameter error

increment $W(k)$ is positive. Lemma 3.15 is a version of Lemma 3.4 tailored to the case that the regression vector is not independent from the excitation vector but related to the latter via step-size matrix \mathbf{D}_k .

Lemma 3.15: Expanding Behaviour for $\tilde{\mathbf{w}}_{k-1} \not\parallel \mathbf{D}_k \tilde{\mathbf{w}}_{k-1}$

For non-stalling adaptation (cf. Assumption 3.1), and if the parameter error vector $\tilde{\mathbf{w}}_{k-1}$ is not completely contained in one single eigenspace of the positive definite step-size matrix \mathbf{D}_k , i.e., $\tilde{\mathbf{w}}_{k-1} \not\parallel \mathbf{D}_k \tilde{\mathbf{w}}_{k-1}$, there always exists at least one excitation vector for which the parameter error distance increases.

Proof. See Appendix D.1.9. However, note that this proof relies on Inequality (3.92), which is obtained further down on page 60. The reader may prefer to temporarily postpone the proof until the latter inequality is derived and explained. A corresponding reminder is included there. \square

Figure 3.8 further down in Section 3.5 gives a geometrically illustrative interpretation of Lemma 3.15. Note that in the context of the SR-LMS algorithm – which also belongs to the class of asymmetric algorithms – [CM81] came to an insight that agrees with Lemma 3.15.

3.4.4 Impact of Matrix Step-Sizes to the Convergence Behaviour

With all the insights obtained in Sections 3.4.1 to 3.4.3, it is now possible to return to the simulation example in Section 3.1. Specifically, the three questions that are raised on page 31, are still open. They are repeated here, for convenience:

1. Does Algorithm II in fact diverge under w.c. excitation?
2. Does the parameter error vector of the other two algorithms actually remain bounded?
3. What exactly makes the difference which decides on boundedness or divergence?

For Algorithm I, Question 2 can be answered based on existing results from literature [RC00]. Accordingly, an asymmetric algorithm with invariant positive definite step-size matrix can be mapped to a symmetric algorithm, i.e., algorithms out of the LMS family, which allows to resort to the wide range of available analyses that have been conducted for the latter. As a consequence, for the step-sizes chosen in the simulation experiments, the parameter error vector of Algorithm I is ensured to remain bounded. In fact, for PE it is even guaranteed to converge – in the noiseless case – to the zero vector [e.g., Bit84; SR96; Hay02; Say03]. Nevertheless, as a first step to the answer of Question 3, the following theorem is given.

Theorem 3.2: Bounded Parameter Error Distance for Constant Matrix Step-Size

If (3.15) is satisfied, and the step-size matrix is positive definite and constant, i.e., $\mathbf{D}_k = \mathbf{D}$, with its minimum and maximum eigenvalue, d_{\min} and d_{\max} , defined by (3.67), then, under w.c. excitation, parameter error vector $\tilde{\mathbf{w}}_k$ converges to one of the eigenspaces $\mathcal{E}(d_i)$, for which

$$\alpha(k) \leq 2 \frac{d_i}{d_{\max}}. \quad (3.71)$$

Proof. For $\tilde{\mathbf{w}}_{k-1} \not\parallel \mathbf{D}\tilde{\mathbf{w}}_{k-1}$, the existence of an \mathbf{u}_k leading to $W(k) > 0$ is ensured by Lemma 3.15. Due to Lemma 3.5, such an increase will additionally turn the parameter error vector into the direction of the regression vector \mathbf{x}_k . As the latter is given by $\mathbf{x}_k = \mathbf{D}\mathbf{u}_k$, Lemma 3.9 allows to conclude that \mathbf{x}_k tends to turn towards the eigenspaces of step-size matrix \mathbf{D} that correspond to eigenvalues with larger magnitude. Therefore, as $\tilde{\mathbf{w}}_{k-1}$ follows \mathbf{x}_k , it also tends to align with the eigenspaces of eigenvalues with larger magnitude. Lemmas 3.11 and 3.15 show that this process goes on until the parameter error vector perfectly aligns with one of the eigenspaces of \mathbf{D} , i.e., $\tilde{\mathbf{w}}_{k-1} \in \mathcal{E}(d_i)$. Then, as long as $\mathbf{u}_k \not\parallel \tilde{\mathbf{w}}_{k-1}$, from Lemma 3.13, it is seen that the next iteration will reduce the energy contained in the component of $\tilde{\mathbf{w}}_{k-1}$ that belongs to $\mathcal{E}(d_i)$, while the remaining components (that are zero before the iteration) increase their energy. Whether this also goes along with an increase of the overall parameter error increment is decided by the step-size bound given in Lemma 3.14. Accordingly, the parameter error increment will only increase if (3.70) is satisfied. Otherwise, it will at most remain constant. In the former case, the before described process will continue. In the latter case, the process has reached its maximum and the parameter error increment will either remain constant if Assumption 3.1 is violated, or decrease. This maximum is reached at latest as $\tilde{\mathbf{w}}_{k-1} \in \mathcal{E}(d_{\max})$. That $\|\tilde{\mathbf{w}}_k\|$ remains bounded during this process is a direct consequence of the above mentioned fact that an asymmetric algorithm with invariant step-size matrix can be mapped to a symmetric algorithm [RC00]. Finally, note that (3.71) is directly obtained from (3.70) by bounding the cosine by one. \square

The arguments used in the proof of Theorem 3.2 also give the answer to Question 2 with respect to Algorithm III. This algorithm shows considerable fluctuations in its step-size matrix. However, it keeps them sorted. Since the step-size matrix is diagonal, this means that also its eigenspaces remain constant – just the eigenvalues change. As the arguments in the above proof are exclusively based on the eigenspaces, from this perspective, the only difference among Algorithm I and III is that in the latter case, d_i and d_{\max} depend on the iteration index k . Note that under the assumption of non-stalling adaptation (cf. Assumption 3.1), (3.71) is always true for i such that $d_i = d_{\max}$, or with respect to Algorithm III, $d_i(k) = d_{\max}(k)$. Consequently, also in the latter case, the parameter error vector will converge to an eigenspaces of step-size matrix \mathbf{D}_k and thus, remain bounded.

Finally, Question 1 and Question 3 can be answered together by the following theorem.

Theorem 3.3: Necessary Condition for Parameter Divergence

If step-size condition (3.15) is satisfied, and the step-size matrix is positive definite, the parameter error vector can only diverge if all of the eigenspaces of the step-size matrix keep changing persistently.

Proof. The proof follows the same lines as the proof of Theorem 3.2. The difference is that due to Lemma 3.15, the ever changing eigenspaces allow for a permanent increase of the parameter error distance. As none of the eigenspaces remains constant, due to parameter leakage shown in Lemma 3.13, it is ensured that the parameter error vector does not get stuck in one of the eigenspaces. \square

As an addition to Theorem 3.3, Lemmas 3.5 and 3.9 allow the loose interpretation that under w.c. excitation, the parameter error vector is “dragged” around in the containing space. Where the direction of change is dictated by the eigenspaces of the step-size matrix.

3.5 Worst Case Excitation – Analytic Approach

Section 3.4.2 is concerned with the existence of expanding behaviour based on the underlying geometric mechanisms that decide on convergence and divergence. This section in turn, provides analytic methods in order to design w.c. excitation sequences for asymmetric algorithms with positive definite diagonal step-size matrix. Again, based on Lemma 3.7 in Section 3.4.2, the such obtained results directly extend to the case of Hermitian step-size matrices and due to Lemma 3.8, they are also valuable for algorithms with non-Hermitian but normal step-size matrix.

Throughout this whole section, iteration index k is suppressed. Symbols $\tilde{\mathbf{w}}$ and $\mathbf{e}_{\tilde{\mathbf{w}}}$, refer to $\tilde{\mathbf{w}}_{k-1}$ and $\mathbf{e}_{\tilde{\mathbf{w}}_{k-1}}$, respectively. As a first step, the expression for parameter error increment W in (3.41) is modified to reflect the assumption of a positive definite diagonal step-size matrix

$$W = |\alpha|^2 |\tilde{\mathbf{w}}^T \mathbf{e}_{\mathbf{u}}|^2 - 2\text{Re} \left\{ \alpha (\tilde{\mathbf{w}}^T \mathbf{e}_{\mathbf{u}})^* \frac{\tilde{\mathbf{w}}^T \mathbf{D} \mathbf{e}_{\mathbf{u}}}{\|\mathbf{D} \mathbf{e}_{\mathbf{u}}\|} \right\}, \quad (3.72)$$

or equivalently,

$$W = \frac{1}{\|\mathbf{D} \mathbf{e}_{\mathbf{u}}\|} \left[\underbrace{|\alpha|^2 \|\mathbf{D} \mathbf{e}_{\mathbf{u}}\| |\tilde{\mathbf{w}}^T \mathbf{e}_{\mathbf{u}}|^2}_{\textcircled{1}} - 2\text{Re} \left\{ \alpha (\tilde{\mathbf{w}}^T \mathbf{e}_{\mathbf{u}})^* \tilde{\mathbf{w}}^T \mathbf{D} \mathbf{e}_{\mathbf{u}} \right\} \right]. \quad (3.73)$$

Term $\textcircled{2}$ in (3.73) is only affected by portions of the excitation vector that are contained in hyperplane

$$\mathcal{S}_{\tilde{\mathbf{w}}^*, \mathbf{D} \tilde{\mathbf{w}}^*} \triangleq \text{span} \{ \tilde{\mathbf{w}}^*, \mathbf{D} \tilde{\mathbf{w}}^* \}. \quad (3.74)$$

Term $\textcircled{1}$, in contrast, also depends on the components of \mathbf{u} that belong to the orthogonal complement of $\mathcal{S}_{\tilde{\mathbf{w}}^*, \mathbf{D} \tilde{\mathbf{w}}^*}$, i.e.,

$$\mathcal{S}_{\tilde{\mathbf{w}}^*, \mathbf{D} \tilde{\mathbf{w}}^*}^\perp \triangleq \left\{ \mathbf{x} \in \mathbb{C}^M \mid \mathbf{y}^H \mathbf{x} = 0, \forall \mathbf{y} \in \mathcal{S}_{\tilde{\mathbf{w}}^*, \mathbf{D} \tilde{\mathbf{w}}^*} \right\}. \quad (3.75)$$

Figure 3.8 schematically depicts the geometric meaning of (3.73) in a real-valued regime, projected onto the plane $\mathcal{S}_{\tilde{\mathbf{w}}^*, \mathbf{D} \tilde{\mathbf{w}}^*}$. The hatched areas represent the case $W > 0$, i.e., the areas of increasing parameter error distance. More specifically, the single hatching indicates those regions where Term $\textcircled{2}$ is less than zero. The double hatching refers to the case where Term $\textcircled{2}$ is positive but still too weak in order to compensate Term $\textcircled{1}$. Note that a similar argumentation has been adopted in the context of the SR-LMS algorithm in [CM81].

As Term $\textcircled{1}$ is non-negative, $W > 0$ is ensured, as soon as Term $\textcircled{2}$ is negative. Hence, sufficient conditions for $W > 0$ can be derived by restricting to an analysis of

$$\text{Re} \left\{ \alpha (\tilde{\mathbf{w}}^T \mathbf{e}_{\mathbf{u}})^* \tilde{\mathbf{w}}^T \mathbf{D} \mathbf{e}_{\mathbf{u}} \right\} < 0. \quad (3.76)$$

The following Section 3.5.1 focuses on excitation vectors – or more precisely the corresponding unit vectors $\mathbf{e}_{\mathbf{u}} \in \mathcal{S}_{\tilde{\mathbf{w}}^*, \mathbf{D} \tilde{\mathbf{w}}^*}$ – that satisfy (3.76) under the assumption of an arbitrary but given $\tilde{\mathbf{w}}$. Section 3.5.2 discusses the ramifications caused by components of the excitation vector that do *not* belong to hyperplane $\mathcal{S}_{\tilde{\mathbf{w}}^*, \mathbf{D} \tilde{\mathbf{w}}^*}$.

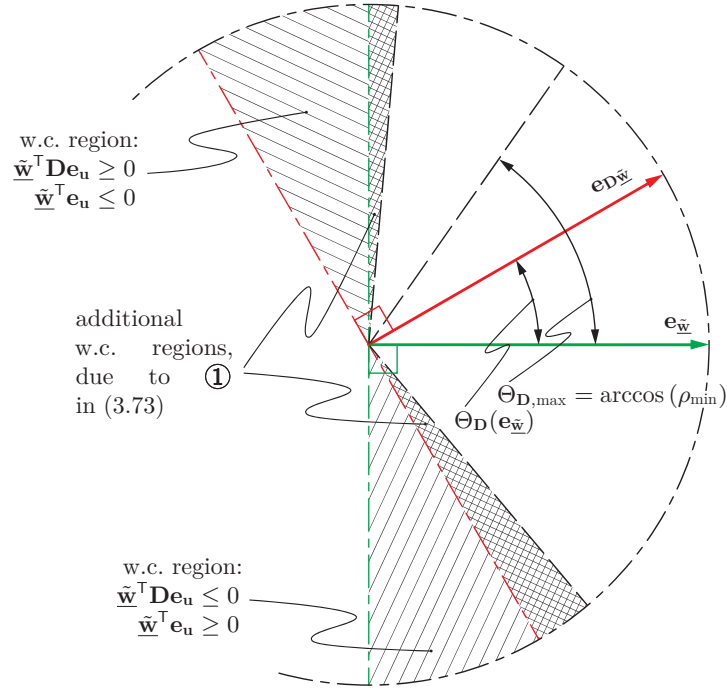


Figure 3.8: Geometric interpretation of the w.c. excitation regions within hyperplane $\mathcal{S}_{\tilde{\mathbf{w}}^*, \mathbf{D}_{\tilde{\mathbf{w}}^*}}$, spanned by the excitation vector and the regression vector. If the projection of some excitation vector onto $\mathcal{S}_{\tilde{\mathbf{w}}^*, \mathbf{D}_{\tilde{\mathbf{w}}^*}}$ is contained within any of the hatched w.c. regions, the parameter error increment $W(k)$ is ensured to be non-negative. Note that the two w.c. sectors caused by ① in (3.73) do not necessarily have the same opening angle. The cosine of the maximally possible angle $\Theta_{\mathbf{D}, \max}$ between $\mathbf{e}_{\tilde{\mathbf{w}}}$ and $\mathbf{e}_{\mathbf{D}_{\tilde{\mathbf{w}}}}$ coincides with ρ_{\min} from (3.66). Note that $\mathbf{e}_{\mathbf{D}_{\tilde{\mathbf{w}}}}$ is the unit vector corresponding to $\mathbf{D}_{\tilde{\mathbf{w}}}$

3.5.1 Identification of Worst Case Excitation Vectors

As this section focuses on the excitation vectors that satisfy (3.76), only those of their components that are contained in $\mathcal{S}_{\tilde{\mathbf{w}}^*, \mathbf{D}_{\tilde{\mathbf{w}}^*}}$ (cf. (3.74)), are relevant here. This is reflected by the decomposition

$$\mathbf{e}_{\mathbf{u}} = a_{\mathbf{u}} \mathbf{e}_{\tilde{\mathbf{w}}}^* + b_{\mathbf{u}} \mathbf{D} \mathbf{e}_{\tilde{\mathbf{w}}}^* = [a_{\mathbf{u}} \mathbf{I} + b_{\mathbf{u}} \mathbf{D}] \mathbf{e}_{\tilde{\mathbf{w}}}^*, \quad (3.77)$$

with coefficients $a_{\mathbf{u}}, b_{\mathbf{u}} \in \mathbb{C}$. In order to satisfy $\|\mathbf{e}_{\mathbf{u}}\| = 1$, they have to satisfy

$$\|\mathbf{e}_{\mathbf{u}}\| = f_{\mathbf{D}}(\mathbf{e}_{\tilde{\mathbf{w}}}, a_{\mathbf{u}}, b_{\mathbf{u}}) \stackrel{!}{=} 1, \quad (3.78)$$

with the newly introduced function

$$f_{\mathbf{D}}(\mathbf{e}_{\tilde{\mathbf{w}}}, a_{\mathbf{u}}, b_{\mathbf{u}}) \triangleq \sqrt{|a_{\mathbf{u}}|^2 + |b_{\mathbf{u}}|^2 \|\mathbf{D} \mathbf{e}_{\tilde{\mathbf{w}}}\|^2 + 2 \operatorname{Re}\{a_{\mathbf{u}}^* b_{\mathbf{u}}\} \|\mathbf{D}^{1/2} \mathbf{e}_{\tilde{\mathbf{w}}}\|^2}. \quad (3.79)$$

Inserting (3.78) in (3.76), together with the substitutions

$$\mathbf{e}_{\tilde{\mathbf{w}}}^{\top} \mathbf{e}_{\mathbf{u}} = a_{\mathbf{u}} + b_{\mathbf{u}} \mathbf{e}_{\tilde{\mathbf{w}}}^{\top} \mathbf{D} \mathbf{e}_{\tilde{\mathbf{w}}}^*, \quad (3.80)$$

$$\mathbf{e}_{\tilde{\mathbf{w}}}^{\top} \mathbf{D} \mathbf{e}_{\mathbf{u}} = a_{\mathbf{u}} \mathbf{e}_{\tilde{\mathbf{w}}}^{\top} \mathbf{D} \mathbf{e}_{\tilde{\mathbf{w}}}^* + b_{\mathbf{u}} \|\mathbf{D} \mathbf{e}_{\tilde{\mathbf{w}}}\|^2, \quad (3.81)$$

after division by $\|\tilde{\mathbf{w}}\|^2$ and with $\alpha \in \mathbb{R}_+$ (cf. Assumption 3.2), leads to

$$\|\mathbf{D}^{1/2} \mathbf{e}_{\tilde{\mathbf{w}}}\|^2 + \operatorname{Re}\{a_{\mathbf{u}}^* b_{\mathbf{u}}\} \left[\|\mathbf{D} \mathbf{e}_{\tilde{\mathbf{w}}}\|^2 - \|\mathbf{D}^{1/2} \mathbf{e}_{\tilde{\mathbf{w}}}\|^4 \right] < 0. \quad (3.82)$$

The cosine of angle $\Theta_{\mathbf{D}}(\mathbf{e}_{\underline{\mathbf{w}}})$ between vectors $\mathbf{e}_{\underline{\mathbf{w}}}$ and $\mathbf{D}\mathbf{e}_{\underline{\mathbf{w}}}$, is given by the ratio

$$0 < \cos(\Theta_{\mathbf{D}}(\mathbf{e}_{\underline{\mathbf{w}}})) \triangleq \frac{\|\mathbf{D}^{1/2}\mathbf{e}_{\underline{\mathbf{w}}}\|^2}{\|\mathbf{D}\mathbf{e}_{\underline{\mathbf{w}}}\|} \leq \bar{\lambda}_1(\mathbf{D}) \triangleq \frac{2\sqrt{d_1 d_M}}{d_1 + d_M} \leq 1. \quad (3.83)$$

The bound on the left-hand side is a direct consequence of the positive definiteness of step-size matrix \mathbf{D} . The bound on the right-hand side corresponds to the first antieigenvalue $\bar{\lambda}_1(\mathbf{D})$ of step-size matrix \mathbf{D} . It is a fundamental notion introduced in the context of operator trigonometry [Gus95; GR97; Gus00]. Details and further definitions can be found in Appendix C.1. Clearly, (3.83) entails

$$0 \leq |\Theta_{\mathbf{D}}(\mathbf{e}_{\underline{\mathbf{w}}})| < \frac{\pi}{2}. \quad (3.84)$$

Equation (3.83) together with the trigonometric identity $\sin^2(\Theta_{\mathbf{D}}(\mathbf{e}_{\underline{\mathbf{w}}})) = 1 - \cos^2(\Theta_{\mathbf{D}}(\mathbf{e}_{\underline{\mathbf{w}}}))$ modifies (3.82) to

$$\cos(\Theta_{\mathbf{D}}(\mathbf{e}_{\underline{\mathbf{w}}})) + \operatorname{Re}\{a_{\mathbf{u}}^* b_{\mathbf{u}}\} \|\mathbf{D}\mathbf{e}_{\underline{\mathbf{w}}}\| \sin^2(\Theta_{\mathbf{D}}(\mathbf{e}_{\underline{\mathbf{w}}})) < 0. \quad (3.85)$$

With the complex argument of the product $a_{\mathbf{u}}^* b_{\mathbf{u}}$,

$$\varphi_{a_{\mathbf{u}} b_{\mathbf{u}}} \triangleq \operatorname{arc}(a_{\mathbf{u}}^* b_{\mathbf{u}}), \quad (3.86)$$

(3.85) becomes

$$\underbrace{\cos(\Theta_{\mathbf{D}}(\mathbf{e}_{\underline{\mathbf{w}}}))}_{\in(0,1]} + \underbrace{|a_{\mathbf{u}}| |b_{\mathbf{u}}|}_{\geq 0} \underbrace{\|\mathbf{D}\mathbf{e}_{\underline{\mathbf{w}}}\|}_{> 0} \underbrace{\sin^2(\Theta_{\mathbf{D}}(\mathbf{e}_{\underline{\mathbf{w}}}))}_{\in(0,1)} \underbrace{\cos(\varphi_{a_{\mathbf{u}} b_{\mathbf{u}}})}_{\in[-1,1]} < 0. \quad (3.87)$$

Thus, (3.82), or equivalently, (3.76), can only be satisfied if

$$|\varphi_{a_{\mathbf{u}} b_{\mathbf{u}}}| \in \left(\frac{\pi}{2}, \pi\right]. \quad (3.88)$$

With (3.88) being fulfilled, Inequalities (3.82) and (3.87) provide the following condition for $W > 0$

$$|a_{\mathbf{u}}| |b_{\mathbf{u}}| |\cos(\varphi_{a_{\mathbf{u}} b_{\mathbf{u}}})| > \frac{\|\mathbf{D}^{1/2}\mathbf{e}_{\underline{\mathbf{w}}}\|^2}{\|\mathbf{D}\mathbf{e}_{\underline{\mathbf{w}}}\|^2 - \|\mathbf{D}^{1/2}\mathbf{e}_{\underline{\mathbf{w}}}\|^4} = \frac{\cos(\Theta_{\mathbf{D}}(\mathbf{e}_{\underline{\mathbf{w}}}))}{\|\mathbf{D}\mathbf{e}_{\underline{\mathbf{w}}}\| \sin^2(\Theta_{\mathbf{D}}(\mathbf{e}_{\underline{\mathbf{w}}}))}. \quad (3.89)$$

Using the complex argument $\varphi_{a_{\mathbf{u}} b_{\mathbf{u}}}$, (3.79) can be equivalently written as

$$f_{\mathbf{D}}(\mathbf{e}_{\underline{\mathbf{w}}}, a_{\mathbf{u}}, b_{\mathbf{u}}) = \sqrt{|a_{\mathbf{u}}|^2 + |b_{\mathbf{u}}|^2 \|\mathbf{D}\mathbf{e}_{\underline{\mathbf{w}}}\|^2 + 2|a_{\mathbf{u}}| |b_{\mathbf{u}}| \cos(\varphi_{a_{\mathbf{u}} b_{\mathbf{u}}}) \|\mathbf{D}^{1/2}\mathbf{e}_{\underline{\mathbf{w}}}\|^2}, \quad (3.90)$$

by which (3.78) entails

$$|a_{\mathbf{u}}|^2 + |b_{\mathbf{u}}|^2 \|\mathbf{D}\mathbf{e}_{\underline{\mathbf{w}}}\|^2 + 2|a_{\mathbf{u}}| |b_{\mathbf{u}}| \cos(\varphi_{a_{\mathbf{u}} b_{\mathbf{u}}}) \|\mathbf{D}^{1/2}\mathbf{e}_{\underline{\mathbf{w}}}\|^2 = 1. \quad (3.91)$$

Condition (3.91) makes clear that the magnitudes of the coefficients, $a_{\mathbf{u}}$ and $b_{\mathbf{u}}$, are elliptically interrelated. This fact is illustrated by Figure 3.9, which also visualises the parametrisation of the coefficients $a_{\mathbf{u}}$ and $b_{\mathbf{u}}$, summarised in Definition Table 3.1. A detailed derivation is provided in Appendix B.

Eventually, this shows that (3.76), and thus $W > 0$, is satisfied if complex argument $\varphi_{a_{\mathbf{u}} b_{\mathbf{u}}}$ and product $|a_{\mathbf{u}}| |b_{\mathbf{u}}|$ fulfil (3.88) and (3.89), respectively. In the $\langle |a_{\mathbf{u}}|, |b_{\mathbf{u}}| \rangle$ -plane, (3.89) covers all points

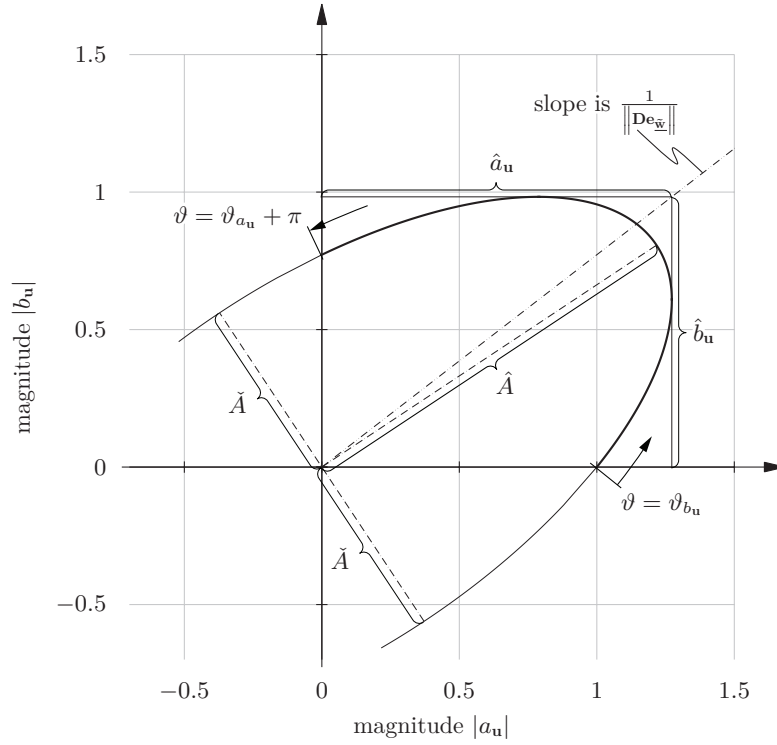


Figure 3.9: Relation among magnitudes $|a_u|$ and $|b_u|$, with effective step-size $\alpha = 1$, strongly decaying step-size matrix $\mathbf{D} = \sqrt{M} \text{diag}_{i=0}^{M-1} \{10^{-3}(M-i)^4\}$, and parameter error vector $\underline{\mathbf{w}} = \mathbf{1}$. Definition Table 3.1 defined the referenced symbols. A detailed derivation can be found in Appendix B.

that lie above a hyperbola, which asymptotes coincide with the $|a_u|$ -axis and $|b_u|$ -axis. Consequently, together with the afore developed insight that $|a_u|$ and $|b_u|$ depend elliptically from each other, the solutions of (3.89) are found by overlapping a hyperbola with an ellipsis. This fact is illustrated in Figure 3.10, where three cases of complex argument $\varphi_{a_u b_u}$ are considered. At this point, details about their meaning are not important, they will be clarified further down, in the context of Inequality (3.92). However, what can already be observed, is that for $|\varphi_{a_u b_u}| = \pi$, a clear overlap occurs. For the other two values of $|\varphi_{a_u b_u}|$, in one case, both geometric objects touch only in one point, in the other case, they are completely disjoint. Accordingly, out of these three scenarios, only for the first one, (3.89) has a solution – in fact, a whole range of solutions. A detailed derivation of the just described intersection process is included in Appendix B. Therein, (B.32) provides the minimum magnitude of angle $\varphi_{a_u b_u}$ that solves (3.89). Accordingly, a solution of the latter only exists, if⁶

$$\cos(\varphi_{a_u b_u}) > \cos(\check{\varphi}_{a_u b_u}^{\text{limit}}) = \frac{2 \|\mathbf{D}\mathbf{e}_{\underline{\mathbf{w}}}\| \|\mathbf{D}^{1/2}\mathbf{e}_{\underline{\mathbf{w}}}\|^2}{\|\mathbf{D}\mathbf{e}_{\underline{\mathbf{w}}}\|^2 + \|\mathbf{D}^{1/2}\mathbf{e}_{\underline{\mathbf{w}}}\|^4} = \frac{2 \cos(\Theta_{\mathbf{D}}(\mathbf{e}_{\underline{\mathbf{w}}}))}{1 + \cos^2(\Theta_{\mathbf{D}}(\mathbf{e}_{\underline{\mathbf{w}}}))}. \quad (3.92)$$

⁶ As a reminder, Inequality (3.92) completes the prerequisites that are required for the proof of Lemma 3.15. Hence, all the arguments in the corresponding Appendix D.1.9 are accessible at this point.

Definition Table 3.1: Parametrisation of Worst Case, given by (3.77)

$$|a_{\mathbf{u}}| = \hat{a}_{\mathbf{u}} \sin(\vartheta - \vartheta_{a_{\mathbf{u}}}), \quad |b_{\mathbf{u}}| = \hat{b}_{\mathbf{u}} \sin(\vartheta - \vartheta_{b_{\mathbf{u}}}), \quad \vartheta \in [\vartheta_{b_{\mathbf{u}}}, \vartheta_{a_{\mathbf{u}}} + \pi], \quad (3.93)$$

with the amplitudes

$$\hat{a}_{\mathbf{u}} \triangleq \|\mathbf{D}\mathbf{e}_{\tilde{\mathbf{w}}}\| \hat{b}_{\mathbf{u}}, \quad (3.94)$$

$$\begin{aligned} \hat{b}_{\mathbf{u}} &\triangleq \frac{\|\mathbf{D}\mathbf{e}_{\tilde{\mathbf{w}}}\|}{\sqrt{\|\mathbf{D}\mathbf{e}_{\tilde{\mathbf{w}}}\|^2 - \|\mathbf{D}^{1/2}\mathbf{e}_{\tilde{\mathbf{w}}}\|^4 \cos^2(\varphi_{a_{\mathbf{u}}b_{\mathbf{u}}})}} \\ &= \frac{1}{\sqrt{1 - \cos^2(\Theta_{\mathbf{D}}(\mathbf{e}_{\tilde{\mathbf{w}}})) \cos^2(\varphi_{a_{\mathbf{u}}b_{\mathbf{u}}})}}. \end{aligned} \quad (3.95)$$

The offset angles are given by

$$\begin{aligned} \vartheta_{a_{\mathbf{u}}} &\triangleq \arctan \left(\frac{\sqrt{\|\mathbf{D}\mathbf{e}_{\tilde{\mathbf{w}}}\|^2 - \|\mathbf{D}^{1/2}\mathbf{e}_{\tilde{\mathbf{w}}}\|^4 \cos^2(\varphi_{a_{\mathbf{u}}b_{\mathbf{u}}})}}{\|\mathbf{D}^{1/2}\mathbf{e}_{\tilde{\mathbf{w}}}\|^2 \cos(\varphi_{a_{\mathbf{u}}b_{\mathbf{u}}})} (1 - \|\mathbf{D}\mathbf{e}_{\tilde{\mathbf{w}}}\|^2 \hat{A}^2) \right) \\ &= \arctan \left(\frac{\sqrt{1 - \cos^2(\Theta_{\mathbf{D}}(\mathbf{e}_{\tilde{\mathbf{w}}})) \cos^2(\varphi_{a_{\mathbf{u}}b_{\mathbf{u}}})}}{\cos(\Theta_{\mathbf{D}}(\mathbf{e}_{\tilde{\mathbf{w}}})) \cos(\varphi_{a_{\mathbf{u}}b_{\mathbf{u}}})} (1 - \|\mathbf{D}\mathbf{e}_{\tilde{\mathbf{w}}}\|^2 \hat{A}^2) \right), \quad (3.96) \\ \vartheta_{b_{\mathbf{u}}} &\triangleq -\arctan \left(\frac{\|\mathbf{D}^{1/2}\mathbf{e}_{\tilde{\mathbf{w}}}\|^2 \cos(\varphi_{a_{\mathbf{u}}b_{\mathbf{u}}})}{\sqrt{\|\mathbf{D}\mathbf{e}_{\tilde{\mathbf{w}}}\|^2 - \|\mathbf{D}^{1/2}\mathbf{e}_{\tilde{\mathbf{w}}}\|^4 \cos^2(\varphi_{a_{\mathbf{u}}b_{\mathbf{u}}})} \hat{A}^2 - 1} \right) + \begin{cases} \pi; & \cos(\varphi_{a_{\mathbf{u}}b_{\mathbf{u}}}) > 0 \\ 0; & \text{otherwise} \end{cases} \\ &= -\arctan \left(\frac{\cos(\Theta_{\mathbf{D}}(\mathbf{e}_{\tilde{\mathbf{w}}})) \cos(\varphi_{a_{\mathbf{u}}b_{\mathbf{u}}})}{\sqrt{1 - \cos^2(\Theta_{\mathbf{D}}(\mathbf{e}_{\tilde{\mathbf{w}}})) \cos^2(\varphi_{a_{\mathbf{u}}b_{\mathbf{u}}})} \hat{A}^2 - 1} \right) + \begin{cases} \pi; & \cos(\varphi_{a_{\mathbf{u}}b_{\mathbf{u}}}) > 0 \\ 0; & \text{otherwise} \end{cases}. \end{aligned} \quad (3.97)$$

The lengths of the semi-major and semi-minor axes of the resulting ellipse are found as

$$\{\hat{A}, \check{A}\} \triangleq \sqrt{\frac{1 + \|\mathbf{D}\mathbf{e}_{\tilde{\mathbf{w}}}\|^2 \pm \sqrt{(1 - \|\mathbf{D}\mathbf{e}_{\tilde{\mathbf{w}}}\|^2)^2 - 4\|\mathbf{D}^{1/2}\mathbf{e}_{\tilde{\mathbf{w}}}\|^4 \cos^2(\varphi_{a_{\mathbf{u}}b_{\mathbf{u}}})}}{2\|\mathbf{D}^{1/2}\mathbf{e}_{\tilde{\mathbf{w}}}\|^4 \cos^2(\varphi_{a_{\mathbf{u}}b_{\mathbf{u}}})}}, \quad (3.98)$$

which is meant in the sense that \hat{A} is obtained by the positive and \check{A} by the negative square-root. Finally, note that the difference $\vartheta_{a_{\mathbf{u}},b_{\mathbf{u}}} \triangleq \vartheta_{a_{\mathbf{u}}} - \vartheta_{b_{\mathbf{u}}}$ of the offset angles satisfies

$$\cos(\vartheta_{a_{\mathbf{u}},b_{\mathbf{u}}}) = \frac{\|\mathbf{D}^{1/2}\mathbf{e}_{\tilde{\mathbf{w}}}\|^2 |\cos(\varphi_{a_{\mathbf{u}}b_{\mathbf{u}}})|}{\|\mathbf{D}\mathbf{e}_{\tilde{\mathbf{w}}}\|} = \cos(\Theta_{\mathbf{D}}(\mathbf{e}_{\tilde{\mathbf{w}}})) |\cos(\varphi_{a_{\mathbf{u}}b_{\mathbf{u}}})|. \quad (3.99)$$

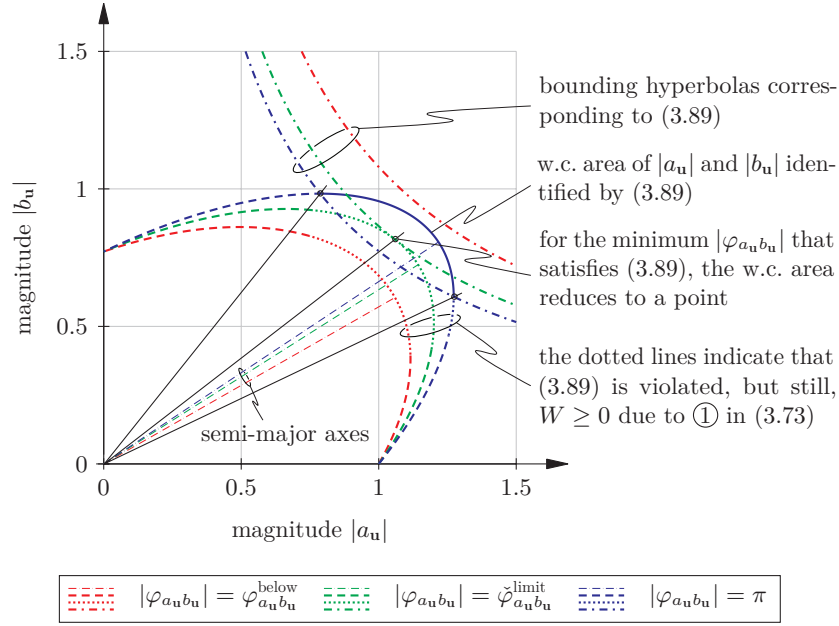


Figure 3.10: Visualisation of the overlapping process described by (3.89). Additionally, the impact of Terms ① and ② in (3.73) can be identified. The solid lines correspond to a negative Term ②, which coincides with an overlap of hyperbola and the ellipsis. The dotted lines represent the case when Term ② is positive but still less than Term ①, again causing $W > 0$. Then, (3.89) does not have a solution, which is represented by $\varphi_{a_u b_u} = \varphi_{a_u b_u}^{\text{below}}$. Dashed parts of the elliptic arcs refer to pairs $\langle a_u, b_u \rangle$ that ensure a *decreasing* parameter error distance.

Returning to Figure 3.10 for a second time, the lacking details can be discussed now. It is easy to see that the range of product $|a_u| |b_u|$ that satisfies (3.89), grows with increasing $|\varphi_{a_u b_u}| \in (\frac{\pi}{2}, \pi]$. This is the reason why in Figure 3.10, for $|\varphi_{a_u b_u}| = \pi$, the overlap between hyperbola and ellipsis is most extensive. According to (3.92), $\varphi_{a_u b_u}^{\text{limit}}$ is the limiting angle (in magnitude) for (3.89). This is represented in Figure 3.10 by the pair of hyperbola and ellipsis that touches only in one point. Finally, for $|\varphi_{a_u b_u}| = \varphi_{a_u b_u}^{\text{below}} < \varphi_{a_u b_u}^{\text{limit}}$, no solution exists for (3.89), which is reflected by the disjoint pair of curves.

In addition to the visual evaluation of (3.89), which only relies on Term ② in (3.73), Figure 3.10 also gives insight to the impact of Term ①. While the solid lines of the elliptic arcs indicate negative values of Term ②, portions for which the latter is positive but still less than Term ①, are depicted by dotted lines. Note that even in the third case for which $|\varphi_{a_u b_u}| = \varphi_{a_u b_u}^{\text{below}}$, a dotted part exists, meaning that there still $W > 0$. This confirms that the limiting angle $\varphi_{a_u b_u}^{\text{limit}}$ in (3.92) is a conservative bound for the complex argument among the pair of coefficients $\langle a_u, b_u \rangle$ that allows for an increase of the parameter error distance.

3.5.2 Influence of Orthogonal Components of the Excitation Vector

In (3.73), it is found that Term ② is only influenced by the portions of \mathbf{u} that belong to hyperplane $\mathcal{S}_{\bar{\mathbf{w}}^*}^*, \mathcal{D}_{\bar{\mathbf{w}}^*}^*$, defined in (3.74). While the same applies to the squared magnitude of the inner product of Term ① in (3.73), squared norm $\|\mathbf{D}\mathbf{e}_u\|^2$ is modified by any change of \mathbf{u} , independently whether inside and outside of $\mathcal{S}_{\bar{\mathbf{w}}^*}^*, \mathcal{D}_{\bar{\mathbf{w}}^*}^*$. This can be quantified, if corresponding unit vector \mathbf{e}_u is decomposed into two orthogonal parts,

$$\mathbf{e}_u = a_S^{\parallel} \mathbf{e}_S^{\parallel} + b_S^{\perp} \mathbf{e}_S^{\perp}, \quad (3.100)$$

with unit vectors (cf. (3.74) and (3.75))

$$\mathbf{e}_S^{\parallel} \in \mathcal{S}_{\tilde{\mathbf{w}}^*, \mathbf{D}\tilde{\mathbf{w}}^*}, \quad \text{and} \quad \mathbf{e}_S^{\perp} \in \mathcal{S}_{\tilde{\mathbf{w}}^*, \mathbf{D}\tilde{\mathbf{w}}^*}^{\perp}. \quad (3.101)$$

Thus, taking into account that \mathbf{e}_S^{\parallel} and \mathbf{e}_S^{\perp} can incorporate any arbitrary phase rotation, w.o.l.o.g., coefficients a_S^{\parallel} and b_S^{\perp} can be restricted to be real-valued, hence,

$$a_S^{\parallel}, b_S^{\perp} \in [0, 1], \quad \text{and} \quad b_S^{\perp} = \sqrt{1 - a_S^{\parallel 2}}. \quad (3.102)$$

Since $\tilde{\mathbf{w}}^{\top} \mathbf{e}_u = a_S^{\parallel} \tilde{\mathbf{w}}^{\top} \mathbf{e}_S^{\parallel}$ and $\tilde{\mathbf{w}}^{\top} \mathbf{D} \mathbf{e}_u = a_S^{\parallel} \tilde{\mathbf{w}}^{\top} \mathbf{D} \mathbf{e}_S^{\parallel}$, inserting (3.100) in (3.73), leads to

$$W = \frac{a_S^{\parallel 2}}{\|\mathbf{D} \mathbf{e}_u\|} \left[|\alpha|^2 \|\mathbf{D} \mathbf{e}_u\| \left| \tilde{\mathbf{w}}^{\top} \mathbf{e}_S^{\parallel} \right|^2 - 2 \operatorname{Re} \left\{ \alpha \left(\tilde{\mathbf{w}}^{\top} \mathbf{e}_S^{\parallel} \right)^* \tilde{\mathbf{w}}^{\top} \mathbf{D} \mathbf{e}_S^{\parallel} \right\} \right], \quad (3.103)$$

where

$$\|\mathbf{D} \mathbf{e}_u\|^2 = a_S^{\parallel 2} \|\mathbf{D} \mathbf{e}_S^{\parallel}\|^2 + (1 - a_S^{\parallel 2}) \|\mathbf{D} \mathbf{e}_S^{\perp}\|^2 + 2a_S^{\parallel} \sqrt{1 - a_S^{\parallel 2}} \operatorname{Re} \left\{ \mathbf{e}_S^{\parallel \text{H}} \mathbf{D} \mathbf{D} \mathbf{e}_S^{\perp} \right\}. \quad (3.104)$$

It is straight forward to see that with the extremal eigenvalues of \mathbf{D} , d_{\min} and d_{\max} , defined in (3.67),

$$\|\mathbf{D} \mathbf{e}_S^{\parallel}\| \in [d_{\min}, d_{\max}], \quad \text{as well as,} \quad \|\mathbf{D} \mathbf{e}_S^{\perp}\| \in [d_{\min}, d_{\max}]. \quad (3.105)$$

The right-most term in (3.104), which in general is complex-valued, can be bounded as

$$0 \leq \left| \operatorname{Re} \left\{ \mathbf{e}_S^{\parallel \text{H}} \mathbf{D} \mathbf{D} \mathbf{e}_S^{\perp} \right\} \right| \leq \left| \mathbf{e}_S^{\parallel \text{H}} \mathbf{D} \mathbf{D} \mathbf{e}_S^{\perp} \right| \leq \frac{d_{\max}^2 - d_{\min}^2}{2}, \quad (3.106)$$

where the maximum is assumed for

$$\mathbf{e}_S^{\parallel} = \frac{1}{\sqrt{2}} (\mathbf{e}_i + \mathbf{e}_j), \quad \mathbf{e}_S^{\perp} = \frac{1}{\sqrt{2}} (\mathbf{e}_i - \mathbf{e}_j), \quad (3.107)$$

if the unit vectors \mathbf{e}_i and \mathbf{e}_j are the eigenvectors that correspond to the minimum and the maximum eigenvalue of \mathbf{D} , respectively. In terms of ordering convention (2.30), this would mean $i = 1$ and $j = M$, or vice versa. That (3.107) actually leads to the maximum in (3.106), is a consequence of orthogonality $\mathbf{e}_S^{\parallel \text{H}} \mathbf{e}_S^{\perp} = 0$ and the Wielandt inequality (see (C.7)) [Rao05; Lin13]. Then,

$$\|\mathbf{D} \mathbf{e}_S^{\parallel}\|^2 = \|\mathbf{D} \mathbf{e}_S^{\perp}\|^2 = \frac{d_{\max}^2 + d_{\min}^2}{2}. \quad (3.108)$$

Comparing (3.103) with (3.73) shows that an analysis which does *not* restrict \mathbf{u} to hyperplane $\mathcal{S}_{\tilde{\mathbf{w}}^*, \mathbf{D}\tilde{\mathbf{w}}^*}$, except from scaling factor $a_S^{\parallel 2}$, does not affect Term ② in (3.73). However, Term ① in (3.73) is not only scaled by $a_S^{\parallel 2}$, since in (3.103), $\|\mathbf{D} \mathbf{e}_u\|$ occurs, instead of $\|\mathbf{D} \mathbf{e}_S^{\parallel}\|$. With all of the above insights, (3.103) can finally be re-written in a form of almost the same structure as (3.73),

$$W = \frac{a_S^{\parallel 2}}{\|\mathbf{D} \mathbf{e}_u\|} \left[|\alpha|^2 \gamma \|\mathbf{D} \mathbf{e}_S^{\parallel}\| \left| \tilde{\mathbf{w}}^{\top} \mathbf{e}_S^{\parallel} \right|^2 - 2 \operatorname{Re} \left\{ \alpha \left(\tilde{\mathbf{w}}^{\top} \mathbf{e}_S^{\parallel} \right)^* \tilde{\mathbf{w}}^{\top} \mathbf{D} \mathbf{e}_S^{\parallel} \right\} \right], \quad (3.109)$$

with factor

$$\begin{aligned} \gamma &\triangleq \frac{\|\mathbf{D}\mathbf{e}_{\mathbf{u}}\|}{\|\mathbf{D}\mathbf{e}_{\mathcal{S}}\|} \\ &= \sqrt{a_{\mathcal{S}}^{\parallel 2} + \underbrace{\left(1 - a_{\mathcal{S}}^{\parallel 2}\right) \frac{\|\mathbf{D}\mathbf{e}_{\mathcal{S}}^{\perp}\|^2}{\|\mathbf{D}\mathbf{e}_{\mathcal{S}}\|^2}}_{\in \left[\frac{d_{\min}^2}{d_{\max}^2}, \frac{d_{\max}^2}{d_{\min}^2}\right]} + 2a_{\mathcal{S}}^{\parallel} \sqrt{1 - a_{\mathcal{S}}^{\parallel 2}} \frac{\|\mathbf{D}\mathbf{e}_{\mathcal{S}}^{\perp}\|}{\|\mathbf{D}\mathbf{e}_{\mathcal{S}}\|} \underbrace{\operatorname{Re} \left\{ \frac{\mathbf{e}_{\mathcal{S}}^{\parallel \text{H}} \mathbf{D} \mathbf{D} \mathbf{e}_{\mathcal{S}}^{\perp}}{\|\mathbf{D}\mathbf{e}_{\mathcal{S}}\| \|\mathbf{D}\mathbf{e}_{\mathcal{S}}^{\perp}\|} \right\}}_{\substack{\text{due to the Wielandt inequality (C.7):} \\ \in \left[-\frac{d_{\max}^2 - d_{\min}^2}{d_{\max}^2 + d_{\min}^2}, \frac{d_{\max}^2 - d_{\min}^2}{d_{\max}^2 + d_{\min}^2} \right]} \right)}. \end{aligned} \quad (3.110)$$

Factor γ reflects how the instantaneous power of excitation vector \mathbf{u} divides into $\mathcal{S}_{\tilde{\mathbf{w}}^*, \mathbf{D}\tilde{\mathbf{w}}^*}$ and $\mathcal{S}_{\tilde{\mathbf{w}}^*, \mathbf{D}\tilde{\mathbf{w}}^*}^{\perp}$. It scales the expression on the left-hand side within the brackets of (3.109), and is contained in interval

$$\gamma \in \left[\frac{d_{\min}}{d_{\max}}, \frac{d_{\max}}{d_{\min}} \right]. \quad (3.111)$$

Figure 3.11 visualises the dependency of γ with respect to coefficient $a_{\mathcal{S}}^{\parallel}$. Shown are the minima and maxima for three different types of real-valued excitation vectors. The underlying step-size matrix is given by $\mathbf{D} = \operatorname{diag}_{i=1}^M \{1 - 0.6(i - 1)\}$. The two unit vectors in (3.100) have a specific mutually orthogonal form, according to

$$\mathbf{e}_{\mathcal{S}}^{\parallel} = \cos(\psi) \mathbf{e}_i + \sin(\psi) \mathbf{e}_j, \quad \mathbf{e}_{\mathcal{S}}^{\perp} = \cos(\psi) \mathbf{e}_i - \sin(\psi) \mathbf{e}_j, \quad (3.112)$$

where angle ψ is swept from $-\pi$ to π . The three cases only differ in the choice of the indices i and j :

Case	i	$j = M - i + 1$
1	1	10
2	3	8
3	5	6

The resulting graphs in Figure 3.11 confirm that components of \mathbf{u} which are orthogonal to $\mathcal{S}_{\tilde{\mathbf{w}}^*, \mathbf{D}\tilde{\mathbf{w}}^*}$, may either increase or reduce the w.c. subspace of \mathbb{C}^M that leads to a growth of the parameter error distance. In any case, vectors \mathbf{u} for which Term ② in (3.73) – or equivalently, the right-hand side term in the brackets of (3.109) – becomes negative, will always cause $W > 0$.

Finally, in order to assess the impact of orthogonal components to the synthesised w.c. sequences, the simulation experiment in Section 3.1, is repeated twice for Algorithm II with $\bar{\mu} = 0.5$. In both cases, w.c. excitation is used. However, in contrast to the original simulation setting in Section 3.1, which employed a search method to identify the w.c. directions, here, this is achieved by the afore introduced analytical approach. Once without any orthogonal components, i.e., $a_{\mathcal{S}}^{\parallel} = 1$. A second time, with excitation power $\|\mathbf{u}\|^2$ randomly distributed over all $M = 10$ dimensions, more specifically, in each iteration, $a_{\mathcal{S}}^{\parallel}$ is drawn equally likely from interval $[0, 1]$. Figure 3.12 depicts estimated parameter mismatch $m(k)$ (cf. (2.19)), for both cases. In accordance with (3.110), the second variant leads to slower growth than the first one, since the latter can resort to the complete excitation power to follow the diverging trajectories. For reference, also the results for the originally performed numerical search, with $N_{\text{w.c.}} = 10\,000$ random trials, is included. This allows to observe that the analytical w.c. synthesis outperforms the search method, with respect to their ability of maximising the rate of divergence.

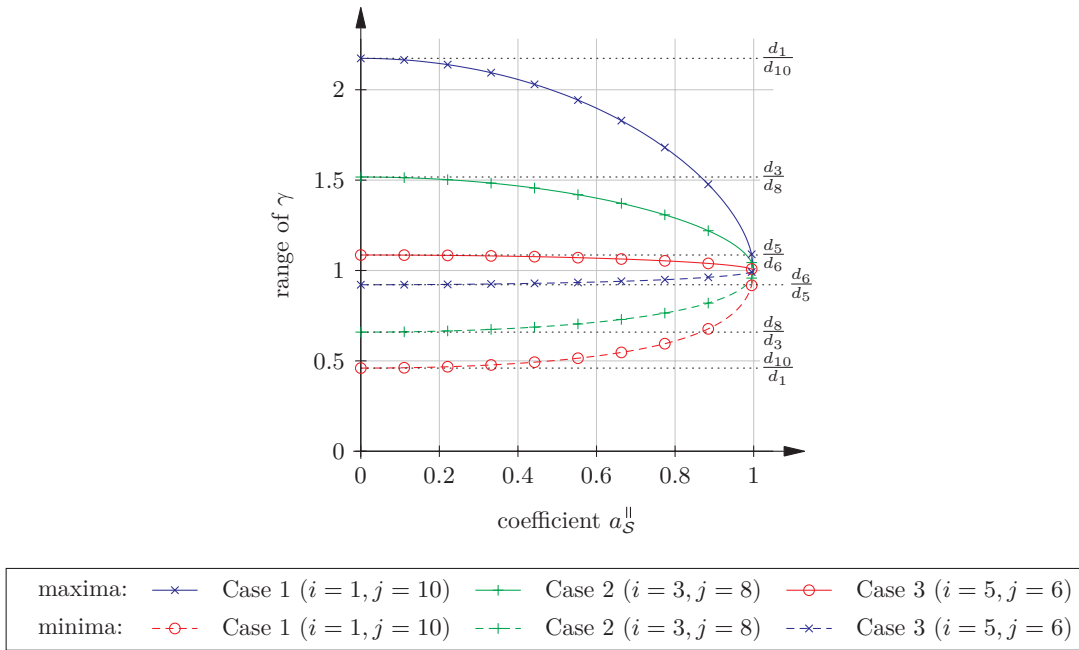


Figure 3.11: Numeric range of γ for three different types of excitation vectors. They are all decomposed according to (3.100), where \mathbf{e}_S^{\parallel} and \mathbf{e}_S^{\perp} are given by (3.112). The three cases only differ in the choice of the indices i and j , the step-size matrix is the same for all of them, and has the form $\mathbf{D} = \text{diag}_{i=1}^M \{1 - 0.6(i - 1)\}$.

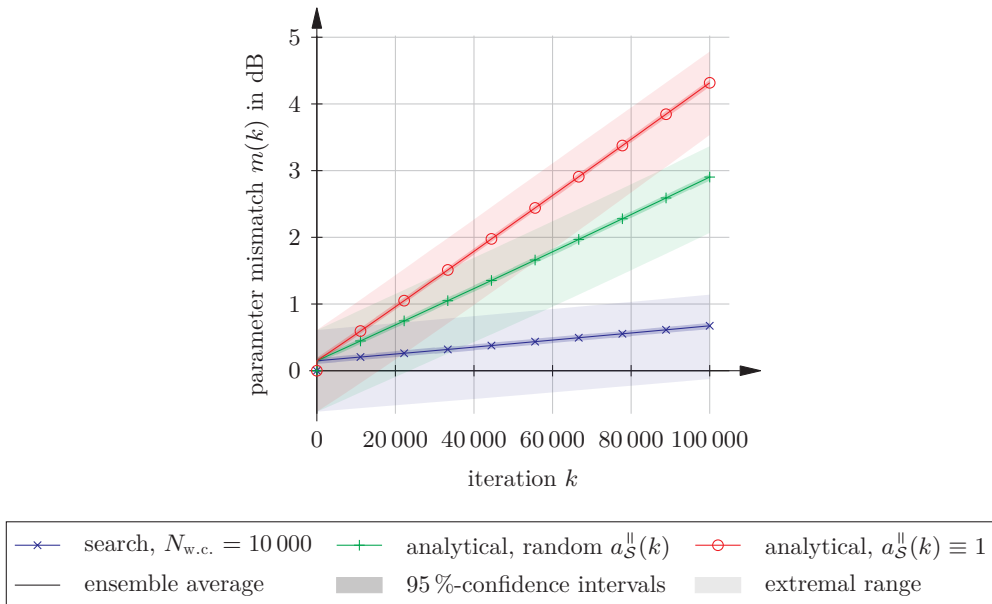


Figure 3.12: Comparison of the analytical w.c. synthesis, with ($a_S^{\parallel}(k)$ random within $[0, 1]$) and without ($a_S^{\parallel}(k) \equiv 1$) components of \mathbf{u}_k that are orthogonal to hyperplane $\mathcal{S}_{\tilde{\mathbf{w}}^*}, \mathcal{D}_{\tilde{\mathbf{w}}^*}$. Additionally, the w.c. search method, with $N_{w.c.} = 10\,000$ trials per iteration, described in Section 3.1, is included for reference. The data is obtained by the simulation experiment described in Section 3.1.

3.6 Worst Case Excitation – Numeric Search

In some situations, synthesis of w.c. excitation vectors is not possible with the analytic approach presented in Section 3.5, e.g., in cases where the step-size matrix is non-normal or, if the excitation space is restricted. As pointed out in Chapter 3, the primer case occurs only rarely – at least from a practical point of view. The second scenario, however, is of high relevance. For example, as described in Section 2.2.1.2, if the reference and the adaptive system represent FIR filters, the excitation vector is given by the delay vector in (2.21). Then, the first entry of \mathbf{u}_k corresponds to the most recent input sample, while the remaining vector elements contain the input samples from the foregoing $M - 1$ consecutive iterations. As the latter ones cannot be changed any more at that point, the space from which \mathbf{u}_k can be chosen collapses to a line in the M -dimensional space. A second example for a restricted excitation space is observed, if the individual elements of the excitation vector are taken from a restricted set. The simplest and most obvious case in context of telecommunications, is a binary symbol alphabet, meaning that each entry in \mathbf{u}_k can only assume one out of two values [BLM04].

Methods which allow to synthesise w.c. excitation sequences in such cases, are focus of this section. The most general formulation is given in terms of (2.17), without any assumption regarding the relation among \mathbf{u}_k and \mathbf{x}_k . Then, a pair of the latter is searched for, which satisfies

$$\langle \mathbf{u}_k, \mathbf{x}_k \rangle_{w.c.,k} \triangleq \arg \max_{\substack{\langle \mathbf{u}_k, \mathbf{x}_k \rangle \\ \|\mathbf{u}_k\| = U(k) \\ \|\mathbf{x}_k\| = X(k)}} \{ \|\mathbf{B}_k \tilde{\mathbf{w}}_{k-1}\| \}, \quad \text{with} \quad \mathbf{B}_k \triangleq \mathbf{I} - \mu(k) \mathbf{x}_k^* \mathbf{u}_k^T, \quad (3.113)$$

where $U(k) > 0$ and $X(k) > 0$ are some given vector lengths. The solution depends on initial value $\tilde{\mathbf{w}}_{-1}$, step-size $\mu(k)$, $U(k)$ and $X(k)$, as well as on the sets that underlie the individual elements of \mathbf{u}_k and \mathbf{x}_k . With respect to hidden divergence, larger values of $\mu(k)$, $U(k)$ and $X(k)$ lead to a larger w.c. space. This is a direct consequence of the findings about the maximum singular value of mapping matrix \mathbf{B}_k in Section 3.3.2. Alternatively, e.g., (3.76) also confirms this.

In the sequel, the search in (3.113) is tailored to two specific types of step-size matrices. Section 3.6.1 starts with the case of a general step-size matrix that maps the excitation vector linearly to the regression vector. The restriction to normal step-size matrices is discussed in Section 3.6.2.

3.6.1 General Step-Size Matrix

As a first step, in this section, (3.113) is reformulated in order to reflect the most general case of an asymmetric algorithm with matrix step-size, i.e., in accordance to (2.9). This means that (3.113) changes to

$$\mathbf{u}_{w.c.,k} \triangleq \arg \max_{\substack{\mathbf{u}_k \\ \|\mathbf{u}_k\| = U(k)}} \{ \|\mathbf{B}_k \tilde{\mathbf{w}}_{k-1}\| \}, \quad \text{with} \quad \mathbf{B}_k = \mathbf{I} - \mu(k) \mathbf{M}_k \mathbf{u}_k^* \mathbf{u}_k^T. \quad (3.114)$$

In contrast to (3.113), regression vector \mathbf{x}_k has here inherently moved to the right-hand side.

Below iteration index k is suppressed. Symbol $\tilde{\mathbf{w}}$ refers to $\tilde{\mathbf{w}}_{k-1}$. In Section 3.3.2, it was found that the left and right-sided singular vectors, \mathbf{r}_1 and \mathbf{t}_1 , corresponding to maximum singular value $\sigma_{\max} = \sigma_1$, as well as, \mathbf{r}_2 and \mathbf{t}_2 , corresponding to minimum singular value $\sigma_{\min} = \sigma_2$, are contained in hyperplane $\mathcal{S}_{\mathbf{u}^*, \mathbf{x}^*}$ (cf. (3.18)). Accordingly, in order to achieve a w.c. situation, $\tilde{\mathbf{w}}$ has to be completely contained in this hyperplane, i.e.,

$$\tilde{\mathbf{w}} = a_{\tilde{\mathbf{w}}} \mathbf{u}^* + a_{\tilde{\mathbf{w}}} b_{\tilde{\mathbf{w}}} \mathbf{x}^* = a_{\tilde{\mathbf{w}}} [\mathbf{I} + b_{\tilde{\mathbf{w}}} \mathbf{M}] \mathbf{u}^*, \quad (3.115)$$

with adequately chosen coefficients $a_{\tilde{\mathbf{w}}} \in \mathbb{C} \setminus \{0\}$, $b_{\tilde{\mathbf{w}}} \in \mathbb{C}$, both typically varying with suppressed iteration index k . If matrix

$$\bar{\mathbf{M}}_{b_{\tilde{\mathbf{w}}}} \triangleq \mathbf{I} + b_{\tilde{\mathbf{w}}}\mathbf{M} \quad (3.116)$$

is invertible, (3.115) gives

$$\mathbf{u} = \frac{1}{a_{\tilde{\mathbf{w}}}^*} \bar{\mathbf{M}}_{b_{\tilde{\mathbf{w}}}}^{-*} \tilde{\mathbf{w}}^*. \quad (3.117)$$

This allows to choose excitation vector \mathbf{u} , such that $\tilde{\mathbf{w}} \in \mathcal{S}_{\mathbf{u}^*, \mathbf{x}^*}$. Inserting (3.117) on the right-hand side of (3.114), yields

$$\mathbf{B} = \mathbf{I} - \frac{\mu}{|a_{\tilde{\mathbf{w}}}|^2} \mathbf{M} \bar{\mathbf{M}}_{b_{\tilde{\mathbf{w}}}}^{-1} \tilde{\mathbf{w}} \tilde{\mathbf{w}}^H \bar{\mathbf{M}}_{b_{\tilde{\mathbf{w}}}}^{-H}. \quad (3.118)$$

Equation (3.118) could already be used to identify w.c. excitation vector $\mathbf{u}_{\text{w.c.},k}$, represented by the pair $\langle a_{\tilde{\mathbf{w}}}, b_{\tilde{\mathbf{w}}} \rangle$ that solves (3.114). However, (3.118) does not provide direct access to the length of \mathbf{u} , this can be circumvented – with $\mathbf{u} \neq \mathbf{0}$ – by substituting $|a_{\tilde{\mathbf{w}}}|$, based on

$$\|\mathbf{u}\| = \frac{\|\bar{\mathbf{M}}_{b_{\tilde{\mathbf{w}}}}^{-1} \tilde{\mathbf{w}}\|}{|a_{\tilde{\mathbf{w}}}|} \stackrel{\mathbf{u} \neq \mathbf{0}}{\Rightarrow} |a_{\tilde{\mathbf{w}}}| = \frac{\|\bar{\mathbf{M}}_{b_{\tilde{\mathbf{w}}}}^{-1} \tilde{\mathbf{w}}\|}{\|\mathbf{u}\|}. \quad (3.119)$$

Then, (3.114) becomes

$$b_{\tilde{\mathbf{w}}, \text{w.c.}, k} \triangleq \arg \max_{\substack{b_{\tilde{\mathbf{w}}, k} \\ \|\mathbf{u}_k\| = U(k)}} \left\{ \left\| \left[\mathbf{I} - \frac{\mu(k) \|\mathbf{u}_k\|^2}{\|\bar{\mathbf{M}}_{b_{\tilde{\mathbf{w}}, k}}^{-1} \tilde{\mathbf{w}}_{k-1}\|^2} \mathbf{M}_k \bar{\mathbf{M}}_{b_{\tilde{\mathbf{w}}, k}}^{-1} \tilde{\mathbf{w}}_{k-1} \tilde{\mathbf{w}}_{k-1}^H \bar{\mathbf{M}}_{b_{\tilde{\mathbf{w}}, k}}^{-H} \right] \tilde{\mathbf{w}}_{k-1} \right\| \right\}. \quad (3.120)$$

Compared to (3.113), in (3.120), the dimension of the search space has massively reduced, as only one complex-valued variable has to be identified. However, the cost function is now strongly non-linear in this single variable, resulting in a solution that is in general only accessibly by numerical methods.

3.6.2 Normal Step-Size Matrix

If step-size matrix \mathbf{M}_k is a normal matrix, Lemma 3.7 applies and it can be verified that also $\bar{\mathbf{M}}_{b_{\tilde{\mathbf{w}}, k}}$ in (3.116) is diagonalised by $\mathbf{Q}_{\mathbf{M}, k}$ according to

$$\bar{\mathbf{M}}_{b_{\tilde{\mathbf{w}}, k}} = \mathbf{Q}_{\mathbf{M}, k} \bar{\boldsymbol{\Lambda}}_{b_{\tilde{\mathbf{w}}, k}} \mathbf{Q}_{\mathbf{M}, k}^H, \quad \text{with} \quad \bar{\boldsymbol{\Lambda}}_{b_{\tilde{\mathbf{w}}, k}} \triangleq \mathbf{I} + b_{\tilde{\mathbf{w}}, k} \boldsymbol{\Lambda}_{\mathbf{M}, k}. \quad (3.121)$$

Then, taking unitary invariance of the Euclidean norm into account, with $\tilde{\mathbf{w}}''_{k-1}$ defined in (3.54), (3.120) modifies to

$$b_{\tilde{\mathbf{w}}, \text{w.c.}, k} \triangleq \arg \max_{\substack{b_{\tilde{\mathbf{w}}, k} \\ \|\mathbf{u}_k\| = U(k)}} \left\{ \left\| \left[\mathbf{I} - \frac{\mu(k) \|\mathbf{u}_k\|^2}{\|\bar{\boldsymbol{\Lambda}}_{b_{\tilde{\mathbf{w}}, k}}^{-1} \tilde{\mathbf{w}}''_{k-1}\|^2} \boldsymbol{\Lambda}_{\mathbf{M}, k} \bar{\boldsymbol{\Lambda}}_{b_{\tilde{\mathbf{w}}, k}}^{-1} \tilde{\mathbf{w}}''_{k-1} \tilde{\mathbf{w}}''_{k-1}^H \bar{\boldsymbol{\Lambda}}_{b_{\tilde{\mathbf{w}}, k}}^{-H} \right] \tilde{\mathbf{w}}''_{k-1} \right\| \right\}. \quad (3.122)$$

Note that although looking similar to (3.120), (3.122) has a much lower complexity, since all contained matrices are diagonal.

Chapter 4

Coupled Adaptive Filters

In Chapter 3, asymmetric gradient type algorithms are studied which contain one isolated asymmetric algorithm that is updated based on one single update error. The latter is obtained by comparison between the responses of reference system and system model. There, special emphasis is given to algorithms which employ unconventional directions for regression. This chapter falls back to the standard symmetric algorithm which uses the complex conjugate of its excitation vector to determine the direction of decent. However, instead of only one such algorithm, here, arbitrarily many are considered, which interfere with each other via a memoryless linear coupling among their individual a priori errors. There are several motivations which raise interest for such a structure.

In practice, such as sensor networks and multichannel ANC, several gradient type algorithms are combined in one system [ASSC02; KM08]. In such situations, interference between the individual algorithms may occur by desire of the designer, or due to imperfect physical conditions, e.g., circuit crosstalk or interference among transducers. In Section 5.3, for example, it is found that the MC-FXLMS applied to ANC can be mapped to the here considered coupled structure, enabling analysis of its stability and convergence behaviour. As motivated in Section 5.2, a similar situation is encountered in the context of cascaded structures consisting of several gradient type algorithms. Analysis of even more complicated structures such as neural networks, are accessible by the here considered structure as well (cf. Section 5.4).

As a consequence, this chapter is dedicated to introduce this special coupled structure and to investigate some of its properties. A detailed description is given in Section 4.1. Followed by an ℓ_2 -stability analysis in Section 4.4, which is based on the concept of input-output stability according to Section 2.4.2. Before this can be accomplished, as a prerequisite, Section 4.2 introduces a method better known in the context of economics that allows to solve specific types of linear systems of inequalities. Complementary to ℓ_2 -stability, Section 4.5 adopts the method of the mapping analysis performed for asymmetric algorithms in Section 3.4, and applies it to the coupled structure. By means of the Khatri-Rao matrix product that is introduced in Section 4.3, a compact mathematical formulation of the underlying mapping mechanisms is presented, which in turn gives access to conclusive conditions for boundedness of the parameter error vector. The chapter closes in Section 4.6 with the discussion of a special scenario, which is characterised by adaptation of all individual gradient type algorithms, based on one single update error. The practical relevance of this specific case will become clear in Chapter 5, which discusses some of its applications.

The most important results in this chapter are found in Sections 4.4 and 4.5. The primer presents Theorems 4.1 and 4.2 which provide bounds ensuring ℓ_2 -stability in terms of absolute and weighted energies, respectively. Section 4.5 states in Lemmas 4.3 and 4.4 conditions for a non-increasing parameter error distance. Of special practical interest is the identical error case, considered in Section 4.6. Finally, the two auxiliary methods introduced in Sections 4.2 and 4.3 deserve attention from a theoretical point of view. Although not new by themselves, they are novel in the here presented context.

4.1 General Coupled Adaptive Structure

In this section, the coupled structure is introduced that is focus of this whole chapter. It consists of $N \geq 2$ symmetric algorithms, i.e., conventional LMS algorithms, which mutually interact with each other via a linear memoryless coupling among their individual a priori errors. Defining the set of indices

$$\mathcal{N} \triangleq \{1, \dots, N\}, \quad (4.1)$$

this means that update error $\tilde{\varepsilon}_i(k)$ of the i^{th} adaptive filter is given by a linear combination of all individual a priori errors $\tilde{e}_j(k)$, $j \in \mathcal{N}$, i.e.,

$$\tilde{\varepsilon}_i(k) \triangleq \sum_{j \in \mathcal{N}} \nu_{ij}(k) \tilde{e}_j(k), \quad (4.2)$$

with coupling factors $\nu_{ij}(k) \in \mathbb{C}$. Out of these, those with identical indices, i.e., $\nu_{ii}(k)$, are distinguished from the others with $i \neq j$, as the primer scale the a priori error that corresponds to the adaptive filter with the same index. In order to reflect their special meaning, these $\nu_{ii}(k)$ are also referred to by the term *main coupling factors*. This is also expressed by (4.2), if re-written as

$$\tilde{\varepsilon}_i(k) \triangleq \nu_{ii}(k) \tilde{e}_i(k) + \sum_{j \in \mathcal{N} \setminus \{i\}} \nu_{ij}(k) \tilde{e}_j(k). \quad (4.3)$$

Each of the parameter vectors $\hat{\mathbf{w}}_{i,k}$, corresponding to adaptive filter i , is updated by a conventional LMS algorithm. Hence, as described in Section 2.1, the adaptive process aims to minimise the cost function on the left-hand side of (2.6), i.e., $E\{|\tilde{e}_i(k)|^2\}$, based on its instantaneous approximation in (2.7), i.e., $|\tilde{e}_i(k)|^2$. Accordingly, due to the interferences in (4.3),

$$\hat{\mathbf{w}}_{i,k} = \hat{\mathbf{w}}_{i,k-1} + \mathbf{u}_{i,k}^* \tilde{\varepsilon}_i(k), \quad (4.4)$$

where $\mathbf{u}_{i,k}$ represents the corresponding excitation vector. Comparing (4.4) with the update equation of the conventional LMS algorithm, i.e., (2.8), with the step-size matrix replaced by identity (cf. (2.5)), indicates that all terms in the sum on the right-hand side of (4.3) act as disturbance for the corresponding update. Adopting the assumptions listed in Section 2.1, parameter vector $\mathbf{w}_{i,k}$ of reference system i has the same length M_i as parameter vector $\hat{\mathbf{w}}_{i,k}$. Thus, the parameter error vector (cf. (2.10))

$$\tilde{\mathbf{w}}_{i,k} \triangleq \mathbf{w}_{i,k} - \hat{\mathbf{w}}_{i,k}, \quad (4.5)$$

can be introduced, which allows to write (4.4) equivalently as,

$$\tilde{\mathbf{w}}_{i,k} = \tilde{\mathbf{w}}_{i,k-1} - \mathbf{u}_{i,k}^* \tilde{\varepsilon}_i(k). \quad (4.6)$$

Figure 4.1 visualises the such obtained coupled adaptive structure. It also includes additive noise $v_i(k)$ that affects the individual reference outputs $d_i(k)$. The meaning of this noise is analogous to $v(k)$, introduced in the context of (2.4) in Section 2.1. Therefore, the a priori errors $\tilde{e}_i(k)$ include some noise, and can thus be split up into

$$\tilde{e}_i(k) \triangleq e_i(k) + v_i(k), \quad \text{with} \quad e_i(k) \triangleq \mathbf{u}_{i,k}^T \tilde{\mathbf{w}}_{i,k-1}. \quad (4.7)$$

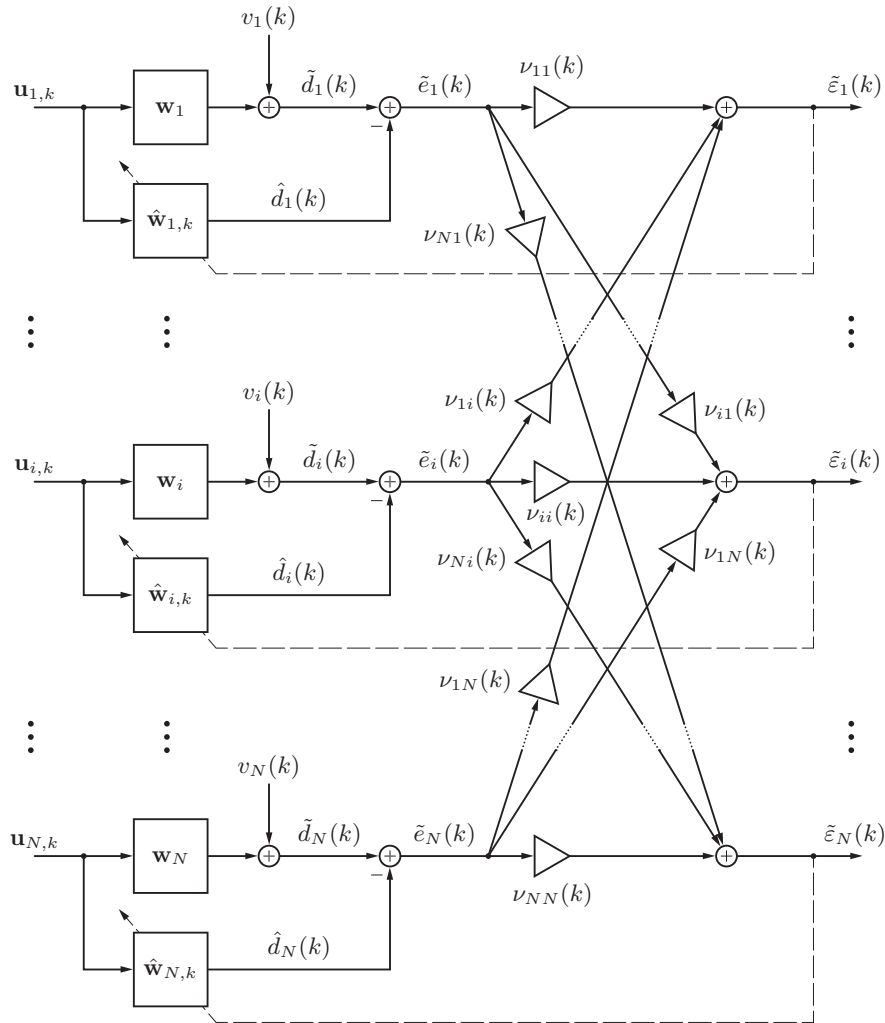


Figure 4.1: The coupled adaptive structure considered in this chapter. It consists of N individual LMS algorithms that mutually interfere with each other via a linear memoryless coupling among their a priori errors $\tilde{e}_i(k)$.

This also allows to separate update errors $\tilde{\varepsilon}_i(k)$ into a noiseless error component $\varepsilon_i(k)$ and additive noise $v_i^{(\varepsilon)}(k)$, i.e.,

$$\tilde{\varepsilon}_i(k) \triangleq \varepsilon_i(k) + v_i^{(\varepsilon)}(k) = \sum_{j \in \mathcal{N}} \nu_{ij}(k) \tilde{e}_j(k), \quad (4.8)$$

with

$$\varepsilon_i(k) \triangleq \sum_{j \in \mathcal{N}} \nu_{ij}(k) e_j(k), \quad \text{and} \quad v_i^{(\varepsilon)}(k) \triangleq \sum_{j \in \mathcal{N}} \nu_{ij}(k) v_j(k). \quad (4.9)$$

Note that (4.4) and (4.6) correspond to an LMS update rule with unit step-size. However, this does not restrict generality. This can be verified by introducing the coupling factors normalised to some step-size $\mu_i(k) \neq 0$,

$$\nu'_{ij}(k) \triangleq \frac{\nu_{ij}(k)}{\mu_i(k)}, \quad \text{with} \quad i, j \in \mathcal{N}, \quad (4.10)$$

and the modified update error

$$\tilde{\varepsilon}'_i(k) \triangleq \frac{\tilde{\varepsilon}_i(k)}{\mu_i(k)} = \sum_{j \in \mathcal{N}} \nu'_{ij}(k) \tilde{e}_j(k), \quad (4.11)$$

The, update equation (4.4)¹ becomes

$$\hat{\mathbf{w}}_{i,k} = \hat{\mathbf{w}}_{i,k} + \mu_i(k) \mathbf{u}_{i,k}^* \tilde{\varepsilon}'_i(k), \quad (4.12)$$

which shows the typical structure that includes a step-size. Table 4.1 summarises all of the so far occurred symbols and their meaning.

4.2 Systems of Inequalities Involving Z -Matrices

Section 4.4 will present an ℓ_2 -stability analysis of the coupled structure introduced in Section 4.1. In Sections 4.4.2 and 4.4.3, this will end up in the problem of solving a linear system of inequalities. As preparation, this section discusses an approach for its solution, based on a method adopted from economics².

Consider a system of N inequalities of the form

$$\mathbf{Z}\mathbf{a} \preceq \mathbf{b}, \quad (4.13)$$

where $\mathbf{Z} \in \mathbb{R}^{N \times N}$ is assumed to be a so called Z -matrix [FP62; BP79], meaning that all of its off-diagonal entries are non-positive, its diagonal entries are arbitrary. The vectors \mathbf{a} and \mathbf{b} , both have length N , and are constrained to contain only non-negative elements. Order relation “ \preceq ” is meant in an elementwise sense. The goal is to investigate if there exist matrices \mathbf{Z} , for which (4.13) entails

$$\mathbf{a} \preceq \mathbf{Z}^{-1}\mathbf{b}, \quad (4.14)$$

¹ Equation (4.6) is modified analogously.

² This system of inequalities in (4.13) is tightly related to Leontief’s input-output analysis in economics [BP79, pp. 242ff.].

Table 4.1: Mathematical Symbols Describing the i^{th} Gradient Type Algorithm

N	total number of individual adaptive filters
\mathcal{N}	set containing all indices, i.e., $\mathcal{N} = \{1, \dots, N\}$
$u_{j,k}^{(i)}$	scalar input that excites dimension j of gradient type algorithm i
$\mathbf{u}_{i,k}$	excitation vector $\mathbf{u}_{i,k} \triangleq [u_{1,k}^{(i)}, u_{2,k}^{(i)}, \dots, u_{M_i,k}^{(i)}]^\top$ of gradient type algorithm i
\mathbf{w}_i	parameter vector of reference system i
$\hat{\mathbf{w}}_{i,k}$	parameter vector of system model i
$\tilde{\mathbf{w}}_{i,k}$	parameter error vector $\tilde{\mathbf{w}}_{i,k} \triangleq \mathbf{w}_i - \hat{\mathbf{w}}_{i,k}$ of gradient type algorithm i
$d_i(k)$	noiseless response of i^{th} reference system, $d_i(k) \triangleq \mathbf{w}_i^\top \mathbf{u}_{i,k}$
$v_i(k)$	additive noise affecting the output of reference system i
$\tilde{d}_i(k)$	noisy response of i^{th} reference system, $\tilde{d}_i(k) \triangleq d_i(k) + v_i(k)$
$\hat{d}_i(k)$	response of i^{th} system model, $\hat{d}_i(k) \triangleq \hat{\mathbf{w}}_{i,k}^\top \mathbf{u}_{i,k}$
$e_i(k)$	noiseless a priori error that occurs between the outputs of reference system i and the corresponding system model, $e_i(k) \triangleq d_i(k) - \hat{d}_i(k)$
$\tilde{e}_i(k)$	noisy a priori error that occurs between the outputs of reference system i and the corresponding system model, $\tilde{e}_i(k) \triangleq \tilde{d}_i(k) - \hat{d}_i(k) = e_i(k) + v_i(k)$
$\varepsilon_i(k)$	update error used by gradient type algorithm i , excluding any noise, cf. (4.9)
$\tilde{\varepsilon}_i(k)$	noisy update error used by gradient type algorithm i , cf. (4.2) and (4.3)
$v_i^{(\varepsilon)}(k)$	overall noise, affecting update error $\tilde{\varepsilon}_i(k)$, cf. (4.9)
$\nu_{ij}(k)$	coupling factor that determines which amount of a priori error $\tilde{e}_j(k)$ is coupled into update error $\tilde{\varepsilon}_i(k)$
$\mu_i(k)$	step-size of i^{th} gradient type algorithm, cf. (4.12)
$\tilde{\varepsilon}'_i(k)$	noisy update error used by gradient type algorithm i with update equation (4.12), i.e., $\tilde{\varepsilon}_i(k)$ normalised by $\mu_i(k)$, cf. (4.11)
$\nu'_{ij}(k)$	coupling factors $\nu_{ij}(k)$ normalised by step-size $\mu_i(k)$, cf. (4.10)

and if so, what criteria such a matrix has to meet. Clearly, invertibility of \mathbf{Z} is necessary for (4.14) to hold. However, since the elements of the vectors \mathbf{a} and \mathbf{b} are constrained to be non-negative, it seems likely that further restrictions have to be imposed. Moreover, it can be expected that the order relation will not be preserved for an arbitrary matrix \mathbf{Z} . A straightforward approach to convert (4.13) into (4.14) would be to apply Gaussian elimination [MS00b, pp. 279ff.]. However, care has to be taken in order not to affect the order relation. Clearly, pivoting and adding up positive multiples of rows does not pose any problem. As soon as the negative multiple of a row is required in order to eliminate an element, the method fails as then the order relation changes direction, and a simple additive combination with one of the other rows is not allowed any more.

Performing the steps of Gaussian elimination, provides more insight. Assuming, w.o.l.o.g., that $(\mathbf{Z})_{11}$ is different from zero, the off-diagonal elements of the first column can be zeroed by adding the first line, multiplied by the non-negative factors $-(\mathbf{Z})_{j1}$, to each of the other lines with $j \in \{2, \dots, N\}$ that in turn are all multiplied by $(\mathbf{Z})_{11}$. This shows that $(\mathbf{Z})_{11}$ has to be positive, otherwise, it would alter the order relation for all of the lines j . Assuming $(\mathbf{Z})_{11} > 0$, the obtained matrix, which is referred to by \mathbf{Z}' , contains entry $(\mathbf{Z}')_{22} = (\mathbf{Z})_{11}(\mathbf{Z})_{22} - (\mathbf{Z})_{12}(\mathbf{Z})_{21}$. Moreover, it is easy to see that all non-positive elements of the original matrix \mathbf{Z} , are ensured to remain non-positive in \mathbf{Z}' . In the next step, the off-diagonal elements of the second column of \mathbf{Z}' have to be turned to zero. Following the same arguments as before, this is only possible if $(\mathbf{Z}')_{22}$ has its sign opposite to all non-zero elements in column 2, below the diagonal of \mathbf{Z}' . Excluding the case that all of them are zero, this entails $(\mathbf{Z}')_{22} > 0$. It can be verified that $(\mathbf{Z}')_{22}$ coincides with the second leading principal minor of \mathbf{Z} (cf. Appendix C.3). Proceeding with this scheme reveals that also all other leading principal minors of \mathbf{Z} have to be positive. This motivates the conjecture that if \mathbf{Z} is a Z -matrix, positivity of all of its leading principal minors is sufficient for the existence of (4.14).

That this conjecture indeed holds can be seen by introducing a vector $\boldsymbol{\delta}$ of slack variables [BV09], in order to re-write (4.13) in terms of an equality with side constraint, i.e.,

$$\mathbf{Z}\mathbf{a} + \boldsymbol{\delta} = \mathbf{b}, \quad \text{under constraint} \quad \boldsymbol{\delta} \succcurlyeq \mathbf{0}. \quad (4.15)$$

Since \mathbf{Z} is per definition, constrained to be a Z -matrix, it has a very special structure. Additionally requiring its leading principal minors to be positive, makes it even more special. The such defined matrix is a so-called M -matrix [FP62; BP79; Moy77], which possesses interesting properties that are summarised in Appendix C.2. Accordingly, the set of solutions for \mathbf{a} in (4.13) is ensured to be bounded, meaning that the order relation is preserved by inverting \mathbf{Z} . This can also be observed directly from (4.15) by recognising the remarkable property that the inverse of an M -matrix exclusively contains positive elements, as then,

$$\mathbf{Z}^{-1} \succ \mathbf{0}, \mathbf{b} \succcurlyeq \mathbf{0}, \boldsymbol{\delta} \succcurlyeq \mathbf{0} \quad \Rightarrow \quad \mathbf{a} = \mathbf{Z}^{-1}\mathbf{b} - \underbrace{\mathbf{Z}^{-1}\boldsymbol{\delta}}_{\succcurlyeq \mathbf{0}} \quad \Rightarrow \quad \mathbf{a} \preccurlyeq \underbrace{\mathbf{Z}^{-1}\mathbf{b}}_{\succcurlyeq \mathbf{0}}. \quad (4.16)$$

At this point, it has to be noted that this result agrees with the criteria stated in [HV83, pp. 203ff.]. As a refinement, based on [Nik68, p. 95], the condition of \mathbf{Z} being an M -matrix is found to be not only sufficient but also necessary for (4.14) to exist.

4.3 The Khatri-Rao Product

The previous section acts as preparation for the ℓ_2 -stability analysis in Section 4.4. Analogously, this section establishes prerequisites required by Section 4.5. There, for the conducted mapping analysis – similar to the one for asymmetric algorithms in Section 3.4 – additional means are required, in

order to achieve compact results on boundedness of the parameter error vector. The here introduced Khatri-Rao product, provides the key to achieve this.

The Khatri-Rao product was originally introduced in [KR68; Rao70] as a column-wise Kronecker product for matrices with the same number of columns. In [HM92], a block-Kronecker product was introduced which can be considered as extension of the original Khatri-Rao product to block matrices. In fact, in more recent literature the term Khatri-Rao addresses matrix products of the latter kind [see, e.g., CZY02; LT08]. Such matrix products can also be considered as generalisation of the Hadamard product to block matrices [HM92]. Alternatively, the conventional Kronecker product is found to be a special case of the Khatri-Rao product [Liu99; CZY02; LT08]. In literature, different symbols are used for the Khatri-Rao product, out of which a common variant is “*” [Liu99; CZY02; LT08]. As in signal processing the latter is almost exclusively reserved for the convolution [see, e.g., OWN97], in order to reduce the risk of confusion, in this thesis, the notation “ \boxtimes ” from [HM92] is adopted.

A detailed definition is included in Definition Table 4.1, on page 76. The matrix obtained by the Khatri-Rao product in (4.20) is a submatrix (cf. Appendix C.3) of Kronecker product $\mathbf{A} \otimes \mathbf{A}'$ [HM92], i.e., $\mathbf{A} \boxtimes \mathbf{A}'$ can be obtained from $\mathbf{A} \otimes \mathbf{A}'$ by deleting certain columns and rows³. Accordingly,

$$\mathbf{A} \boxtimes \mathbf{A}' = \mathbf{S}_r^T (\mathbf{A} \otimes \mathbf{A}') \mathbf{S}_c, \quad (4.17)$$

where matrices $\mathbf{S}_r \in \{0, 1\}^{MM' \times M^\boxtimes}$ and $\mathbf{S}_c \in \{0, 1\}^{NN' \times N^\boxtimes}$ are block matrices that consist of identity and zero blocks. Further down, (4.24) represents a special example for such a matrix. As a consequence, it can be concluded [HM92] that the singular values $\sigma_i(\mathbf{A} \boxtimes \mathbf{A}')$ interlace the singular values $\sigma_j(\mathbf{A} \otimes \mathbf{A}')$. Appendix C.3 reviews this relation in more detail. Specifically, (C.9) allows to state this fact more precisely [HJ99, Corollary 3.1.3],

$$\sigma_j(\mathbf{A} \otimes \mathbf{A}') \geq \sigma_j(\mathbf{A} \boxtimes \mathbf{A}') \geq \sigma_{j+r}(\mathbf{A} \otimes \mathbf{A}'), \quad j \in \{1, \dots, \min\{MM', NN'\}\}, \quad (4.18)$$

assuming decreasingly sorted singular values, and given that

$$r = MM' - M^\boxtimes + NN' - N^\boxtimes \quad (4.19)$$

is the number of deleted rows and columns. If moreover both matrices \mathbf{A} and \mathbf{A}' are Hermitian, and symmetrically (but not necessarily identically) partitioned, then, $\mathbf{A} \boxtimes \mathbf{A}'$ and $\mathbf{A} \otimes \mathbf{A}'$ are both Hermitian and the interlacing property also holds for the eigenvalues. If \mathbf{A} and \mathbf{A}' are additionally positive semi-definite, then, also $\mathbf{A} \boxtimes \mathbf{A}'$ is positive semi-definite [HM92].

³ Note that [LT08, p. 164] presents a slightly differing statement. There, the matrices \mathbf{S}_r and \mathbf{S}_c in (4.17) not only perform deletions of certain rows and columns but they additionally include permutations. This however, destroys the fact that $\mathbf{A} \boxtimes \mathbf{A}'$ is a submatrix of $\mathbf{A} \otimes \mathbf{A}'$, which in turn prohibits the use of the interlacing property for the singular values. [LT08] does not present a proof and refers to [ZYC02; KNW91]. This brings me to the supposition that the statement in [LT08] was derived in two steps: [ZYC02] shows that the Khatri-Rao product is a submatrix of the Tracy-Singh product, the latter in turn is proven in [KNW91] to be related to the Kronecker product via permutations that are based on the commutation matrix, introduced in [MN79]. If in [LT08] the permutation is trivial, i.e., identity, then, it agrees with [HM92]. In order to face this unclear situation, I verified that the special structure of the Khatri-Rao products that occur in this thesis is in fact a submatrix of the corresponding Kronecker product. Hence, the applicability of [HM92] is ensured.

Definition Table 4.1: The Khatri-Rao Product [Liu99; HM92]

Let $\mathbf{A} \in \mathbb{C}^{M \times N}$ and $\mathbf{A}' \in \mathbb{C}^{M' \times N'}$ be partitioned into blocks $\mathbf{A}_{ij} \in \mathbb{C}^{M_i \times N_j}$ and $\mathbf{A}'_{ij} \in \mathbb{C}^{M'_i \times N'_j}$, with $i \in \{1, \dots, I\}$ and $j \in \{1, \dots, J\}$, where

$$1 \leq I \leq \min \{M, M'\}, \quad \text{and} \quad 1 \leq J \leq \min \{N, N'\},$$

such that

$$\begin{aligned} \sum_{i=1}^I M_i &= M, & \text{and} & & \sum_{i=1}^I M'_i &= M', \\ \sum_{j=1}^J N_j &= N, & \text{and} & & \sum_{j=1}^J N'_j &= N', \end{aligned}$$

Then, the partitioning of the matrices \mathbf{A} and \mathbf{A}' has the form

$$\mathbf{A} \triangleq \begin{bmatrix} \mathbf{A}_{11} & \mathbf{A}_{12} & \cdots & \mathbf{A}_{1J} \\ \mathbf{A}_{21} & \mathbf{A}_{22} & \cdots & \mathbf{A}_{2J} \\ \vdots & \vdots & \ddots & \vdots \\ \mathbf{A}_{I1} & \mathbf{A}_{I2} & \cdots & \mathbf{A}_{IJ} \end{bmatrix}, \quad \mathbf{A}' \triangleq \begin{bmatrix} \mathbf{A}'_{11} & \mathbf{A}'_{12} & \cdots & \mathbf{A}'_{1J} \\ \mathbf{A}'_{21} & \mathbf{A}'_{22} & \cdots & \mathbf{A}'_{2J} \\ \vdots & \vdots & \ddots & \vdots \\ \mathbf{A}'_{I1} & \mathbf{A}'_{I2} & \cdots & \mathbf{A}'_{IJ} \end{bmatrix}.$$

The Khatri-Rao product of the matrices \mathbf{A} and \mathbf{A}' is contained in $\mathbb{C}^{M^\boxtimes \times N^\boxtimes}$, and defined as

$$\mathbf{A} \boxtimes \mathbf{A}' \triangleq \begin{bmatrix} \mathbf{A}_{11} \otimes \mathbf{A}'_{11} & \mathbf{A}_{12} \otimes \mathbf{A}'_{12} & \cdots & \mathbf{A}_{1J} \otimes \mathbf{A}'_{1J} \\ \mathbf{A}_{21} \otimes \mathbf{A}'_{21} & \mathbf{A}_{22} \otimes \mathbf{A}'_{22} & \cdots & \mathbf{A}_{2J} \otimes \mathbf{A}'_{2J} \\ \vdots & \vdots & \ddots & \vdots \\ \mathbf{A}_{I1} \otimes \mathbf{A}'_{I1} & \mathbf{A}_{I2} \otimes \mathbf{A}'_{I2} & \cdots & \mathbf{A}_{IJ} \otimes \mathbf{A}'_{IJ} \end{bmatrix}, \quad (4.20)$$

with

$$M^\boxtimes \triangleq \sum_{i=1}^I M_i M'_i, \quad N^\boxtimes \triangleq \sum_{j=1}^J N_j N'_j. \quad (4.21)$$

Finally, the notion of a symmetric partitioning is introduced, using matrix \mathbf{A} as example. The matrix \mathbf{A} is said to be partitioned symmetrically if $I = J$ and $M_i = N_i, \forall i \in \{1, \dots, I\}$.

In this thesis, the encountered Khatri-Rao products are of a special kind, which is obtained if matrix \mathbf{A} in Definition Table 4.1 is of dimension $I \times J$ and each of its elements is scalar, i.e., $(\mathbf{A})_{ij} = A_{ij}$, with $M_i = 1, \forall 1 \leq i \leq I = M$, and $N_j = 1, \forall 1 \leq j \leq J = N$. Then, in (4.20) the Kronecker product in each of the blocks reduces to a simple multiplication of a matrix by a scalar,

$$\mathbf{A} \boxtimes \mathbf{A}' = \begin{bmatrix} A_{11} \mathbf{A}'_{11} & A_{12} \mathbf{A}'_{12} & \cdots & A_{1J} \mathbf{A}'_{1J} \\ A_{21} \mathbf{A}'_{21} & A_{22} \mathbf{A}'_{22} & \cdots & A_{2J} \mathbf{A}'_{2J} \\ \vdots & \vdots & \ddots & \vdots \\ A_{I1} \mathbf{A}'_{I1} & A_{I2} \mathbf{A}'_{I2} & \cdots & A_{IJ} \mathbf{A}'_{IJ} \end{bmatrix}. \quad (4.22)$$

It is easy to verify that in this case

$$\mathbf{A} \boxtimes \mathbf{A}' = \mathbf{S}_r^\top (\mathbf{A} \otimes \mathbf{A}') \mathbf{S}_c, \quad (4.23)$$

with selection matrix (no permutations required)

$$\mathbf{S}_r^\top \triangleq \begin{bmatrix} \mathbf{I}_{M_1} & \mathbf{0}_{M_1 \times (M' - N_1)} & \mathbf{0}_{M_1 \times M'} & \mathbf{0}_{M_1 \times M'} & \mathbf{0}_{M_1 \times M'} \\ \mathbf{0}_{M_2 \times M'} & \mathbf{0} & \mathbf{I}_{M_2} & \mathbf{0}_{M_2 \times \sum_{i=3}^I M_i} & \mathbf{0}_{M_2 \times M'} \\ \mathbf{0}_{M_3 \times M'} & \mathbf{0}_{M_3 \times M'} & \mathbf{0} & \mathbf{I}_{M_3} & \mathbf{0}_{M_3 \times \sum_{i=4}^I M_i} \\ \vdots & \vdots & \vdots & \vdots & \vdots \\ \mathbf{0}_{M_I \times M'} & \mathbf{0}_{M_I \times M'} & \mathbf{0}_{M_I \times M'} & \mathbf{0}_{M_I \times (M' - M_I)} & \mathbf{I}_{M_I} \end{bmatrix} \quad (4.24)$$

where $M_i \triangleq M'_i$ and $N_j \triangleq N'_j$ was used. Note that

$$\mathbf{S}_r^\top \mathbf{S}_r = \mathbf{I}_{M^\boxtimes}, \quad (4.25)$$

and

$$\mathbf{S}_r \mathbf{S}_r^\top = \bigoplus_{i=1}^I (\mathbf{I}_{M_i} \oplus \mathbf{0}_{M'}), \quad (4.26)$$

where the direct sum [HJ13, Section 0.9] is employed to construct the block diagonal matrix in (4.26). Due to its similarity to \mathbf{S}_r , for selection matrix \mathbf{S}_c , expressions analogous to (4.24) and (4.26), are simply obtained by replacing all symbols, M and I , by symbols, N and J , respectively.

If in addition, the partitioning of matrix \mathbf{A}' is symmetric, the two selection matrices are identical and $\mathbf{A} \boxtimes \mathbf{A}'$ is a principal submatrix of $\mathbf{A} \otimes \mathbf{A}'$ [HM92]. Finally, two lemmas are presented which are required in Section 4.5.

Lemma 4.1: Matrix Product of two Khatri-Rao Products

Let $\mathbf{A}, \mathbf{A}' \in \mathbb{C}^{I \times I}$ be partitioned elementwise. Let moreover $\mathbf{C}, \mathbf{C}' \in \mathbb{C}^{M \times M}$ be symmetrically partitioned in the same way, such that their partitioning agrees with the partitioning of \mathbf{A} and \mathbf{A}' . Then,⁴

$$(\mathbf{A} \boxtimes \mathbf{C})(\mathbf{A}' \boxtimes \mathbf{C}')^H = \sum_{i=1}^I (\mathbf{a}_i \mathbf{a}_i^H) \boxtimes \left(\begin{matrix} \text{col} \\ \text{row} \end{matrix} \left\{ \mathbf{C}_{ji} \right\}_{j=1}^I \right) \left(\begin{matrix} \text{row} \\ \text{col} \end{matrix} \left\{ \mathbf{C}'_{ji} \right\}_{j=1}^I \right)^H, \quad (4.27)$$

where \mathbf{a}_i and \mathbf{a}'_i denote the columns of matrices \mathbf{A} and \mathbf{A}' , respectively, and \mathbf{C}_{ij} and \mathbf{C}'_{ij} denote the blocks obtained by the partitioning of matrices \mathbf{C} and \mathbf{C}' , respectively.

Proof. See Appendix D.2.1. □

⁴ The symbol \mathbf{C}_{ij}^H denotes the conjugate transpose of the matrix block \mathbf{C}_{ij} (in row i and column j of block matrix \mathbf{C}). Thus,

$$\begin{matrix} \text{row} \\ \text{col} \end{matrix} \left\{ \mathbf{C}_{ij}^H \right\}_{j=1}^I = \left(\begin{matrix} \text{col} \\ \text{row} \end{matrix} \left\{ \mathbf{C}_{ji} \right\}_{j=1}^I \right)^H. \quad (4.28)$$

Finally, a special case of Lemma 4.1 is presented that leads to a considerable simplification, which will be of great value in the proof of Lemma 4.3.

Lemma 4.2: Special Case of Lemma 4.1

Consider the mixed product in (4.27). If the assumptions of Lemma 4.1 are adopted, and if additionally

$$\text{col}_{j=1}^I \left\{ \mathbf{C}_{ji} \right\} \text{row}_{j=1}^I \left\{ \mathbf{C}'_{ji} \right\} = c(i) \mathbf{C}, \quad (4.29)$$

with $c(i) \in \mathbb{C}$, $\forall i \in \{1, \dots, I\}$, and $\mathbf{C} \in \mathbb{C}^{M \times M}$. Then,

$$(\mathbf{A} \boxtimes \mathbf{C}) (\mathbf{A}' \boxtimes \mathbf{C}')^H = \left(\mathbf{A} \text{diag}_{i=1}^I \{c(i)\} \mathbf{A}'^H \right) \boxtimes \mathbf{C}. \quad (4.30)$$

Proof. See Appendix D.2.2. □

4.4 ℓ_2 -Stability of Coupled Adaptive Filters

This section presents an input-output stability analysis for the coupled adaptive structure from Section 4.1. As a result, sufficient conditions for two versions of ℓ_2 -stability are obtained in Theorems 4.1 and 4.2. For the reader unfamiliar with this kind of stability theory, Section 2.4.2 is recommended as starting point, as it provides a smooth introduction, by briefly repeating the derivation of ℓ_2 -stability for the conventional LMS algorithm [RS96a; SR96]. Although the coupled structure considered in this section is considerably more complex, the underlying principles remain the same.

First, in Section 4.4.1, general passivity, as well as, relations among error and noise energies are derived. With this basis, Sections 4.4.2 and 4.4.3 apply the findings of Section 4.2, in order to identify ℓ_2 -stability in terms of absolute and weighted energies, respectively.

4.4.1 Energy Relations for Coupled Adaptive Filters

In this section, the principles introduced in Section 2.4.2 are adopted to complete the first step in the derivation of ℓ_2 -stability conditions for the coupled structure described in Section 4.1. The goal is to derive energy relations in the style of (2.59), separately for each of the adaptive filters in Figure 4.1. Analogous to Section 2.4.2, starting point is update equation (4.6) of one individual filter, for which the squared Euclidean norm is found to satisfy

$$\|\tilde{\mathbf{w}}_{i,k}\|^2 = \|\tilde{\mathbf{w}}_{i,k-1}\|^2 + \|\mathbf{u}_{i,k}\|^2 |\tilde{\varepsilon}_i(k)|^2 - 2\text{Re} \{e_i(k)^* \tilde{\varepsilon}_i(k)\}, \quad (4.31)$$

where (4.7) was used. The next step is to insert $\tilde{\varepsilon}_i(k)$ from (4.6). To do so, temporarily the *overall disturbance* $v'_i(k)$ is defined that affects adaptive filter i ,

$$v'_i(k) \triangleq v_i(k) + \sum_{j \in \mathcal{N} \setminus \{i\}} \frac{\nu_{ij}(k)}{\nu_{ii}(k)} \tilde{\varepsilon}_j(k). \quad (4.32)$$

At this point a restriction has to be imposed.

Assumption 4.1: Real-Valued Main Coupling Factors

For all iteration steps k , the main coupling factors $\nu_{ii}(k)$, $i \in \mathcal{N}$ are all real-valued and non-zero, i.e., $\nu_{ii}(k) \in \mathbb{R} \setminus \{0\}$.

With this assumption, inserting (4.32) into (4.31), leads to

$$\|\tilde{\mathbf{w}}_{i,k}\|^2 = \|\tilde{\mathbf{w}}_{i,k-1}\|^2 + \|\mathbf{u}_{i,k}\|^2 |\tilde{\varepsilon}_i(k)|^2 - 2\nu_{ii}(k) |e_i(k)|^2 - 2\nu_{ii}(k) \operatorname{Re} \{e_i(k)^* v'_i(k)\}. \quad (4.33)$$

Expanding on the right-hand side with $\nu_{ii}(k) |v'_i(k)|^2 - \nu_{ii}(k) |v'_i(k)|^2$ and recognising that

$$|e_i(k) + v'_i(k)|^2 = |e_i(k)|^2 + 2\operatorname{Re} \{e_i(k)^* v'_i(k)\} + |v'_i(k)|^2, \quad (4.34)$$

yields

$$\|\tilde{\mathbf{w}}_{i,k}\|^2 = \|\tilde{\mathbf{w}}_{i,k-1}\|^2 + \|\mathbf{u}_{i,k}\|^2 |\tilde{\varepsilon}_i(k)|^2 - \nu_{ii}(k) |e_i(k)|^2 - \nu_{ii}(k) |e_i(k) + v'_i(k)|^2 + \nu_{ii}(k) |v'_i(k)|^2. \quad (4.35)$$

Finally, using Assumption 4.1 for a second time, together with $\tilde{\varepsilon}_i(k) = \nu_{ii}(k) (e_i(k) + v'_i(k))$, gives

$$\|\tilde{\mathbf{w}}_{i,k}\|^2 + \nu_{ii}(k) |e_i(k)|^2 = \|\tilde{\mathbf{w}}_{i,k-1}\|^2 + \nu_{ii}(k) |v'_i(k)|^2 + |\tilde{\varepsilon}_i(k)|^2 \left(\|\mathbf{u}_{i,k}\|^2 - \frac{1}{\nu_{ii}(k)} \right). \quad (4.36)$$

Thus, analogous to (2.57), condition

$$0 < \nu_{ii}(k) \leq \frac{1}{\|\mathbf{u}_{i,k}\|^2}, \quad (4.37)$$

allows to conclude passivity, such that after calculation of the update, the overall error power is never larger than the power of disturbances, i.e.,

$$\|\tilde{\mathbf{w}}_{i,k}\|^2 + \nu_{ii}(k) |e_i(k)|^2 \leq \|\tilde{\mathbf{w}}_{i,k-1}\|^2 + \nu_{ii}(k) |v'_i(k)|^2. \quad (4.38)$$

Summing (4.38) up, on both sides from the first iteration $k = 0$, up to a certain iteration $K \geq 0$, with initial state $k = -1$, and applying the Minkowsky inequality [MS00b, p. 871], leads to an energy relation analogous to (2.59),

$$\sqrt{\sum_{k=0}^K \nu_{ii}(k) |e_i(k)|^2} \leq \|\tilde{\mathbf{w}}_{i,-1}\| + \sqrt{\sum_{k=0}^K \nu_{ii}(k) |v'_i(k)|^2}. \quad (4.39)$$

While in case of the LMS algorithm, in (2.59) the derivation was complete after this step, here, the situation is different. This becomes obvious by reinserting overall disturbance $v'_i(k)$, defined in (4.32), and splitting up a priori error $\tilde{\varepsilon}_i(k)$, into its noiseless component and its additive noise as done in (4.7),

$$\sqrt{\sum_{k=0}^K \nu_{ii}(k) |e_i(k)|^2} \leq \|\tilde{\mathbf{w}}_{i,-1}\| + \sqrt{\sum_{k=0}^K \nu_{ii}(k) \left| \sum_{j \in \mathcal{N} \setminus \{i\}} \frac{\nu_{ij}(k)}{\nu_{ii}(k)} e_j(k) + \sum_{j \in \mathcal{N}} \frac{\nu_{ij}(k)}{\nu_{ii}(k)} v_j(k) \right|^2}. \quad (4.40)$$

The reason why the derivation cannot stop at this point, is that not only $e_i(k)$ is an output of the

system, but all $e_j(k)$, $j \in \mathcal{N} \setminus \{i\}$ as well. As the latter occur on the right-hand side of (4.40), this inequality does not constitute any useful bound. This becomes even more obvious by applying the triangle inequality [MS00b, p. 72], and after resorting to the Minkowsky inequality for another time,

Erratum 7

$$\sqrt{\sum_{k=0}^K \nu_{ii}(k) |e_i(k)|^2} \leq \|\tilde{\mathbf{w}}_{i,-1}\| + \sqrt{\sum_{k=0}^K \sum_{j \in \mathcal{N} \setminus \{i\}} \frac{|\nu_{ij}(k)|^2}{\nu_{ii}(k)} |e_j(k)|^2} + \sqrt{\sum_{k=0}^K \sum_{j \in \mathcal{N}} \frac{|\nu_{ij}(k)|^2}{\nu_{ii}(k)} |v_j(k)|^2}. \quad (4.41)$$

Clearly, (4.41) constitutes a system of inequalities with respect to some sort of energies of the noiseless update errors $e_i(k)$. This is now the point where Section 4.2 proves useful. The following two sections apply the corresponding findings in order to state conditions for two types of ℓ_2 -stability. It has to be emphasised that above as well as in Sections 4.4.2 and 4.4.3, the derivations are based on the triangle inequality and the Minkowsky inequality, which both are applicable for any ℓ_p -norm. Thus, it is possible – yet not presented here – to generalise the results, i.e., Theorems 4.1 and 4.2, such that they are formulated in terms of ℓ_p -stability.

4.4.2 ℓ_2 -Stability in Terms of Absolute Energies

In this section, conditions for ℓ_2 -stability of the coupled structure presented in Section 4.1 are deduced. This is achieved by bringing (4.41) into a system of inequalities of the same type as discussed in Section 4.2. In Section 4.4.3 similar arguments will lead to ℓ_2 -stability in a different sense. As a first step, further definitions are required which are presented in Definition 4.1.

Definition 4.1: Absolute Energies up to Iteration K

Vector composed by the absolute energies $E_i(K)$ of the individual noiseless a priori errors

$$\mathbf{e}_K \triangleq [E_1(K) \quad \cdots \quad E_N(K)]^T, \quad \text{with} \quad E_i(K) \triangleq \sqrt{\sum_{k=0}^K |e_i(k)|^2}. \quad (4.42)$$

Vector composed by the absolute energies $E_i^{(\varepsilon)}(K)$ of the noiseless update errors

$$\boldsymbol{\varepsilon}_K \triangleq [E_1^{(\varepsilon)}(K) \quad \cdots \quad E_N^{(\varepsilon)}(K)]^T, \quad \text{with} \quad E_i^{(\varepsilon)}(K) \triangleq \sqrt{\sum_{k=0}^K |\varepsilon_i(k)|^2}. \quad (4.43)$$

Vector composed by the absolute energies $V_i(K)$ of the individual additive noise sequences

$$\mathbf{v}_K \triangleq [V_1(K) \quad \cdots \quad V_N(K)]^T, \quad \text{with} \quad V_i(K) \triangleq \sqrt{\sum_{k=0}^K |v_i(k)|^2}. \quad (4.44)$$

Additionally, some bounds of the coupling factors as well as related matrices are required that can be found in Definition Table 4.2 on page 83. Before the derivation can start, it is convenient to

collect the energies contained in the initial parameter error vectors in vector

$$\boldsymbol{\omega}_{-1} \triangleq [\|\tilde{\mathbf{w}}_{1,-1}\| \quad \cdots \quad \|\tilde{\mathbf{w}}_{N,-1}\|]^\top. \quad (4.45)$$

With this at hand, since

$$\sqrt{\check{\nu}_{ii}(K)} \sqrt{\sum_{k=0}^K |e_i(k)|^2} \leq \sqrt{\sum_{k=0}^K \nu_{ii}(k) |e_i(k)|^2}, \quad (4.46)$$

by reordering of sums and a further application of Minkowski's inequality, (4.41) modifies to

$$\sqrt{\sum_{k=0}^K |e_i(k)|^2} \leq \frac{\|\tilde{\mathbf{w}}_{i,-1}\|}{\sqrt{\check{\nu}_{ii}(K)}} + \sum_{j \in \mathcal{N} \setminus \{i\}} \frac{\hat{\eta}_{ij}(K)}{\sqrt{\check{\nu}_{ii}(K)}} \sqrt{\sum_{k=0}^K |e_j(k)|^2} + \sum_{j \in \mathcal{N}} \frac{\hat{\eta}_{ij}(K)}{\sqrt{\check{\nu}_{ii}(K)}} \sqrt{\sum_{k=0}^K |v_j(k)|^2}, \quad (4.47)$$

which holds for all $e_i(k)$, thus, with the elementwise order relation “ \preceq ” and Definition Table 4.2,

$$\mathbf{e}_K \preceq \check{\mathbf{D}}_{\nu,K}^{-1} \boldsymbol{\omega}_{-1} + (\mathbf{I} - \bar{\mathbf{\Delta}}_K) \mathbf{e}_K + \check{\mathbf{D}}_{\nu,K}^{-1} \left(\hat{\mathbf{D}}_{\nu,K} + \mathbf{I} - \bar{\mathbf{\Delta}}_K \right) \mathbf{v}_K. \quad (4.48)$$

The set of inequalities in (4.48) can be brought to the structure of (4.13),

$$\bar{\mathbf{\Delta}}_K \mathbf{e}_K \preceq \underbrace{\check{\mathbf{D}}_{\nu,K}^{-1} \boldsymbol{\omega}_{-1}}_{\succ \mathbf{0}} + \underbrace{\check{\mathbf{D}}_{\nu,K}^{-1} \left(\hat{\mathbf{D}}_{\nu,K} + \mathbf{I} - \bar{\mathbf{\Delta}}_K \right) \mathbf{v}_K}_{\succ \mathbf{0}}. \quad (4.49)$$

For the noiseless update error $\varepsilon_i(k)$, an expression similar to (4.49) can be found, as due to the triangle inequality [MS00b, p. 72], with from (4.9), it holds that

$$|\varepsilon_i(k)|^2 \leq \nu_{ii}^2(k) |e_i(k)|^2 + \sum_{j \in \mathcal{N} \setminus \{i\}} |\nu_{ij}(k)|^2 |e_j(k)|^2, \quad (4.50)$$

for which the Minkowsky inequality leads to the energy bound

$$\sqrt{\sum_{k=0}^K |\varepsilon_i(k)|^2} \leq \sqrt{\sum_{k=0}^K \nu_{ii}^2(k) |e_i(k)|^2} + \sqrt{\sum_{k=0}^K \sum_{j \in \mathcal{N} \setminus \{i\}} |\nu_{ij}(k)|^2 |e_j(k)|^2}. \quad (4.51)$$

With maximum coupling factors $\hat{\nu}_{ij}(K)$, defined in Definition Table 4.2, after exchanging sums and application of the Minkowsky inequality, the energy of the noiseless update error is bounded by

$$\sqrt{\sum_{k=0}^K |\varepsilon_i(k)|^2} \leq \sum_{j \in \mathcal{N}} \hat{\nu}_{ij}(K) \sqrt{\sum_{k=0}^K |e_j(k)|^2}, \quad (4.52)$$

or equivalently,

$$\boldsymbol{\varepsilon}_K \preceq \hat{\mathbf{\Delta}}_{\nu,K} \mathbf{e}_K. \quad (4.53)$$

Eventually, (4.49), (4.53), and the insights from Section 4.2, open up access to the following theorem.

Theorem 4.1: ℓ_2 -Stability in Terms of Absolute Energies

Consider the structure of coupled adaptive gradient type algorithms defined by (4.4)–(4.9), with the real-valued main coupling factors fulfilling for all $i \in \mathcal{N}$, $k = 0, \dots, K$,

$$0 < \nu_{ii}(k) \leq \|\mathbf{u}_{i,k}\|^{-2}, \quad (4.54)$$

and the cross coupling factors $\nu_{ij}(k) \in \mathbb{C}$. With $\boldsymbol{\omega}_{-1}$ from (4.45), Definition 4.1, and Definition Table 4.2, positive definiteness of the matrix relating absolute energies, i.e.,

$$\bar{\Delta}_K > 0 \quad (4.55)$$

is sufficient for ℓ_2 -stability in terms of individual a priori error energies, according to

$$\mathbf{e}_K \preceq \bar{\Delta}_K^{-1} \check{\mathbf{D}}_{\nu,K}^{-1} \left(\boldsymbol{\omega}_{-1} + \hat{\Delta}_{\eta,K} \mathbf{v}_K \right), \quad (4.56)$$

as well as, in terms of update error energies, according to

$$\boldsymbol{\varepsilon}_K \preceq \hat{\Delta}_{\nu,K} \bar{\Delta}_K^{-1} \check{\mathbf{D}}_{\nu,K}^{-1} \left(\boldsymbol{\omega}_{-1} + \hat{\Delta}_{\eta,K} \mathbf{v}_K \right). \quad (4.57)$$

Erratum 9

4.4.3 ℓ_2 -Stability in Terms of Weighted Energies

The ideas and derivations in this section tightly follow the arguments of Section 4.4.2. Thus, explanations are kept rather brief here. Vectors $\boldsymbol{\varepsilon}_K$ and $\boldsymbol{\omega}_{-1}$ containing the absolute energies of the noiseless update errors and the energy of the individual initial parameter error vectors, respectively, as well as diagonal matrix $\hat{\mathbf{D}}_{\nu,K}$ of maximum main coupling magnitudes, are left unchanged and can be found in Definition Table 4.2. Further required entities are specified in Definitions 4.2 and 4.3. To emphasise their analogy, except from being augmented by the prime character ($'$), the used symbols remain the same as in Section 4.4.2.

Definition 4.2: Bounds for the Coupling Factors and Related Matrices, used in Context of the ℓ_2 -Stability in terms of Weighted Energies

Maximum magnitude of the normalised coupling factors up to iteration K

$$\hat{\eta}'_{ij}(K) \triangleq \max_{0 \leq k \leq K} \left\{ \frac{|\nu_{ij}(k)|}{\sqrt{\nu_{ii}(k)\nu_{jj}(k)}} \right\}. \quad (4.58)$$

Matrix relating weighted energies

$$\bar{\Delta}'_K \triangleq \begin{bmatrix} 1 & -\hat{\eta}'_{12}(K) & \cdots & -\hat{\eta}'_{1N}(K) \\ -\hat{\eta}'_{21}(K) & 1 & \cdots & -\hat{\eta}'_{2N}(K) \\ \vdots & \vdots & \ddots & \vdots \\ -\hat{\eta}'_{N1}(K) & -\hat{\eta}'_{N2}(K) & \cdots & 1 \end{bmatrix}. \quad (4.59)$$

Bounding matrix for weighted energies

$$\hat{\Delta}'_{\eta,K} \triangleq 2\mathbf{I} - \bar{\Delta}'_K. \quad (4.60)$$

Definition Table 4.2: Bounds for the Coupling Factors and Related Matrices, used in Context of ℓ_2 -Stability for Absolute Energies

Minimum and maximum magnitude of coupling factors $\nu_{ij}(k)$, up to iteration K

$$\check{\nu}_{ij}(K) \triangleq \min_{0 \leq k \leq K} \{|\nu_{ij}(k)|\}, \quad \hat{\nu}_{ij}(K) \triangleq \max_{0 \leq k \leq K} \{|\nu_{ij}(k)|\}, \quad (4.61)$$

and the related diagonal matrices of minimum and maximum main coupling square roots

$$\check{\mathbf{D}}_{\nu,K} \triangleq \text{diag} \left\{ \sqrt{\check{\nu}_{ii}(K)} \right\}, \quad \hat{\mathbf{D}}_{\nu,K} \triangleq \text{diag} \left\{ \sqrt{\hat{\nu}_{ii}(K)} \right\}. \quad (4.62)$$

Matrix of maximum coupling magnitudes

$$\hat{\mathbf{\Delta}}_{\nu,K} \triangleq \begin{bmatrix} \hat{\nu}_{11}(K) & \cdots & \hat{\nu}_{1N}(K) \\ \vdots & \ddots & \vdots \\ \hat{\nu}_{N1}(K) & \cdots & \hat{\nu}_{NN}(K) \end{bmatrix}. \quad (4.63)$$

Maximum magnitudes of normalised coupling factors, up to iteration K (note that due to Assumption 4.1, $\nu_{ii}(k) \in \mathbb{R} \setminus \{0\}$)

$$\hat{\eta}_{ij}(K) \triangleq \max_{0 \leq k \leq K} \left\{ \frac{|\nu_{ij}(k)|}{\sqrt{\nu_{ii}(k)}} \right\}. \quad (4.64)$$

Matrix relating absolute energies

$$\bar{\mathbf{\Delta}}_K \triangleq \begin{bmatrix} 1 & -\frac{\hat{\eta}_{12}(K)}{\sqrt{\hat{\nu}_{11}(K)}} & \cdots & -\frac{\hat{\eta}_{1N}(K)}{\sqrt{\hat{\nu}_{11}(K)}} \\ -\frac{\hat{\eta}_{21}(K)}{\sqrt{\hat{\nu}_{22}(K)}} & 1 & \cdots & -\frac{\hat{\eta}_{2N}(K)}{\sqrt{\hat{\nu}_{22}(K)}} \\ \vdots & \vdots & \ddots & \vdots \\ -\frac{\hat{\eta}_{N1}(K)}{\sqrt{\hat{\nu}_{NN}(K)}} & -\frac{\hat{\eta}_{N2}(K)}{\sqrt{\hat{\nu}_{NN}(K)}} & \cdots & 1 \end{bmatrix}. \quad (4.65)$$

Bounding matrix for absolute energies

$$\hat{\mathbf{\Delta}}_{\eta,K} \triangleq \hat{\mathbf{D}}_{\nu,K} + \check{\mathbf{D}}_{\nu,K} (\mathbf{I} - \bar{\mathbf{\Delta}}_K). \quad (4.66)$$

Definition 4.3: Weighted Energies up to Iteration K

Vector composed by the weighted energies $E'_i(K)$ of the individual noiseless output errors

$$\mathbf{e}'_K \triangleq [E'_1(K) \ \cdots \ E'_N(K)]^T, \quad \text{with} \quad E'_i(K) \triangleq \sqrt{\sum_{k=0}^K \nu_{ii}(k) |e_i(k)|^2}, \quad (4.67)$$

Vector composed by the weighted energies $V'_i(K)$ of the individual additive noise sequences

$$\mathbf{v}'_K \triangleq [V'_1(K) \ \cdots \ V'_N(K)]^T, \quad \text{with} \quad V'_i(K) \triangleq \sqrt{\sum_{k=0}^K \nu_{ii}(k) |v_i(k)|^2}. \quad (4.68)$$

Re-writing energy relation (4.41) as

$$\begin{aligned} \sqrt{\sum_{k=0}^K \nu_{ii}(k) |e_i(k)|^2} \leq \|\tilde{\mathbf{w}}_{i,-1}\| + \sqrt{\sum_{k=0}^K \sum_{j \in \mathcal{N} \setminus \{i\}} \frac{|\nu_{ij}(k)|^2}{\nu_{ii}(k)\nu_{jj}(k)} \nu_{jj}(k) |e_j(k)|^2} \\ + \sqrt{\sum_{k=0}^K \sum_{j \in \mathcal{N}} \frac{|\nu_{ij}(k)|^2}{\nu_{ii}(k)\nu_{jj}(k)} \nu_{jj}(k) |v_j(k)|^2}, \quad (4.69) \end{aligned}$$

based on the Minkowsky inequality, the following bound can be found

$$\begin{aligned} \sqrt{\sum_{k=0}^K \nu_{ii}(k) |e_i(k)|^2} \leq \|\tilde{\mathbf{w}}_{i,-1}\| + \sum_{j \in \mathcal{N} \setminus \{i\}} \hat{\eta}'_{ij}(K) \sqrt{\sum_{k=0}^K \nu_{jj}(k) |e_j(k)|^2} \\ + \sum_{j \in \mathcal{N}} \hat{\eta}'_{ij}(K) \sqrt{\sum_{k=0}^K \nu_{jj}(k) |v_j(k)|^2}. \quad (4.70) \end{aligned}$$

This is equivalent to a system of inequalities of the same type as in Section 4.2,

$$\bar{\Delta}'_K \mathbf{e}'_K \preceq \boldsymbol{\omega}_{-1} + \hat{\Delta}'_{\eta,K} \mathbf{v}'_K. \quad (4.71)$$

To show that ℓ_2 -stability with respect to the individual noiseless a priori errors $e_i(k)$ also entails ℓ_2 -stability in terms of the noiseless update errors, (4.50) is modified to

Erratum 10

$$|\varepsilon_i(k)|^2 \leq \nu_{ii}(k) \left(\nu_{ii}(k) |e_i(k)|^2 + \sum_{j \in \mathcal{N} \setminus \{i\}} \frac{|\nu_{ij}(k)|^2}{\nu_{ii}(k)\nu_{jj}(k)} \nu_{jj}(k) |e_j(k)|^2 \right). \quad (4.72)$$

After a few basic steps and application of the Minkowsky inequality, the following bound is obtained

$$\sqrt{\sum_{k=0}^K |\varepsilon_i(k)|^2} \leq \sqrt{\hat{\nu}_{ii}(K)} \left(\sqrt{\sum_{k=0}^K \nu_{ii}(k) |e_i(k)|^2} + \sum_{j \in \mathcal{N} \setminus \{i\}} \hat{\eta}'_{ij}(K) \sqrt{\sum_{k=0}^K \nu_{jj}(k) |e_j(k)|^2} \right), \quad (4.73)$$

and as a consequence,

$$\boldsymbol{\varepsilon}_K \preceq \hat{\mathbf{D}}_{\nu,K} \hat{\boldsymbol{\Delta}}'_{\eta,K} \mathbf{e}'_K \preceq \hat{\mathbf{D}}_{\nu,K} \hat{\boldsymbol{\Delta}}'_{\eta,K} \left(2\mathbf{I} - \hat{\boldsymbol{\Delta}}'_{\eta,K}\right)^{-1} \left(\boldsymbol{\omega}_{-1} + \hat{\boldsymbol{\Delta}}'_{\eta,K} \mathbf{v}'_K\right). \quad (4.74)$$

Based on (4.71) and (4.74), together with Section 4.2, the following theorem can be formulated.

Theorem 4.2: ℓ_2 -Stability in Terms of Weighted Energies

Consider the structure of coupled adaptive gradient type algorithms defined by (4.4)–(4.9), with the real-valued main coupling factors fulfilling for all $i \in \mathcal{N}$, $k = 0, \dots, K$,

$$0 \leq \nu_{ii}(k) \leq \|\mathbf{u}_{i,k}\|^{-2}, \quad (4.75)$$

and the cross coupling factors $\nu_{ij}(k) \in \mathbb{C}$. With $\boldsymbol{\omega}_{-1}$ from (4.45), and Definitions 4.2 and 4.3, positive definiteness of the matrix relating weighted energies, i.e.,

$$\bar{\boldsymbol{\Delta}}'_K > 0 \quad (4.76)$$

is sufficient for ℓ_2 -stability in terms of individual weighted a priori error energies, according to

$$\mathbf{e}'_K \preceq \bar{\boldsymbol{\Delta}}'^{-1}_K \left(\boldsymbol{\omega}_{-1} + \hat{\boldsymbol{\Delta}}'_{\eta,K} \mathbf{v}'_K\right), \quad (4.77)$$

as well as, in terms of update error energies, according to

$$\boldsymbol{\varepsilon}_K \preceq \hat{\mathbf{D}}_{\nu,K} \hat{\boldsymbol{\Delta}}'_{\eta,K} \bar{\boldsymbol{\Delta}}'^{-1}_K \left(\boldsymbol{\omega}_{-1} + \hat{\boldsymbol{\Delta}}'_{\eta,K} \mathbf{v}'_K\right), \quad (4.78)$$

where $\boldsymbol{\varepsilon}_K$ is given by (4.43) and $\hat{\mathbf{D}}_{\nu,K}$ by (4.62).

Erratum 11

Note that although claiming to be expressed in terms of weighted energies, (4.78) in Theorem 4.2 provides bounds for the update error energies without any weighting. This is done, as the obtained form is also sufficient for ℓ_2 -stability in terms of the weighted update error energies, which can be verified from (4.73).

4.5 Mapping Analysis of Coupled Adaptive Filters

After considering ℓ_2 -stability of the coupled structure presented in Section 4.1, in this section, the view point is switched from input-output stability to the mapping behaviour of the homogeneous recursion. The underlying idea is the same as presented in Section 2.3.3. First, based on the Khatri-Rao product introduced in Section 4.3, Lemma 4.3 provides a strict condition for non-increasing parameter error distance. As the latter contains a rather involved dependency among coupling factors $\nu_{ij}(k)$ and excitation vectors $\mathbf{u}_{i,k}$, a more convenient but only sufficient condition is presented in Lemma 4.4. The latter still depends on the excitation vectors but only in terms of their norms. In order to further improve applicability, Lemma 4.5 states a useful expression that is necessary for Lemma 4.4 to hold. Extensions – which will be discussed in place – to Lemma 4.5 are established by Lemma 4.6 and Conjecture 4.1. Finally, Theorem 4.3 reformulates Lemma 4.3 for an arbitrary number of iterations.

As in Section 3.3, starting point is a homogeneous but nonautonomous recursion of the form

(2.18), i.e.,

$$\tilde{\mathbf{w}}_k = \mathbf{B}_k \tilde{\mathbf{w}}_{k-1}. \quad (4.79)$$

The only difference is that now the parameter error vector is a combination of all separate parameter error vectors $\tilde{\mathbf{w}}_{i,k}$, i.e.,

$$\tilde{\mathbf{w}}_k \triangleq \text{col}_{i=1}^N \{ \tilde{\mathbf{w}}_{i,k} \} \in \mathbb{C}^M, \quad \text{with} \quad M \triangleq \sum_{i \in N} M_i. \quad (4.80)$$

As a consequence, mapping matrix \mathbf{B}_k that in (2.16) corresponds to an asymmetric algorithm, has to be modified adequately in order to resemble the structure of Figure 4.1. It is straightforward to see that (4.79) with the parameter error vector given by (4.80), is in the noiseless case, equivalent to a combination of recursions (4.6), if

$$\mathbf{B}_k = \mathbf{I} - \begin{bmatrix} \nu_{11}(k) \mathbf{u}_{1,k}^* \mathbf{u}_{1,k}^\top & \cdots & \nu_{1N}(k) \mathbf{u}_{1,k}^* \mathbf{u}_{N,k}^\top \\ \vdots & & \vdots \\ \nu_{N1}(k) \mathbf{u}_{N,k}^* \mathbf{u}_{1,k}^\top & \cdots & \nu_{NN}(k) \mathbf{u}_{N,k}^* \mathbf{u}_{N,k}^\top \end{bmatrix}. \quad (4.81)$$

At this point, it is time to resort to Section 4.3 which introduces the Khatri-Rao product. The latter allows to write \mathbf{B}_k in a very compact form. Moreover, in Lemma 4.4, it opens up access to the derivation of a practically useful sufficient condition for non-expanding behaviour. As a first step, analogous to (4.80), let

$$\mathbf{u}_k \triangleq \text{col}_{i=1}^N \{ \mathbf{u}_{i,k} \} \in \mathbb{C}^M, \quad (4.82)$$

be the combination of all individual excitation vectors $\mathbf{u}_{i,k}$, and

$$\mathbf{U}_k \triangleq \mathbf{u}_k^* \mathbf{u}_k^\top \in \mathbb{C}^{M \times M}. \quad (4.83)$$

be the complex conjugate of its outer product. Additionally, introducing the coupling matrix

$$\mathbf{\Delta}_k \triangleq \begin{bmatrix} \nu_{11}(k) & \cdots & \nu_{1N}(k) \\ \vdots & & \vdots \\ \nu_{N1}(k) & \cdots & \nu_{NN}(k) \end{bmatrix}, \quad (4.84)$$

containing all the individual coupling factors, (4.81) is compactly written as

$$\mathbf{B}_k = \mathbf{I} - \mathbf{\Delta}_k \boxtimes \mathbf{U}_k. \quad (4.85)$$

The partitioning of the Khatri-Rao product in (4.85) is elementwise for $\mathbf{\Delta}_k$, and for \mathbf{U}_k done according to the partitioning vector

$$\mathbf{p}_u \triangleq [M_1 \quad M_2 \quad \cdots \quad M_N]^\top. \quad (4.86)$$

The compact version of mapping matrix \mathbf{B}_k in (4.85) allows to derive a strict condition for non-increasing parameter error distance, provided by the following lemma.

Lemma 4.3: A Strict Condition for Non-Expanding Behaviour of \mathbf{B}_k

Mapping matrix \mathbf{B}_k in (4.85), with \mathbf{U}_k and Δ_k given by (4.82) and (4.84), respectively, has no singular value larger than one, iff

$$\Gamma_k \boxtimes \mathbf{U}_k \geq 0, \quad (4.87)$$

where

$$\Gamma_k \triangleq \Delta_k + \Delta_k^H - \Delta_k^H \mathbf{D}_{\mathbf{u},k} \Delta_k, \quad \text{and} \quad \mathbf{D}_{\mathbf{u},k} \triangleq \text{diag} \left\{ \|\mathbf{u}_{i,k}\|^2 \right\}_{i=1}^N. \quad (4.88)$$

Proof. See Appendix D.2.3. □

Deriving practically feasible bounds from (4.87), is expected to be rather involved in practical situations. Hence, a simplification is desirable, which is provided by the following lemma.

Lemma 4.4: Sufficient Condition for Non-Expanding Behaviour of \mathbf{B}_k

Mapping matrix \mathbf{B}_k in (4.85), with \mathbf{U}_k and Δ_k given by (4.82) and (4.84), respectively, has at least $M - N$ unit singular values. Moreover, no singular value is larger than one, if the matrix Γ_k in (4.88) is positive semi-definite, i.e.,

$$\Gamma_k \geq 0. \quad (4.89)$$

Proof. See Appendix D.2.4. □

Although (4.89) is less involved compared to the strict condition in (4.87), it still may be challenging to deduce practically feasible convergence bounds. Hence, the next lemma aims to provide some further support. The achieved simplification is noteworthy as it only depends on the eigenvalues of coupling matrix Δ_k and on the minimum of all norms $\|\mathbf{u}_{i,k}\|$.

Lemma 4.5: Necessary Condition for $\Gamma_k \geq 0$ (cf. (4.89))

With non-vanishing excitation, i.e., $\mathbf{u}_{i,k} \neq 0$, for all $i \in \mathcal{N}$, in order to satisfy (4.89), it is necessary that all the eigenvalues $\lambda_i(\Delta_k)$ of the (non-nilpotent) coupling matrix Δ_k in (4.84), comply with

$$0 \leq \text{Re} \{ \lambda_i(\Delta_k) \} \leq \frac{1}{2} |\lambda_i(\Delta_k)|^2 \mathbf{q}_i^H(\Delta_k) \mathbf{D}_{\mathbf{u}} \mathbf{q}_i(\Delta_k), \quad (4.90)$$

where $\mathbf{q}_i(\Delta_k)$ denotes the eigenvectors of Δ_k . Clearly, (4.90) is ensured if

$$0 \leq \text{Re} \{ \lambda_i(\Delta_k) \} \leq \frac{1}{2} |\lambda_i(\Delta_k)|^2 \min_{i \in \mathcal{N}} \left\{ \|\mathbf{u}_{i,k}\|^2 \right\}. \quad (4.91)$$

Proof. See Appendix D.2.5. □

According to (4.90), the eigenvalues of Δ_k have to be contained in a circle in the complex plane, centred on the real axis at the value of its radius, which is given by $[\mathbf{q}_i^H(\Delta) \mathbf{D}_u \mathbf{q}_i(\Delta_k)]^{-1}$. The drawback of (4.91) is that it is only necessary but not sufficient for (4.89). Hence, the latter is ensured to be violated, if (4.91) is violated, but the reversed implication is not necessarily true.

Finally, the following lemma, ensures that for a normal coupling matrix, Lemma 4.5 can be satisfied. Conjecture 4.1 argues that in most cases of a non-normal coupling matrix, the opposite is the case.

Lemma 4.6: Complement to Lemma 4.5, for Δ_k being a Normal Matrix

If the coupling matrix Δ_k is normal, the order relation on the left-hand side of (4.90) and (4.91) is ensured to hold.

Proof. See Appendix D.2.6. □

Conjecture 4.1: Complement to Lemma 4.5, if Δ_k is not a Normal Matrix

If the coupling matrix Δ_k is not normal, the order relation on the left-hand side of (4.90) and (4.91) is (in most cases) violated.

(Partial) Proof. See Appendix D.2.7. □

Lemma 4.6 and Conjecture 4.1 show a strong analogy to Chapter 3. There, it was found that (excluding trivial cases) asymmetric algorithms always have a mapping matrix \mathbf{B}_k with a singular value larger than one. Only if the regression vector is the complex conjugate of the excitation vector, a symmetric algorithm is obtained for which \mathbf{B}_k can be ensured to be non-expanding. From this point of view, Lemma 4.6 can be considered as condition leading to a generalised form of a symmetric algorithm, while if violated, the algorithm behaves like a generalised asymmetric algorithm.

Finally, Lemmas 4.3 and 4.4 are extended from a per-iteration point of view to a global statement.

Theorem 4.3: Non-Expanding Behaviour in the Noiseless Case

Consider the structure of coupled adaptive gradient type algorithms defined by (4.4)–(4.9), with coupling factors $\nu_{ij}(k) \in \mathbb{C}$. Let Δ_k be the matrix of coupling factors, defined in (4.84), and \mathbf{U}_k be the outer product of excitation vector $\mathbf{u}_{i,k}$, defined in (4.83), then, (4.87) is necessary and sufficient, (4.89) only sufficient for

$$\|\tilde{\mathbf{w}}_k\| \leq \|\tilde{\mathbf{w}}_{k-1}\|, \quad \forall k = 0, \dots \quad (4.92)$$

i.e., the length of the combined parameter error vector $\tilde{\mathbf{w}}_k$ as introduced in (4.80) will never increase with increasing iteration index k .

Proof. This Theorem 4.3 directly follows from Lemmas 4.3 and 4.4. □

4.6 Identical Error Case

A special situation occurs, if some of the individual coupled adaptive algorithms in Figure 4.1 rely on the same update error for the calculation of their parameter estimates. This case occurs more often than possibly expected, as, e.g., cascaded adaptive structures can be mapped to this case (cf. Section 5.2). In the sequel, w.o.l.o.g., it is assumed that the first $N' \leq N$ algorithms do their adaptation based on one common update error, except from a scaling factor $\mu_{i'}(k)$, for which the same symbols is used as for the step-size in (4.10)–(4.12), since their algorithmic effect is identical. Let

$$\mathcal{N}' \triangleq \{1, \dots, N'\} \subseteq \mathcal{N} \quad (4.93)$$

denote the set of indices which addresses the group of algorithms that are updated by the joint error. The latter, denoted by $\tilde{\varepsilon}'(k)$, is defined below in (4.96). The corresponding coupling factors $\nu_{i'j}(k)$, $i' \in \mathcal{N}'$, $j \in \mathcal{N}$, can be factorised by

$$\nu_{i'j}(k) = \mu_{i'}(k)\nu_j(k), \quad (4.94)$$

leading for the individual update errors (4.8) to

$$\tilde{\varepsilon}_{i'}(k) = \sum_{j \in \mathcal{N}} \mu_{i'}(k)\nu_j(k)\tilde{e}_j(k) = \mu_{i'}(k) \sum_{j \in \mathcal{N}} \nu_j(k)\tilde{e}_j(k) = \mu_{i'}(k)\tilde{\varepsilon}'(k), \quad (4.95)$$

with common update error

$$\tilde{\varepsilon}'(k) \triangleq \sum_{j \in \mathcal{N}} \nu_j(k)\tilde{e}_j(k). \quad (4.96)$$

Note that the sums in (4.95) and (4.96) cover the whole index range and are not restricted to the subset \mathcal{N}' . Inserting coupling factors $\nu_{i'j}(k)$ into the coupling matrix $\mathbf{\Delta}_k$ in (4.84), clearly causes the latter to become rank deficient with $\text{rank}\{\mathbf{\Delta}_k\} \leq N - N' + 1$. As a consequence, (4.55) and (4.76) are violated, entailing Theorems 4.1 and 4.2 to be inapplicable. Thus, no statement regarding the ℓ_2 -stability of the coupled structure with (partially) identical update errors can be made. It is important to notice that this situation does *not* allow to conclude instability in the ℓ_2 -sense. It only indicates that the identical error case cannot be analysed by Theorems 4.1 and 4.2.

For the mapping analysis in Section 4.5, the underlying theory does not require $\mathbf{\Delta}_k$ to be invertible. In fact, since Lemma 4.3 is necessary and sufficient, it is accessible for arbitrary coupling matrices. Also the practically more relevant Lemma 4.4 remains valid for singular coupling matrices. Based on Lemma 4.5, together with the extending statements, Lemma 4.6 and Conjecture 4.1, the following conjecture is found.

Conjecture 4.2: $\mathbf{\Gamma}_k \geq 0$ in the Identical Error Case

In the identical error case, Condition (4.89) in Lemma 4.4 can only be satisfied if the coupling matrix $\mathbf{\Delta}_k$ is normal.

Proof. For a normal $\mathbf{\Delta}_k$, Lemma 4.6 ensures $\mathbf{\Gamma}_k \geq 0$. Conjecture 4.1 in turn, shows that non-normal $\mathbf{\Delta}_k$ lead to $\mathbf{\Gamma} \not\geq 0$. If Conjecture 4.1 could be shown to hold for any non-normal coupling matrix,

the above statement would become strict. \square

Conjecture 4.2 has a strong impact to the degrees of freedom for $\mu_{i'}(k)$ and $\nu_j(k)$. As the following Lemma 4.7 shows, in the case that the coupling matrix is not only normal but also Hermitian, it entails that coupled adaptive filters with common update error behave identical to a symmetric algorithm. For simplicity reasons, w.o.l.o.g., assume that $\mathcal{N}' = \mathcal{N}$. Then, inserting (4.96) in (4.6), together with the combined parameter error vector in (4.80), and the combined excitation vector in (4.82), the overall update equation in the noiseless case is obtained as

$$\tilde{\mathbf{w}}_k = \tilde{\mathbf{w}}_{k-1} - \left(\bigoplus_{i=1}^N \mu_i(k) \mathbf{I}_{M_i} \right) \mathbf{u}_k^* \mathbf{u}_k^\top \left(\bigoplus_{i=1}^N \nu_i(k) \mathbf{I}_{M_i} \right) \tilde{\mathbf{w}}_{k-1}, \quad (4.97)$$

where the block diagonal matrices are expressed by the direct sum [HJ13, Section 0.9].

Lemma 4.7: Identical Error Case with Hermitian coupling matrix

In the identical error case, the coupling matrix Δ_k is Hermitian iff all $\mu_{i'}(k)$ are related to the corresponding $\nu_{i'}^(k)$, $i' \in \mathcal{N}'$, by the same proportionality constant $a(k) \in \mathbb{C}$, i.e.,*

$$\nu_{i'}(k) = a(k) \mu_{i'}^*(k). \quad (4.98)$$

Proof. A Hermitian coupling matrix requires $\nu_{i'j}(k) = \nu_{ji}^*(k)$, which due to (4.94) entails $\mu_{i'}(k) \nu_j(k) = \mu_j^*(k) \nu_{i'}^*(k)$. Thus,

$$\frac{\mu_{i'}(k)}{\mu_j^*(k)} = \frac{\nu_{i'}^*(k)}{\nu_j(k)} \Rightarrow \nu_{i'}(k) = \nu_1^*(k) \frac{\nu_{i'}(k)}{\nu_1^*(k)} = \nu_1^*(k) \frac{\mu_{i'}^*(k)}{\mu_1(k)} = \frac{\nu_1^*(k)}{\mu_1(k)} \mu_{i'}^*(k). \quad \square$$

Inserting (4.98) into (4.97), leads to

$$\tilde{\mathbf{w}}_k = \tilde{\mathbf{w}}_{k-1} - a(k) \underbrace{\left(\bigoplus_{i=1}^N \mu_i(k) \mathbf{I}_{M_i} \right)}_{\mathbf{u}_k'^*} \mathbf{u}_k^* \mathbf{u}_k^\top \underbrace{\left(\bigoplus_{i=1}^N \nu_i(k) \mathbf{I}_{M_i} \right)}_{\mathbf{u}_k'^\top} \tilde{\mathbf{w}}_{k-1}. \quad (4.99)$$

This algorithm obviously behaves like a symmetric algorithm with step-size $a(k)$ and excitation vector \mathbf{u}_k' . In the general case, with non-zero coupling factors, defining the transformed excitation vector

$$\mathbf{u}_k' \triangleq \left(\bigoplus_{i=1}^N \nu_i(k) \mathbf{I}_{M_i} \right) \mathbf{u}_k, \quad (4.100)$$

(4.97) becomes

$$\tilde{\mathbf{w}}_k = \tilde{\mathbf{w}}_{k-1} - \left(\bigoplus_{i=1}^N \frac{\mu_i(k)}{\nu_i(k)} \mathbf{I}_{M_i} \right) \mathbf{u}_k'^* \mathbf{u}_k'^\top \tilde{\mathbf{w}}_{k-1}, \quad (4.101)$$

which obviously corresponds to the homogeneous update equation of a gradient type algorithm with matrix step-size, according to (2.8).

For practical usage, Conjecture 4.2 would be more adequate if it would state conditions regarding the singular values of \mathbf{B}_k . However, at the moment when I am writing these lines, a missing link exists which prevents me from doing so. Let me point this out in more detail. Lemmas 4.5 and 4.6 and Conjecture 4.1 provide necessary conditions for $\mathbf{\Gamma}_k \geq 0$, which due to Lemma 4.4 are in turn sufficient for a non-expanding \mathbf{B}_k . Consequently, a violation of Lemma 4.5, Lemma 4.6, and/or Conjecture 4.1 ensures $\mathbf{\Gamma}_k \not\geq 0$. The latter however does *not* allow to conclude that \mathbf{B}_k is expanding, as Lemma 4.4 is only sufficient and not necessary. Thus, the mentioned missing link is a statement of the form “ $\mathbf{\Gamma}_k \not\geq 0 \Rightarrow \mathbf{\Gamma}_k \boxtimes \mathbf{U}_k \not\geq 0$ ”, which I have not been able to show up to now.

Chapter 5

Examples and Applications

After the considerations of Chapters 3 and 4 with strong theoretical focus, this chapter presents four different applications. As an introduction, Section 5.1.1 considers two adaptive filters that are coupled according to Chapter 4. Two configurations of coupling factors are discussed. The first one shows perfectly symmetric coupling and provides insight to the application of Theorems 4.1 and 4.2 and Lemmas 4.3 and 4.4. The second configuration represents an identical error case as introduced in Section 5.1.3.2, and demonstrates its relation to asymmetric algorithms. Simulation experiments are included for further illustration.

The Wiener model which is mentioned in Section 1.1, as one of the main motivations that lead to this thesis, is analysed in Section 5.2. As it can be represented as an identical error case, according to Section 4.6, Lemma 4.7 gives access to a condition that allows to ensure ℓ_2 -stability and a non-expanding parameter error vector.

The third application is found in Section 5.3, which thoroughly studies ℓ_2 -stability and the mapping behaviour of the MC-FXLMS algorithm in the context of ANC. The main results are developed step by step, starting in Section 5.3.1 with a scenario that only contains one reference microphone and one cancelling loudspeaker, but several error microphones. The case of an arbitrary number of reference microphones and cancelling loudspeakers but with only one single error microphone is covered by Section 5.3.2. Section 5.3.3 eventually states conditions for ℓ_2 -stability and non-expanding mapping behaviour of the general MC-FXLMS algorithm.

Finally, in Section 5.4, the whole apparatus of Chapter 4 is harnessed to extend the insights to the still not completely understood convergence behaviour of the backpropagation algorithm, employed for the training of a neural network, more specifically, a multilayer perceptron.

5.1 Special Case of Two Coupled Adaptive Filters

As first application of the theory presented in Chapter 4, this section considers a strongly simplified and rather generic example of two coupled filters, i.e., in (4.1) $N = 2$ and $\mathcal{N} = \{1, 2\}$. Figure 5.1 shows the specific structure that is obtained from Figure 4.1 in this case. The reason for choosing this example is twofold. First, it gives a good overview about the difference between the ℓ_2 -stability bounds obtained in Section 4.4.2, and the convergence conditions in Section 4.5. Second, the structure will also be of value in the following Section 5.2.

The obtained results are tightly related to the ones presented in [DR09b; DR15]. However, there, the derivations are a priori restricted to $N = 2$, and do not cover the general case of arbitrary $N > 2$. Moreover, in these works, the coupling factors are inherently restricted to be real-valued.

Section 5.1.1 briefly discusses ℓ_2 -stability for the objective coupled structure. The mapping behaviour in terms of the parameter error vector is analysed in Section 5.1.2, which is condensed in Corollary 5.1. Finally, two generic examples with strong symmetries of their coupling factors are considered in Section 5.1.3. The first one, is tailored to comprehensively carve out the strictness of

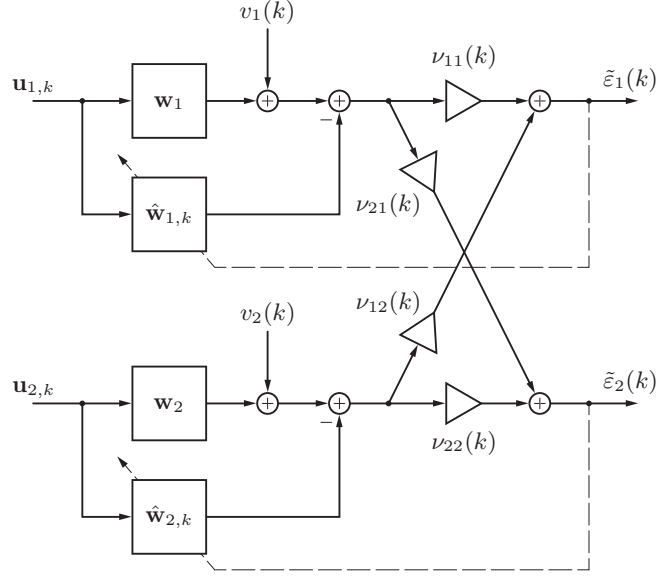


Figure 5.1: Two Coupled Adaptive Filters. This structure is obtained from Figure 4.1 for $N = 2$.

Corollary 5.1. The second one, also applies Corollary 5.1 in order to illustrate the implications of the identical error case from Section 4.6.

5.1.1 ℓ_2 -Stability of Two Coupled Adaptive Gradient Type Algorithms

For the coupled structure in Figure 5.1, ℓ_2 -stability bounds are obtained from Theorems 4.1 and 4.2, by inserting $N = 2$. Both theorems require the main coupling factors to be real-valued and to satisfy,

$$0 \leq \nu_{ii}(k) \leq \frac{1}{\|\mathbf{u}_{i,k}\|^2}, \quad (5.1)$$

with $i \in \mathcal{N}$. Then, according to Theorem 4.1, additional positive definiteness of coupling matrix $\bar{\Delta}_K$, defined in Definition Table 4.2, i.e.,

$$\bar{\Delta}_K = \begin{bmatrix} 1 & -\frac{1}{\sqrt{\nu_{11}(k)}} \max_{0 \leq k \leq K} \left\{ \frac{|\nu_{12}(k)|}{\sqrt{\nu_{11}(k)}} \right\} \\ -\frac{1}{\sqrt{\nu_{22}(k)}} \max_{0 \leq k \leq K} \left\{ \frac{|\nu_{21}(k)|}{\sqrt{\nu_{22}(k)}} \right\} & 1 \end{bmatrix} > \mathbf{0}. \quad (5.2)$$

is sufficient for ℓ_2 -stability in terms of absolute energies. Equivalently [HJ13, Observation 7.1.2], since the elements on the main diagonal are ensured to be positive, $\det(\bar{\Delta}_K) > 0$ leads to

$$\left(\max_{0 \leq k \leq K} \left\{ \frac{|\nu_{12}(k)|}{\sqrt{\nu_{11}(k)}} \right\} \right) \left(\max_{0 \leq k \leq K} \left\{ \frac{|\nu_{21}(k)|}{\sqrt{\nu_{22}(k)}} \right\} \right) < \sqrt{\nu_{11}(k)\nu_{22}(k)}. \quad (5.3)$$

Similarly, due to (4.76) in Theorem 4.2, positive definiteness of matrix $\bar{\Delta}'_K$, defined in Definition 4.3, is sufficient to ensure ℓ_2 -stability in terms of weighted energies. As before, the equivalent condition

$\det(\bar{\Delta}'_K) > 0$ gives

$$\left(\max_{0 \leq k \leq K} \left\{ \frac{|\nu_{12}(k)|}{\sqrt{\nu_{11}(k)\nu_{22}(k)}} \right\} \right) \left(\max_{0 \leq k \leq K} \left\{ \frac{|\nu_{21}(k)|}{\sqrt{\nu_{11}(k)\nu_{22}(k)}} \right\} \right) < 1. \quad (5.4)$$

For constant coupling factors, Conditions (5.3) and (5.4) coincide and simplify to

$$|\nu_{12}| |\nu_{21}| < \nu_{11}\nu_{22} \leq \frac{1}{\max_{k \geq 0} \left\{ \|\mathbf{u}_{1,k}\|^2 \right\} \max_{k \geq 0} \left\{ \|\mathbf{u}_{2,k}\|^2 \right\}}, \quad (5.5)$$

where the bound on the right-hand side is a consequence of (5.1). This perfectly agrees with the result in [DR09b]. The only difference is that there, the coupling factors do not inherently include the step-sizes of the underlying gradient type algorithms. The equivalence can easily be verified based on (4.10)–(4.12).

5.1.2 Convergence Behaviour of Two Coupled Gradient Type Algorithms

In this section, instead of ℓ_2 -stability, the mapping behaviour of the corresponding homogeneous recursion is considered, according to Section 4.5. The elements of matrix $\mathbf{\Gamma}_k$ in (4.88) are identified as

$$(\mathbf{\Gamma}_k)_{11} = 2\operatorname{Re}\{\nu_{11}(k)\} - |\nu_{11}(k)|^2 \|\mathbf{u}_{1,k}\|^2 - |\nu_{21}(k)|^2 \|\mathbf{u}_{2,k}\|^2, \quad (5.6)$$

$$(\mathbf{\Gamma}_k)_{22} = 2\operatorname{Re}\{\nu_{22}(k)\} - |\nu_{22}(k)|^2 \|\mathbf{u}_{2,k}\|^2 - |\nu_{12}(k)|^2 \|\mathbf{u}_{1,k}\|^2, \quad (5.7)$$

$$(\mathbf{\Gamma}_k)_{12} = (\mathbf{\Gamma}_k)_{21}^* = \nu_{12}(k) + \nu_{21}^*(k) - \nu_{11}^*(k)\nu_{12}(k) \|\mathbf{u}_{1,k}\|^2 - \nu_{22}(k)\nu_{21}^*(k) \|\mathbf{u}_{2,k}\|^2. \quad (5.8)$$

According to Lemma 4.4, in the noiseless case, non-expanding behaviour of the homogeneous recursion is guaranteed if $\mathbf{\Gamma}_k \geq \mathbf{0}$, or equivalently [HJ13, Observation 7.1.2],

$$[(\mathbf{\Gamma}_k)_{11} \geq 0] \wedge [(\mathbf{\Gamma}_k)_{22} \geq 0] \quad \wedge \quad \det(\mathbf{\Gamma}_k) = (\mathbf{\Gamma}_k)_{11}(\mathbf{\Gamma}_k)_{22} - |(\mathbf{\Gamma}_k)_{12}|^2 \geq 0. \quad (5.9)$$

Equation (5.9) is rather concise. However, as it is based on Lemma 4.4, it is only sufficient for non-expanding behaviour. Nevertheless, the simplicity of the here considered case, due to $N = 2$, allows to directly evaluate Lemma 4.3 which opens up access to sufficient *and necessary* conditions. The corresponding Corollary 5.1 leads to the same result as in [DR15], here, extended to the complex-valued case.

Corollary 5.1: Strict Condition for Non-Expanding Behaviour if $N = 2$

Consider the structure of two coupled adaptive gradient type algorithms, i.e., $N = 2$, defined by (4.4)–(4.9). Then, the elements of the 2×2 matrix $\mathbf{\Gamma}_k$ in (4.88) are given by (5.6)–(5.8). Under the assumption that $\mathbf{u}_{i,k} \neq \mathbf{0}$, $i \in \mathcal{N} = \{1, 2\}$, with the three conditions

- A. $(\mathbf{\Gamma}_k)_{11} (\mathbf{\Gamma}_k)_{22} \geq |(\mathbf{\Gamma}_k)_{12}|^2$,
- B. $(\mathbf{\Gamma}_k)_{11} \|\mathbf{u}_{1,k}\|^2 + (\mathbf{\Gamma}_k)_{22} \|\mathbf{u}_{2,k}\|^2 > 0$,
- C. $(\mathbf{\Gamma}_k)_{11} \|\mathbf{u}_{1,k}\|^2 + (\mathbf{\Gamma}_k)_{22} \|\mathbf{u}_{2,k}\|^2 < 0$,

for increasing $k \geq 0$, norm $\|\tilde{\mathbf{w}}_k\|$ of the combined parameter error vector in (4.80),

1. can never increase, iff, $(A \wedge B)$,
2. can never decrease, iff $(A \wedge C)$,
3. can do both, increase or decrease, depending on $\mathbf{u}_{i,k}$, iff A is violated, and $(B \vee C)$,
4. is ensured to remain constant, iff B and C are violated.

Proof. See Appendix D.3.1. □

Although (5.9) was obtained from Lemma 4.4 as sufficient condition for non-expanding behaviour, a comparison with Corollary 5.1 shows that it almost precisely captures the strict condition for non-expanding behaviour from the latter. For $(\mathbf{\Gamma}_k)_{ii} \geq 0$ both conditions actually coincide. Nevertheless, Corollary 5.1 provides much more insight to the possible mapping mechanisms.

5.1.3 Two Illustrative Examples with Strong Symmetries

Finally, in this section, the results of Sections 5.1.1 and 5.1.2 are illustrated by two specific configurations of the coupled structure in Figure 5.1. Both of them show strong symmetries which are idealised and probably rarely met in practice. However, they lead to a very clear picture of the corresponding bounds. First, Section 5.1.3.1 considers two coupled gradient type algorithms with identical main and cross coupling factors. Then, Section 5.1.3.2 analyses a simple configuration with identical update errors.

5.1.3.1 Symmetric Cross Coupling

In this section, it is assumed that the coupling factors in Figure 5.1 satisfy

$$\nu_{11} = \nu_{22} = \mu, \quad \nu_{12} = \nu_{21} = \mu\nu, \quad (5.10)$$

with real-valued constants μ and ν . Moreover, the excitation sequences are assumed to have invariant and identical power, i.e.,

$$\|\mathbf{u}_{1,k}\|^2 = \|\mathbf{u}_{2,k}\|^2 = U > 0. \quad (5.11)$$

This is not as restricting as it may seem at the first glance. Indeed, it is perfectly met if, e.g., the excitation vectors represent the delay line of FIR filters, as described in Section 2.2.1.2, and if the

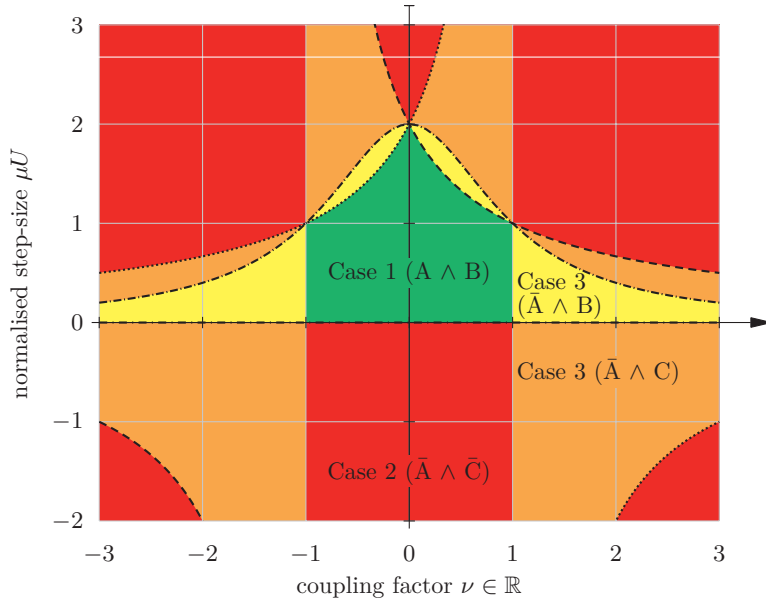


Figure 5.2: Graphical representation of the 4 cases in Corollary 5.1, for two coupled gradient type algorithms that satisfy the symmetry requirements in (5.10).

samples of the two corresponding scalar input sequences contain by the baseband symbols of a constant envelope modulation scheme [Pro95; BLM04].

For such a configuration, (5.5) provides the ℓ_2 -stability bound [DR09b]

$$|\nu| < 1, \quad 0 \leq \mu U \leq 1. \quad (5.12)$$

With respect to the mapping analysis, inserting (5.10) in (5.6)–(5.8) gives

$$(\mathbf{\Gamma}_k)_{11} = (\mathbf{\Gamma}_k)_{22} = \mu [2 - \mu U (1 + \nu^2)], \quad (\mathbf{\Gamma}_k)_{12} = (\mathbf{\Gamma}_k)_{21} = 2\mu\nu (1 - \mu U), \quad (5.13)$$

which modifies the three conditions in Corollary 5.1 to

- A. $(\mu = 0) \vee (|\nu| = 1) \vee \left\langle (|\nu| \neq 1) \wedge \left[\left(\mu U - \frac{2}{1+|\nu|} \right) \left(\mu U - \frac{2}{1-|\nu|} \right) \geq 0 \right] \right\rangle$,
- B. $\mu [2 - \mu U (1 + \nu^2)] > 0$,
- C. $\mu [2 - \mu U (1 + \nu^2)] < 0$.

Figure 5.2 visualises the evaluation of the four cases in Corollary 5.1, after inserting the above conditions. Clearly, for two coupled gradient type algorithms that satisfy (5.10), non-expanding behaviour can only be ensured for

$$-1 \leq \nu \leq 1, \quad \text{and} \quad 0 \leq \mu U \leq \frac{2}{1+|\nu|}. \quad (5.14)$$

Table 5.1: Values of Normalised Step-Size μU obtained for ν in (5.18)

ν	bound for μU in (5.14)	μU 1% below bound	μU 1% above bound
0	2	1.980	2.020
0.25	1.6	1.584	1.616
0.5	1.3	1.320	1.347
0.75	$\overline{1.142857}$	1.131	1.154
1	1	0.990	1.010

It can be verified that these bounds coincide with the sufficient conditions that are obtained from (5.9). Consequently, in this symmetric scenario, Lemma 4.4 is necessary and sufficient.

The following simulation experiments demonstrate the strictness of (5.9). Either of the reference systems as well as the system models of the here considered coupled structure are FIR filters comprising of five taps, i.e.,

$$M_1 = M_2 = M = 5. \quad (5.15)$$

The individual filter weights of the reference systems are drawn from $\mathcal{N}_{\mathbb{C}}(0, 1)$. Similarly, the individual entries $\hat{w}_i(-1)$ of the adaptive parameter vectors are randomly initialised by drawing them from $\mathcal{N}_{\mathbb{C}}(0, \frac{1}{M})$. In order to ensure (5.11), the elements of sequences, $\{u_1(k)\}$ and $\{u_2(k)\}$, that excite the two branches of the coupled structure, are taken from a quadrature phase shift keying (QPSK) alphabet [Pro95; BLM04], i.e, with $i \in \mathcal{N}$,

$$u_i(k) \in \left\{ \frac{1+j}{\sqrt{2}}, \frac{-1+j}{\sqrt{2}}, -\frac{1+j}{\sqrt{2}}, \frac{1-j}{\sqrt{2}} \right\}. \quad (5.16)$$

Hence,

$$U = \|\mathbf{u}_{i,k}\|^2 = M = 5. \quad (5.17)$$

The response of each of the reference systems is affected by additive noise $v_i(k)$ that is randomly generated from $\mathcal{N}_{\mathbb{C}}(0, \sigma_v^2)$, with variance $\sigma_v^2 = 10^{-4}$. For each of the below specified parameter settings, $N_{\text{avg}} = 200$ Monte Carlo runs are performed.

For five values of coupling factor ν ,

$$\nu \in \{0, 0.25, 0.5, 0.75, 1\}, \quad (5.18)$$

four cases are investigated. The first pair of simulations chooses the normalised step-size μU one percent *below* the bound in (5.14) and studies the resulting convergence behaviour for random, as well as for w.c. excitation. The second pair is almost identical, however, μU is selected one percent *above* the bound in (5.14). Table 5.1 gives an overview of the actual values. For the case of random excitation, the input samples $u_i(k)$, drawn from (5.16), are independently and identically distributed. Worst case excitation is achieved by a full search that is performed for each iteration k . The search selects the excitation vectors, $\mathbf{u}_{1,k}$ and $\mathbf{u}_{2,k}$, such that the instantaneous combined parameter error distance $\|\text{col}\{\tilde{\mathbf{w}}_{1,k}, \tilde{\mathbf{w}}_{2,k}\}\|$ is maximised. Due to the restricted domain (5.16) of the excitation samples, and the shift dependency that results from the FIR structure of the individual filters (cf. (2.21)), the search space is restricted to only 16 variants per iteration. This is, as the shift dependency entails that only the first element of each of the two excitation vectors can be modified,

the other elements contain the preceding samples of the excitation sequences. Due to the restricted domain in turn, these two remaining variables can each only assume one out of four values. Hence, $2^4 = 16$ possible excitations cases exist per iteration.

Figures 5.3(a) and 5.3(b) allows to observe that with normalised step-size μU chosen one percent below the bound in (5.14), neither random, nor w.c. excitation lead to divergence of the combined parameter mismatch (cf. (2.19)), i.e., the parameter mismatch that refers to the stacked parameter error vector $\text{col}\{\tilde{\mathbf{w}}_{1,k}, \tilde{\mathbf{w}}_{2,k}\}$ (cf. (4.82)). For μU selected one percent above the bound in (5.14), the results are still similar for random excitation. As Figure 5.3(c) shows, the coupling factors $\nu \in \{0.25, 0.5, 0.75\}$ lead to convergence of the combined parameter error vector towards the steady state that results from the additive noise. For $\nu \in \{0, 1\}$, diverging behaviour can be observed. In the primer case, this is not surprising, as $\nu = 0$ entails that the two gradient type algorithms are independent. Hence, this scenario is equivalent to two isolated NLMS algorithms that are both operated beyond their (sharp) step-size limit [NN67; Hay02; Say03]. Case $\nu = 1$ coincides with the upper bound on the left-hand side of (5.14) and also results in divergence of the combined parameter error vector. Since this effect does not occur for $\nu = 1$ in Figures 5.3(a) and 5.3(b), it can be concluded that (5.14) is also tight for $\nu = 1$. Finally, the results for w.c. excitation depicted in Figure 5.3(d), unveil that also for $\nu \in \{0.25, 0.5, 0.75\}$ divergence of the combined parameter error vector occurs in almost¹ all cases. Consequently, (5.14) is indeed tight for all of the here considered values of coupling factor ν in (5.18).

5.1.3.2 Identical Error Case

In this section, the coupled structure in Figure 5.1 is considered in the case of identical update errors. It is a specific scenario of the system analysed in Section 4.6, with the coupling factors given by

$$\nu_{11} = \nu_{12} = \mu, \quad \nu_{22} = \nu_{21} = a\mu, \quad (5.19)$$

where $a, \mu \in \mathbb{R}$. As in Section 5.1.3.1, the excitation sequences are assumed to have constant and identical power, hence, (5.11) remains valid. In contrast to Section 5.1.3.1, here, (5.5) is not applicable since

$$|\nu_{12}| |\nu_{21}| = a\mu^2 \not\leq \nu_{11}\nu_{22} = a\mu^2. \quad (5.20)$$

Consequently, a statement regarding ℓ_2 -stability is not possible based on the theory in Section 4.4. Yet, a study of the mapping behaviour according to Section 4.5 is still accessible. Inserting (5.11) and (5.19) in (5.6)–(5.8) gives

$$(\mathbf{\Gamma}_k)_{11} = \mu [2 - \mu U (1 + a^2)], \quad (5.21)$$

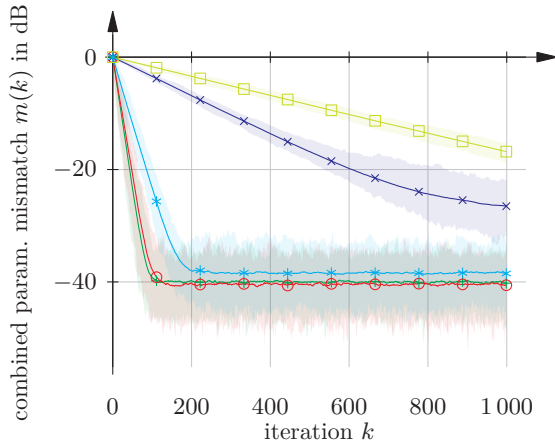
$$(\mathbf{\Gamma}_k)_{22} = \mu [2a - \mu U (1 + a^2)] = (\mathbf{\Gamma}_k)_{11} - 2\mu(1 - a), \quad (5.22)$$

$$(\mathbf{\Gamma}_k)_{12} = (\mathbf{\Gamma}_k)_{21} = \mu [1 + a - \mu U (1 + a^2)] = (\mathbf{\Gamma}_k)_{11} - \mu(1 - a). \quad (5.23)$$

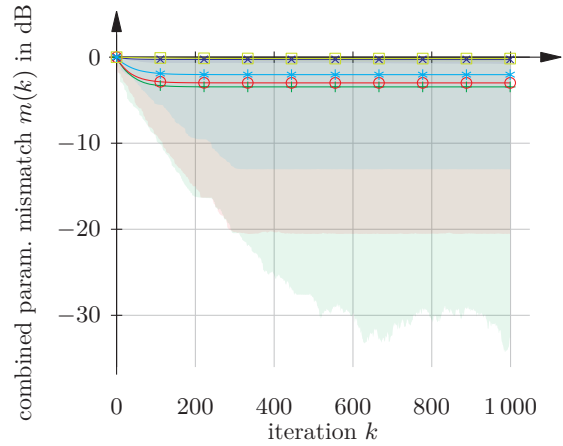
Hence,

$$(\mathbf{\Gamma}_k)_{11} (\mathbf{\Gamma}_k)_{22} - |(\mathbf{\Gamma}_k)_{12}|^2 = -\mu^2 (1 - a)^2 \leq 0 \quad \Rightarrow \quad (\mathbf{\Gamma}_k)_{11} (\mathbf{\Gamma}_k)_{22} \leq |(\mathbf{\Gamma}_k)_{12}|^2, \quad (5.24)$$

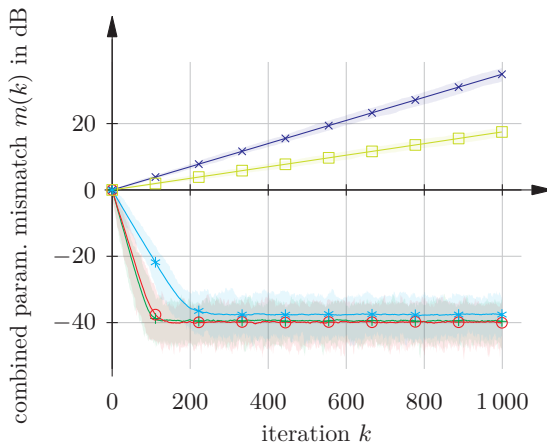
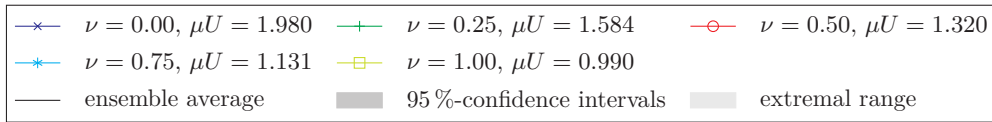
¹ Note that the ensemble minima in Figure 5.3(d) do not continue to grow with increasing k . However, this behaviour is ensured to apply only to a few outliers of the ensemble as the average, as well as the 95 %-confidence intervals show divergence.



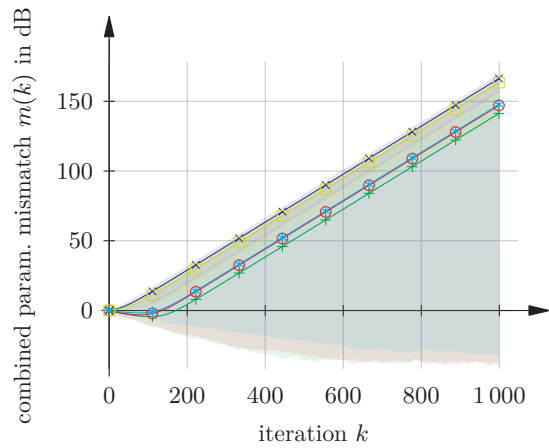
(a) Normalised step-size μU , chosen 1% below the bound in (5.14), i.e., the values are given by the second column on the right-hand of Table 5.1. Excitation of both gradient type algorithms is *random*.



(b) Normalised step-size μU , chosen 1% below the bound in (5.14), i.e., the values are given by the second column on the right-hand of Table 5.1. Here, in contrast to Figure 5.3(a), *w.c.* excitation is used.



(c) In contrast to Figures 5.3(a) and 5.3(b), normalised step-size μU is chosen 1% above the bound in (5.14), i.e., the values are given by the right column in Table 5.1. Excitation of both gradient type algorithms is *random*.



(d) As in Figure 5.3(c), normalised step-size μU is chosen 1% above the bound in (5.14), i.e., the values are given by the right column in Table 5.1. Here, *w.c.* excitation is used.

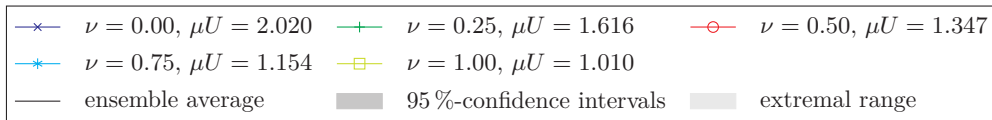


Figure 5.3: Evaluation of bound (5.14) that applies to the coupled structure in Figure 5.1 with coupling symmetries in (5.11) and (5.12). The five values of coupling factor ν in (5.18) are considered. The domain of the excitation sequences is restricted to the QPSK-symbols in (5.16).

which entails that Condition A in Corollary 5.1 can only be satisfied (by identity), if $\mu = 0$ or $a = 1$. Inserting this in (5.21)–(5.23) shows that then, for $\mu = 0$, the constant Case 4 occurs in Corollary 5.1. For $a = 1$, all four elements of $\mathbf{\Gamma}_k$ are identical and the coupled structure reduces to a symmetric algorithm, which is an inherent application of Lemma 4.7. In all other situations, i.e., $\mu \neq 0$ and $a \neq 1$, in Corollary 5.1, Condition A is violated and either Condition B or Condition C holds, resulting in the indifferent Case 3.

For illustration of the above findings, two simulation experiments are performed. Almost all of the simulation settings described in Section 5.1.3 remain valid, here. The only difference is found in the choice of the coupling factors which have to be modified in order to reflect (5.19). As found in Section 4.6, the identical error case, maps to an gradient type algorithm with matrix step-size (cf. (4.101)). Hence, analogous to the simulation experiments in Section 3.1, choosing

$$\mu = \frac{\bar{\mu}}{(1+a)U}. \quad (5.25)$$

with normalised step-size $\bar{\mu}$, the excitation power is normalised and the spectral radius of the corresponding mapping matrix is ensured to be less than one, if $0 < \bar{\mu} < 2$ (cf. Lemma 3.1). Two values for a and three values for $\bar{\mu}$ are considered

$$a \in \{0.5, 1\}, \quad \text{and} \quad \bar{\mu} \in \{0.5, 1.95, 2.05\}, \quad (5.26)$$

respectively. Hence, each simulation experiment investigates six parameter constellations. In a first step, the coupled structure is excited by random QPSK symbols drawn from (5.16). Figure 5.4(a) shows the results in terms of the combined parameter mismatch (cf. (2.19) and (4.82)). Clearly, only for $\bar{\mu} = 2.05$, independently from a , divergence occurs. This is not surprising as it leads to a violation of Lemma 3.1, which necessarily provokes divergence. Note that due to $a = 1$, the scheme coincides with an NLMS algorithm. Hence, this observation perfectly agrees with the corresponding well known step-size bound [NN67; Hay02; Say03]. A repetition of the same experiment with w.c. excitation leads to the graphs in Figure 5.4(b). Although quantitatively different, they are qualitatively similar to those in Figure 5.4(a). Even if the restriction to FIR filters is discarded and linear combiner (cf. Section 2.2.1.1) are used instead, all cases with $\bar{\mu} < 2$, end up in convergence – due to its similarity no figure included. For $a = 0.5$, the asymmetric nature of the algorithm may tempt to expect divergence, also for $\bar{\mu} < 2$. The answer for this possibly counterintuitive observation is found in Section 3.4.4. Accordingly, since a and μ are constant, also the step-size matrix of the equivalent asymmetric algorithm is invariant, which in turn ensures a parameter error distance that remains bounded (cf. Theorem 3.2).

5.2 The (Simplified) Wiener Model

In many system identification applications the (unknown) reference system shows non-linear behaviour [KH86; KAWC95; GS01; DLA03; RZV05; GH09]. If such a system – which is here assumed to be SISO – is memoryless, i.e., at any arbitrary time instant, its output only depends on the instantaneous² input value, the system model is required to implement a (non-linear) one-to-one mapping, i.e., a look-up table (LUT). In such a case, the parametrisation based on a non-linear basis, as introduced in Section 2.2.1.3, leads to a model that is linear in its parameters. This again allows to use a gradient type algorithm in order to perform the adaptive system identification process. The situation becomes more involved, if the output of the reference system additionally depends on

² A fixed and known delay between input and output would also be acceptable.

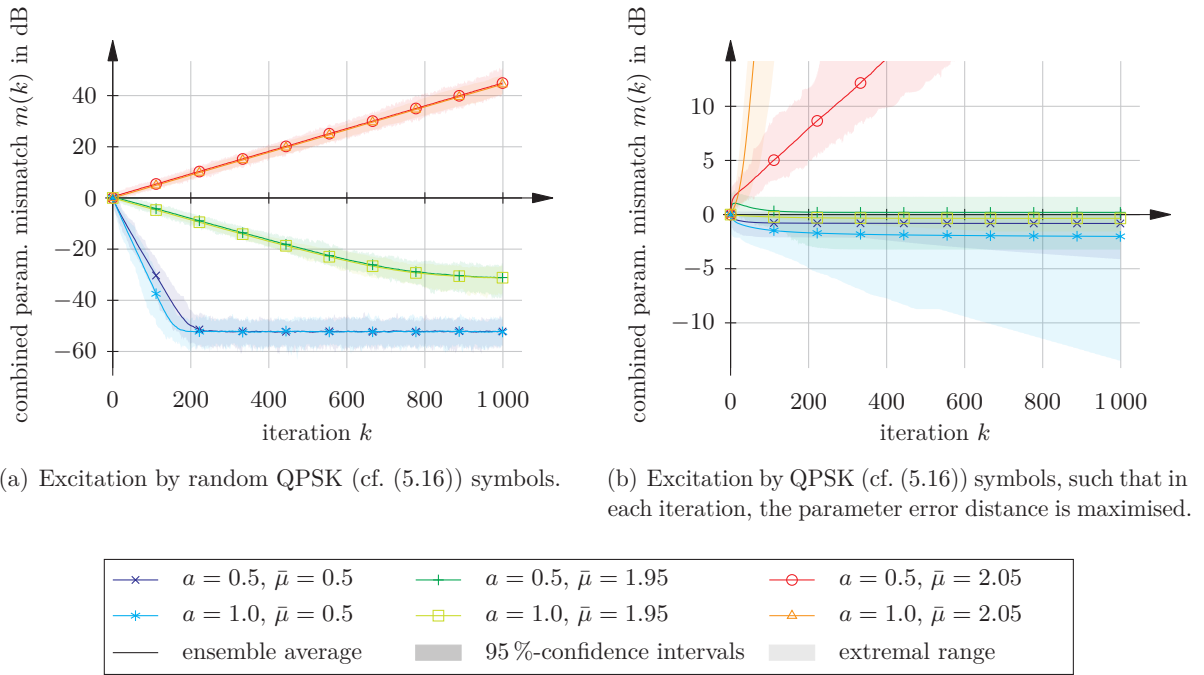


Figure 5.4: Convergence behaviour of the two coupled adaptive filters in Figure 5.1, in the case of identical update errors. The coupling factors are given by (5.26).

the history of its input. Then, one of the most general approaches would be to use Volterra Series (cf. Section 2.2.1.4). While this again leads to a model that is linear in parameters, the downside is the immense number of parameters that has to be estimated, even for reasonable non-linearity orders and short memory lengths. Hence, in scenarios which give access to some a priori knowledge about the unknown reference system, simplifications are desired which allow to reduce computational complexity and speed up adaptation.

One such approach that remarkably reduces the number of parameters, is the Wiener model. It contains the cascade of a linear filter followed by a memoryless non-linearity. Figure 5.5 depicts an adaptive system identification structure, where the reference system as well as the system model are represented by a Wiener model. As pointed out at the beginning of Section 2.1, any behaviour of the reference system that cannot be described by the Wiener model, is subsumed in additive noise $v(k)$.

For the structure in Figure 5.5, several adaptive algorithms and stability analyses are found in

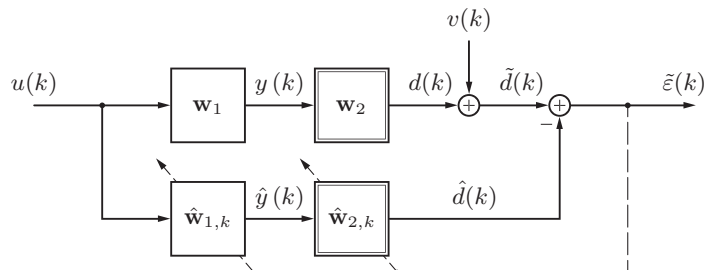


Figure 5.5: An adaptive system identification system based on the Wiener model that consists of a cascade of a linear filter and a memoryless non-linearity. Here, the unknown reference system in the top branch is assumed to have the same structure as the adaptive system model in the bottom branch. Inaccuracies of modelling are subsumed in the additive noise $v(k)$.

literature. One approach is given in [Gre92; PHW07], which describe the linear part by a state-space model and use a non-parametric representation of the non-linearity. The primer is identified by least-squares, the latter by an adaptive kernel method. Convergence is analysed in terms of first and second order moments. Two further identification methods are proposed in [RZV05]. Both of them represent the linear dynamic system as an FIR filter and use a non-linear basis expansion to describe the non-linear part. The first proposed identification algorithm is based on alternating projections, the second one on a minimum norm argument. Finally, [Wig94; Wig95] assume the non-linearity to be known a priori and employ the Gauß-Newton algorithm to identify the linear part represented by an IIR filter. Analyses of local and global convergence are performed. The extension to an unknown non-linearity that is described by either piecewise linear or piecewise quadratic functions is covered in [Wig90].

All of the above described approaches require a considerable amount of computational power. The case of computationally less expensive pure gradient type algorithms is considered in [BCV00; CBV00; CBV01]. First and second order moments analysis as well as mean tracking behaviour of the parameter error vector is analysed under common independence assumptions [Hay02; Say03]. In the sequel, a complementary deterministic analysis for this type of adaptive Wiener model is discussed based on the theories in Chapters 3 and 4. The underlying idea has been published in [DR10]. An improvement for the therein used gradient type algorithm was proposed in [DR12].

Following the lines of [BCV00; CBV00; CBV01; AR03], the output of the first block in the cascade, represented by an FIR filter, is given by

$$y(k) \triangleq \mathbf{u}_k^T \mathbf{w}_1, \quad \hat{y}(k) \triangleq \mathbf{u}_k^T \hat{\mathbf{w}}_{1,k-1}, \quad (5.27)$$

where excitation vector \mathbf{u}_k contains the M_1 entries of the delay line corresponding to the FIR filters, as described in Section 2.2.1.2. Assuming that a non-linear basis has been chosen consisting of M_2 basis functions $\psi_m : \mathbb{R} \mapsto \mathbb{R}$, $m \in \{1, \dots, M_2\}$, the non-linear one-to-one mappings of the second blocks in the cascade can be defined as

$$h_{\mathbf{w}_2}(y(k)) \triangleq \sum_{m=1}^{M_2} w_{2,m} \psi_m(y(k)) = \mathbf{w}_2^T \boldsymbol{\psi}(y(k)), \quad (5.28)$$

$$h_{\hat{\mathbf{w}}_2}(\hat{y}(k)) \triangleq \sum_{m=1}^{M_2} \hat{w}_{2,m}(k-1) \psi_m(\hat{y}(k)) = \hat{\mathbf{w}}_{2,k-1}^T \boldsymbol{\psi}(\hat{y}(k)), \quad (5.29)$$

where the vector of basis functions $\boldsymbol{\psi}(\cdot) \in \mathbb{R}^{M_2}$ has been introduced in accordance to (2.22), i.e.,

$$\boldsymbol{\psi}(\cdot) \triangleq [\psi_1(\cdot) \quad \dots \quad \psi_{M_2}(\cdot)]^T. \quad (5.30)$$

Assuming that the linear part has been identified perfectly, the adaptive update of the non-linear part can be done using the conventional LMS algorithm algorithm, i.e.,

$$\hat{\mathbf{w}}_{2,k} = \hat{\mathbf{w}}_{2,k-1} + \mu_{\text{nl}}(k) \boldsymbol{\psi}(\hat{y}(k)) \tilde{\varepsilon}(k), \quad (5.31)$$

with some real-valued positive step-size $\mu_{\text{nl}}(k)$, and

$$\tilde{\varepsilon}(k) = \tilde{d}(k) - \hat{d}(k) = \underbrace{d(k) - \hat{d}(k)}_{\varepsilon(k)} + v(k) = \underbrace{\hat{\mathbf{w}}_{2,k-1}^T \boldsymbol{\psi}(\hat{y}(k))}_{\varepsilon(k)} + v(k). \quad (5.32)$$

If a stochastic gradient update is used also for the linear part, and if analogous to (2.6) and (2.7),

cost function $E\{\tilde{\varepsilon}^2(k)\}$ is employed, the following gradient is obtained (suppressing iteration index k in the next line)

$$\frac{\partial \tilde{\varepsilon}^2}{\partial \hat{\mathbf{w}}_1} = 2\tilde{\varepsilon} \frac{\partial \tilde{\varepsilon}}{\partial \hat{\mathbf{w}}_1} = 2\tilde{\varepsilon} \frac{\partial}{\partial \hat{\mathbf{w}}_1} \{h_{\mathbf{w}_2}(\mathbf{w}_1^\top \mathbf{u}) - h_{\hat{\mathbf{w}}_2}(\hat{\mathbf{w}}_1^\top \mathbf{u}) + v\} = -2\tilde{\varepsilon} h'_{\hat{\mathbf{w}}_2}(\hat{\mathbf{w}}_1^\top \mathbf{u}) \mathbf{u}^\top. \quad (5.33)$$

Including the constant factor 2 into the real-valued positive step-size $\mu_{\text{lin}}(k)$, this leads to the stochastic gradient update of parameter vector $\hat{\mathbf{w}}_{1,k}$, according to

$$\hat{\mathbf{w}}_{1,k} = \hat{\mathbf{w}}_{1,k-1} + \mu_{\text{lin}}(k) \mathbf{u}_k h'_{\hat{\mathbf{w}}_{2,k-1}}(\hat{\mathbf{w}}_{1,k-1}^\top \mathbf{u}_k) \tilde{\varepsilon}(k). \quad (5.34)$$

Note that the gradient descent can only reliably lead to the actual minimum of the cost function, if the latter does not show local minima. While this is ensured for (5.31), it is in general not guaranteed for (5.34), as it contains an – at this point almost arbitrary – non-linearity in its auxiliary path. With the vector consisting of the first order derivatives of the basis functions ψ_m ,

$$\boldsymbol{\psi}'(\cdot) \triangleq \left[\frac{d\psi_1(\cdot)}{d\cdot} \quad \dots \quad \frac{d\psi_{M_2}(\cdot)}{d\cdot} \right]^\top, \quad (5.35)$$

based on (5.29), (suppressing iteration index k for the remainder of this sentence), derivative $h'_{\hat{\mathbf{w}}_2}(\hat{y})$ is equivalent to (note that for derivative $h'_{\mathbf{w}_2}(y)$ an analogous relation holds)

$$h'_{\hat{\mathbf{w}}_2}(\hat{y}) = \frac{d}{d\hat{y}} \left\{ \sum_{m=1}^{M_2} \hat{w}_{2,m} \psi_m(\hat{y}) \right\} = \sum_{m=1}^{M_2} \hat{w}_{2,m} \frac{d\psi_m(\hat{y})}{d\hat{y}} = \hat{\mathbf{w}}_2^\top \boldsymbol{\psi}'(\hat{y}). \quad (5.36)$$

Inserting (5.36) in (5.34) gives the completely equivalent update equation

$$\hat{\mathbf{w}}_{1,k} = \hat{\mathbf{w}}_{1,k-1} + \mu_{\text{lin}}(k) \mathbf{u}_k \hat{\mathbf{w}}_{2,k-1}^\top \boldsymbol{\psi}'(\hat{\mathbf{w}}_{1,k-1}^\top \mathbf{u}_k) \tilde{\varepsilon}(k). \quad (5.37)$$

In the sequel, the goal is to map the combination of the two gradient type algorithms given by (5.31) and (5.34) to the coupled structure introduced in Chapter 4, more specifically, to the one in Figure 5.1. To do so, as a first step, the noiseless a priori error $\varepsilon(k)$ is expanded to

$$\varepsilon(k) = d(k) - \hat{d}(k) = h_{\mathbf{w}_2}(y(k)) - h_{\hat{\mathbf{w}}_{2,k-1}}(\hat{y}(k)) \quad (5.38)$$

$$= \underbrace{h_{\mathbf{w}_2}(y(k)) - h_{\mathbf{w}_2}(\hat{y}(k))}_{\textcircled{1}} + \underbrace{h_{\mathbf{w}_2}(\hat{y}(k)) - h_{\hat{\mathbf{w}}_{2,k-1}}(\hat{y}(k))}_{\textcircled{2}}. \quad (5.39)$$

At this point it is necessary to assume that the non-linear one-to-one mapping $h_{\mathbf{w}_2}$ is differentiable on the open interval $(y(k), \hat{y}(k))$. Then, due to the mean value theorem [MS00b, p. 626; HSK94, pp. 11ff.; SR95a; RS96b; RS97]³,

$$h_{\mathbf{w}_2}(y(k)) - h_{\mathbf{w}_2}(\hat{y}(k)) = h'_{\mathbf{w}_2}(\eta(k)) (y(k) - \hat{y}(k)) \quad (5.40)$$

$$= h'_{\mathbf{w}_2}(\eta(k)) (\mathbf{u}_k^\top \mathbf{w}_1 - \mathbf{u}_k^\top \hat{\mathbf{w}}_{1,k-1}) \quad (5.41)$$

$$= h'_{\mathbf{w}_2}(\eta(k)) \mathbf{u}_k^\top \tilde{\mathbf{w}}_{1,k-1}, \quad (5.42)$$

with some intermediate value $\eta(k) \in [y(k), \hat{y}(k)]$. Equation (5.42) obviously coincides with $\textcircled{1}$ in

³ Note that the mean value theorem for vector valued functions in [McL65] ensures that the identity in (5.40) also holds if $h_{\mathbf{w}_2}$ is replaced by the decomposition in (5.28).

(5.39). For ②, basis expansions (5.28) and (5.29), give

$$h_{\mathbf{w}_{2,k-1}}(\hat{y}(k)) - h_{\hat{\mathbf{w}}_{2,k-1}}(\hat{y}(k)) = (\mathbf{w}_2 - \hat{\mathbf{w}}_{2,k-1})^\top \boldsymbol{\psi}(\hat{y}(k)) = \tilde{\mathbf{w}}_{2,k-1}^\top \boldsymbol{\psi}(\hat{y}(k)). \quad (5.43)$$

Hence, with (5.42) and (5.43), noiseless a priori error (5.39) is found to be equivalent to

$$\varepsilon(k) = h'_{\mathbf{w}_2}(\eta(k)) \tilde{\mathbf{w}}_{1,k-1}^\top \mathbf{u}_k + \tilde{\mathbf{w}}_{2,k-1}^\top \boldsymbol{\psi}(\hat{y}(k)). \quad (5.44)$$

Eventually, substituting the individual noiseless a priori errors,

$$e_1(k) \triangleq \tilde{\mathbf{w}}_{1,k-1}^\top \mathbf{u}_k, \quad e_2(k) \triangleq \tilde{\mathbf{w}}_{2,k-1}^\top \boldsymbol{\psi}(\hat{y}(k)), \quad (5.45)$$

in (5.44), yields the (noisy) a priori error $\tilde{\varepsilon}(k)$

$$\tilde{\varepsilon}(k) = h'_{\mathbf{w}_2}(\eta(k)) e_1(k) + e_2(k) + v(k), \quad (5.46)$$

that has the structure of the a priori error in (4.96), for the coupled structure with identical errors. Inserting (5.46) in (5.31) and (5.34), leads to the desired set of update equations

$$\hat{\mathbf{w}}_{1,k} = \hat{\mathbf{w}}_{1,k-1} + \mu_{\text{lin}}(k) \mathbf{u}_k h'_{\hat{\mathbf{w}}_{2,k-1}}(\hat{\mathbf{w}}_{1,k-1}^\top \mathbf{u}_k) \left[h'_{\mathbf{w}_2}(\eta(k)) e_1(k) + e_2(k) + v(k) \right], \quad (5.47)$$

$$\hat{\mathbf{w}}_{2,k} = \hat{\mathbf{w}}_{2,k-1} + \mu_{\text{nl}}(k) \boldsymbol{\psi}(\hat{y}(k)) \left[h'_{\mathbf{w}_2}(\eta(k)) e_1(k) + e_2(k) + v(k) \right]. \quad (5.48)$$

Comparing, (5.47) and (5.48) with the identical error case discussed in Section 4.6, it is found that the adaptive system in Figure 5.5, updated according to (5.31) and (5.34), is equivalent to the coupled structure in Figure 5.1. With the factorisation of the coupling factors in (4.94), the (effective) step-sizes and coupling factors are identified as

$$\mu_1(k) = \mu_{\text{lin}}(k) h'_{\hat{\mathbf{w}}_{2,k-1}}(\hat{\mathbf{w}}_{1,k-1}^\top \mathbf{u}_k), \quad \nu_1(k) = h'_{\mathbf{w}_2}(\eta(k)), \quad (5.49)$$

$$\mu_2(k) = \mu_{\text{nl}}(k), \quad \nu_2(k) = 1. \quad (5.50)$$

As pointed out in Section 4.6, such a structure is in general not accessible too the ℓ_2 -stability analysis in Section 4.4. Yet, according to [AR03], conditions for ℓ_2 -stability of such a structure can indeed be established. This confirms the remark in Section 4.6 that failing of the theory in Section 4.4 does *not* allow to conclude instability in the ℓ_2 -stable-sense. Moreover, in Section 4.6, it is found that the identical error case can be mapped to an asymmetric algorithm implying the validity of all the findings of Chapter 3. Specifically, Lemma 4.7 is applicable, which provides a condition that guarantees the algorithm to reduce to a symmetric algorithm. This in turn, entails non-expanding behaviour (for adequately chosen step-sizes). Applying the latter lemma to the step-sizes and coupling factors in (5.49) and (5.50), translates to condition

$$\mu_{\text{lin}}(k) h'_{\hat{\mathbf{w}}_{2,k-1}}(\hat{\mathbf{w}}_{1,k-1}^\top \mathbf{u}_k) = \mu_{\text{nl}}(k) h'_{\mathbf{w}_2}(\eta(k)). \quad (5.51)$$

Note that since in practical situations, the reference system is unknown and only its input $u(k)$ and output $\tilde{d}(k)$ are accessible, in (5.51) neither $h_{\mathbf{w}_2}$, nor $\eta(k)$ can be determined exactly. Nevertheless, under the assumption of uniform convergence [Rud09, p. 255],

$$\hat{\mathbf{w}}_{2,k} \rightarrow \mathbf{w}_2 \Rightarrow h_{\hat{\mathbf{w}}_{2,k}} \rightarrow h_{\mathbf{w}_2}, \quad (5.52)$$

and due to

$$\hat{\mathbf{w}}_{1,k} \rightarrow \mathbf{w}_1 \Rightarrow \hat{y}(k) \rightarrow y(k) \Rightarrow \eta(k) \rightarrow \hat{\mathbf{w}}_{1,k-1}^T \mathbf{u}_k, \quad (5.53)$$

it becomes clear that increasing accuracy of estimates $\hat{\mathbf{w}}_{1,k}$ and $\hat{\mathbf{w}}_{2,k}$, facilitates an approximate satisfaction of (5.51). Similarly, this confirms that parameter initialisation also influences the risk of hidden divergence.

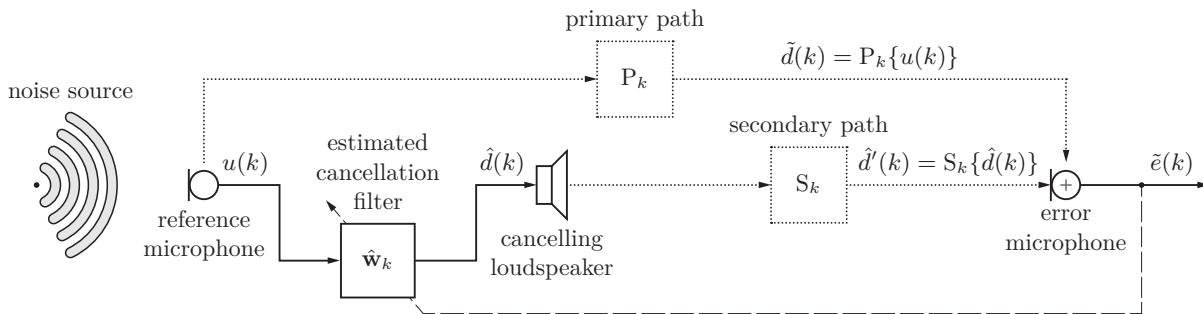
Finally, stepping back to Section 3.4.4, it is known that asymmetric algorithms do not necessarily lead to parameter divergence under w.c. excitation. Hence, even if (5.51) is violated, the parameter error vector of the resulting algorithm may still be ensured to remain unconditionally bounded. In fact, based on Section 4.6, it is found that the step-size matrix of the equivalent asymmetric algorithm in (4.101) is diagonal with M_1 entries given by the quotient, obtained by dividing the left-hand side of (5.49) by its right-hand side, and M_2 entries equal to $\mu_2(k)$ in (5.50). Accordingly, the resulting step-size matrix has only two different eigenvalues with multiplicities M_1 and M_2 . As a consequence, the step-sizes, $\mu_{\text{lin}}(k)$ and $\mu_{\text{nl}}(k)$, provide means to inhibit the fulfilment of the necessary condition for parameter divergence in Theorem 3.3. This in turn shows that although (5.51) cannot be precisely satisfied in practical situations, the parameter error of the adaptive Wiener model still can in most cases be ensured to converge to a finite limit – even under w.c. excitation.

5.3 Multichannel Filtered- x LMS Algorithm

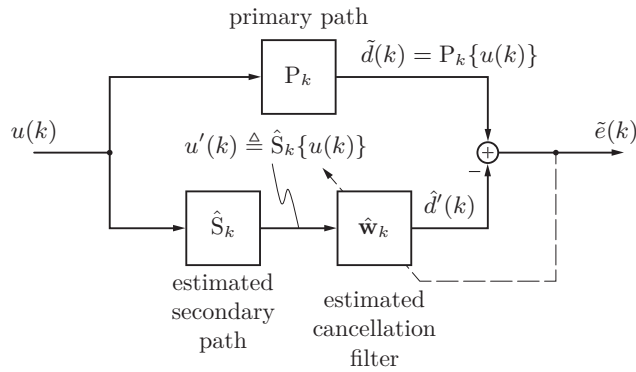
In this section, the results of Chapter 4 are applied to the MC-FXLMS algorithm which is, e.g., used in broadband feed-forward ANC applications [KM99; KM08; KGK12; Tab12; GP13]. In simple geometric settings, such as a narrow duct, in which an almost plane sound wave propagates, the FXLMS algorithm achieves considerable noise suppression. In less regular scenarios, the resulting complicated sound field requires further effort. As a direct consequence, the MC-FXLMS algorithm has been independently proposed by [Mor80; WSS81] as a MIMO extension of the FXLMS algorithm. Figure 5.6 depicts a SISO broadband feed-forward ANC system and its corresponding system model. The underlying principle is that the cancelling loudspeaker in Figure 5.6(a) emits a sound wave (corresponding to signal $\hat{d}(k)$), such that due to destructive interference, in the vicinity of the error microphone, the inbound noise (represented by signal $\tilde{e}(k)$) is evened out. In such a feed-forward system, the compensation signal is generated by filtering the arriving noise signal $u(k)$ that is received by the reference microphone. The required filter (with parameter vector $\hat{\mathbf{w}}_k$) is estimated based on reference (noise) signal $u(k)$ and error signal $\tilde{e}(k)$. Identification of the filter by means of the conventional LMS algorithm is degraded or even inhibited due to the delay and dispersion introduced by the secondary path S_k between the cancelling loudspeaker and the error microphone.

Assuming slowly changing acoustic channels and purely linear behaviour, the system in Figure 5.6(b) has equivalent behaviour to the scenario in Figure 5.6(a). However, here, reference signal $u'(k)$ is pre-filtered by an estimate \hat{S}_k of the secondary path. This allows to compensate the afore mentioned delay and dispersion, and describes the principle underlying the famous FXLMS algorithm. A crucial point here, is necessity for estimate \hat{S}_k of the secondary path. However, observations have shown that in many cases the accuracy of the secondary path model is not critical. Often even a one tap filter, i.e., a simple delay, suffices in order to achieve a possibly slowly converging but still reliable performance [LLP89; FBL93; LLP92; Bja95; KM08; TA10; KGK12].

The FXLMS algorithm is well studied, yet research of its convergence is still ongoing [TA10]. A stochastic analysis of the FXLMS algorithm for spherically invariant excitation processes as well as a good overview about available results can be found in [Bja95]. Stability in the mean is treated in [FBL93]. A mean square analysis for different secondary path models can be found in [TA10;



(a) Physical system. Dotted lines indicate acoustic paths. The “+” sign in the error microphone indicates that there, noise compensation is achieved by acoustic superposition.



(b) Equivalent system model under the assumption of slowly changing primary and secondary paths as well as small step-sizes. Moreover, acoustic feedback from the cancelling loudspeaker to the primary microphone is neglected.

Figure 5.6: Broadband feed-forward ANC based on the FXLMS algorithm.

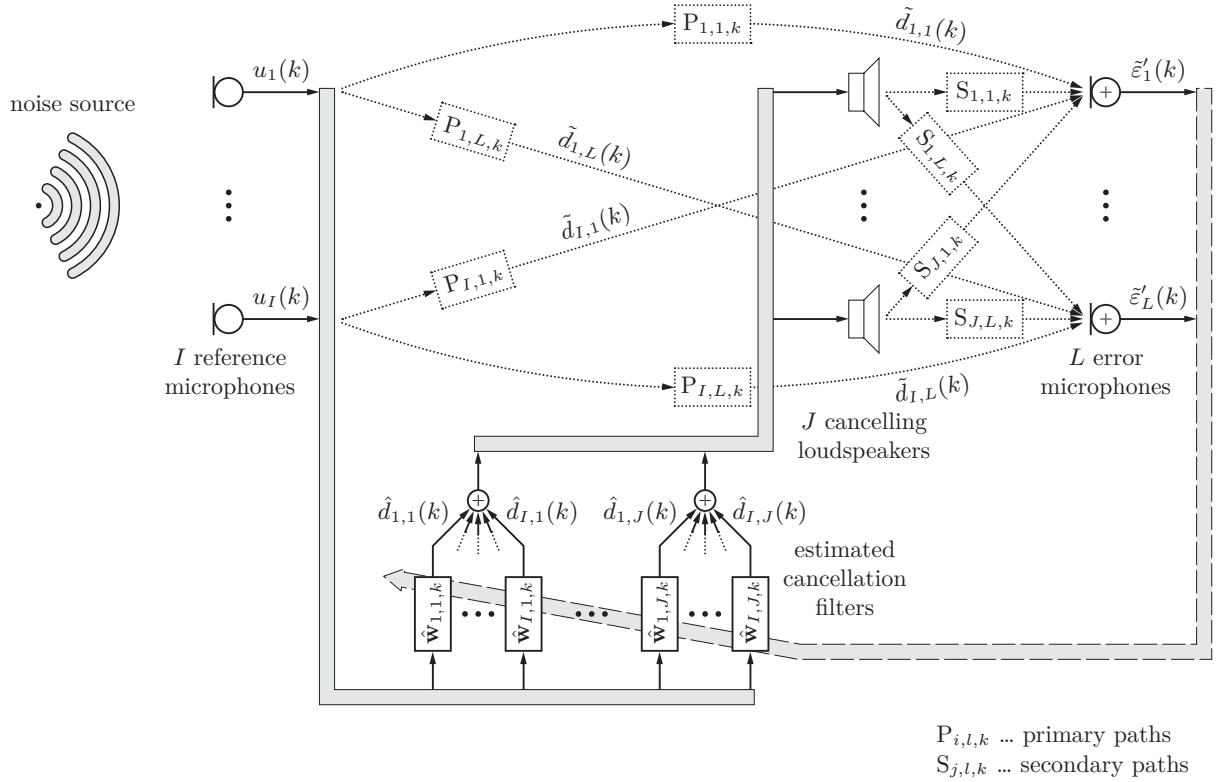


Figure 5.7: Multichannel broadband feed-forward ANC. Dotted lines indicate acoustic paths. The “+” sign in the error microphones indicates that there, noise compensation is achieved by acoustic superposition.

TA11; Tab12], as well as in [LLP89; LLP92; RF94]. A deterministic study for sinusoidal excitation is given in [ESN87; VM06]. An alternative deterministic approach is pursued in [RS96a; RS98], which investigate ℓ_2 -stability of the FXLMS algorithm based on the small gain theorem.

The here considered MC-FXLMS algorithm is a direct extension of the FXLMS algorithm. Accordingly, the system underlying its application to ANC depicted in Figure 5.7 is straightforwardly obtained from the structures in Figure 5.6, by using I reference microphones, J cancelling loudspeakers, and L error microphones instead of only one of each. An overview of related symbols can be found in Table 5.2. Note that in this section, indices which are fixed to one single value are omitted. This is done for the sake of notational simplicity. The resulting ambiguity is minimised by the context. With $i \in \{1, \dots, I\}$, $j \in \{1, \dots, J\}$, and $l \in \{1, \dots, L\}$, the individual parameter vectors $\hat{\mathbf{w}}_{i,j,k}$ are updated by

$$\hat{\mathbf{w}}_{i,j,k} = \hat{\mathbf{w}}_{i,j,k-1} + \sum_{l=1}^L \mu_{i,j,l}(k) \mathbf{u}_{i,j,l}^{l*} \tilde{\varepsilon}'_l(k), \quad (5.54)$$

with

$$\tilde{\varepsilon}'_l(k) \triangleq \sum_{i=1}^I \sum_{j=1}^J \tilde{e}_{i,j,l}(k) = \underbrace{\sum_{i=1}^I \sum_{j=1}^J e_{i,j,l}(k)}_{\varepsilon'_l(k)} + \underbrace{\sum_{i=1}^I \sum_{j=1}^J v_{i,j,l}(k)}_{v_l^{(\varepsilon')}(k)}, \quad (5.55)$$

Table 5.2: List of Mathematical Symbols Describing the Multichannel Filtered- x LMS

I	number of reference microphones, corresponding index i is taken from $\{1, \dots, I\}$
J	number of cancelling loudspeakers, corresponding index j is taken from $\{1, \dots, J\}$
L	number of error microphones, corresponding index l is taken from $\{1, \dots, L\}$
$P_{i,l,k}$	(acoustical) primary path between reference microphone i and error microphone l
$S_{j,l,k}$	(acoustical) secondary path between cancelling loudspeaker j and error microphone l
$\hat{S}_{j,l,k}$	estimate of secondary path $S_{j,l,k}$
$u_i(k)$	discrete time signal at reference microphone i
$\mathbf{u}_{i,k}$	excitation vector, i.e., tapped delay line, at output of reference microphone i
$u'_{i,j,l}(k)$	excitation signal, corresponding to $u_i(k)$ filtered by estimated secondary path $\hat{S}_{j,l,k}$
$\mathbf{u}'_{i,j,l,k}$	excitation vector, i.e., tapped delay line, of adaptive filter $\langle i, j \rangle$, if excited by $u'_{i,j,l}(k)$
$\mathbf{w}_{i,j}$	parameter vector representing the reference system between reference microphone i , and cancelling loudspeaker j
$\hat{\mathbf{w}}_{i,j,k}$	adaptively estimated version of parameter vector $\mathbf{w}_{i,j}$
$\tilde{\mathbf{w}}_{i,j,k}$	parameter error vector $\tilde{\mathbf{w}}_{i,j,k} = \mathbf{w}_{i,j} - \hat{\mathbf{w}}_{i,j,k}$
$M_{i,j}$	length of parameter vectors $\mathbf{w}_{i,j}$ and $\hat{\mathbf{w}}_{i,j,k}$, which are assumed to have the same length
M	total number of parameters, i.e., sum over all $M_{i,j}$
$\mu_{i,j,l}(k)$	step-size of adaptive filter $\langle i, j \rangle$, using the signal of error microphone l
$d_{i,l}(k)$	noiseless output of primary path $\langle i, l \rangle$
$\tilde{d}_{i,l}(k)$	output of primary path $\langle i, l \rangle$, including noise; represents the (acoustic) signal which would be received by error microphone l , in absence of an ANC
$\hat{d}_{i,j}(k)$	output of adaptive filter $\langle i, j \rangle$, if excited by $u_i(k)$
$\hat{d}'_{i,j,l}(k)$	output of adaptive filter $\langle i, j \rangle$, if excited by pre-filtered $u'_{i,j,l}(k)$
$e_{i,j,l}(k)$	noiseless a priori error of adaptive filter $\langle i, j \rangle$, using error microphone l (cf. (5.56))
$v_{i,j,l}(k)$	additive noise present at error microphone l , “seen” by adaptive filter $\langle i, j \rangle$
$\tilde{e}_{i,j,l}(k)$	noisy version of $e_{i,j,l}(k)$
$\varepsilon'_l(k)$	noiseless error at error microphone l (cf. (5.55))
$v_l^{(\varepsilon')}(k)$	overall noise “seen” by error microphone l
$\tilde{\varepsilon}'_l(k)$	noisy version of $\varepsilon'_l(k)$ and actual output of error microphone l
\mathbf{U}'_k	matrix combining all pre-filtered excitation vectors (cf. (5.59))
\mathbf{e}_k	vector of noiseless overall a priori errors in the SIMO case (cf. (5.60))
\mathbf{v}_k	vector of additive noise signals in the SIMO case (cf. (5.61))
$\tilde{\mathbf{e}}_k$	noisy version of \mathbf{e}_k (cf. (5.62))
\mathbf{D}_k	step-size matrix (cf. (5.63))
ε'_k	vector of noiseless overall a priori errors in the MIMO case (cf. (5.92))
$\mathbf{v}_k^{(\varepsilon')}$	vector of additive noise signals in the MIMO case (cf. (5.93))
$\mathbf{D}_{l,k}$	step-size matrix in the MIMO case, using error signal l (cf. (5.82))
$f_{\mathcal{I}\mathcal{J}}(\cdot)$	bijective function, mapping one dimensional indices to two-dimensional indices (cf. (5.72))
\ddot{i}	one-dimensional index which is equivalent to $\langle i, j \rangle$

and

$$\tilde{e}_{i,j,l}(k) \triangleq \underbrace{\tilde{\mathbf{w}}_{i,j,k-1}^T \mathbf{u}'_{i,j,l,k}}_{e_{i,j,l}(k)} + v_{i,j,l}(k). \quad (5.56)$$

Also the MC-FXLMS algorithm has been investigated in literature with respect to its convergence, robustness, and stability. A frequency domain stability analysis for a discrete spectrum of the primary source is presented in [ESN87; EBN92]. A different approach is taken in [WR99], which applies the ordinary differential equation method [Lju77; Lju99], in order to study convergence with probability one for the single input MC-FXLMS algorithm, i.e., $I = 1$. Based on, e.g., [IS96; LLM98], asymptotic convergence with respect to stochastic uncertainties of the secondary path is investigated in [Fra04; FVE07; FEV07].

In the sequel, these results are complemented by an analysis of ℓ_2 -stability and an investigation of the mapping behaviour, under the assumption of perfectly known secondary paths. This is an idealised and debatable scenario. Nevertheless, it seems tolerable for two reasons. First, as pointed out in some of the above mentioned works, the FXLMS algorithm and its MIMO extension are rather robust with respect to modelling errors of the secondary path. Second, this assumption allows to obtain results which are conclusive despite being idealised. Indeed, many works in literature also resort to this simplifications, in order to end up with comprehensive results [ESN87; EBN92; FBL93; Bja95; Ell00].

The analysis of the MC-FXLMS algorithm is presented in three steps. Section 5.3.1 considers the simplest extension of the FXLMS algorithm by only increasing the number of error microphones, i.e., $I = J = 1$, $L > 1$. In Section 5.3.2, this restriction is reversed, meaning that an arbitrary number of reference microphones and cancelling loudspeakers is opposed by only one single error microphone, i.e., $I > 1$, $J > 1$, $L = 1$. Finally, Section 5.3.3 combines the results of Sections 5.3.1 and 5.3.2, in order to analyse the general case. The terms SIMO, MISO, and MIMO will be used to address the respective versions of the MC-FXLMS algorithm. In order to prevent confusion, it is emphasised that here, the term “single/multiple output” does *not* refer to the number of cancelling loudspeakers, but instead to the number of error microphones. The justification for this choice will become clear further down in Figure 5.8, which visualises that the existence of more than one cancelling loudspeakers translates to an increase of effective inputs to the MC-FXLMS algorithm.

5.3.1 The Single Input Multiple Output Case

The simplest extension of the FXLMS algorithm is obtained if in Figure 5.7, only one reference microphone and one cancelling loudspeaker is used, i.e., $I = J = 1$, whereas multiple error microphones are employed, i.e., $L > 1$. Then, only one single adaptive filter is updated according to the update equation

$$\hat{\mathbf{w}}_k = \hat{\mathbf{w}}_{k-1} + \sum_{l=1}^L \mu_l(k) \mathbf{u}_{l,k}^{l*} \tilde{e}'_l(k), \quad \text{with} \quad \tilde{e}'_l(k) = \tilde{e}_l(k) \triangleq \underbrace{\tilde{\mathbf{w}}_{k-1}^T \mathbf{u}'_{l,k}}_{\varepsilon'_l(k)=e_l(k)} + \underbrace{v_l(k)}_{v_l^{(\varepsilon')} (k)}, \quad (5.57)$$

where parameter error vector $\tilde{\mathbf{w}}_k$ is defined in (2.10). In (5.57), the symbols stick with the notation introduced in the introductory part of this section, while additionally the convention is adopted that trivial indices, i.e., indices which only assume one single value, are omitted. The such obtained adaptive algorithm in (5.57) coincides with the averaged LMS found in [KD75; HC90]. It is a specific version of the more general higher order LMS from [Glo79]. Yet, it has to be pointed out that it

differs from similar data-reusing LMS algorithms, as, e.g., in [SW83; RS89], the parameter vector is updated several times based on the *same* input/output (I/O) data, or alternatively, in [SJ93], past I/O data are used to “upsample” adaptation of the parameter vector. In terms of the parameter error vector, (5.57) modifies to

$$\tilde{\mathbf{w}}_k = \tilde{\mathbf{w}}_{k-1} - \sum_{l=1}^L \mu_l(k) \mathbf{u}_{l,k}^* \tilde{e}_l(k), \quad (5.58)$$

which becomes even more compact by introducing

$$\mathbf{U}'_k \triangleq [\mathbf{u}'_{1,k} \ \cdots \ \mathbf{u}'_{L,k}], \quad (5.59)$$

$$\mathbf{e}_k \triangleq [\mathbf{u}_{1,k}^T \tilde{\mathbf{w}}_{k-1} \ \cdots \ \mathbf{u}_{L,k}^T \tilde{\mathbf{w}}_{k-1}]^T = \mathbf{U}'_k{}^T \tilde{\mathbf{w}}_{k-1}, \quad (5.60)$$

$$\mathbf{v}_k \triangleq [v_1(k) \ \cdots \ v_L(k)]^T, \quad (5.61)$$

$$\tilde{\mathbf{e}}_k \triangleq \mathbf{e}_k + \mathbf{v}_k, \quad (5.62)$$

$$\mathbf{D}_k \triangleq \text{diag} \{ \mu_l(k) \}_{l=1}^L, \quad (5.63)$$

leading to

$$\tilde{\mathbf{w}}_k = \tilde{\mathbf{w}}_{k-1} - \mathbf{U}'_k{}^* \mathbf{D}_k \tilde{\mathbf{e}}_k. \quad (5.64)$$

Equation (5.64) has a structure similar to a symmetric algorithm in the sense of Section 2.1. The only difference is that excitation vector is replaced by matrix \mathbf{U}'_k of excitation vectors. Moreover, scalar step-size $\mu(k)$ is in general replaced by diagonal matrix \mathbf{D}_k . At this point, it is emphasised that although the latter is a step-size matrix and uses the same symbol as the diagonalised version of step-size matrix \mathbf{M}_k in Section 3.4.3, (5.64) does *not* represent an asymmetric algorithm. Actually, the analogy of (5.64) to the conventional LMS algorithm allows to extend the ℓ_2 -stability analysis from [RS96a; SR96] that is also sketched in Section 2.4.2. Thus, the theory established in Section 4.4, and specifically, Theorems 4.1 and 4.2, do not even need to be consulted to state the following lemma.

Lemma 5.1: ℓ_2 -Stability of the SIMO MC-FXLMS

The SIMO MC-FXLMS algorithm described by (5.57), or equivalently by (5.59)–(5.64), with $\mu_l(k) \in \mathbb{R}_+$, $l \in \{1, \dots, L\}$, is ℓ_2 -stable, in the sense

$$\sqrt{\sum_{k=0}^K \mathbf{e}_k^H \mathbf{D}_k \mathbf{e}_k} \leq \|\tilde{\mathbf{w}}_{-1}\| + \sqrt{\sum_{k=0}^K \mathbf{v}_k^H \mathbf{D}_k \mathbf{v}_k}, \quad (5.65)$$

if

$$\mathbf{D}_k^{-1} \geq \mathbf{U}'_k{}^T \mathbf{U}'_k{}^*, \quad \text{or equivalently,} \quad \mathbf{U}'_k{}^T \mathbf{D}_k \mathbf{U}'_k{}^* \leq \mathbf{I}. \quad (5.66)$$

Proof. See Appendix D.3.2. □

Also the mapping behaviour of the homogeneous first-order system of linear difference equations in the noiseless case is similar to the analysis for the conventional LMS algorithm. Based on Section 2.3, the corresponding findings are summarised in the next lemma.

Lemma 5.2: Non-Expanding Behaviour of the SIMO MC-FXLMS

For the SIMO MC-FXLMS algorithm described by (5.57), or equivalently by (5.59)–(5.64), in the noiseless case, the norm of the parameter error vector is ensured to satisfy

$$\|\tilde{\mathbf{w}}_k\| \leq \|\tilde{\mathbf{w}}_{k-1}\|, \quad \forall k = 0, \dots \quad (5.67)$$

iff

$$\mathbf{D}_k^{-1} \geq \frac{1}{2} \mathbf{U}_k'^T \mathbf{U}_k'^*, \quad \text{or equivalently,} \quad \mathbf{U}_k'^* \mathbf{D}_k \mathbf{U}_k'^T \leq 2\mathbf{I}. \quad (5.68)$$

Proof. See Appendix D.3.3. □

Clearly, (5.68) allows twice as large step-sizes $\mu_l(k)$ than (5.66). For the latter, a rough sufficient condition can directly be found by the fact that the maximum eigenvalue of a matrix is bounded from above by its trace, leading to

$$\max_{l=1}^L \{\mu_l(k)\} \leq \frac{1}{\text{tr}\{\mathbf{U}_k'^T \mathbf{U}_k'^*\}} = \frac{1}{\sum_{l=1}^L \|\mathbf{u}'_{l,k}\|^2}. \quad (5.69)$$

Multiplying the upper bound in (5.69) by two, provides a sufficient condition for (5.68). Finally, it is pointed out that if all step-sizes are identical, i.e., $\mu_l(k) \equiv \mu(k)$, (5.68) in Lemma 5.2 resembles the result given in [EBN92, therein, right after (15)], which is obtained for excitation of a leaky MC-FXLMS algorithm with discrete sinusoidal signals.

5.3.2 The Multiple Input Single Output Case

As seen in the previous section, the SIMO MC-FXLMS algorithm is equivalent to an averaged LMS algorithm. As the latter can be considered as a matrix version of the conventional LMS algorithm, the analysis of its ℓ_2 -stability as well as its mapping behaviour are obtained by a straightforward extension of the derivations for the conventional LMS algorithm. Hence, if the conditions are modified accordingly, averaging preserves ℓ_2 -stability, as well as contracting behaviour. In fact, also in the MIMO case, the use of multiple error microphones can be considered as a way of averaging. Before this general situation is investigated in Section 5.3.3, this section focuses on the MISO case as an intermediate step.

Based on Figures 5.6(b) and 5.7, it is straightforward to identify the equivalent structure in Figure 5.8. As in Figure 5.6(b), the assumption of slowly changing primary and secondary paths as well as small step-sizes is required. Again, feedback from the cancelling loudspeakers to the reference microphones is neglected. Excluding the SISO case, i.e., the conventional FXLMS algorithm with $I = J = L = 1$, the obtained structure in Figure 5.8 covers all three cases, possible with $L = 1$, i.e., (i) $I = 1, J > 1$, (ii) $I > 1, J = 1$, and (iii) $I > 1, J > 1$. The parameter update is performed by

$$\hat{\mathbf{w}}_{i,j,k} = \hat{\mathbf{w}}_{i,j,k-1} + \mu_{i,j}(k) \mathbf{u}'_{i,j,k} \tilde{\varepsilon}'(k), \quad (5.70)$$

with

$$\tilde{\varepsilon}'(k) \triangleq \sum_{i=1}^I \sum_{j=1}^J \tilde{e}_{i,j}(k) = \underbrace{\sum_{i=1}^I \sum_{j=1}^J e_{i,j}(k)}_{\varepsilon'(k)} + \underbrace{\sum_{i=1}^I \sum_{j=1}^J v_{i,j}(k)}_{v^{(\varepsilon')}(k)}, \quad (5.71)$$

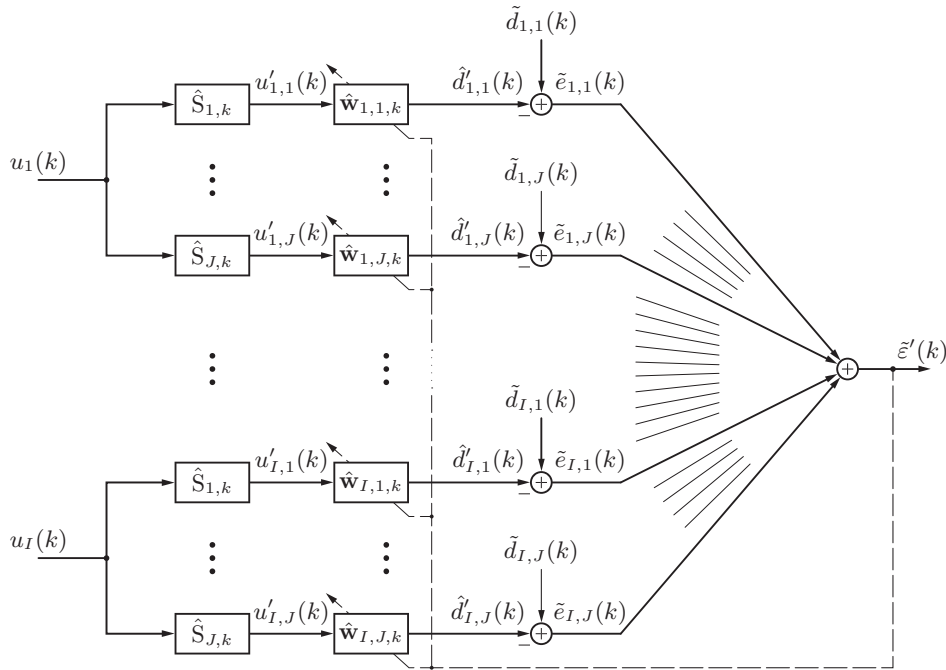


Figure 5.8: Equivalent coupled structure of the MISO MC-FXLMS algorithm under the assumption of slowly changing primary and secondary paths as well as small step-sizes. Moreover, acoustic feedback from the cancelling loudspeaker to the primary microphone is neglected.

where $\tilde{e}_{i,j}(k)$ and $e_{i,j}(k)$ are given by (5.56), after collapsing trivial index l . Clearly, all parameter updates are based on the same update error. Without any further detailed identification of the coupling factors, this shows that the MISO MC-FXLMS algorithm leads to an identical error case in the sense of Section 4.6. As a consequence, the coupling matrix Δ_k in (4.84) is ensured to be rank deficient and the ℓ_2 -stability analysis in Section 4.4 is only applicable if condition (4.98) in Lemma 4.7 is satisfied. Then, also due to Conjecture 4.2 also contracting behaviour of the MISO MC-FXLMS algorithm can be established. As a first step, care has to be taken regarding the indexing of the coupling factors. Comparing (5.71) with (4.8) shows strong similarities. However, while (4.8) only sums up along one index, (5.71) is found to sum up along two indices. This is in fact only a side-effect of the notation introduced in Figure 5.8. In this figure, the choice for a two-dimensional indexing is used in order to reflect the underlying regular structure. In fact, introducing any arbitrary bijective function

$$f_{\mathcal{IJ}} : \{1, \dots, IJ\} \mapsto \{1, \dots, I\} \times \{1, \dots, J\} \quad (5.72)$$

that allows to unambiguously map a one dimensional index $\tilde{i} \in \{1, \dots, IJ\}$ to a pair of indices $\langle i, j \rangle$ with $i \in \{1, \dots, I\}$ and $j \in \{1, \dots, J\}$, (5.71) can be rewritten as

$$\tilde{e}'(k) = \sum_{\tilde{i}=1}^{IJ} \tilde{e}_{f_{\mathcal{IJ}}(\tilde{i})}(k), \quad (5.73)$$

which now structurally agrees with (4.96). Comparing the latter with (5.73) shows that all coupling factors $\nu_i(k)$ are identical to one. Hence, due to Lemma 4.7, all step-sizes $\mu_{i,j}(k)$ have to be identical.

This insight leads to the following lemma.

Lemma 5.3: Non-Expanding Behaviour of the MISO MC-FXLMS

For the MISO MC-FXLMS algorithm described by (5.70) and (5.71), in the noiseless case, the overall squared norm over all parameter error vectors is ensured to satisfy

$$\sum_{i=1}^I \sum_{j=1}^J \|\tilde{\mathbf{w}}_{i,j,k}\|^2 \leq \sum_{i=1}^I \sum_{j=1}^J \|\tilde{\mathbf{w}}_{i,j,k-1}\|^2, \quad \forall k = 0, \dots \quad (5.74)$$

if for all $i \in \{1, \dots, I\}$ and $j \in \{1, \dots, J\}$, $\mu_{i,j}(k) = \mu(k)$, and if additionally,

$$|\mu(k)|^2 \sum_{i=1}^I \sum_{j=1}^J \|\mathbf{u}'_{i,j,k}\|^2 \leq 2\text{Re}\{\mu(k)\}. \quad (5.75)$$

Proof. See Appendix D.3.4. □

With all the step-sizes being identical, mapping matrix \mathbf{B}_k in (4.79) that corresponds to the MISO MC-FXLMS algorithm, is found to be Hermitian. Moreover, due to (4.99), the resulting algorithm is symmetric, and \mathbf{B}_k corresponds to (2.16) with identity step-size matrix. Therefore, (5.75) is equivalent to (3.15). The geometric meaning of (5.75) in the complex plane, is that step-size $\mu(k)$ is contained inside or on a circle with centre $r_\mu(k) + j0$ and radius

$$r_\mu(k) = \frac{1}{\sum_{i=1}^I \sum_{j=1}^J \|\mathbf{u}'_{i,j,k}\|^2}. \quad (5.76)$$

Finally, with the ℓ_2 -stability analysis for the conventional LMS algorithm in Section 2.4.2, the following lemma can be directly formulated.

Lemma 5.4: ℓ_2 -Stability of the MISO MC-FXLMS

For the MISO MC-FXLMS algorithm described by (5.70) and (5.71), with $\varepsilon'(k)$ and $v^{(\varepsilon')}(k)$ defined in (5.71), ℓ_2 -stability in the sense

$$\sqrt{\sum_{k=0}^K \mu(k) |\varepsilon'(k)|^2} \leq \sqrt{\sum_{i=1}^I \sum_{j=1}^J \|\tilde{\mathbf{w}}_{i,j,-1}\|^2} + \sqrt{\sum_{k=0}^K \mu(k) |v^{(\varepsilon')}(k)|^2}, \quad (5.77)$$

is ensured, if for all $i \in \{1, \dots, I\}$ and $j \in \{1, \dots, J\}$, $\mu_{i,j}(k) = \mu(k) \in \mathbb{R}_{0+}$, and

$$\mu(k) \leq r_\mu(k), \quad (5.78)$$

with $r_\mu(k)$ given in (5.76).

5.3.3 The Multiple Input Multiple Output Case

Eventually, this section considers the general case of a MIMO MC-FXLMS algorithm, given by (5.54)–(5.56), based on the findings of the foregoing sections. In contrast to the MISO case considered

in Section 5.3.2, now, more than one error microphones exist. As already identified in Section 5.3.1, this situation leads to an averaged version of the corresponding MISO algorithm. However, while in the SIMO case, in Section 5.3.1, the algorithm was found to behave equivalent to a generalised symmetric algorithm, here, the MIMO case can be identified as a generalised asymmetric algorithm. To see this, the bijective index transformation function $f_{\mathcal{I}\mathcal{J}}$ in (5.73) is applied to (5.54)–(5.56). With $\ddot{i} \in \{1, \dots, IJ\}$, this gives the completely equivalent set of expressions,

$$\hat{\mathbf{w}}_{f_{\mathcal{I}\mathcal{J}}(\ddot{i}),k} = \hat{\mathbf{w}}_{f_{\mathcal{I}\mathcal{J}}(\ddot{i}),k-1} + \sum_{l=1}^L \mu_{f_{\mathcal{I}\mathcal{J}}(\ddot{i}),l}(k) \mathbf{u}'_{f_{\mathcal{I}\mathcal{J}}(\ddot{i}),l,k} \tilde{\varepsilon}'_l(k), \quad (5.79)$$

with

$$\tilde{\varepsilon}'_l(k) = \sum_{\ddot{i}=1}^{IJ} \tilde{e}_{f_{\mathcal{I}\mathcal{J}}(\ddot{i}),l}(k) = \underbrace{\sum_{\ddot{i}=1}^{IJ} e_{f_{\mathcal{I}\mathcal{J}}(\ddot{i}),l}(k)}_{\varepsilon'_l(k)} + \underbrace{\sum_{\ddot{i}=1}^{IJ} v_{f_{\mathcal{I}\mathcal{J}}(\ddot{i}),l}(k)}_{v'_l(\varepsilon')_l(k)}. \quad (5.80)$$

By introducing the stacked parameter vector analogous to (4.80), and the l^{th} stacked excitation vector analogous to (4.82),

$$\hat{\mathbf{w}}_k \triangleq \text{col}_{\ddot{i}=1}^{IJ} \{ \hat{\mathbf{w}}_{f_{\mathcal{I}\mathcal{J}}(\ddot{i}),k} \}, \quad \text{and} \quad \mathbf{u}'_{l,k} \triangleq \text{col}_{\ddot{i}=1}^{IJ} \{ \mathbf{u}'_{f_{\mathcal{I}\mathcal{J}}(\ddot{i}),k} \}, \quad (5.81)$$

respectively, the combination of (5.79), for all $\ddot{i} \in \{1, \dots, IJ\}$, is compactly written as

$$\hat{\mathbf{w}}_k = \hat{\mathbf{w}}_{k-1} + \sum_{l=1}^L \underbrace{\left(\bigoplus_{\ddot{i}=1}^{IJ} \mu_{f_{\mathcal{I}\mathcal{J}}(\ddot{i}),l}(k) \mathbf{I}_{M_{\ddot{i}}} \right)}_{\text{step-size matrix } \mathbf{D}_{l,k}} (\mathbf{u}'_{l,k})^* \tilde{\varepsilon}'_l(k), \quad (5.82)$$

where $M_{\ddot{i}}$ represents the number of parameters in $\hat{\mathbf{w}}_{f_{\mathcal{I}\mathcal{J}}(\ddot{i}),k}$. Thus, the total number M of parameters, i.e., the length of $\hat{\mathbf{w}}_k$ is obtained as

$$M = \sum_{\ddot{i}=1}^{IJ} M_{\ddot{i}}. \quad (5.83)$$

Reverting for a moment to the MISO MC-FXLMS algorithm in Section 5.3.2, i.e., the here considered algorithm restricted to one single error microphone, hence, $L = 1$, (5.82) is found to have the same structure as (2.8). This shows that in the general case, the MISO MC-FXLMS algorithm is equivalent to an asymmetric algorithm and all the findings in Chapter 3 are applicable. It also confirms that the requirement for identical step-sizes in Lemma 5.3 leads to a symmetric algorithm. With these insights, returning to the MIMO case, the MC-FXLMS algorithm is found to behave like an averaged asymmetric algorithm.

While for this general case, ℓ_2 -stability cannot be analysed with the theory of Section 4.4, a mapping analysis of the underlying homogeneous first-order system of linear difference equations in the noiseless case is possible. Based on (5.80)–(5.82), with parameter error vector $\tilde{\mathbf{w}}_k$, corresponding to the stacked parameter vector $\hat{\mathbf{w}}_k$ in (5.81),

$$\varepsilon'_l(k) = \tilde{\mathbf{w}}_k^T \mathbf{u}'_{l,k}, \quad (5.84)$$

mapping matrix \mathbf{B}_k in the corresponding recursion of the form (4.79) is found to be given by

$$\mathbf{B}_k = \mathbf{I} - \sum_{l=1}^L \mathbf{D}_{l,k} (\mathbf{u}'_{l,k})^* (\mathbf{u}'_{l,k})^\top = \frac{1}{L} \sum_{l=1}^L \underbrace{[\mathbf{I} - L\mathbf{D}_{l,k} (\mathbf{u}'_{l,k})^* (\mathbf{u}'_{l,k})^\top]}_{\mathbf{B}_{l,k}}. \quad (5.85)$$

Analysing the singular values of \mathbf{B}_k in an exact way, would lead to a necessary and sufficient criterion for non-expanding behaviour of recursion (4.79). Here, the derivation is simplified, leading to only sufficient criteria which, however, still provide considerable insight. Assuming a descending sorting of the individual singular values $\sigma_m(\mathbf{B}_{l,k})$, $m \in \{1, \dots, M\}$, with [HJ99, Theorem 3.3.16], the largest singular value of \mathbf{B}_k is bounded by

$$\sigma_{\max}(k) \leq \frac{1}{L} \sum_{l=1}^L \sigma_1(\mathbf{B}_{l,k}), \quad (5.86)$$

hence,

$$\sigma_1(\mathbf{B}_{l,k}) \leq 1, \quad \forall l \in \{1, \dots, L\} \quad \Rightarrow \quad \sigma_{\max}(k) \leq 1. \quad (5.87)$$

As found in Section 3.3.2, the left-hand side in (5.86) can only be satisfied if all of the individual mapping matrices $\mathbf{B}_{l,k}$ correspond to a symmetric algorithm. This in turn requires that the regression vector of each of the individual mappings is in parallel with the respective excitation vector. The latter requirement entails that step-size matrices $\mathbf{D}_{l,k}$ have to be a multiple of the identity matrix, which is only possible if for all $l \in \{1, \dots, L\}$,

$$\mu_{f_{\mathcal{I}\mathcal{J}}(1),l}(k) = \dots = \mu_{f_{\mathcal{I}\mathcal{J}}(IJ),l}(k) = \mu_l(k), \quad (5.88)$$

as then,

$$\mathbf{D}_{l,k} = \mu_l(k) \mathbf{I}_M. \quad (5.89)$$

Then, Lemma 5.3 applies and leads to the following slightly modified theorem.

Theorem 5.1: Non-Expanding Behaviour of the MIMO MC-FXLMS

For the MIMO MC-FXLMS algorithm described by (5.54)–(5.56), in the noiseless case, the overall squared norm over all parameter error vectors is ensured to satisfy

$$\sum_{i=1}^I \sum_{j=1}^J \|\tilde{\mathbf{w}}_{i,j,k}\|^2 \leq \sum_{i=1}^I \sum_{j=1}^J \|\tilde{\mathbf{w}}_{i,j,k-1}\|^2, \quad \forall k = 0, \dots \quad (5.90)$$

if for all $i \in \{1, \dots, I\}$, $j \in \{1, \dots, J\}$, and $l \in \{1, \dots, L\}$, $\mu_{i,j,l}(k) = \mu_l(k)$, and if additionally,

$$|\mu_l(k)|^2 \sum_{i=1}^I \sum_{j=1}^J \|\mathbf{u}'_{i,j,l,k}\|^2 \leq \frac{2}{L} \operatorname{Re} \{\mu_l(k)\}. \quad (5.91)$$

Proof. Most of this proof is already covered by the above conducted derivation. The division by L on the right-hand side of (5.91) directly follows from (5.85), since the power of the excitation vectors is scaled by the factor \sqrt{L} . \square

Since under constraint (5.88), (5.82) perfectly agrees with (5.57), also ℓ_2 -stability can be ensured based on the following theorem.

Theorem 5.2: ℓ_2 -Stability of the MIMO MC-FXLMS

If for all $i \in \{1, \dots, I\}$, $j \in \{1, \dots, J\}$, and $l \in \{1, \dots, L\}$, $\mu_{i,j,l}(k) = \mu_l(k) \in \mathbb{R}_+$, the diagonal positive definite step-size matrix \mathbf{D}_k can be defined according to (5.63). Using (5.81), let moreover (5.60) and (5.61) be modified to

$$\boldsymbol{\varepsilon}'_k \triangleq [\varepsilon'_1(k) \ \cdots \ \varepsilon'_L(k)]^T, \quad (5.92)$$

$$\mathbf{v}_k^{(\varepsilon')} \triangleq [v_1^{(\varepsilon')}(k) \ \cdots \ v_L^{(\varepsilon')}(k)]^T, \quad (5.93)$$

with $\varepsilon'_l(k)$ and $v_l^{(\varepsilon')}(k)$ defined in (5.80). Then, the MIMO MC-FXLMS algorithm described by (5.79) and (5.80) is ℓ_2 -stable, in the sense

$$\sqrt{\sum_{k=0}^K \boldsymbol{\varepsilon}'_k{}^H \mathbf{D}_k \boldsymbol{\varepsilon}'_k} \leq \|\tilde{\mathbf{w}}_{-1}\| + \sqrt{\sum_{k=0}^K \mathbf{v}_k^{(\varepsilon')}{}^H \mathbf{D}_k \mathbf{v}_k^{(\varepsilon')}}}, \quad (5.94)$$

if

$$\mathbf{D}_k^{-1} \geq \mathbf{U}_k{}^T \mathbf{U}_k{}^*, \quad \text{or equivalently,} \quad \mathbf{U}_k{}^T \mathbf{D}_k \mathbf{U}_k{}^* \leq \mathbf{I}, \quad (5.95)$$

where excitation matrix $\mathbf{U}_k{}^*$, defined in (5.59), contains the stacked excitation vectors in (5.81).

5.4 Multilayer Perceptrons Trained by the Backpropagation Algorithm

Finally, this section, applies the formalism established in Chapter 4 in order to gain further insight into the mapping behaviour of a multilayer perceptron⁴. The latter is a feed forward neural network [Hay94] and has a wide range of applications, such as image recognition, handwriting recognition, speech recognition, and natural language processing [see, e.g., Hay94; Roj96; Nie14]. Supervised learning is a common method to train such structures and often implemented by the backpropagation algorithm which basically is a gradient descent scheme [GT92; RHW86a; RHW86b]. The latter seems to date back to a work of Bryson *et al.* [BH69] and was independently proposed in different flavours and contexts by several authors [BH69; Wer74; Par82; LeC86; RHW86b]. For a brief historical overview see, e.g., [RHW86a; Hec89; Wer90], a more detailed introduction can be found in, e.g., [Hay94; Roj96; Nie14].

To my knowledge, for a multilayer perceptron of arbitrary size that is trained by the backpropagation algorithm, no general analysis of convergence exists. According to [Hay94, p. 153], the backpropagation algorithm cannot be shown to converge. Moreover, [GG91; APT99] point out that there barely exists any analysis considering the dynamical behaviour of multilayer perceptrons, i.e., their boundedness and convergence. In literature, it is well documented that the cost function of the backpropagation algorithm may manifest several local minima as well as regions of marginal slope. Both are reason, why under adverse circumstances, the learning performance of this algorithm is poor.

⁴ In this work, the here considered kind of multilayer neural network is addressed by the common term multilayer perceptron as done, e.g., in [Bis92; Hay94; Roj96; She12]. However, as pointed out in [Nie14, Chapter 1], it should be noted that the underlying structure does *not* contain perceptrons in a strict sense, as the activation function of the latter is assumed to be step-shaped. Thus, it is not differentiable. Here, in contrast, differentiability of the activation function is of central importance in order to apply the backpropagation algorithm [Hay94; Roj96].

Hence, a multitude of methods have been published which aim to circumvent these problems [Hay94; Roj96; Møl97; She12]. In the context of pattern classification, under certain assumptions, the existence of local minima can be precluded if the training patterns are linearly separable into disjoint classes. In this framework, convergence of a single layer perceptron is proved in [SS89b], and extended to a more general multilayer structure in [GT92].

Here, an approach is adopted that does not impose any restriction to the occurring input patterns. The perspective is motivated from a system identification point of view, and considers the multilayer perceptron trained by the backpropagation algorithm in a pattern-by-pattern mode. By this, it complements the findings in [HSK94; SR95a; RS96b; RS97], which investigate H^∞ -optimality under PE and ℓ_2 -stability for the single layer case. The latter two works also allow for recurrence, i.e., a feedback from the network output to the input. Additionally, [Set92] derives a persistence of excitation condition that guarantees local exponential stability for a single layer perceptron trained by the backpropagation algorithm and claims that the result can be extended to multilayer perceptrons, if adequate identifiability assumptions for the reference neural network are available. The key assumption made therein is that in the corresponding homogeneous recursion of type (4.79), a sliding average over a certain number of consecutive mapping matrices \mathbf{B}_k shows sufficiently slow variations.

The most central assumption made here, is that the training data, i.e., the set of observed I/O pairs, is (or could be) obtained from a reference multilayer perceptron, which is constant and of known structure. Of course, the corresponding network weights are considered unknown. The goal of the system identification process is to adapt a multilayer perceptron of the same structure, such that, in the limit, its weights coincide with the weights of the reference multilayer perceptron. An important subtlety is the fact that the training data are not required to actually originate from a multilayer perceptron, they can actually be provided by any arbitrary reference source. However, they are required to belong to the space of training data that can be represented by the assumed network structure. It may be possible to relax this restriction by including additive noise, as explained in Section 2.1, but this is beyond the scope of the here presented analysis.

In the sequel, details on the functionality of the multilayer perceptron and the backpropagation algorithm are not covered extensively, as they can be found in most of the above mentioned literature [e.g., Hay94; Roj96; Nie14]. Instead, only the structural and algorithmic details are described that are of relevance, here. The used notation is mostly motivated by [Roj96], however, with slight differences. The convention of this thesis is retained that symbols with a caret, e.g., $\hat{\mathbf{w}}_j^{(l)}$, refer to the (adaptive) system model, those without, to the (unknown) reference system. The used symbols and their meaning are listed in Table 5.3. Note that there, if applicable, the symbols are shown with caret. Hence, they refer to the adaptive multilayer perceptron, i.e., the system model. Nevertheless, due to the assumption of identical structure, omitting the caret directly gives the symbols that correspond to the reference system. Figure 5.9 provides a graphical representation of the considered multilayer perceptron. Each neuron is assumed to use the same activation function f which is here only required to be real-valued and differentiable. The vertical dashed lines indicate the boundaries between the individual network layers. Hence, except from the left-most and the right-most boundary, the outputs of layer l coincide with the inputs of the following layer $l + 1$. Layer 0 represents the input layer, and does not contain any computational resources. It is assumed that the set of inputs of each layer is fully meshed with its neurons. Although not explicitly demonstrated here, the analysis still holds for networks with incompletely meshed layers. The only reason for excluding this more general case, is that it would make notation even more difficult to follow. Anyhow, connections that cross layer borders are *not* allowed.

After this structural description of the multilayer perceptron, the update mechanism is explained that is achieved by the backpropagation algorithm. The vectors $\hat{\mathbf{w}}_j^{(l)}$ containing the weights of all

Table 5.3: List of Mathematical Symbols Describing the Multilayer Perceptron

L	number of layers
\mathcal{L}_0	set of indices addressing all layers; $\mathcal{L} \triangleq \{0, \dots, L\}$, thus, below $l \in \mathcal{L}$
\mathcal{L}	set of indices addressing all layers except from the input layer; $\mathcal{L} \triangleq \mathcal{L}_0 \setminus \{0\}$, thus, here, in most cases $l \in \mathcal{L}$, it will be explicitly stated if $l \in \mathcal{L}_0$
N_l	number of neurons in layer l , $l \in \mathcal{L}_0$
\mathcal{N}_l	set of indices addressing the neurons in layer l ; $\mathcal{N}_l \triangleq \{1, \dots, N_l\}$, $l \in \mathcal{L}_0$
$\hat{w}_{ij}^{(l)}$	real-valued weight of edge, from neuron i , layer $l-1$ to neuron j , layer l , $i \in \mathcal{N}_{l-1}$, $j \in \mathcal{N}_l$
$\hat{\mathbf{w}}_j^{(l)}$	vector of all edge weights that end at neuron j in layer l , thus, $\hat{\mathbf{w}}_j^{(l)} \in \mathbb{R}^{N_{l-1}}$, $j \in \mathcal{N}_l$
$\hat{\mathbf{W}}^{(l)}$	matrix containing all weights of layer l ; $\hat{\mathbf{W}}^{(l)} \triangleq \begin{bmatrix} \hat{\mathbf{w}}_1^{(l)} & \dots & \hat{\mathbf{w}}_{N_l}^{(l)} \end{bmatrix} \in \mathbb{R}^{N_{l-1} \times N_l}$
$\hat{\xi}_j^{(l)}$	stimulus level of neuron j in layer l ; $\hat{\xi}_j^{(l)} \triangleq \hat{\mathbf{w}}_j^{(l)\top} \hat{\mathbf{x}}^{(l-1)} \in \mathbb{R}$, $j \in \mathcal{N}_l$
$\hat{\boldsymbol{\xi}}^{(l)}$	vector of stimulus levels of all neurons in layer l ; $\hat{\boldsymbol{\xi}}^{(l)} \triangleq \begin{bmatrix} \hat{\xi}_1^{(l)} & \dots & \hat{\xi}_{N_l}^{(l)} \end{bmatrix}^\top = \hat{\mathbf{W}}^{(l)\top} \hat{\mathbf{x}}^{(l-1)} \in \mathbb{R}^{N_l}$
$f(\cdot)$	activation function with derivative $f'(\cdot)$, here, most generally, $f : \mathbb{R} \mapsto \mathbb{R}$ and $f' : \mathbb{R} \mapsto \mathbb{R}_{0+}$
$\hat{x}_j^{(l)}$	activation level of neuron j in layer l ; $\hat{x}_j^{(l)} \triangleq f(\hat{\xi}_j^{(l)}) \in \mathbb{R}$, $l \in \mathcal{L}_0$
$\hat{\mathbf{x}}^{(l)}$	vector of activation levels of all neurons in layer l ; $\hat{\mathbf{x}}^{(l)} \triangleq \begin{bmatrix} \hat{x}_1^{(l)} & \dots & \hat{x}_{N_l}^{(l)} \end{bmatrix}^\top \in \mathbb{R}^{N_l}$, $l \in \mathcal{L}_0$
$\delta_j^{(l)}$	real-valued error, propagating back to neuron j in layer l , $j \in \mathcal{N}_l$
$\boldsymbol{\delta}^{(l)}$	vector of errors propagated back to the neurons in layer l ; $\boldsymbol{\delta}^{(l)} \in \mathbb{R}^{N_l}$
$\mu_j^{(l)}$	step-size used to update weight vector $\hat{\mathbf{w}}_j^{(l)}$, $\mu_j^{(l)} \in \mathbb{R}_{0+}$
$\mathbf{D}_\mu^{(l)}$	diagonal matrix containing the step-sizes used in the update process of the neurons in layer l ; $\mathbf{D}_\mu^{(l)} \triangleq \text{diag}_{j \in \mathcal{N}_l} \left\{ \mu_j^{(l)} \right\} \in \mathbb{R}_{0+}^{N_l \times N_l}$
$\mathbf{F}^{(l)}$	diagonal matrix containing the derivatives of the activation function evaluated at the current stimulus level of each neuron in layer l ; $\mathbf{F}^{(l)} \triangleq \text{diag}_{j \in \mathcal{N}_l} \left\{ f'(\hat{\xi}_j^{(l)}) \right\} \in \mathbb{R}_{0+}^{N_l \times N_l}$
$\eta_j^{(l)}$	mean stimulus value lying in the interval $[\hat{\xi}_j^{(l)}, \xi_j^{(l)}]$
$\mathbf{F}_\eta^{(l)}$	diagonal matrix containing the derivatives of the activation function evaluated at the mean values $\eta_j^{(l)}$; $\mathbf{F}_\eta^{(l)} \triangleq \text{diag}_{j \in \mathcal{N}_l} \left\{ f'(\eta_j^{(l)}) \right\} \in \mathbb{R}_{0+}^{N_l \times N_l}$
$\tilde{w}_{ij}^{(l)}$	difference between weight $w_{ij}^{(l)}$ of the reference system and weight $\hat{w}_{ij}^{(l)}$ of the adaptive neural network; $\tilde{w}_{ij}^{(l)} \triangleq w_{ij}^{(l)} - \hat{w}_{ij}^{(l)}$
$\tilde{\mathbf{w}}_j^{(l)}$	analogous to $\tilde{w}_{ij}^{(l)}$, the weight error vector of layer l ; $\tilde{\mathbf{w}}_j^{(l)} \triangleq \mathbf{w}_j^{(l)} - \hat{\mathbf{w}}_j^{(l)}$
$\tilde{\mathbf{W}}^{(l)}$	analogous to $\tilde{w}_{ij}^{(l)}$ and $\tilde{\mathbf{w}}_j^{(l)}$, the weight error matrix of layer l ; $\tilde{\mathbf{W}}^{(l)} \triangleq \mathbf{W}^{(l)} - \hat{\mathbf{W}}^{(l)}$
$\Delta x_j^{(l)}$	deviation between the activation of node j in layer l of the reference system and the activation of the same node in the adaptive neural network; $\Delta x_j^{(l)} \triangleq x_j^{(l)} - \hat{x}_j^{(l)}$, $l \in \mathcal{L}_0$
$\Delta \mathbf{x}^{(l)}$	vector of all deviations $\Delta x_j^{(l)}$ of layer l ; $\Delta \mathbf{x}^{(l)} \triangleq \begin{bmatrix} \Delta x_1^{(l)} & \dots & \Delta x_{N_l}^{(l)} \end{bmatrix}^\top \in \mathbb{R}^{N_l}$, $l \in \mathcal{L}_0$
$e_j^{(l)}$	generic deviation of the stimulus level of node j in layer l in the adaptive neural network, from the stimulus level of the same node in the reference system, if the latter would be stimulated by the same input vector $\hat{\mathbf{x}}^{(l-1)}$: $e_j^{(l)} \triangleq \mathbf{w}_j^{(l)\top} \hat{\mathbf{x}}^{(l-1)} - \hat{\xi}_j^{(l)} = \mathbf{w}_j^{(l)\top} \hat{\mathbf{x}}^{(l-1)} - \hat{\mathbf{w}}_j^{(l)\top} \hat{\mathbf{x}}^{(l-1)} = \tilde{\mathbf{w}}_j^{(l)\top} \hat{\mathbf{x}}^{(l-1)}$, $l \in \mathcal{L}_0$
$\mathbf{e}^{(l)}$	vector of all generic stimulus deviations $e_j^{(l)}$ in layer l : $\mathbf{e}^{(l)} \triangleq \begin{bmatrix} e_1^{(l)} & \dots & e_{N_l}^{(l)} \end{bmatrix}^\top = \tilde{\mathbf{W}}^{(l)\top} \hat{\mathbf{x}}^{(l-1)} \in \mathbb{R}^{N_l}$, $l \in \mathcal{L}_0$

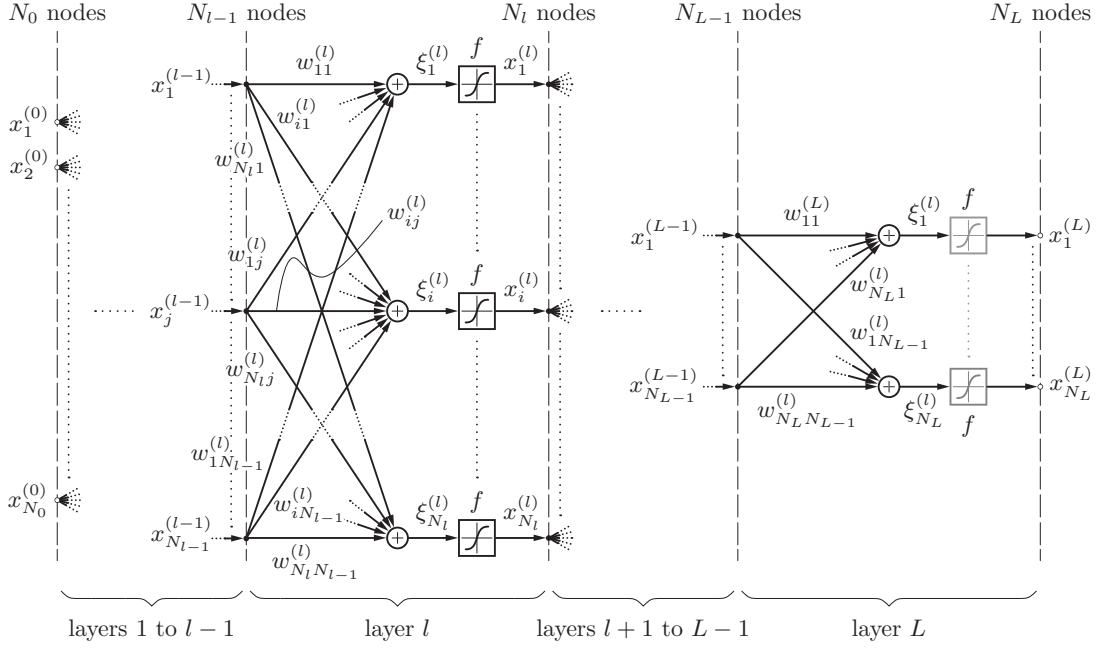


Figure 5.9: General structure of the here considered multilayer perceptron. In the output layer $l = L$, the activation functions are slightly shaded as their existence depends on the chosen cost function. Including them, leads to the minimisation of the squared error. If in turn the cross-entropy cost function is used as error measure, they can be omitted.

edges that end at neuron j of layer l , are updated according to⁵

$$\hat{\mathbf{w}}_{j,\text{new}}^{(l)} = \hat{\mathbf{w}}_j^{(l)} + \mu_j^{(l)} \hat{\mathbf{x}}^{(l-1)} \delta_j^{(l)}. \quad (5.96)$$

The similarity of (5.96) with (2.8) well resembles that backpropagation is a gradient type algorithm with identity step-size matrix. Clearly, the update is proportional to the back propagated error $\delta_j^{(l)}$. Combining all of the N_l vectors $\hat{\mathbf{w}}_j^{(l)}$ belonging to layer l , column by column, in matrix $\hat{\mathbf{W}}^{(l)}$, the weight update for the whole layer l is compactly written as

$$\hat{\mathbf{W}}_{\text{new}}^{(l)} = \hat{\mathbf{W}}^{(l)} + \hat{\mathbf{x}}^{(l-1)} \boldsymbol{\delta}^{(l)\top} \mathbf{D}_\mu^{(l)}. \quad (5.97)$$

Equation (5.97) introduces vector $\boldsymbol{\delta}^{(l)}$ of errors, back propagated to neuron j of layer l , as well as diagonal step-size matrix $\mathbf{D}_\mu^{(l)}$ that contains the step-sizes of the individual neurons (cf. Table 5.3). It is important to notice that the influence of this matrix is different from the step-size matrices occurring in the context of asymmetric algorithms in Chapter 3. Here, $\mathbf{D}_\mu^{(l)}$ is simply introduced for reasons of a compact notation. Still, the separate algorithms are given by (5.96) and are thus symmetric.

Up to now, the actual meaning of back propagated error $\delta_j^{(l)}$ is not further specified. To make up for this, consider deviation $\Delta x_j^{(l)} = x_j^{(l)} - \hat{x}_j^{(l)}$ between the output, i.e., the activation level, $\hat{x}_j^{(l)}$ of neuron j in layer l , belonging to the adaptive multilayer perceptron, and the corresponding

⁵ In contrast to the rest of this work, in this section, no iteration index k is used here. This is mainly done to reduce the number of subscripts, superscripts and arguments. Of course, the involved entities generally change from update to update.

activation level $x_j^{(l)}$ of the reference system. In the real world, the only deviations $x_j^{(l)}$ that can be observed, are those at the output layer $l = L$ and those at the input layer $l = 0$. While inputs to the neural network traverse the structure in Figure 5.9 from left to right, the idea of the backpropagation algorithm is, to let the (accessible) errors at the output propagate backwards (from right to left), in order to quantify the necessary modification of the network weights. On their way back to the input nodes, the output errors are scaled by the edge weights and by the differential gains that are introduced by the non-linearity in each of the passed neurons. For a certain neuron, this gain is given by the first derivative of the activation function, evaluated at its stimulus level, i.e., the sum of all weighted inputs arriving at this neuron. Eventually, referring to the definitions in Table 5.3, due to the chain rule, error vectors $\boldsymbol{\delta}^{(l)}$, $l \in \{1, \dots, L-1\}$, are found as [Roj96, p. 171]

$$\boldsymbol{\delta}^{(l)} = \mathbf{F}^{(l)} \hat{\mathbf{W}}^{(l+1)} \dots \mathbf{F}^{(L-1)} \hat{\mathbf{W}}^{(L)} \boldsymbol{\delta}^{(L)}. \quad (5.98)$$

Depending on whether the squared error or the cross-entropy cost function [Nie14] should be minimised by the backpropagation algorithm, in the output layer, i.e., $l = L$, error vector $\boldsymbol{\delta}^{(L)}$ is given by

$$\boldsymbol{\delta}^{(L)} = \mathbf{F}^{(L)} \Delta \mathbf{x}^{(L)}, \quad \text{or} \quad \boldsymbol{\delta}^{(L)} = \Delta \mathbf{x}^{(L)}, \quad (5.99)$$

respectively. Defining

$$\mathbf{F}_C \triangleq \begin{cases} \mathbf{F}^{(L)} & \text{for a squared error cost function} \\ \mathbf{I}_{N_L} & \text{for a cross-entropy cost function} \end{cases}, \quad (5.100)$$

and matrix⁶

$$\boldsymbol{\Omega}^{(l)} \triangleq \begin{cases} \left(\prod_{m=l}^{\overrightarrow{L-1}} \mathbf{F}^{(m)} \hat{\mathbf{W}}^{(m+1)} \right) \mathbf{F}_C & l \in \mathcal{L} \setminus \{L\} \\ \mathbf{F}_C & l = L \end{cases}, \quad (5.101)$$

of dimension the $N_l \times N_L$, (5.98) and (5.99) can be combined to

$$\boldsymbol{\delta}^{(l)} = \boldsymbol{\Omega}^{(l)} \Delta \mathbf{x}^{(L)}. \quad (5.102)$$

So far, the derivation does not contain any essential difference with respect to literature. This changes at this point, as below, the multilayer perceptron in Figure 5.9, trained by the backpropagation algorithm, is shown to be representable as a coupled structure in the sense of Section 4.1. As a first step, observe that the errors between the reference activation levels and the activation levels of the adaptive multilayer perceptron in layer l are given by (cf. Table 5.3)

$$\Delta \mathbf{x}^{(l)} = \mathbf{x}^{(l)} - \hat{\mathbf{x}}^{(l)} = \underset{j=1}{\text{col}}^{N_l} \left\{ f\left(\xi_j^{(l)}\right) - f\left(\hat{\xi}_j^{(l)}\right) \right\}. \quad (5.103)$$

Similarly to Section 5.2, applying the mean value theorem [MS00b, p. 626; HSK94, pp. 11ff.; SR95a;

⁶ The arrow on top of the product operator indicates how the operands are ordered with increasing index.

RS96b; RS97] in each row, leads to (cf. Table 5.3)

$$\Delta \mathbf{x}^{(l)} = \underset{j=1}{\text{col}}^{N_l} \left\{ f'(\eta_j^{(l)}) \left(\xi_j^{(l)} - \hat{\xi}_j^{(l)} \right) \right\} = \mathbf{F}_\eta^{(l)} \underset{j=1}{\text{col}}^{N_l} \left\{ \xi_j^{(l)} - \hat{\xi}_j^{(l)} \right\} = \mathbf{F}_\eta^{(l)} \left(\boldsymbol{\xi}^{(l)} - \hat{\boldsymbol{\xi}}^{(l)} \right) \quad (5.104)$$

$$= \mathbf{F}_\eta^{(l)} \left(\mathbf{W}^{(l)\top} \mathbf{x}^{(l-1)} - \hat{\mathbf{W}}^{(l)\top} \hat{\mathbf{x}}^{(l-1)} \right) \quad (5.105)$$

$$= \mathbf{F}_\eta^{(l)} \left(\left(\mathbf{W}^{(l)} - \hat{\mathbf{W}}^{(l)} \right)^\top \mathbf{x}^{(l-1)} + \hat{\mathbf{W}}^{(l)\top} \left(\mathbf{x}^{(l-1)} - \hat{\mathbf{x}}^{(l-1)} \right) \right) \quad (5.106)$$

$$= \mathbf{F}_\eta^{(l)} \left(\tilde{\mathbf{W}}^{(l)\top} \mathbf{x}^{(l-1)} + \hat{\mathbf{W}}^{(l)\top} \Delta \mathbf{x}^{(l-1)} \right) \quad (5.107)$$

$$= \mathbf{F}_\eta^{(l)} \left(\left(\mathbf{W}^{(l)} - \hat{\mathbf{W}}^{(l)} \right)^\top \hat{\mathbf{x}}^{(l-1)} + \mathbf{W}^{(l)\top} \left(\mathbf{x}^{(l-1)} - \hat{\mathbf{x}}^{(l-1)} \right) \right) \quad (5.108)$$

$$= \mathbf{F}_\eta^{(l)} \left(\tilde{\mathbf{W}}^{(l)\top} \hat{\mathbf{x}}^{(l-1)} + \mathbf{W}^{(l)\top} \Delta \mathbf{x}^{(l-1)} \right). \quad (5.109)$$

While the backpropagation algorithm describes how the error at the output layer propagates back to the nodes of the hidden layers, (5.107) and (5.109) describe how the deviations of each layer accumulate up to the overall deviation in the output layer. Therefore, they can be considered as a reversed form of the backpropagation algorithm.

In the learning phase, the I/O-pairs $\{\mathbf{x}^{(0)}, \mathbf{x}^{(L)}\}$ are provided. On the one hand, as the input of the reference system is the same as the input of the adaptive multilayer perceptron, i.e., $\mathbf{x}^{(0)} = \hat{\mathbf{x}}^{(0)}$, the deviation $\Delta \mathbf{x}^{(0)} = \mathbf{0}$. On the other hand, the deviation in the output layer is directly accessible and thus known. Therefore, due to (5.109),

$$l = 0: \quad \Delta \mathbf{x}^{(0)} = \mathbf{0}$$

$$l = 1: \quad \Delta \mathbf{x}^{(1)} = \mathbf{F}_\eta^{(1)} \left(\tilde{\mathbf{W}}^{(1)\top} \hat{\mathbf{x}}^{(0)} + \mathbf{W}^{(1)\top} \Delta \mathbf{x}^{(0)} \right) = \mathbf{F}_\eta^{(1)} \tilde{\mathbf{W}}^{(1)\top} \hat{\mathbf{x}}^{(0)}$$

$$l = 2: \quad \Delta \mathbf{x}^{(2)} = \mathbf{F}_\eta^{(2)} \left(\tilde{\mathbf{W}}^{(2)\top} \hat{\mathbf{x}}^{(1)} + \mathbf{W}^{(2)\top} \Delta \mathbf{x}^{(1)} \right) = \\ = \mathbf{F}_\eta^{(2)} \tilde{\mathbf{W}}^{(2)\top} \hat{\mathbf{x}}^{(1)} + \mathbf{F}_\eta^{(2)} \mathbf{W}^{(2)\top} \mathbf{F}_\eta^{(1)} \tilde{\mathbf{W}}^{(1)\top} \hat{\mathbf{x}}^{(0)}$$

$$l = 3: \quad \Delta \mathbf{x}^{(3)} = \mathbf{F}_\eta^{(3)} \tilde{\mathbf{W}}^{(3)\top} \hat{\mathbf{x}}^{(2)} + \mathbf{F}_\eta^{(3)} \mathbf{W}^{(3)\top} \mathbf{F}_\eta^{(2)} \tilde{\mathbf{W}}^{(2)\top} \hat{\mathbf{x}}^{(1)} + \mathbf{F}_\eta^{(3)} \mathbf{W}^{(3)\top} \mathbf{F}_\eta^{(2)} \mathbf{W}^{(2)\top} \mathbf{F}_\eta^{(1)} \tilde{\mathbf{W}}^{(1)\top} \hat{\mathbf{x}}^{(0)}$$

$$\vdots$$

$$l = L: \quad \Delta \mathbf{x}^{(L)} = \mathbf{F}_\eta^{(L)} \tilde{\mathbf{W}}^{(L)\top} \hat{\mathbf{x}}^{(L-1)} + \mathbf{F}_\eta^{(L)} \mathbf{W}^{(L)\top} \mathbf{F}_\eta^{(L-1)} \tilde{\mathbf{W}}^{(L-1)\top} \hat{\mathbf{x}}^{(L-2)} \\ + \dots + \mathbf{F}_\eta^{(L)} \mathbf{W}^{(L)\top} \dots \mathbf{F}_\eta^{(2)} \mathbf{W}^{(2)\top} \mathbf{F}_\eta^{(1)} \tilde{\mathbf{W}}^{(1)\top} \hat{\mathbf{x}}^{(0)}. \\ \underbrace{\hspace{10em}}_{L-3 \text{ terms}}$$

From the last expression, it can be concluded that for $l \in \mathcal{L}$,

$$\Delta \mathbf{x}^{(l)} = \sum_{m=1}^l \left[\left(\prod_{n=m+1}^l \mathbf{F}_\eta^{(n)} \mathbf{W}^{(n)\top} \right) \mathbf{F}_\eta^{(m)} \underbrace{\tilde{\mathbf{W}}^{(m)\top} \hat{\mathbf{x}}^{(m-1)}}_{\mathbf{e}^{(m)}} \right] \quad (5.110)$$

$$= \sum_{m=1}^l \boldsymbol{\Theta}_l^{(m)} \mathbf{e}^{(m)}, \quad (5.111)$$

with the $N_l \times N_m$ matrix

$$\Theta_l^{(m)} \triangleq \left(\prod_{n=m+1}^l \mathbf{F}_\eta^{(n)} \mathbf{W}^{(n)\top} \right) \mathbf{F}_\eta^{(m)}. \quad (5.112)$$

Especially, for $\Delta \mathbf{x}^{(L)}$, this entails

$$\Delta \mathbf{x}^{(L)} = \Theta \mathbf{e}, \quad (5.113)$$

with the vector of length $N \triangleq \sum_{l \in \mathcal{L}} N_l$,

$$\mathbf{e} \triangleq \operatorname{col}_{l=1}^L \left\{ \mathbf{e}^{(l)} \right\}, \quad (5.114)$$

and the $N_L \times N$ matrix

$$\Theta \triangleq \operatorname{row}_{l=1}^L \left\{ \Theta^{(l)} \right\}. \quad (5.115)$$

By inserting (5.113) in (5.102), the following compact relation between $\delta^{(l)}$ and \mathbf{e} is found,

$$\delta^{(l)} = \Omega^{(l)} \Theta \mathbf{e}, \quad (5.116)$$

with $\Omega^{(l)}$, defined by (5.100) and (5.101), and Θ according to (5.112) and (5.115). Each element of \mathbf{e} corresponds to one combination of $\tilde{\mathbf{w}}_j^{(l)\top} \hat{\mathbf{x}}^{(l-1)}$, for $j \in \mathcal{N}_l$, and $l \in \mathcal{L}$. Each $\delta_j^{(l)}$ in turn, is a linear combination of those entries. With this in mind, after inserting (5.116) in update equation (5.96), it can be seen that the multilayer perceptron has algorithmically the same structure as the coupled structure given by (4.4)–(4.9). Therefore, its stability can be analysed based on the results presented in Chapter 4.

To do so, first recognise that the coupling matrices in Sections 4.4 and 4.5 all relate the individual a priori errors to the update errors. Here, the former are represented by the elements of \mathbf{e} , the latter by the elements of all the $\delta^{(l)}$. Hence, coupling matrix Δ_{MLP} (cf. (4.84)) that corresponds to the multilayer perceptron can be identified, according to

$$\delta \triangleq \operatorname{col}_{l=1}^L \left\{ \delta^{(l)} \right\} = \operatorname{col}_{l=1}^L \left\{ \Omega^{(l)} \Theta \mathbf{e} \right\} = \underbrace{\operatorname{col}_{l=1}^L \left\{ \Omega^{(l)} \right\}}_{\triangleq \Omega} \Theta \mathbf{e} = \underbrace{\Omega \Theta}_{\Delta_{\text{MLP}}} \mathbf{e}. \quad (5.117)$$

Matrix Ω is upright rectangular and has N_L columns, matrix Θ in turn is a lying rectangular matrix with N_L rows. Accordingly, due to Sylvester's inequality [HJ13, Section 0.4.5] regarding the rank of a matrix product, the rank of the corresponding coupling matrix Δ_{MLP} is bounded by

$$\operatorname{rank} \{ \Delta_{\text{MLP}} \} \leq N_L. \quad (5.118)$$

Therefore, Δ_{MLP} is rank deficient and consequently, in the best case positive semi-definite. This entails that Theorems 4.1 and 4.2 cannot be applied, inhibiting any statement regarding ℓ_2 -stability of the multilayer perceptron trained by the backpropagation algorithm. However, Lemma 4.3 is not affected by Δ_{MLP} being singular. Taking into account the complicated structure of the latter, in general, it can be expected to be a non-normal matrix. Hence, based on Conjecture 4.1, in most cases, Lemma 4.4 will not hold. As a consequence, also Lemma 4.3 seems hard to satisfy, which eventually allows to conjecture that for the multilayer perceptron trained by the backpropagation

algorithm, non-expanding mapping behaviour in terms of the weight error matrices, can hardly be ensured. Furthermore, analogously to the Wiener model discussed in Section 5.2, this result also confirms that the initialisation of the edge weights directly affects the convergence behaviour of the backpropagation algorithm.

Note that the above derivation puts one detail aside. The output of an artificial neuron typically does not only depend on its inputs, i.e., its stimulus level, but also on a threshold value that may be constant or adaptive as well. The here considered structure seems to ignore this point. However, this is justified for the following reasons. On the one hand, as explained in [Roj96, Chapter 7.3], bias weights can easily be taken into account by extending the neural network. Moreover, the backpropagating errors do not need to traverse the corresponding bias edges, as they are not connected to any preceding layer. On the other hand, the applied theory in Chapter 4 completely ignores the fact that the inputs of intermediate layers are given by the outputs of their preceding neighbour layers. Thus, the only step that is necessary to reflect the existence of such thresholds, is to modify the weight matrices appropriately. As this modification is not expected to essentially affect the above found insights, a more detailed investigation is skipped here and left for future work.

Chapter 6

Conclusions

Identification of unknown systems based on observable data is an ubiquitous problem encountered in many disciplines of science and engineering. In some situations, such as weather forecast, these unknown systems are of substantial complexity. However, their identification can resort to a vast amount of data and a high-performance infrastructure for numeric solutions. In other scenarios in turn, only a moderate complexity is faced, while strong restrictions with respect to available computational capacity are imposed. This thesis completely focuses on the latter case.

One main motivation for its contents arose in the context of DPD for microwave power amplifiers. There, a typical low complexity approach makes use of adaptive Wiener models, i.e., two-block models which consist of a linear filter followed by a non-linear one-to-one mapping. The investigation of convergence and stability of such systems triggered the development of the presented methods. With progress of the conducted research, the original focus on adaptive two-block models has been extended towards more general structures. As a result, the presented methods became more and more independent, and in the current form, they establish a widely self contained theory.

Below, Section 6.1 briefly points out the key results presented in this thesis, reviews some interrelations, and gives complementary comments. A critical discussion about open issues and possible directions for future research is provided in Section 6.2. Finally, this work is closed by a few concluding remarks in Section 6.3.

6.1 Summary of Key Results

The two main topics in this thesis – the analysis of asymmetric algorithms in Chapter 3, and the study of coupled gradient type algorithms in Chapter 4 – on the first glance, appear rather unrelated. However, especially the identical error case, discussed in Section 4.6, reveals how the primer helps to understand the latter. Two insights of Chapter 3 stand out. On the one hand, Theorem 3.1 shows that the most typical kind of asymmetric algorithms, the LMS algorithm with matrix step-size, inherently introduces the risk of parameter divergence. The reason why such divergence cannot always be provoked, and conditions for its existence, are presented in Section 3.4.4 (cf. Theorems 3.2 and 3.3). In conjunction with the simulation experiments introduced in Section 3.1, and their reconsideration in Section 3.2, it is made clear that the necessary condition for parameter divergence given in Theorem 3.3, is novel and extends existing knowledge about this kind of algorithms. As Theorem 3.3 is only necessary and lacks sufficiency, in some situations, a reliable verdict on convergence may not be accessible. Then, as an alternative, Sections 3.5 and 3.6 provide analytical as well as numerical means for synthesis of w.c. excitation sequences. By this, simulation experiments can be conducted, in order to test given algorithms for existence of diverging modes. If possible, the numerical method should only be employed, if the analytical approach is not applicable (cf. Section 3.6 for details), as the latter *ensures* to find diverging modes, if they exist at all. Moreover, the achieved simulation times are a fraction of those required by the numerical method.

The coupled structure introduced in Section 4.1 may appear rather generic at first. For sure, in this context, the topic most debated with colleagues and scientific reviewers, are the circumstances which may cause the errors of several gradient type algorithms to become coupled in such a way. As pointed out at the beginning of Chapter 4, one can imagine physical effects that introduce interference. Alternatively, this structure opens up the possibility to intentionally introduce a dependency among the quality of several estimates. Hence, the designer may on purpose make use of such a linear coupling. However, the most important reason for the coupled structure of Chapter 4 to occur, is attributed to algorithmic analysis. The four applications discussed in Chapter 5 are intended to justify this fact. Specifically, the investigation of the MC-FXLMS algorithm in Section 5.3, shows how this method opens up access to systematic derivation of concise mapping and stability conditions. The investigation of the multilayer perceptron trained by the backpropagation algorithm, in Section 5.4, in turn, demonstrates that considerable effort may be required to successfully map a given algorithm to such a coupled structure.

While the investigations of asymmetric algorithms, presented in Chapter 3 provide incremental contributions to a widely studied family of algorithms, the coupled structure in Chapter 4, has not been considered by other authors. Hence, the obtained results are novel to a wide extent. Although ℓ_2 -stability is a well established notion (cf. Section 2.4.2), its extension based on the theory of M -matrices (cf. Section 4.2), to a system of gradient type algorithms (cf. Section 4.4), is to my best knowledge, new in this field. Similarly, the results of the mapping analysis conducted in Section 4.5 appear to be original contributions. One intention of Chapter 5 is to demonstrate that this mapping analysis has a somewhat wider reach compared to ℓ_2 -stability. This is seen as the latter fails specifically in all identical error cases, i.e., Sections 5.1.3.2, 5.2, and 5.3. Then, the mapping analysis is still applicable, and allows to identify conditions for a non-expanding parameter error distance via Lemma 4.7. The latter lemma establishes the link to Chapter 3 and has a remarkable side-effect: as it leads to algorithms that are symmetric, the (originally failing) ℓ_2 -stability analyses of Section 4.4 become employable again.

6.2 Critical Discussion, Open Issues, and Outlook

The theory developed in Chapters 3 and 4 rests upon rigorous derivations and provides several new insights to the characteristics that inhere gradient type algorithms, respectively, combinations of them. Although general applicability and completeness has been one of the goals pursued in this thesis, open issues remain. These are addressed in the sequel of this section. Section 6.2.1 focuses on the derivations regarding asymmetric algorithms in Chapter 3. The results obtained for the coupled structure in Chapter 4 are discussed in Section 6.2.2. However, at first, one restriction is pointed out that applies in either case.

Throughout this thesis, the parameter vector of the reference system is assumed to be constant (cf. Section 2.1). Hence, from a formal point of view, any variation of the latter would cause the presented results to fail. Yet, intuitively, up to a certain degree, drifts and small fluctuations are expected to be acceptable. Nevertheless, being based on intuition, this is just a speculation and its verification requires further investigation.

6.2.1 Considerations with Respect to Asymmetric Algorithms in Chapter 3

The mapping analysis for the homogeneous recursion of asymmetric algorithms in Chapter 3 gives a detailed picture about the mechanisms that occur during one iteration. It also allows to deduce the progress over a finite number of iterations. What is not completely covered, is the extension to behaviour in the limit, i.e., for $k \rightarrow \infty$. This is specifically reflected in the proof of Theorem 3.2,

which has to resort to [RC00], in order to ensure boundedness of the described mapping process. This is necessary, as without any further reasoning, the convergence of the parameter error vector to one of the eigenspaces of the step-size matrix, does *not* inherently entail its boundedness.

Also Theorem 3.3 leaves space for improvement. It requires a persistent change of *all* eigenspaces of the step-size matrix. Intuitively, the same is expected to hold, if some of the eigenspaces are invariant, as long as the one, corresponding to the eigenvalue with maximum real part, is *not* amongst them. Consequently, it is desirable to state Theorem 3.3 more precisely, clarifying the corresponding details.

Regardless which of the approaches presented in Sections 3.5 and 3.6 is chosen, the numerical assessment of hidden divergence for a given asymmetric algorithm bares two limiting subtleties, which are not that obvious at first glance. The first one is of relevance, if a real-world system identification process has to be analysed – in contrast to a simulated one. Then, the parameter vector of the reference system is unknown, causing the parameter error vector to be inaccessible. Hence, neither the analytic approach, nor the numeric search for w.c. excitation vectors can be employed. Consequently, the synthesis of w.c. excitation sequences, based on the methods in Sections 3.5 and 3.6, is restricted to simulations.

The second limiting subtlety concerns the fact that divergence of the parameter error vector may depend on its initial state. Thus, a set of Monte Carlo simulations that does not reveal an unbounded growth of the parameter error vector, does *not* allow to conclude unconditional boundedness of the latter. Only the contrary situation leads to a conclusive result. Accordingly, if a Monte Carlo simulations ends up in at least one run with diverging parameter error vector, it is ensured that the considered algorithm is not guaranteed to converge.

As pointed out at the end of Section 3.2.4, it is not completely clarified how the here revealed hidden divergence of asymmetric algorithm blends with the phenomena described in [SLJB86; Set92; Nas99], which are all in some sense caused by insufficient persistency of excitation. The in this work observed rates of divergence as well as the numerically verified fulfilment of PE, both indicate that the here observed behaviour is of different nature. Yet, a formal investigation remains open.

A last possible direction for future research with respect to the asymmetric algorithms in Chapter 3 addresses parameter leakage. The latter is known to be a measure which effectively reduces the parameter drift that can be observed for the conventional LMS algorithm [CM81; Nas99]. This motivates to study parameter divergence for leaky asymmetric algorithms, or specifically, for a leaky version of the LMS algorithm with matrix step-size.

6.2.2 Considerations with Respect to the Coupled Structure in Chapter 4

The bounds ensuring ℓ_2 -stability of the coupled structure in Section 4.4 have to be expected to be conservative in most cases. The reason for this is the repeated application of triangle and Minkowsky inequality in the derivations of Theorems 4.1 and 4.2. Hence, an interesting open topic is the identification of alternative arguments which allow to circumvent the frequent use of these latter two inequalities.

The possibly most prevalent open issues with respect to the mapping analysis of the homogeneous recursion that underlies the coupled structure in Chapter 4, are two weak links in the chain of statements in Section 4.5. The first one is based on the fact that Lemma 4.4 is sufficient for non-expanding behaviour of the parameter error vector. The following Lemma 4.5, however, is only

necessary for Lemma 4.4. Hence, the latter – and thus non-expanding behaviour – is *not* ensured to hold, if Lemma 4.5 is satisfied. Moreover, a violation of Lemma 4.5 entails Lemma 4.4 to fail. Yet, as the latter is a sufficient condition, even then, non-expanding w.c. behaviour is possible. Thus, as pointed out at the end of Section 4.6, the first mentioned missing link is a statement, complementary to Lemma 4.4, of the form “ $\mathbf{\Gamma}_k \not\geq 0 \Rightarrow \mathbf{\Gamma}_k \boxtimes \mathbf{U}_k \not\geq 0$ ”, and/or a sufficient counterpart to Lemma 4.5.

The second weak link is of less significance but still desirable to be reinforced. As some unusual but still possible coupling matrices are not covered by the proof of Conjecture 4.1, it is incomplete. A specific consequence is that in the identical error case, Lemma 4.7 has only the limited rigour of a conjecture, as it does not strictly clarify whether the coupling matrix has to be normal in order to ensure Lemma 4.4.

Chapter 5 demonstrates how the findings about the coupled structure in Chapter 4 can be leveraged to study the behaviour of cascaded and otherwise combined gradient type algorithms. With respect to the mapping analysis in the sense of Section 4.5, it has to be noted that all of the excitation vectors are inherently assumed to be independent. Based on Chapter 5, it becomes clear that this is only partially the case, if the coupled structure is obtained as an intermediate step in the analysis of some specific algorithm. Dependencies among the excitation vectors do not cause the obtained results to be invalid. Yet, it has to be kept in mind that then, the original algorithm may show more benign convergence behaviour than the equivalent coupled structure. In other words, the obtained convergence conditions may be rather conservative. In some situations, Monte Carlo simulations employing Section 3.5 or Section 3.6 in order to provoke w.c. excitation, allow to assess the tightness of the theoretically derived bounds.

Finally, one further idea for extension of the coupled structure in Chapter 4 is sketched. The analysis of the MC-FXLMS algorithm in Section 5.3 assumes perfect knowledge of the secondary paths. If this assumption is dropped, the obtained structure modifies to a combination of gradient type algorithms, where each of the individual regression vectors deviates from the conjugate of the corresponding excitation vector. Hence, a system of coupled *asymmetric* algorithms is obtained. Accordingly, as Chapter 4 restricts the individual gradient type algorithms to be symmetric, an extension towards asymmetric algorithms is desirable.

6.3 Conclusion

More than half a century ago, with the seminal works of Widrow and Hoff [WH60] and Kalman [Kal60], adaptive filtering gained more and more attention. Meanwhile, the amount of available literature dealing with this topic has become remarkably vast. Nevertheless, still, open questions remain. This work aims to answer yet another few of them.

Although the phenomenon of hidden diverging modes in asymmetric algorithms has already been investigated in earlier works by other authors (cf. Section 3.2), this thesis provides novel means in order to explain, reveal, and prevent their occurrence. Additionally, it extends the understanding of the underlying mechanisms. Altogether, this enables the designer of such algorithms to act with more awareness regarding convergence and stability.

Although separately operating gradient type algorithms are well understood, their combination still poses challenges with respect to convergence and stability. The in this work presented structure of interfering gradient type algorithms (cf. Chapter 4), together with the developed theory, is intended to ease design and analysis of such systems that incorporate several interacting gradient type algorithms. Specifically, its application to the adaptive Wiener model and the MC-FXLMS in context of ANC, leads to novel interpretations and bounds, and well demonstrates its effectiveness.

Appendix A

Singular Values of Mapping Matrix \mathbf{B}_k

This appendix provides the derivations related to Section 3.3.2. First, Appendix A.1 derives the quadratic equation that directly leads to (3.22). Then, Appendix A.2 presents a detailed discussion of the dependency of the two non-unit singular values, σ_1 and σ_2 , on the effective step-size α , the correlation coefficient ρ , and the complex argument $\varphi_{\alpha\rho^*}$ among them – cf. (3.11)–(3.13), respectively. Along the way, Appendix A.2.3 provides the proof for Lemma 3.2. Moreover, based on the obtained insights, Appendix A.3 determines the extremal behaviour of σ_1 and σ_2 , leading to the bounds in Theorem 3.1. *Until the end of this appendix, iteration index k is suppressed.*

A.1 Derivation of the Non-Unit Singular Values of \mathbf{B}_k

The singular values of mapping matrix \mathbf{B} are defined as the solutions to the equation

$$\det(\mathbf{B}^H\mathbf{B} - \sigma^2\mathbf{I}) = 0. \quad (\text{A.1})$$

It can be straightforwardly solved by the Sherman-Morrison-Woodbury formula¹ [HJ13, Section 0.7.4] and Cauchy’s formula for the determinant of a rank-one perturbation (cf. footnote on 130). However, here, an even simpler approach is adopted based on Vieta’s formulas. In Section 3.3.2, it is found that \mathbf{B} has a unit singular value with multiplicity $M - 2$. For the remaining two, the following relations hold [see, e.g., HJ13, Section 1.2]

$$\text{tr}(\mathbf{B}^H\mathbf{B}) = \sum_{i=1}^M \sigma_i^2 = \sigma_1^2 + \sigma_2^2 + M - 2, \quad (\text{A.4})$$

$$\det(\mathbf{B}^H\mathbf{B}) = |\det(\mathbf{B})|^2 = \prod_{i=1}^M \sigma_i^2 = \sigma_1^2\sigma_2^2, \quad (\text{A.5})$$

¹ For an invertible matrix $\mathbf{A} \in \mathbb{C}^{M_A \times M_A}$ and some matrices $\mathbf{C} \in \mathbb{C}^{M_A \times M_D}$, $\mathbf{D} \in \mathbb{C}^{M_D \times M_D}$, and $\mathbf{E} \in \mathbb{C}^{M_D \times M_A}$, such that $\mathbf{D}^{-1} + \mathbf{E}\mathbf{A}^{-1}\mathbf{C}$ is invertible, it can be shown that

$$(\mathbf{A} + \mathbf{CDE})^{-1} = \mathbf{A}^{-1} - \mathbf{A}^{-1}\mathbf{C}(\mathbf{D}^{-1} + \mathbf{E}\mathbf{A}^{-1}\mathbf{C})^{-1}\mathbf{E}\mathbf{A}^{-1}. \quad (\text{A.2})$$

Especially, for $M_D = 1$, the matrix \mathbf{D} reduces to a scalar $d \in \mathbb{C}$, and the matrices $\mathbf{C} = \mathbf{c} \in \mathbb{C}^{M_A}$ and $\mathbf{E} = \mathbf{e}^T$, with $\mathbf{e} \in \mathbb{C}^{M_A}$, reduce to a column vector, respectively, a row vector. For $d\mathbf{e}^T\mathbf{A}^{-1}\mathbf{c} \neq -1$, this leads to

$$(\mathbf{A} + d\mathbf{c}\mathbf{e}^T)^{-1} = \mathbf{A}^{-1} - \frac{d}{1 + d\mathbf{e}^T\mathbf{A}^{-1}\mathbf{c}}\mathbf{A}^{-1}\mathbf{c}\mathbf{e}^T\mathbf{A}^{-1}. \quad (\text{A.3})$$

where equivalently, $\mathbf{B}\mathbf{B}^H$ could have been used instead of $\mathbf{B}^H\mathbf{B}$. Consequently, from (A.4) together with (3.16), or (3.17), (3.11) and (3.12), it follows that

$$\sigma_1^2 + \sigma_2^2 = 2 + |\alpha|^2 - 2\operatorname{Re}\{\alpha\rho^*\}, \quad (\text{A.6})$$

and from (A.5), using Cauchy's formula for the determinant of a rank-one perturbation² [HJ13, Equation 0.8.5.11],

$$\sigma_1^2\sigma_2^2 = |1 - \alpha\rho^*|^2. \quad (\text{A.7})$$

With this at hand, Vieta's formulas directly lead to the quartic equation,

$$\sigma_i^4 - \sigma_i^2 \left(2 + |\alpha|^2 - 2\operatorname{Re}\{\alpha\rho^*\} \right) + |1 - \alpha\rho^*|^2 = 0. \quad (\text{A.9})$$

Since (A.9) does neither contain a first nor a third order term, its roots are found via the equivalent quadratic equation in σ_i^2 . It can be verified that all of the four roots are ensured to be real-valued. As a consequence, two of them are non-negative, the other two are non-positive, where the latter have the same magnitudes as the primer. Taking into account that the singular values are by definition non-negative, the negative roots can be discarded, by which the two singular values in (3.22) are obtained.

A.2 Analysis of the two Non-Unit Singular Values of \mathbf{B}_k

This appendix thoroughly analyses the dependency of the two non-unit singular values of mapping matrix \mathbf{B} , on the effective step-size α , the correlation coefficient ρ , and the complex argument $\varphi_{\alpha\rho^*}$. The goal is to develop a clear picture of the corresponding functions, in order to prepare for the specification of bounds and extremal ratings in the following Appendix A.3. In order to improve readability, first the following definitions and abbreviations are introduced:

$$a \triangleq |\alpha| \in \mathbb{R}_{0+}, \quad \varphi_\alpha \triangleq \operatorname{arc}\{\alpha\} \in (-\pi, \pi] \quad \Rightarrow \quad \alpha = ae^{j\varphi_\alpha}, \quad (\text{A.10})$$

$$r \triangleq |\rho| \in [0, 1], \quad \varphi_\rho \triangleq \operatorname{arc}\{\rho\} \in (-\pi, \pi] \quad \Rightarrow \quad \rho = re^{j\varphi_\rho}, \quad (\text{A.11})$$

$$\varphi \triangleq \varphi_\alpha - \varphi_\rho \text{ mapped to } (-\pi, \pi] \quad \Rightarrow \quad \varphi = \operatorname{arc}\{\alpha\rho^*\}, \quad (\text{A.12})$$

$$g = f_g(a, r, \varphi) \triangleq \frac{a}{2} - r \cos(\varphi) \in \left[\frac{a}{2} - r, \frac{a}{2} + r \right] \subset [-1, \infty), \quad (\text{A.13})$$

$$\eta_i = f_{\eta,i}(a, r, \varphi) \triangleq g + s_i \sqrt{1 + g^2 - r^2} \quad \Rightarrow \quad \sigma_i^2 = 1 + a\eta_i. \quad (\text{A.14})$$

In (A.14) the sign factor s_i is introduced, which is defined as

$$s_i \triangleq (-1)^{i-1}. \quad (\text{A.15})$$

Note that $0 \leq \eta_1 \leq |g| + \sqrt{1 + g^2}$, where the bound from below is due to the fact that since $0 \leq r \leq 1$, the square-root is always larger than or equal to the magnitude of g . The bound from above is trivially verified from (A.14). For η_2 , it analogously follows, $-|g| - \sqrt{1 + g^2} \leq \eta_2 \leq 0$.

² For an invertible square matrix $\mathbf{A} \in \mathbb{C}^{M \times M}$ and two vectors $\mathbf{a}, \mathbf{b} \in \mathbb{C}^M$, the following relation holds

$$\det(\mathbf{A} + \mathbf{a}\mathbf{b}^T) = \det(\mathbf{A}) \left(1 + \mathbf{b}^T \mathbf{A}^{-1} \mathbf{a} \right). \quad (\text{A.8})$$

According to the right-hand side of (A.14), both η_i affinely map to the two non-unit singular values. Hence, in order to locate their extrema – respectively, the extrema of their squares – the first order partial derivatives of g and η_i with respect to a , r , and φ are required. These are found to evaluate to

$$\frac{\partial g}{\partial a} = \frac{1}{2}, \quad \frac{\partial g}{\partial r} = -\cos(\varphi), \quad \frac{\partial g}{\partial \varphi} = r \sin(\varphi), \quad (\text{A.16})$$

and

$$\frac{\partial \eta_i}{\partial a} = \frac{\partial g}{\partial a} \underbrace{\left(1 + s_i \frac{g}{\sqrt{1+g^2-r^2}}\right)}_{\in[0,2]} = s_i \frac{\eta_i}{2\sqrt{1+g^2-r^2}} = \frac{|\eta_i|}{2\sqrt{1+g^2-r^2}}, \quad (\text{A.17})$$

$$\frac{\partial \eta_i}{\partial r} = \frac{\partial g}{\partial r} + s_i \frac{g \frac{\partial g}{\partial r} - r}{\sqrt{1+g^2-r^2}} = -\left(\cos(\varphi) + s_i \frac{g \cos(\varphi) + r}{\sqrt{1+g^2-r^2}}\right) = -\frac{|\eta_i| \cos(\varphi) + s_i r}{\sqrt{1+g^2-r^2}}, \quad (\text{A.18})$$

$$\frac{\partial \eta_i}{\partial \varphi} = \frac{\partial g}{\partial \varphi} \left(1 + s_i \frac{g}{\sqrt{1+g^2-r^2}}\right) = s_i \frac{\eta_i r \sin(\varphi)}{\sqrt{1+g^2-r^2}} = \frac{|\eta_i| r \sin(\varphi)}{\sqrt{1+g^2-r^2}}. \quad (\text{A.19})$$

A.2.1 Dependency with respect to the Magnitude of the Effective Step-Size

The first order partial derivative of η_i with respect to a in (A.17) is always non-negative. However, this is not true for the corresponding first order partial derivative of σ_i^2 ,

$$\frac{\partial(\sigma_i^2)}{\partial a} = \eta_i + a \frac{\partial \eta_i}{\partial a} \stackrel{(\text{A.17})}{=} \eta_i \left(1 + \frac{s_i a}{2\sqrt{1+g^2-r^2}}\right). \quad (\text{A.20})$$

Accordingly, for σ_1^2 , the first order partial derivative with respect to a is non-negative,

$$\frac{\partial(\sigma_1^2)}{\partial a} \geq 0, \quad (\text{A.21})$$

with identity at the roots of η_1 , i.e., for

$$r = 1 \wedge |\varphi| \leq \frac{\pi}{2} \wedge a \leq 2 \cos(\varphi). \quad (\text{A.22})$$

For σ_2^2 , i.e., with sign factor $s_2 = -1$, (A.20) is zero at the roots of η_2 , which occur at

$$r = 1 \wedge \left[\frac{\pi}{2} \leq |\varphi| \leq \pi \vee \left(|\varphi| < \frac{\pi}{2} \wedge a \geq 2 \cos(\varphi)\right)\right], \quad (\text{A.23})$$

complemented by the roots of the bracket expression in (A.20). Only for $r > 0 \wedge |\varphi| < \frac{\pi}{2}$ one such additional root exists, found at

$$\check{a}_2 = \frac{1 - r^2 \sin^2(\varphi)}{r \cos(\varphi)}. \quad (\text{A.24})$$

For $\frac{\pi}{2} \leq |\varphi| \leq \pi$, the bracket expression in (A.20) is non-negative (identical to zero for $r = 1 \wedge |\varphi| = \frac{\pi}{2}$ and in the limit for $a \rightarrow \infty$). This entails that then, the first order derivative of σ_2^2 with respect to a is in any case less than or equal to zero. If in contrast, a valid, i.e., a non-negative, root (A.24)

exists, the bracket expression in (A.20) is (greater than|less than)³, zero for $\langle a < \check{a}_2 | a > \check{a}_2 \rangle$. Thus, the behaviour of the first order partial derivative of σ_2^2 with respect to a can be summarised as

$$\frac{\partial(\sigma_2^2)}{\partial a} \begin{cases} < 0; & \text{for } \frac{\pi}{2} < |\varphi| \leq \pi \vee (|\varphi| = \frac{\pi}{2} \wedge r < 1) \vee [|\varphi| < \frac{\pi}{2} \wedge (r > 0 \wedge a < \check{a}_2) \vee (r = 1 \wedge a < 2 \cos(\varphi))] \\ = 0; & \text{for } \langle r = 1 \wedge [\frac{\pi}{2} \leq |\varphi| \leq \pi \vee (|\varphi| < \frac{\pi}{2} \wedge a \geq 2 \cos(\varphi))] \rangle \vee [r > 0 \wedge |\varphi| < \frac{\pi}{2} \wedge a = \check{a}_2] \\ > 0; & \text{for } 0 < r < 1 \wedge |\varphi| < \frac{\pi}{2} \wedge a > \check{a}_2 \end{cases}$$

The maximum of σ_2^2 is always one and occurs at $a = 0$, and for $r = 1$ also at $a \geq 2 \cos(\varphi)$. The minimum is either

$$\min_{a \in \mathbb{R}_{0+}} \sigma_2^2 = r^2 \sin^2(\varphi), \quad (\text{A.25})$$

located at \check{a}_2 if $r > 0$ and $|\varphi| \leq \frac{\pi}{2}$, or

$$\min_{a \in \mathbb{R}_{0+}} \sigma_2^2 = r^2, \quad (\text{A.26})$$

which is only reached in the limit $a \rightarrow \infty$, for $\frac{\pi}{2} < |\varphi| \leq \pi$.

A.2.2 Dependency with respect to the Magnitude of the Correlation Coefficient

The first order partial derivative of σ_i^2 with respect to r is found to be

$$\frac{\partial(\sigma_i^2)}{\partial r} = a \frac{\partial \eta_i}{\partial r} \stackrel{(\text{A.18})}{=} - \frac{a}{\sqrt{1+g^2-r^2}} \begin{cases} \eta_1 \cos(\varphi) + r; & \text{for } i = 1 \\ |\eta_2| \cos(\varphi) - r; & \text{for } i = 2 \end{cases}. \quad (\text{A.27})$$

For $a = 0$, (A.27) becomes zero for both cases. Acknowledging that, for the rest of this appendix, *the focus is kept on $a > 0$* . Then, (A.27) gives

$$\frac{\partial(\sigma_1^2)}{\partial r} < 0 \quad \Leftrightarrow \quad \eta_1 \cos(\varphi) + r > 0, \quad (\text{A.28})$$

$$\frac{\partial(\sigma_2^2)}{\partial r} < 0 \quad \Leftrightarrow \quad |\eta_2| \cos(\varphi) - r > 0. \quad (\text{A.29})$$

Anticipating following findings, at this point, three special values of a are introduced:

$$a_1 = 2 \cos(\varphi) - \frac{1}{\cos(\varphi)} = \frac{\cos(2\varphi)}{\cos(\varphi)} = \cos(\varphi) (1 - \tan^2(\varphi)) \geq 0, \text{ for } |\varphi| \in \left[0, \frac{\pi}{4}\right] \cup \left(\frac{\pi}{2}, \frac{3\pi}{4}\right], \quad (\text{A.30})$$

$$a_2 = 2 \cos(\varphi) - \frac{1}{2 \cos(\varphi)} = \frac{3 - 4 \sin^2(\varphi)}{2 \cos(\varphi)} = \frac{\cos(\varphi)}{2} (3 - \tan^2(\varphi)) \geq 0, \text{ for } |\varphi| \in \left[0, \frac{\pi}{3}\right] \cup \left(\frac{\pi}{2}, \frac{2\pi}{3}\right], \quad (\text{A.31})$$

$$a_3 = 2 \cos(\varphi) \geq 0, \text{ for } |\varphi| \leq \frac{\pi}{2}. \quad (\text{A.32})$$

Each of the values is tied to a certain range of angle φ . Outside of these ranges, the corresponding value becomes negative and is thus not a valid value for magnitude a . Furthermore, note that under

³ The abbreviated notation "...A|B) ...C|D) ..." expands to two statements: "...A ...C ...", and "...B ...D ...".

the assumption of their existence, a_1 , a_2 , and a_3 satisfy the following relations

$$0 < a_3 < a_2 < a_1, \quad \text{for} \quad \frac{\pi}{2} < |\varphi| < \pi, \quad (\text{A.33})$$

$$0 < a_1 < a_2 < a_3, \quad \text{for} \quad |\varphi| < \frac{\pi}{2}. \quad (\text{A.34})$$

In the next step, the roots for the right-hand side of (A.28) and (A.29) are calculated. From (A.22) and (A.23), it is already known that $\eta_i \neq 0$ if $r < 1$. Therefore, even if $a = 0$, the value $r = 0$ can only be a root iff $|\varphi| = \frac{\pi}{2}$. Keeping this in mind, in the following, *the cases $r = 0$ and $|\varphi| = \frac{\pi}{2}$ do not need to be considered further*. This, together with restriction $a > 0$ that has been introduced right after (A.27), in combination with the facts, $\eta_1 \geq 0$ and $\eta_2 \leq 0$, leads to

$$\frac{\partial(\sigma_1^2)}{\partial r} < 0, \quad \text{for} \quad |\varphi| < \frac{\pi}{2}, \quad (\text{A.35})$$

$$\frac{\partial(\sigma_2^2)}{\partial r} > 0, \quad \text{for} \quad \frac{\pi}{2} < |\varphi| < \pi. \quad (\text{A.36})$$

A.2.2.1 Details for the First Singular Value

For $|\varphi| < \frac{\pi}{2}$, expression (A.35) is already available. Hence, what remains open for singular value σ_1 , is the analysis for $\frac{\pi}{2} < |\varphi| \leq \pi$. This is done by identifying the magnitude r – further down in (A.39), the solution is denoted \hat{r}_1 – that solves the right-hand side of (A.28), with identity to zero. Re-inserting η_1 from (A.14), leads to

$$r^2 \sin^2(\varphi) - ra |\cos(\varphi)| - \cos^2(\varphi) = 0, \quad (\text{A.37})$$

under the constraint

$$a \leq \frac{2r \sin^2(\varphi)}{|\cos(\varphi)|}. \quad (\text{A.38})$$

Equation (A.37) is solved by (note that the second solution would be less than zero which is no valid value for r)

$$\hat{r}_1 = \frac{a |\cos(\varphi)|}{2 \sin^2(\varphi)} \left[1 + \sqrt{1 + \left(\frac{2}{a}\right)^2 \sin^2(\varphi)} \right]. \quad (\text{A.39})$$

In order to ensure $\hat{r}_1 \leq 1$, magnitude a additionally has to be bounded from above by a_1 in (A.30), i.e.,

$$a \leq a_1, \quad (\text{A.40})$$

which imposes the additional restriction $\frac{\pi}{2} < |\varphi| < \frac{3\pi}{4}$ to the range of φ for which a valid \hat{r}_1 exists. Note that (A.38) is implied by (A.40), since here, only $\frac{\pi}{2} < |\varphi| \leq \pi$ is of relevance. If a valid \hat{r}_1 exists, the right-hand side expression of (A.28) is ⟨negative|positive⟩, for ⟨ $r < \hat{r}_1$ | $r > \hat{r}_1$ ⟩, which shows that \hat{r}_1 is a maximum of σ_1^2 . Eventually, the behaviour of the first order derivative of σ_1^2 can

be carved out:

$$\frac{\partial(\sigma_1^2)}{\partial r} \begin{cases} < 0; & \text{for } a > 0 \wedge [|\varphi| < \frac{\pi}{2} \vee (|\varphi| = \frac{\pi}{2} \wedge r > 0) \vee (\frac{\pi}{2} < |\varphi| < \frac{3\pi}{4} \wedge a \leq a_1 \wedge r > \hat{r}_1)] \\ = 0; & \text{for } a = 0 \vee (r = 0 \wedge |\varphi| = \frac{\pi}{2}) \vee (\frac{\pi}{2} < |\varphi| < \frac{3\pi}{4} \wedge a \leq a_1 \wedge r = \hat{r}_1) \\ > 0; & \text{for } a > 0 \wedge \{ \frac{\pi}{2} < |\varphi| < \frac{3\pi}{4} \wedge [(a \leq a_1 \wedge r < \hat{r}_1) \vee a > a_1] \} \vee \frac{3\pi}{4} \leq |\varphi| \leq \pi \} \end{cases}$$

Accordingly, for $a > 0$, and if either $r > 0$ or $|\varphi| \neq \frac{\pi}{2}$, σ_1^2 assumes its maximum at

$$r = 0, \quad \text{for} \quad |\varphi| \leq \frac{\pi}{2}, \quad (\text{A.41})$$

$$r = \hat{r}_1, \quad \text{for} \quad \frac{\pi}{2} < |\varphi| < \frac{3\pi}{4} \wedge a < a_1, \quad (\text{A.42})$$

$$r = 1, \quad \text{for} \quad \left(\frac{\pi}{2} < |\varphi| < \frac{3\pi}{4} \wedge a > a_1 \right) \vee \frac{3\pi}{4} \leq |\varphi| \leq \pi. \quad (\text{A.43})$$

As a consequence, the minimum of σ_1^2 with respect to r is found at its limits, i.e., $r = 0$ or $r = 1$. From (A.10)–(A.14), the corresponding values are obtained as

$$\sigma_1^2|_{r=0} = 1 + \frac{a^2}{2} + a\sqrt{1 + \frac{a^2}{4}}, \quad (\text{A.44})$$

$$\sigma_1^2|_{r=1, \frac{\pi}{2} < |\varphi| \leq \pi} = 1 + a^2 + 2a|\cos(\varphi)|. \quad (\text{A.45})$$

It can be verified that $\sigma_1^2|_{r=0} > \sigma_1^2|_{r=1, \frac{\pi}{2} < |\varphi| \leq \pi}$, for $a < a_2$ (cf. (A.31)), which allows to conclude that the minimum of σ_1^2 is found at

$$r = 0, \quad \text{for} \quad \left(\frac{\pi}{2} < |\varphi| \leq \frac{2\pi}{3} \wedge a \geq a_2 \right) \vee \frac{2\pi}{3} < |\varphi| \leq \pi, \quad (\text{A.46})$$

$$r = 1, \quad \text{for} \quad \left(\frac{\pi}{2} < |\varphi| \leq \frac{2\pi}{3} \wedge a \leq a_2 \right) \vee |\varphi| < \frac{\pi}{2}. \quad (\text{A.47})$$

At $a = a_2$, the minimum value of σ_1^2 occurs at $r = 0$ as well as at $r = 1$. Note moreover that (A.47) is only valid if $\frac{\pi}{2} < |\varphi| \leq \frac{2\pi}{3}$.

A.2.2.2 Details for the Second Singular Value

Stepping back to (A.29), remembering that (A.36) already covered the case $\frac{\pi}{2} < |\varphi| < \pi$, and keeping in mind that the above analysis has been restricted to $a > 0$, $r > 0$, and $|\varphi| < \frac{\pi}{2}$, below, a similar path is followed as in Appendix A.2.2.1. First, the magnitude r is sought which solves the right-hand side of (A.29), with identity to zero, i.e., after re-inserting for η_2 from (A.14),

$$r^2 \sin^2(\varphi) + ra \cos(\varphi) - \cos^2(\varphi) = 0, \quad (\text{A.48})$$

which differs from (A.37), only in the sign of the term linear in r . The root of (A.48) is found at (note that as for (A.37), the second solution would be less than zero which is not a valid value for r)

$$\check{r}_2 = \begin{cases} \frac{1}{a}; & \text{for } \varphi = 0 \\ \frac{a \cos(\varphi)}{2 \sin^2(\varphi)} \left[-1 + \sqrt{1 + \left(\frac{2}{a}\right)^2 \sin^2(\varphi)} \right]; & \text{otherwise} \end{cases}. \quad (\text{A.49})$$

In order to ensure $r \leq 1$ in (A.49), condition $a \geq a_1$ has to be satisfied. Bound a_1 is defined in (A.30), from which it is also found that for the relevant range of φ , a_1 only exists if $|\varphi| < \frac{\pi}{4}$. Hence, for $|\varphi| \in [\frac{\pi}{4}, \frac{\pi}{2}]$, (A.48) always has a (non-negative) root in domain of r , i.e., $[0, 1]$. It can easily be verified that the right-hand side expression in (A.29) is positive for $r < \check{r}_2$, and negative for $r > \check{r}_2$. This clarifies that $r = \check{r}_2$ is a minimum of σ_2^2 . Finally, the point is reached, where the first order derivative of σ_2^2 , with respect to r , can be specified:

$$\frac{\partial(\sigma_2^2)}{\partial r} \begin{cases} < 0; & \text{for } a > 0 \wedge \langle |\varphi| < \frac{\pi}{4} \wedge [a < a_1 \vee (a \geq a_1 \wedge r < \check{r}_2)] \vee (\frac{\pi}{4} \leq |\varphi| < \frac{\pi}{2} \wedge r < \check{r}_2) \rangle \\ = 0; & \text{for } a = 0 \vee (r = 0 \wedge |\varphi| = \frac{\pi}{2}) \vee \langle r = \check{r}_2 \wedge [(|\varphi| < \frac{\pi}{4} \wedge a \geq a_1) \vee \frac{\pi}{4} \leq |\varphi| < \frac{\pi}{2}] \rangle \\ > 0; & \text{for } a > 0 \wedge \{ \langle [(|\varphi| < \frac{\pi}{4} \wedge a \geq a_1) \vee \frac{\pi}{4} \leq |\varphi| < \frac{\pi}{2}] \wedge r > \check{r}_2 \rangle \vee \frac{\pi}{2} < |\varphi| < \pi \} \end{cases}.$$

Consequently, for $a > 0$, and with either $r > 0$ or $|\varphi| \neq \frac{\pi}{2}$, the minimum of σ_2^2 is found at (note that $\check{r}_2 = 1$ for $a = a_1$ and a valid angle φ)

$$r = 0, \quad \text{for} \quad \frac{\pi}{2} < |\varphi| < \pi, \quad (\text{A.50})$$

$$r = \check{r}_2, \quad \text{for} \quad \left(|\varphi| < \frac{\pi}{4} \wedge a \geq a_1 \right) \vee \frac{\pi}{4} \leq |\varphi| < \frac{\pi}{2}, \quad (\text{A.51})$$

$$r = 1, \quad \text{for} \quad |\varphi| < \frac{\pi}{4} \wedge a \leq a_1. \quad (\text{A.52})$$

Analogous to Appendix A.2.2.1, it can be concluded that the maximum occurs either at $r = 0$ or $r = 1$. From (A.10)–(A.14), it is found that

$$\sigma_2^2|_{r=0} = 1 + \frac{a^2}{2} - a\sqrt{1 + \frac{a^2}{4}}, \quad (\text{A.53})$$

$$\sigma_2^2|_{r=1, |\varphi| < \frac{\pi}{2}} = \begin{cases} 1 + a^2 - 2a \cos(\varphi); & \text{for } a < a_3 \\ 1; & \text{for } a \geq a_3 \end{cases}, \quad (\text{A.54})$$

with a_3 defined in (A.32). Based on (A.53) and (A.54), it can be observed that $\sigma_2^2|_{r=0} > \sigma_2^2|_{r=1, |\varphi| < \frac{\pi}{2}}$, for $0 < a < a_2$. Therefore, the maximum of σ_2^2 is found at

$$r = 0, \quad \text{for} \quad \left(|\varphi| < \frac{\pi}{3} \wedge a \leq a_2 \right), \quad (\text{A.55})$$

$$r = 1, \quad \text{for} \quad \left(|\varphi| < \frac{\pi}{3} \wedge a \geq a_2 \right) \vee \left(\frac{\pi}{3} < |\varphi| < \frac{\pi}{2} \vee \frac{\pi}{2} < |\varphi| \leq \pi \right). \quad (\text{A.56})$$

At $|\varphi| = \frac{\pi}{2}$, σ_2^2 is constant with respect to r . Moreover, for $a = a_2$, the maximum of σ_2^2 occurs at $r = 0$, as well as at $r = 1$.

A.2.3 Dependency with respect to the Phase Offset

The first order partial derivative of σ_i^2 with respect to φ is obtained from (A.12), as

$$\frac{\partial(\sigma_i^2)}{\partial \varphi} = a \frac{\partial \eta_i}{\partial \varphi} \stackrel{(\text{A.19})}{=} a \frac{|\eta_i| r \sin(\varphi)}{\sqrt{1 + g^2 - r^2}}. \quad (\text{A.57})$$

Clearly, the sign on the right-hand side of (A.57) is dictated by the sine of φ . Consequently, $\varphi = 0$ leads to the smallest achievable value of σ_i , $\varphi = \pi$ to the largest achievable value. Thus, both non-unit singular values increase monotonously with $|\varphi|$. This proves Lemma 3.2.

A.3 Bounds on the Singular Values of \mathbf{B}_k

Eventually, the results obtained in Appendix A.2 can be summarised in order to justify Theorem 3.1. For reasons of orientation, a schematic overview of the results is provided in Figure A.1, which allows to identify the location of minima and maxima with respect to magnitude r , parametrised by the pair $\langle a, \varphi \rangle$. The first important fact to keep in mind – expressed by (A.57) – is that both of the singular values increase with an increasing magnitude of angle φ (mapped to the interval $(-\pi, \pi]$). Moreover, due to (A.21), σ_1 always grows together with magnitude a . Finally, as found at the end of Appendix A.2.1, $\sigma_2 \leq 1$.

In order to obtain the upper bound (3.31) on σ_1 , first it is observed that due to (A.35) for $|\varphi| \leq \frac{\pi}{2}$, the maximum is found at $r = 1$. Moreover, (A.57) entails that σ_1 further grows with $|\varphi| > \frac{\pi}{2}$. Then, (A.43) shows that for $|\varphi| = \pi$, the maximum remains at $r = 1$. Hence, maximum $\hat{\sigma}_1$ is found at $r = 1$, $\varphi = \pi$. Upper bound $\hat{\sigma}_2 = 1$ in (3.32) has already been identified at the end of Appendix A.2.1. The location $r = 1$, $\varphi = 0$ for lower bound $\check{\sigma}_1 = 1$ in (3.33), directly follows from (A.35) and (A.57). Finally, lower bound $\check{\sigma}_1 = 1$ in (3.34) requires to distinguish two cases. Due to (A.52), up to $a = 1$, the minimum is found at $r = 1$, $\varphi = 0$ – where at $a = 1$, the minimum has reached zero. For $a > 1$, (A.51) has to be used, which allows to verify that for $\varphi = 0$, $\check{r}_2 = \frac{1}{a}$, the minimum remains at zero.

Note that additionally, from (3.32), (3.33), (A.6), and (A.57),

$$\sigma_1^2 \geq \begin{cases} 1 + a^2 - 2ar \cos(\varphi); & \text{for } a \neq 0 \text{ and } a > 2r \cos(\varphi) \\ 1; & \text{otherwise} \end{cases}, \quad (\text{A.58})$$

can be derived. Similarly,

$$\sigma_2^2 \leq \begin{cases} 1 + a^2 - 2ar \cos(\varphi); & \text{for } a < a < 2r \cos(\varphi) \\ 1; & \text{otherwise} \end{cases}. \quad (\text{A.59})$$

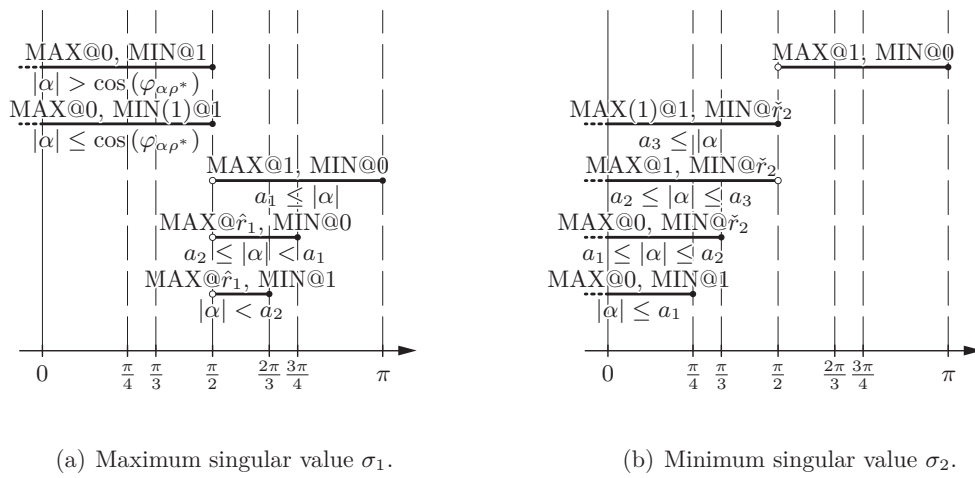


Figure A.1: This diagram abstractly describes the behaviour of the two non-unit singular values σ_1 and σ_2 , by summarising the results obtained in Appendix A.2. The ordinate does not carry any information. Each horizontal line indicates the interval of the complex argument φ , for which the corresponding configuration can occur. A filled circle at the line end indicates that the value of φ is included, an empty circle indicates an exclusion. The actual configuration is described on top of the horizontal line. The number or symbol following the character “@”, specifies the location of the minimum (MIN), respectively, the maximum (MAX), in terms of magnitude r . In two simple cases, the corresponding value of the singular value is also given in brackets. The valid range for magnitude a is found below the horizontal line. The behaviour is symmetric with respect to $\varphi = 0$, except from the fact that $\varphi = -\pi$ is not included since $\varphi \in (-\pi, \pi]$.

Appendix B

Complement to Section 3.5

This appendix provides the derivations that provide the basis for Section 3.5, and specifically, (3.92). For sake of brevity, the following substitutions are introduced (*suppressing iteration index k , $\mathbf{e}_{\tilde{\mathbf{w}}}$ is the unit vector that corresponds to $\tilde{\mathbf{w}}_{k-1}$*)

$$a_1 = |a_{\mathbf{u}}|, \quad a_2 = |b_{\mathbf{u}}|, \quad (\text{B.1})$$

$$\beta = \|\mathbf{D}\mathbf{e}_{\tilde{\mathbf{w}}}\|, \quad \gamma = \cos(\varphi_{a_{\mathbf{u}}b_{\mathbf{u}}}) \|\mathbf{D}^{1/2}\mathbf{e}_{\tilde{\mathbf{w}}}\|^2, \quad (\text{B.2})$$

and with the cosine between $\mathbf{e}_{\tilde{\mathbf{w}}}$ and $\mathbf{D}\mathbf{e}_{\tilde{\mathbf{w}}}$ denoted by $\cos(\Theta_{\mathbf{D}}(\mathbf{e}_{\tilde{\mathbf{w}}}))$ (cf. (3.83)),

$$v = \frac{\|\mathbf{D}^{1/2}\mathbf{e}_{\tilde{\mathbf{w}}}\|^2}{|\cos(\varphi_{a_{\mathbf{u}}b_{\mathbf{u}}})| \left[\|\mathbf{D}\mathbf{e}_{\tilde{\mathbf{w}}}\|^2 - \|\mathbf{D}^{1/2}\mathbf{e}_{\tilde{\mathbf{w}}}\|^4 \right]} = \frac{\cos(\Theta_{\mathbf{D}}(\mathbf{e}_{\tilde{\mathbf{w}}}))}{|\cos(\varphi_{a_{\mathbf{u}}b_{\mathbf{u}}})| \|\mathbf{D}\mathbf{e}_{\tilde{\mathbf{w}}}\| \sin^2(\Theta_{\mathbf{D}}(\mathbf{e}_{\tilde{\mathbf{w}}}))}. \quad (\text{B.3})$$

Then, (3.91) is equivalent to

$$f_{\Phi}(a_1, a_2) \triangleq a_1^2 + \beta^2 a_2^2 + 2\gamma a_1 a_2 = \mathbf{a}^{\top} \mathbf{A} \mathbf{a} = 1, \quad (\text{B.4})$$

with

$$a_1, a_2 \in \mathbb{R}, \quad \mathbf{a} \triangleq [a_1 \quad a_2]^{\top}, \quad \mathbf{A} \triangleq \begin{bmatrix} 1 & \gamma \\ \gamma & \beta^2 \end{bmatrix}, \quad \beta \in \mathbb{R}_+, \quad \gamma \in [-\beta, \beta]. \quad (\text{B.5})$$

B.1 Semi-Minors and Semi-Majors of the Ellipse

Equation (B.4) describes an ellipse in the $\langle a_1, a_2 \rangle$ -plane that is parametrised by β and γ . Accordingly, the lengths of its semi-minor and semi-major are given by the square-root of the reciprocal eigenvalues of matrix \mathbf{A} , i.e., $\frac{1}{\sqrt{\lambda_1(\mathbf{A})}}$, and $\frac{1}{\sqrt{\lambda_2(\mathbf{A})}}$, respectively. The latter eigenvalues are given by

$$\lambda_i(\mathbf{A}) = \frac{1 + \beta^2}{2} + (-1)^{i-1} \sqrt{\left(\frac{1 + \beta^2}{2}\right)^2 + \gamma^2 - \beta^2} = \frac{1 + \beta^2}{2} + (-1)^{i-1} \sqrt{\left(\frac{1 - \beta^2}{2}\right)^2 + \gamma^2}, \quad (\text{B.6})$$

with $i \in \{1, 2\}$. Since $\beta^2 - \gamma^2 \geq 0$, it follows that

$$0 \leq \left(\frac{1-\beta^2}{2}\right)^2 \leq \left(\frac{1+\beta^2}{2}\right)^2 + \gamma^2 - \beta^2 = \left(\frac{1-\beta^2}{2}\right)^2 + \gamma^2 \leq \left(\frac{1+\beta^2}{2}\right)^2, \quad (\text{B.7})$$

which in turn allows to state

$$0 \leq \lambda_2(\mathbf{A}) \leq \min\{1, \beta^2\} \leq 1 \leq \max\{1, \beta^2\} \leq \lambda_1(\mathbf{A}) \leq 1 + \beta^2. \quad (\text{B.8})$$

The corresponding eigenvectors evaluate to

$$\mathbf{q}_i(\mathbf{A}) = \frac{|\gamma|}{\sqrt{(1-\lambda_j(\mathbf{A}))^2 + \gamma^2}} \begin{bmatrix} \frac{1-\lambda_j(\mathbf{A})}{\gamma} & 1 \end{bmatrix}^\top, \quad (\text{B.9})$$

where $j = \{1, 2\} \setminus \{i\}$. Hence, for $\gamma > 0$, the semi-majors ($i = 2, j = 1$) fall into the second and fourth quadrant of the $\langle a_1, a_2 \rangle$ -plane, for $\gamma < 0$, they fall into the first and third quadrant. For the semi-minors the contrary applies. The acute angles, θ_1 and θ_2 , that the semi-axes enclose with the a_1 -axis are given by

$$\cos(\theta_i) = \frac{|1 - \lambda_j(\mathbf{A})|}{\sqrt{(1 - \lambda_j(\mathbf{A}))^2 + \gamma^2}} = \frac{|\gamma|}{\sqrt{(1 - \lambda_i(\mathbf{A}))^2 + \gamma^2}}. \quad (\text{B.10})$$

Thus,

$$\gamma \geq 0 \Rightarrow \theta_1 \in \left[0, \frac{\pi}{2}\right), \theta_2 \in \left[-\frac{\pi}{2}, 0\right), \quad \gamma < 0 \Rightarrow \theta_1 \in \left(-\frac{\pi}{2}, 0\right), \theta_2 \in \left(0, \frac{\pi}{2}\right), \quad (\text{B.11})$$

and

$$\sin(\theta_i) = -\frac{\text{sign}(\gamma)(1 - \lambda_i(\mathbf{A}))}{\sqrt{(1 - \lambda_i(\mathbf{A}))^2 + \gamma^2}} = \frac{\gamma(-1)^{i-1}}{\sqrt{(1 - \lambda_j(\mathbf{A}))^2 + \gamma^2}}. \quad (\text{B.12})$$

Moreover, it can be verified that

$$\tan(2\theta_i) = \frac{2\gamma}{1 - \beta^2}, \quad (\text{B.13})$$

and that $\tan(\theta_1) = -\cot(\theta_2)$.

B.2 Parametrisation of the Ellipse

Based on the results of Appendix B.1, it is straightforward to parametrise the elliptical arc in the first quadrant – which is the only valid one as $a_1 \geq 0, a_2 \geq 0$ – of the $\langle a_1, a_2 \rangle$ -plane, with angle $\vartheta \in [\vartheta_2, \vartheta_1 + \pi]$, according to

$$a_1 = \frac{\cos(\theta_1)}{\sqrt{\lambda_1(\mathbf{A})}} \cos(\vartheta) - \frac{\sin(\theta_1)}{\sqrt{\lambda_2(\mathbf{A})}} \sin(\vartheta) = \hat{a}_1 \sin(\vartheta - \vartheta_1), \quad (\text{B.14})$$

$$a_2 = \frac{\sin(\theta_1)}{\sqrt{\lambda_1(\mathbf{A})}} \cos(\vartheta) + \frac{\cos(\theta_1)}{\sqrt{\lambda_2(\mathbf{A})}} \sin(\vartheta) = \hat{a}_2 \sin(\vartheta - \vartheta_2), \quad (\text{B.15})$$

where

$$\hat{a}_i \triangleq \sqrt{\frac{\cos^2(\theta_i)}{\lambda_1(\mathbf{A})} + \frac{\sin^2(\theta_i)}{\lambda_2(\mathbf{A})}} \Rightarrow \hat{a}_1 = \beta \hat{a}_2 = \frac{\beta}{\sqrt{\lambda_1(\mathbf{A}) \lambda_2(\mathbf{A})}} = \frac{\beta}{\sqrt{\beta^2 - \gamma^2}}, \quad (\text{B.16})$$

$$\vartheta_1 \triangleq \arctan \left(\sqrt{\frac{\lambda_2(\mathbf{A})}{\lambda_1(\mathbf{A})}} \cot(\theta_1) \right), \quad (\text{B.17})$$

$$\vartheta_2 \triangleq \arctan \left(\sqrt{\frac{\lambda_2(\mathbf{A})}{\lambda_1(\mathbf{A})}} \cot(\theta_2) \right) + \begin{cases} \pi; & \gamma > 0 \\ 0; & \text{otherwise} \end{cases}. \quad (\text{B.18})$$

Moreover, without presenting the details of the derivation, for the difference

$$\vartheta_{12} \triangleq \vartheta_1 - \vartheta_2, \quad (\text{B.19})$$

it can be shown that

$$\cos(\vartheta_{12}) = -\frac{\gamma}{\beta}. \quad (\text{B.20})$$

B.3 Maximum of Product $a_1 a_2$

As a preparation for the in Appendix B.4 performed intersection of the ellipse with a hyperbola, here, the rectangle with side lengths a_1 and a_2 is sought that encloses the largest surface area $A_{\square, \max}(\beta, \gamma)$, i.e.,

$$A_{\square, \max}(\beta, \gamma) \triangleq \max_{\substack{a_1, a_2 \\ \text{s.t. (B.4)}}} \{A_{\square}(a_1, a_2)\}, \quad (\text{B.21})$$

with

$$A_{\square}(a_1, a_2) \triangleq a_1 a_2. \quad (\text{B.22})$$

Clearly, $A_{\square, \max}(\beta, \gamma)$ equivalently provides the minimum upper bound for the product $a_1 a_2$. Here, point $\langle a_1, a_2 \rangle$ that leads to $A_{\square, \max}(\beta, \gamma)$, is identified based on the fact that at this point, the tangent along the ellipse coincides with the tangent along the hyperbola, described by (B.22) with $A_{\square}(a_1, a_2)$ kept constant.

The partial derivatives of the implicitly defined functions in (B.4) and (B.22) are obtained as

$$\frac{\partial f_{\Phi}(a_1, a_2)}{\partial a_1} = \frac{\partial f_{\Phi}(a_1, a_2)}{\partial a_2} \frac{da_2}{da_1} = 2 \left[a_1 + \beta^2 a_2 \frac{da_2}{da_1} + \gamma \left(a_2 + a_1 \frac{da_2}{da_1} \right) \right], \quad (\text{B.23})$$

$$\frac{\partial A_{\square}(a_1, a_2)}{\partial a_1} = \frac{\partial A_{\square}(a_1, a_2)}{\partial a_2} \frac{da_2}{da_1} = a_2 + a_1 \frac{da_2}{da_1}. \quad (\text{B.24})$$

If (B.22) is maximised, the partial derivative in (B.24) has to evaluate to zero, i.e.,

$$\frac{\partial A_{\square}(a_1, a_2)}{\partial a_1} \stackrel{!}{=} 0 \Rightarrow \frac{da_2}{da_1} = -\frac{a_2}{a_1}. \quad (\text{B.25})$$

Hence, since the tangents of both graphs have to coincide,

$$\frac{\partial f_{\Phi}(a_1, a_2)}{\partial a_1} \stackrel{!}{=} 0 \Rightarrow \frac{da_2}{da_1} = -\frac{a_1 + \gamma a_2}{\gamma a_1 + \beta^2 a_2}, \quad (\text{B.26})$$

leading to

$$\frac{a_2}{a_1} \stackrel{!}{=} \frac{a_1 + \gamma a_2}{\gamma a_1 + \beta^2 a_2} \Rightarrow a_1 = \pm \beta a_2. \quad (\text{B.27})$$

Thus, in the $\langle a_1, a_2 \rangle$ -plane, the maximum is found along the two lines with slope $\pm \frac{1}{\beta}$, and

$$A_{\square, \max}(\beta, \gamma) = \beta a_2^2. \quad (\text{B.28})$$

Inserting the right-hand side of (B.27) in (B.4) gives

$$a_2^2 = \frac{1}{2\beta(\beta + \gamma)}, \quad (\text{B.29})$$

which finally provides the maximum surface area, exclusively in terms of β and γ ,

$$A_{\square, \max}(\beta, \gamma) = \frac{1}{2(\beta + \gamma)}. \quad (\text{B.30})$$

B.4 Intersecting the Ellipse with a Hyperbola

The bound (3.89) describes a hyperbola in the $\langle a_1, a_2 \rangle$ -plane, which is identical to

$$f_{\nabla}(a_1, a_2) \triangleq \frac{a_1 a_2}{v} = 1, \quad (\text{B.31})$$

with $v \neq 0$ given by (B.3). Based on the insights from Appendix B.3, it is clear that hyperbola $f_{\nabla}(a_1, a_2)$ in (B.31) intersects with ellipse f_{\ominus} in (B.4), iff

$$A_{\square, \max}(\beta, \gamma) \geq v \Rightarrow \frac{1}{2(\beta + \gamma)} \geq v, \quad (\text{B.32})$$

which is equivalent to bound (3.92).

Moreover, from (B.31), it follows with $i \in \{1, 2\}$, $j \in \{1, 2\} \setminus \{i\}$ that

$$a_i = \frac{v}{a_j}. \quad (\text{B.33})$$

Inserting (B.33) in (B.4), leads to

$$a_1^4 + a_1^2(2\gamma v - 1) + \beta^2 v^2 = 0, \quad (\text{B.34})$$

and

$$(\beta a_2)^4 + (\beta a_2)^2(2\gamma v - 1) + \beta^2 v^2 = 0. \quad (\text{B.35})$$

Accordingly,

$$a_1^2 = \beta^2 a_2^2 = \frac{1}{2} - \gamma v \pm \sqrt{\left(\frac{1}{2} - \gamma v\right)^2 - \beta^2 v^2}, \quad (\text{B.36})$$

where the argument of the square-root is non-negative iff (B.32) is satisfied. As the squares on the left-hand side of (B.36) have to be non-negative, the solution on the right-hand side has to be

non-negative as well. Hence, with $\beta \neq 0$ and $v \neq 0$, it is found that this entails

$$\gamma v < \frac{1}{2}. \quad (\text{B.37})$$

Finally, if Conditions (B.32) and (B.37) are satisfied, based on (B.31) and (B.36) the four intersection points are obtained by

$$\mathbf{a}^{(i)} = \left[a_+ \quad \frac{a_-}{\beta} \right]^T, \quad \mathbf{a}^{(ii)} = \left[a_- \quad \frac{a_+}{\beta} \right]^T, \quad \mathbf{a}^{(iii)} = \left[-a_+ \quad -\frac{a_-}{\beta} \right]^T, \quad \mathbf{a}^{(iv)} = \left[-a_- \quad -\frac{a_+}{\beta} \right]^T, \quad (\text{B.38})$$

with

$$a_+ \triangleq \sqrt{\frac{1}{2} - \gamma v + \sqrt{\left(\frac{1}{2} - \gamma v\right)^2 - \beta^2 v^2}}, \quad a_- \triangleq \sqrt{\frac{1}{2} - \gamma v - \sqrt{\left(\frac{1}{2} - \gamma v\right)^2 - \beta^2 v^2}}. \quad (\text{B.39})$$

The angles $\theta^{(i)}$ to $\theta^{(iv)}$, enclosed by the a_1 -axis and the four rays from the origin through those intersection points, can be calculated from

$$\tan(\theta^{(i)}) = \frac{a_2^{(i)}}{a_1^{(i)}} = \tan(\theta^{(iii)}) = \frac{a_2^{(iii)}}{a_1^{(iii)}} = \frac{|v|}{a_-^2}, \quad (\text{B.40})$$

$$\tan(\theta^{(ii)}) = \frac{a_2^{(ii)}}{a_1^{(ii)}} = \tan(\theta^{(iv)}) = \frac{a_2^{(iv)}}{a_1^{(iv)}} = \frac{|v|}{a_+^2}, \quad (\text{B.41})$$

and their difference obeys

$$\theta^{(i)} - \theta^{(ii)} = \theta^{(iii)} - \theta^{(iv)} = \arctan\left(\frac{\sqrt{\left(\frac{1}{v} - 2\gamma\right)^2 - 4\beta^2}}{1 + \beta^2}\right). \quad (\text{B.42})$$

Appendix C

Mathematical Supplement

This appendix briefly introduces some mathematical concepts and notions that are required in this thesis. Appendix C.1 presents basics about operator trigonometry and is specifically relevant for Sections 3.4.2 and 3.5. The M -matrices defined in Appendix C.2 are key to the solution of the system of linear difference equations in Section 4.2 and thus, fundamental for the ℓ_2 -stability analysis of the coupled structure in Section 4.4.1. Finally, Appendix C.3 provides some facts about submatrices, minors, and leading principal minors of a matrix. They are of special importance for the mapping analysis of the coupled structure in Section 4.5 that resorts to Section 4.3.

C.1 Operator Trigonometry

Operator trigonometry dates back to 1966 and is coined by Karl Gustafson [Gus00]. Originally, it was restricted to positive definite matrices. However, meanwhile it is extended to arbitrary invertible matrices [ibid.]. It is tightly related to the notion of antieigenvalues and antieigenvectors, which can be considered as the opposite of eigenvalues and eigenvectors. This becomes clear by comparing their definitions. While the eigenvectors are by definition [Definition 1.1.2 HJ13] the invariant directions attributed to a matrix¹ $\mathbf{A} \in \mathbb{C}^{M \times M}$, $\mathbf{A} > \mathbf{0}$, the antieigenvectors are the directions to which \mathbf{A} imposes the strongest angular change. Further insight is gained by comparing the maximum eigenvalue $\lambda_1(\mathbf{A})$ and the maximum antieigenvalue $\bar{\lambda}_1(\mathbf{A})$. The primer can be defined based on the Rayleigh quotient [Theorem 4.2.2 HJ13],

$$\lambda_1(\mathbf{A}) \triangleq \max_{\mathbf{x} \in \mathbb{C}^M \setminus \{0\}} \frac{\mathbf{x}^H \mathbf{A} \mathbf{x}}{\|\mathbf{x}\|^2}, \quad (\text{C.1})$$

the latter is defined as [Gus00]

$$\bar{\lambda}_1(\mathbf{A}) \triangleq \min_{\mathbf{x} \in \mathbb{C}^M \setminus \{0\}} \frac{\mathbf{x}^H \mathbf{A} \mathbf{x}}{\|\mathbf{x}\| \|\mathbf{A} \mathbf{x}\|}. \quad (\text{C.2})$$

The maximum antieigenvalue is found to coincide with the cosine of the largest (acute) angle that can occur between a vector $\mathbf{x} \neq \mathbf{0}$ and its image $\mathbf{A} \mathbf{x}$.

More generally, the antieigenvalues $\bar{\lambda}_i(\mathbf{A})$, $i \in \{1, \dots, \lfloor \frac{M}{2} \rfloor\}$ are defined as [Gus00; Rao05]

$$\bar{\lambda}_i(\mathbf{A}) \triangleq \min_{\mathbf{x} \perp \mathcal{S}_i} \frac{\mathbf{x}^H \mathbf{A} \mathbf{x}}{\|\mathbf{x}\| \|\mathbf{A} \mathbf{x}\|} = \frac{2\sqrt{\lambda_i(\mathbf{A}) \lambda_j(\mathbf{A})}}{\lambda_j(\mathbf{A}) + \lambda_i(\mathbf{A})}, \quad (\text{C.3})$$

¹ For simplicity reasons, here, only the case of positive definite non-derogatory matrices is considered, i.e., all eigenvalues are positive and unique. Details about the more general cases, i.e, matrices that posses non-positive or complex-valued eigenvalues, possibly with multiplicities higher than one, can be found in [Gus00].

where $j = M - i + 1$, and with the set of eigenvectors $\mathbf{q}_l(\mathbf{A})$, $l \in \{1, \dots, M\}$ of matrix \mathbf{A} , $\bar{\mathcal{S}}_i$ denote the spaces

$$\bar{\mathcal{S}}_i \triangleq \begin{cases} \emptyset; & i = 1 \\ \text{span} \{ \mathbf{q}_1(\mathbf{A}), \dots, \mathbf{q}_{i-1}(\mathbf{A}), \mathbf{q}_{j+1}(\mathbf{A}), \dots, \mathbf{q}_M(\mathbf{A}) \}; & \text{otherwise} \end{cases}. \quad (\text{C.4})$$

The corresponding pairs of antieigenvector $\bar{\mathbf{q}}_i(\mathbf{A}) \in \mathbb{C}^M$ are given by

$$\bar{\mathbf{q}}_i^\pm(\mathbf{A}) \triangleq \pm \sqrt{\frac{\lambda_j(\mathbf{A})}{\lambda_i(\mathbf{A}) + \lambda_j(\mathbf{A})}} \mathbf{q}_i(\mathbf{A}) + \sqrt{\frac{\lambda_i(\mathbf{A})}{\lambda_i(\mathbf{A}) + \lambda_j(\mathbf{A})}} \mathbf{q}_j(\mathbf{A}). \quad (\text{C.5})$$

An extension to derogatory positive definite matrices is found in [Gus00, Theorem 3.1].

A direct consequence of (C.3) is the so called Kantorovich inequality [GR97, pp. 50f.; Rao05],

$$1 \geq \frac{\mathbf{x}^H \mathbf{A} \mathbf{x}}{\|\mathbf{x}\| \|\mathbf{A} \mathbf{x}\|} \geq \frac{2\sqrt{\lambda_1(\mathbf{A}) \lambda_M(\mathbf{A})}}{\lambda_1(\mathbf{A}) + \lambda_M(\mathbf{A})} = \bar{\lambda}_1(\mathbf{A}). \quad (\text{C.6})$$

Finally, for two orthogonal vectors, $\mathbf{x}, \mathbf{z} \in \mathbb{R}^M$, $\mathbf{x} \perp \mathbf{z}$, the Wielandt inequality states the following bound [Rao05]

$$\frac{(\mathbf{x}^T \mathbf{A} \mathbf{z})^2}{(\mathbf{x}^T \mathbf{A} \mathbf{x})(\mathbf{z}^T \mathbf{A} \mathbf{z})} \leq \frac{\lambda_1(\mathbf{A}) - \lambda_M(\mathbf{A})}{\lambda_1(\mathbf{A}) + \lambda_M(\mathbf{A})} = 1 - \bar{\lambda}_1^2(\mathbf{A}) \leq 1. \quad (\text{C.7})$$

C.2 M -Matrices

In this appendix, some facts and properties of the class of M -matrices² are summarised. Detailed information can be found in [FP62], where M -matrices in general, and non-singular M -matrices, are referred to by the terms “matrix of class \mathbf{K}_0 ”, and “matrix of class \mathbf{K} ”, respectively. Moreover, [BP79] and [HJ99, pp. 112ff.] treat this topic elaborately. A brief introduction can be found, e.g., in [Moy77]. Below, the scalars, vectors and matrices are all assumed to be real-valued.

Definition C.1: M -Matrices [BP79, p. 133]

Any matrix \mathbf{A} of the form³

$$\mathbf{A} \triangleq s\mathbf{I} - \mathbf{C}, \quad s > 0, \quad \mathbf{C} \succcurlyeq \mathbf{0}, \quad (\text{C.8})$$

for which $s \geq S(\mathbf{C})$, is called an M -matrix.

Such matrices have some remarkable properties, of which a few are presented below. The following conditions are equivalent to the fact that \mathbf{A} is a non-singular M -matrix:

1. \mathbf{A} is given by (C.8) and $s > S(\mathbf{C})$,
2. each real eigenvalue is positive,
3. all leading principal minors (cf. Appendix C.3) of \mathbf{A} are positive,

² According to [HV83] M -matrices are a generalisation of Minkowski matrices [Won53].

³ The order relation “ \succcurlyeq ” is understood elementwise. $S(\mathbf{C})$ denotes the spectral radius of matrix \mathbf{C} .

4. all principal minors (cf. Appendix C.3) of \mathbf{A} are positive,
5. \mathbf{A} is a monotone matrix, i.e., $\mathbf{A}\mathbf{x} \succcurlyeq \mathbf{0} \Rightarrow \mathbf{x} \succcurlyeq \mathbf{0}$,
6. \mathbf{A} is a positive stable matrix, i.e., the real part of all eigenvalues is positive,
7. the inverse of \mathbf{A} has no negative entries, i.e., it is a non-negative matrix,
8. for each $\mathbf{y} \succcurlyeq \mathbf{0}$, the set $\{\mathbf{x} \succcurlyeq \mathbf{0} | \mathbf{A}\mathbf{x} \preccurlyeq \mathbf{y}\}$ is bounded, and \mathbf{A} is non-singular.

Moreover, note that for a positive (definite) diagonal matrix \mathbf{D} and an M -matrix \mathbf{A} , the products $\mathbf{D}\mathbf{A}$ and $\mathbf{A}\mathbf{D}$ are again M -matrices.

C.3 Submatrices and Minors

Definition C.2: Submatrices and Minors [HJ13, Section 0.7]

Let $\mathbf{A} \in \mathbb{C}^{M \times N}$ be an arbitrary matrix. Then $\mathbf{A}' \in \mathbb{C}^{M' \times N'}$, with $M' \leq M$ and $N' \leq N$, is called a submatrix of \mathbf{A} , if it is obtained by deleting a certain number of rows and/or columns of \mathbf{A} . If specifically, with deletion of the i^{th} row, with $i \in \{1, \dots, \min\{M, N\}\}$ also column i is deleted, then, the resulting matrix is called a principal submatrix. If \mathbf{A} is additionally square, i.e., $M = N$, and \mathbf{A}' contains all rows and columns of \mathbf{A} up to, or starting from, a certain index $\hat{i} \leq M$, matrix \mathbf{A}' is called a leading, or a trailing, principal minor of \mathbf{A} , respectively.

If \mathbf{A}' is a submatrix of \mathbf{A} , determinant $\det(\mathbf{A}')$ is called a minor of \mathbf{A} . Analogously, $\det(\mathbf{A}')$ is called a principal minor, a leading principal minor, or a trailing principal minor of \mathbf{A} , if \mathbf{A}' is a principal submatrix, a leading, or a trailing principal submatrix of \mathbf{A} , respectively.

According to [HJ99, Corollary 3.1.3], if $r \in \mathbb{N}_0$ is the number of deleted rows and columns. Then, the singular values $\sigma_i(\mathbf{A})$ of \mathbf{A} are interlaced by the singular values $\sigma_{i'}(\mathbf{A}')$ of \mathbf{A}' , in the following sense

$$\sigma_j(\mathbf{A}) \geq \sigma_j(\mathbf{A}') \geq \sigma_{j+r}(\mathbf{A}), \quad j \in \{1, \dots, \min\{M, N\}\}, \quad (\text{C.9})$$

where the singular values of each matrix are assumed to be sorted in descending order, i.e., $\sigma_i(\mathbf{A}) \geq \sigma_j(\mathbf{A})$, for $i \geq j$, and $\sigma_{i'}(\mathbf{A}') \geq \sigma_{j'}(\mathbf{A}')$, for $i' \geq j'$. Moreover, all singular values $\sigma_i(\mathbf{A}) \equiv 0$, for any $i > \min\{M, N\}$, and $\sigma_{i'}(\mathbf{A}') \equiv 0$, for any $i' > \min\{M', N'\}$.

Appendix D

Proofs

In several of the following proofs, iteration index k is suppressed. They are marked by a grey bar in the outer page margin. Underlined symbols refer to a priori entities, e.g., $\underline{\tilde{\mathbf{w}}}$ is equivalent to $\tilde{\mathbf{w}}_{k-1}$, and $\underline{\tilde{w}}_i$ corresponds to $\tilde{w}_i(k-1)$.

D.1 Proofs for Chapter 3

D.1.1 Proof of Lemma 3.4

The proof uses the fact that (3.41) is always satisfied if its right-hand side is negative. Two cases have to be considered:

1. $\mathbf{u} \nparallel \mathbf{x}$ and $\rho \neq 0$: Let the regression vector and the parameter error vector be decomposed as

$$\mathbf{e}_x = \rho \left(\mathbf{e}_u + x_u^\perp \mathbf{e}_u^\perp \right), \quad \text{with } x_u^\perp \in \left\{ z \in \mathbb{C} \mid |z| = \sqrt{|\rho|^{-2} - 1} \right\}, \quad (\text{D.1})$$

$$\underline{\tilde{\mathbf{w}}} = w_u \mathbf{e}_u^* + w_u^\perp \mathbf{e}_u^{\perp*} + w_{u,x}^\perp \mathbf{e}_{u,x}^\perp, \quad \text{with } w_u, w_u^\perp, w_{u,x}^\perp \in \mathbb{C}, \quad (\text{D.2})$$

where \mathbf{e}_u , \mathbf{e}_u^\perp , and $\mathbf{e}_{u,x}^\perp$ are mutually orthogonal, and $w_u \neq 0$ since (3.39) is satisfied. Then,

$$2\text{Re} \left\{ \alpha \left(\underline{\tilde{\mathbf{w}}}^\top \mathbf{e}_u \right) \left(\underline{\tilde{\mathbf{w}}}^\top \mathbf{e}_x \right)^* \right\} = 2|\alpha| |\rho| \text{Re} \left\{ e^{j\varphi_{\alpha\rho^*}} \left(1 + x_u^\perp \frac{w_u^\perp}{w_u} \right)^* \right\} \quad (\text{D.3})$$

can always become negative as $\text{arc}(x_u^\perp) \in (-\pi, \pi]$ and $|x_u^\perp| \in \mathbb{R}_{0+}$.

2. $\mathbf{u} \nparallel \mathbf{x}$ and $\rho = 0$, i.e., $\mathbf{u} \perp \mathbf{x}$: In this case, (D.1) is unnecessary, and in (D.2), $\mathbf{e}_u^\perp = \mathbf{e}_x$, thus,

$$2\text{Re} \left\{ \alpha \left(\underline{\tilde{\mathbf{w}}}^\top \mathbf{e}_u \right) \left(\underline{\tilde{\mathbf{w}}}^\top \mathbf{e}_x \right)^* \right\} = 2|\alpha| \text{Re} \left\{ e^{j(\text{arc}(\alpha))} w_u w_u^{\perp*} \right\}, \quad (\text{D.4})$$

where the complex argument of w_u^\perp is determined by the choice of \mathbf{e}_x . As the latter is assumed to be unconstrained, it can always be chosen such that (D.4) is negative.

D.1.2 Proof of Lemma 3.5

Erratum 14 For the first part of Lemma 3.5, consider

$$\left| \tilde{\mathbf{w}}^H \mathbf{e}_u^* \right|^2 = \left| \tilde{\mathbf{w}}^H (\mathbf{I} - \alpha^* \mathbf{e}_u^* \mathbf{e}_x^T) \mathbf{e}_u^* \right|^2 = \left| \tilde{\mathbf{w}}^H \mathbf{e}_u^* \right|^2 |1 - \alpha^* \rho|^2 = 1 + |\alpha \rho|^2 - 2 |\alpha \rho| \cos(\varphi_{\alpha \rho^*}), \quad (\text{D.5})$$

which by inserting $|\alpha \rho| \leq 2 \cos(\varphi_{\alpha \rho^*})$ from (3.15), leads to $|\tilde{\mathbf{w}}^H \mathbf{e}_u^*|^2 \leq |\tilde{\mathbf{w}}^H \mathbf{e}_u^*|$. Since furthermore $\|\tilde{\mathbf{w}}\|^2 > \|\tilde{\mathbf{w}}\|^2$ due to (3.42), it follows that the acute angle¹ enclosed by $\tilde{\mathbf{w}}$ and \mathbf{u} is larger than the acute angle between $\tilde{\mathbf{w}}$ and \mathbf{u} .

For the second part, first it is assumed that $\tilde{\mathbf{w}}^T \mathbf{e}_x \neq 0$, with Lemma 3.1 the following holds

$$\begin{aligned} \left| \tilde{\mathbf{w}}^H \mathbf{e}_x^* \right|^2 &= \left| \tilde{\mathbf{w}}^H (\mathbf{I} - \alpha^* \mathbf{e}_u^* \mathbf{e}_x^T) \mathbf{e}_x^* \right|^2 = \left| \tilde{\mathbf{w}}^H \mathbf{e}_x^* \right|^2 \left| 1 - \left(\frac{\alpha \tilde{\mathbf{w}}^T \mathbf{e}_u}{\tilde{\mathbf{w}}^T \mathbf{e}_x} \right)^* \right|^2 \\ &= \left| \tilde{\mathbf{w}}^H \mathbf{e}_x^* \right|^2 \left[1 + \left| \frac{\alpha \tilde{\mathbf{w}}^T \mathbf{e}_u}{\tilde{\mathbf{w}}^T \mathbf{e}_x} \right|^2 \left(1 - 2 \operatorname{Re} \left\{ \frac{\tilde{\mathbf{w}}^T \mathbf{e}_x}{\alpha \tilde{\mathbf{w}}^T \mathbf{e}_u} \right\} \right) \right] \geq \left| \tilde{\mathbf{w}}^H \mathbf{e}_x^* \right|^2. \end{aligned} \quad (\text{D.6})$$

The fact that $\|\tilde{\mathbf{w}}\|^2 > \|\tilde{\mathbf{w}}\|^2$, together with (D.6), yields the second statement of Lemma 3.5. To complete the proof, for the before excluded case $\tilde{\mathbf{w}}^T \mathbf{e}_x = 0$, from the first line of (D.6) and from (3.39), which is implied by (3.42), it directly follows that $|\tilde{\mathbf{w}}^H \mathbf{e}_x^*|^2 = |\alpha|^2 |\tilde{\mathbf{w}}^H \mathbf{e}_u^*|^2 > 0 = |\tilde{\mathbf{w}}^H \mathbf{e}_x^*|^2$.

D.1.3 Proof of Lemma 3.6

Condition $|\rho| = 1$ is equivalent to $\mathbf{e}_x^T \mathbf{e}_u^* = \exp(j \operatorname{arc}(\rho))$. Thus, $\mathbf{e}_x = \exp(j \operatorname{arc}(\rho)) \mathbf{e}_u$, which causes the violation of the condition for expanding w.c. behaviour (3.42), since

$$\operatorname{Re} \left\{ \frac{\tilde{\mathbf{w}}^T \mathbf{e}_x}{\alpha \tilde{\mathbf{w}}^T \mathbf{e}_u} \right\} = \operatorname{Re} \left\{ e^{-j \varphi_{\alpha \rho^*}} \frac{\tilde{\mathbf{w}}^T \mathbf{e}_u}{|\alpha| \tilde{\mathbf{w}}^T \mathbf{e}_u} \right\} = \frac{\cos(\varphi_{\alpha \rho^*})}{|\alpha|} \geq \frac{1}{2}, \quad (\text{D.7})$$

where the order relation on the right-hand side is a consequence of the step-size bound (3.15), which due to $|\rho| = 1$, results in $|\alpha| \leq 2 \cos(\varphi_{\alpha \rho^*})$.

¹ Note that in the proof of Lemma 3.5, arguments regarding the angle between two complex-valued vectors are derived, based on the magnitude of their inner product. This is not the only way, an angle between two vectors in the multidimensional complex-valued space can be defined. An alternative definition replaces the magnitude by the real-part. Both of these definitions have their justification. The latter preserves validity of the law of cosines in Euclidean geometry. However, e.g., for the inner product of some (non-zero) vector with the same vector multiplied by j , it returns zero, i.e., an angle of $\pm \frac{\pi}{2}$. From the purely geometric point of view adopted in that proof, an arbitrary non-zero multiple of a vector does not change the line of its direction. Hence, multiplying the operands of an inner product by a (complex-valued non-zero) factor should *not* change its result. Especially, the angle between a vector and the same vector multiplied by a non-zero scalar should in any case evaluate to zero. This is the reason why here, the definition based on the magnitude is chosen, as it satisfies these geometric requirements [Sch01; RKS10; LS12].

D.1.4 Proof of Lemma 3.8

Let

$$\mathbf{\Lambda}_{|\lambda|} \triangleq \text{diag} \{ |\lambda_i(\mathbf{M})| \}_{i=1}^M, \quad \mathbf{\Lambda}_{\text{arc}(\lambda)} \triangleq \text{diag} \{ \exp(j \text{arc}(\lambda_i(\mathbf{M}))) \}_{i=1}^M. \quad (\text{D.8})$$

Contemplate two cases, (A) a positive semi-definite diagonal step-size matrix $\mathbf{\Lambda}_{\mathbf{M},\text{A}} = \mathbf{\Lambda}_{|\lambda|}$, and (B) a general diagonal step-size matrix $\mathbf{\Lambda}_{\mathbf{M},\text{B}} = \mathbf{\Lambda}_{|\lambda|} \mathbf{\Lambda}_{\text{arc}(\lambda)}$ with complex entries that have the same magnitudes as in Case A. First, notice that the effective step-size α defined in (3.11) is identical in both cases. Furthermore, using (3.12), the corresponding correlation coefficients are given by

$$\rho_{\text{A}} = \frac{\mathbf{u}^{\text{T}} \mathbf{\Lambda}_{|\lambda|} \mathbf{u}^*}{\|\mathbf{u}\| \|\mathbf{\Lambda}_{|\lambda|} \mathbf{u}\|} \in \mathbb{R}_{0+}, \quad \rho_{\text{B}} = \frac{\mathbf{u}^{\text{T}} \mathbf{\Lambda}_{|\lambda|} \mathbf{\Lambda}_{\text{arc}(\lambda)}^* \mathbf{u}^*}{\|\mathbf{u}\| \|\mathbf{\Lambda}_{|\lambda|} \mathbf{u}\|} \in \mathbb{C}. \quad (\text{D.9})$$

Since $\mu \in \mathbb{R}_{0+}$ and $\rho_{\text{A}} \in \mathbb{R}_{0+}$, the squared maximum singular values are obtained from (3.22) as

$$\begin{aligned} \sigma_{\text{max},\text{A}}^2 &= 1 + \frac{\alpha^2}{2} - \alpha \rho_{\text{A}} + \sqrt{\left(\frac{\alpha^2}{2} - \alpha \rho_{\text{A}}\right)^2 + \alpha^2 (1 - \rho_{\text{A}}^2)}, \\ \sigma_{\text{max},\text{B}}^2 &= 1 + \frac{\alpha^2}{2} - \alpha \text{Re}\{\rho_{\text{B}}\} + \sqrt{\left(\frac{\alpha^2}{2} - \alpha \text{Re}\{\rho_{\text{B}}\}\right)^2 + \alpha^2 (1 - |\rho_{\text{B}}|^2)}, \end{aligned} \quad (\text{D.10})$$

which leads to

$$\sigma_{\text{max},\text{A}}^2 - \sigma_{\text{max},\text{B}}^2 = \alpha \left(\text{Re}\{\rho_{\text{B}}\} - \rho_{\text{A}} + \sqrt{\frac{\alpha^2}{4} - \alpha \rho_{\text{A}} + 1} - \sqrt{\frac{\alpha^2}{4} - \alpha \text{Re}\{\rho_{\text{B}}\} - \text{Im}^2\{\rho_{\text{B}}\} + 1} \right). \quad (\text{D.11})$$

From (D.9), it follows that

$$-2\rho_{\text{A}} \leq \text{Re}\{\rho_{\text{B}}\} - \rho_{\text{A}} = \frac{\sum_{i=1}^M |\lambda_i(\mathbf{M})| |u_i|^2 [\cos(\text{arc}(\lambda_i(\mathbf{M}))) - 1]}{\|\mathbf{u}\| \|\mathbf{\Lambda}_{|\lambda|} \mathbf{u}\|} \leq 0, \quad (\text{D.12})$$

which together with the fact that the difference of the two square-roots in (D.11) is never larger than zero (with identity at $\rho_{\text{B}} = \rho_{\text{A}}$), allows to conclude that $\sigma_{\text{max},\text{A}}^2 \leq \sigma_{\text{max},\text{B}}^2$. The transition from a diagonal step-size matrix to a normal step-size matrix is established by Lemma 3.7. The proof for the minimum singular values is analogous and not presented here.

Erratum 15

D.1.5 Proof of Lemma 3.9

Let $\lambda_i(\mathbf{A})$ and $\mathbf{q}_{\mathbf{A},i}$, $i \in \{1, \dots, M\}$, be the eigenvalues and the eigenvectors, respectively, of some normal matrix $\mathbf{A} \in \mathbb{C}^{M \times M}$. Let further $\mathcal{M}(\lambda_i(\mathbf{A})) \subseteq \{1, \dots, M\}$ denote the set of all indices for which $i, j \in \mathcal{M}(\lambda_i(\mathbf{A})) \Rightarrow \lambda_i(\mathbf{A}) = \lambda_j(\mathbf{A})$. Then, all $\lambda_j(\mathbf{A})$, with $j \in \mathcal{M}(\lambda_i(\mathbf{A}))$, correspond to one eigenvalue of \mathbf{A} with (geometric and algebraic) multiplicity $|\mathcal{M}(\lambda_i(\mathbf{A}))|$, and eigenspace $\mathcal{E}(\lambda_i(\mathbf{A}))$ spanned by $\mathbf{q}_{\mathbf{A},j}$. For some non-zero vector \mathbf{x} and the $(M \times |\mathcal{M}(\lambda_i(\mathbf{A}))|)$

matrix

$$\mathbf{Q}_{\lambda_i(\mathbf{A})} \triangleq \underset{j \in \mathcal{M}(\lambda_i(\mathbf{A}))}{\text{row}} \{ \mathbf{q}_{\mathbf{A},j} \}, \quad (\text{D.13})$$

the component of \mathbf{Ax} inside $\mathcal{E}(\lambda_i(\mathbf{A}))$, and its corresponding norm, are given by

$$\mathbf{Q}_{\lambda_i(\mathbf{A})}^H \mathbf{Ax} = \lambda_i(\mathbf{A}) \mathbf{Q}_{\lambda_i(\mathbf{A})}^H \mathbf{x}, \quad \text{respectively,} \quad \left\| \mathbf{Q}_{\lambda_i(\mathbf{A})}^H \mathbf{Ax} \right\| = |\lambda_i(\mathbf{A})| \left\| \mathbf{Q}_{\lambda_i(\mathbf{A})}^H \mathbf{x} \right\|. \quad (\text{D.14})$$

Thus, the relative increase imposed by the mapping \mathbf{Ax} to the component of \mathbf{x} inside $\mathcal{E}(\lambda_i(\mathbf{A}))$ is

$$\frac{\left\| \mathbf{Q}_{\lambda_i(\mathbf{A})}^H \mathbf{Ax} \right\| - \left\| \mathbf{Q}_{\lambda_i(\mathbf{A})}^H \mathbf{x} \right\|}{\left\| \mathbf{Q}_{\lambda_i(\mathbf{A})}^H \mathbf{x} \right\|} = |\lambda_i(\mathbf{A})| - 1.$$

D.1.6 Proof of Lemma 3.12

The update of i^{th} element \tilde{w}_i of parameter error vector $\tilde{\mathbf{w}}$ is given by

$$\tilde{w}_i = \tilde{w}_i - \alpha \frac{d_i e_{\mathbf{u},i}^*}{\|\mathbf{D}^* \mathbf{e}_{\mathbf{u}}\|} \mathbf{e}_{\mathbf{u}}^T \tilde{\mathbf{w}}. \quad (\text{D.15})$$

Thus, with a positive definite step-size matrix \mathbf{D} , i.e., $d_i \in \mathbb{R}_+$, the difference of the squared magnitudes is obtained as

$$|\tilde{w}_i|^2 - |\underline{\tilde{w}}_i|^2 = \frac{d_i}{\|\mathbf{D} \mathbf{e}_{\mathbf{u}}\|} \left[|\alpha|^2 \frac{d_i |e_{\mathbf{u},i}|^2}{\|\mathbf{D} \mathbf{e}_{\mathbf{u}}\|} |\mathbf{e}_{\mathbf{u}}^T \tilde{\mathbf{w}}|^2 - 2 \text{Re} \{ \alpha e_{\mathbf{u},i}^* \tilde{w}_i^* \mathbf{e}_{\mathbf{u}}^T \tilde{\mathbf{w}} \} \right]. \quad (\text{D.16})$$

If $|\tilde{w}_i| > |\underline{\tilde{w}}_i|$ should hold for all $i \in \{1, \dots, M\}$, it follows from (D.16) that

$$|\alpha|^2 \frac{d_i |e_{\mathbf{u},i}|^2}{\|\mathbf{D} \mathbf{e}_{\mathbf{u}}\|} |\mathbf{e}_{\mathbf{u}}^T \tilde{\mathbf{w}}|^2 > 2 \text{Re} \{ \alpha e_{\mathbf{u},i}^* \tilde{w}_i^* \mathbf{e}_{\mathbf{u}}^T \tilde{\mathbf{w}} \}, \quad \forall i \in \{1, \dots, M\}. \quad (\text{D.17})$$

Summing (D.17) up on both sides, from $i = 1$ to $i = M$, preserves the order relation and leads to

$$|\alpha|^2 \rho |\mathbf{e}_{\mathbf{u}}^T \tilde{\mathbf{w}}|^2 > 2 |\mathbf{e}_{\mathbf{u}}^T \tilde{\mathbf{w}}|^2 \text{Re} \{ \alpha \}, \quad (\text{D.18})$$

where the order of summation and real-part operation has been exchanged. Moreover, due to $\mathbf{D} > 0 \Rightarrow \rho \in (0, 1]$, the identities

$$\sum_{i=1}^M \frac{d_i |e_{\mathbf{u},i}|^2}{\|\mathbf{D} \mathbf{e}_{\mathbf{u}}\|} = |\rho| = \rho, \quad \text{and} \quad \sum_{i=1}^M e_{\mathbf{u},i}^* \tilde{w}_i^* = (\mathbf{e}_{\mathbf{u}}^T \tilde{\mathbf{w}})^*, \quad (\text{D.19})$$

have been inserted. Under Assumption 3.1, (D.18) entails $|\alpha| \rho > 2 \cos(\arccos(\alpha))$, which clearly contradicts to (3.15), as $\arccos(\alpha \rho^*) = \arccos(\alpha)$. Thus, (D.17) cannot hold for all i , yielding (3.68).

D.1.7 Proof of Lemma 3.13

Let $\mathcal{M}(d_i) \subseteq \{1, \dots, M\}$ denote the set of indices that address the unit vectors which belong to eigenspace $\mathcal{E}(d_i)$. Since $\tilde{\mathbf{w}} \in \mathcal{E}(d_i)$, for a component \tilde{w}_j that is not contained in $\mathcal{E}(d_i)$, i.e., $j \notin \mathcal{M}(d_i)$, $\tilde{w}_j = 0$, and (D.16) becomes

$$|\tilde{w}_j|^2 - |\tilde{w}_j|^2 = |\tilde{w}_j|^2 = \left[|\alpha| \frac{d_j |e_{\mathbf{u},j}|}{\|\mathbf{D}\mathbf{e}_{\mathbf{u}}\|} |\mathbf{e}_{\mathbf{u}}^{\top} \tilde{\mathbf{w}}| \right]^2 \geq 0. \quad (\text{D.20})$$

For the remaining components \tilde{w}_j , summing up (D.16) on both sides over all $j \in \mathcal{M}(d_i)$, with

$$\sum_{j \in \mathcal{M}(d_i)} \frac{d_j |e_{\mathbf{u},j}|^2}{\|\mathbf{D}\mathbf{e}_{\mathbf{u}}\|} = |\rho| = \rho, \quad \text{and} \quad \sum_{j \in \mathcal{M}(d_i)} e_{\mathbf{u},j}^* \tilde{w}_j^* = (\mathbf{e}_{\mathbf{u}}^{\top} \tilde{\mathbf{w}})^*, \quad (\text{D.21})$$

gives with Assumption 3.1

$$\sum_{j \in \mathcal{M}(d_i)} \left(|\tilde{w}_j|^2 - |\tilde{w}_j|^2 \right) = \frac{d_i |\alpha|}{\|\mathbf{D}\mathbf{e}_{\mathbf{u}}\|} |\mathbf{e}_{\mathbf{u}}^{\top} \tilde{\mathbf{w}}|^2 [|\alpha| \rho - 2 \cos(\arccos(\alpha))] \leq 0, \quad (\text{D.22})$$

where the upper bound is reached with $\mathbf{D} > 0 \Rightarrow \rho \in (0, 1]$, if α and ρ achieve the limit of step-size condition (3.15).

D.1.8 Proof of Lemma 3.14

For $\tilde{\mathbf{w}} \in \mathcal{E}(d_i)$, with $\mathbf{D} > 0 \Rightarrow \rho \in (0, 1]$, (3.41) gives

$$W = |\alpha| |\tilde{\mathbf{w}}^{\top} \mathbf{e}_{\mathbf{u}}|^2 \left[|\alpha| - \frac{2d_i \cos(\arccos(\alpha))}{\|\mathbf{D}\mathbf{e}_{\mathbf{u}}\|} \right] = \frac{2\text{Re}\{\alpha\}}{\rho} |\tilde{\mathbf{w}}^{\top} \mathbf{e}_{\mathbf{u}}|^2 \left[\frac{|\alpha| \rho}{2 \cos(\arccos(\alpha))} - \frac{d_i \rho}{\|\mathbf{D}\mathbf{e}_{\mathbf{u}}\|} \right] \quad (\text{D.23})$$

In order to ensure the existence of a vector $\mathbf{e}_{\mathbf{u}}$ such that $W > 0$, this leads to the condition (indicated by the exclamation mark)

$$1 \underset{(3.15)}{\geq} \frac{|\alpha| \rho}{2 \cos(\arccos(\alpha))} \underset{(3.41)}{!} \frac{d_i \rho}{\|\mathbf{D}\mathbf{e}_{\mathbf{u}}\|} = d_i \frac{\mathbf{e}_{\mathbf{u}}^{\top} \mathbf{D} \mathbf{e}_{\mathbf{u}}^*}{\mathbf{e}_{\mathbf{u}}^{\top} \mathbf{D}^2 \mathbf{e}_{\mathbf{u}}^*} = d_i \underbrace{\frac{(\mathbf{D}\mathbf{u})^{\top} \mathbf{D}^{-1} (\mathbf{D}\mathbf{u})^*}{(\mathbf{D}\mathbf{u})^{\top} (\mathbf{D}\mathbf{u})^*}}_{\text{Rayleigh quotient}} \geq \frac{d_i}{d_{\max}}, \quad (\text{D.24})$$

where the lower bound on the right-hand side directly follows from the properties of the Rayleigh quotient (cf. (C.1)). For a given step-size α , the left-hand side of (D.24) assumes its maximum for $\rho = 1$, i.e., if $\mathbf{e}_{\mathbf{u}}$ is completely contained in one of the eigenspaces of step-size matrix \mathbf{D} . Especially, if this eigenspace corresponds to d_{\max} , the Rayleigh quotient on the right-hand side reaches its minimum. Therefore, (3.70) is necessary and sufficient in order to guarantee the existence of at least one excitation vector that causes the parameter error distance to increase. For $d_i = d_{\max}$, the right-hand side of (D.24) becomes one. In this case, due to step-size condition (3.15), no solving α can be found.

D.1.9 Proof of Lemma 3.15

If the pair of coefficients $\langle a_{\mathbf{u}}, b_{\mathbf{u}} \rangle$ satisfies (3.88), (3.92) ensures the existence of at least one excitation vector that satisfies (3.82), which in turn is sufficient for $W > 0$. Thus, in order to prove Lemma 3.15, it is only necessary to show that (3.92) can always be fulfilled as long as $\tilde{\mathbf{w}}$ is not completely contained in one single eigenspace of step-size matrix \mathbf{D} . It is easy to see from (3.83) and can also be verified in [Gus95; GR97; Gus00] that the latter requirement ensures $\cos(\Theta_{\mathbf{D}}(\mathbf{e}_{\tilde{\mathbf{w}}})) < 1$ from (3.83), as then $\tilde{\mathbf{w}} \not\parallel \mathbf{D}\tilde{\mathbf{w}}$, or equivalently in terms of the unit vectors, $\mathbf{e}_{\tilde{\mathbf{w}}} \not\parallel \mathbf{D}\mathbf{e}_{\tilde{\mathbf{w}}}$. This entails the right-hand side of (3.92) to be strictly less than one. Consequently, as for $\varphi_{a_{\mathbf{u}}b_{\mathbf{u}}} = \pi$ the left-hand side equals one and thus satisfies (3.92), for $\mathbf{e}_{\tilde{\mathbf{w}}} \not\parallel \mathbf{D}\mathbf{e}_{\tilde{\mathbf{w}}}$, e.g., using decomposition (3.77), it is always possible to find an $\mathbf{e}_{\mathbf{u}}$ such that $W > 0$.

D.2 Proofs for Chapter 4

D.2.1 Proof of Lemma 4.1

Since both matrices \mathbf{C} and \mathbf{C}' have the same symmetric partitioning, both of them can be represented via the Kronecker product using (4.23), where the selection matrices are identical. Let \mathbf{S} denote this common selection matrix, then,

$$(\mathbf{A} \boxtimes \mathbf{C})(\mathbf{A}' \boxtimes \mathbf{C}')^{\text{H}} = \mathbf{S}^{\text{T}} (\mathbf{A} \otimes \mathbf{C}) \mathbf{S} \mathbf{S}^{\text{T}} (\mathbf{A}'^{\text{H}} \otimes \mathbf{C}'^{\text{H}}) \mathbf{S} \quad (\text{D.25})$$

$$= \mathbf{S}^{\text{T}} \prod_{i=1}^I \left\{ \mathbf{a}_i \otimes \mathbf{C} \right\} \mathbf{S} \mathbf{S}^{\text{T}} \prod_{i=1}^I \left\{ \mathbf{a}_i'^{\text{H}} \otimes \mathbf{C}'^{\text{H}} \right\} \mathbf{S}. \quad (\text{D.26})$$

The matrix $\mathbf{S} \mathbf{S}^{\text{T}}$ in the middle of the above line is given by (4.26). It deletes columns of the matrix to the left and analogously rows in the matrix to the right. Taking this into account, gives

$$(\mathbf{A} \boxtimes \mathbf{C})(\mathbf{A}' \boxtimes \mathbf{C}')^{\text{H}} = \mathbf{S}^{\text{T}} \prod_{i=1}^I \left\{ \mathbf{a}_i \otimes \text{col}_{j=1}^I \left\{ \mathbf{C}_{ji} \right\} \right\} \prod_{i=1}^I \left\{ \mathbf{a}_i'^{\text{H}} \otimes \text{row}_{j=1}^I \left\{ \mathbf{C}_{ji}'^{\text{H}} \right\} \right\} \mathbf{S} \quad (\text{D.27})$$

$$= \mathbf{S}^{\text{T}} \sum_{i=1}^I \left(\mathbf{a}_i \otimes \text{col}_{j=1}^I \left\{ \mathbf{C}_{ji} \right\} \right) \left(\mathbf{a}_i'^{\text{H}} \otimes \text{row}_{j=1}^I \left\{ \mathbf{C}_{ji}'^{\text{H}} \right\} \right) \mathbf{S} \quad (\text{D.28})$$

$$= \mathbf{S}^{\text{T}} \sum_{i=1}^I \left(\mathbf{a}_i \mathbf{a}_i'^{\text{H}} \right) \otimes \left(\text{col}_{j=1}^I \left\{ \mathbf{C}_{ji} \right\} \text{row}_{j=1}^I \left\{ \mathbf{C}_{ji}'^{\text{H}} \right\} \right) \mathbf{S}, \quad (\text{D.29})$$

which is found via (4.23) to result in (4.27).

D.2.2 Proof of Lemma 4.2

Inserting (4.29) in (D.29), leads to

$$(\mathbf{A} \boxtimes \mathbf{C})(\mathbf{A}' \boxtimes \mathbf{C}') = \mathbf{S}^{\text{T}} \sum_{i=1}^I \left(\mathbf{a}_i \mathbf{a}_i'^{\text{H}} \right) \otimes (c(i) \mathbf{C}) \mathbf{S} \quad (\text{D.30})$$

$$= \mathbf{S}^{\text{T}} \left(\left(\sum_{i=1}^I c(i) \mathbf{a}_i \mathbf{a}_i'^{\text{H}} \right) \otimes \mathbf{C} \right) \mathbf{S} \quad (\text{D.31})$$

$$= \mathbf{S}^{\text{T}} \left[\left(\mathbf{A} \text{diag}\{c(i)\} \mathbf{A}'^{\text{H}} \right) \otimes \mathbf{C} \right] \mathbf{S}, \quad (\text{D.32})$$

which is equivalent to (4.30).

D.2.3 Proof of Lemma 4.3

The singular values $\sigma_i(\mathbf{B}_k)$ of \mathbf{B}_k can be calculated via the eigenvalues of its Gramian

$$\mathbf{B}_k^H \mathbf{B}_k = (\mathbf{I} - \Delta_k \boxtimes \mathbf{U}_k)^H (\mathbf{I} - \Delta_k \boxtimes \mathbf{U}_k) \quad (\text{D.33})$$

$$= \mathbf{I} - \Delta_k \boxtimes \mathbf{U}_k - (\Delta_k \boxtimes \mathbf{U}_k)^H + (\Delta_k \boxtimes \mathbf{U}_k)^H (\Delta_k \boxtimes \mathbf{U}_k), \quad (\text{D.34})$$

which will be simplified in the sequel. First notice that in the above Khatri-Rao products both matrices Δ_k and \mathbf{U}_k are symmetrically partitioned (see Definition Table 4.1), thus, according to Section 4.3, a selection matrix \mathbf{S} exists such that

$$\Delta_k \boxtimes \mathbf{U}_k = \mathbf{S}^T (\Delta_k \otimes \mathbf{U}_k) \mathbf{S}. \quad (\text{D.35})$$

Hence,

$$(\Delta_k \boxtimes \mathbf{U}_k)^H = \mathbf{S}^T (\Delta_k \otimes \mathbf{U}_k)^H \mathbf{S} = \mathbf{S}^T (\Delta_k^H \otimes \mathbf{U}_k^H) \mathbf{S} = \Delta_k^H \boxtimes \mathbf{U}_k, \quad (\text{D.36})$$

where the transition to the right-most term is possible since \mathbf{U}_k is Hermitian. Equation (D.34) can be consulted in order to simplify the mixed product on the right-hand side of (D.34). However, beforehand, it is necessary to verify whether (4.29) applies. This is in fact the case, which can be seen by inserting the individual blocks of \mathbf{U}_k , i.e.,

$$\mathbf{U}_{ij,k} \triangleq \mathbf{u}_{i,k}^* \mathbf{u}_{j,k}^T \quad \text{with} \quad i, j \in \mathcal{N}, \quad (\text{D.37})$$

in (4.29). This together with the partitioning in (4.86), leads to

$$\underset{i=1}{\overset{N}{\text{col}}} \left\{ \mathbf{U}_{ij,k} \right\} \underset{i=1}{\overset{N}{\text{row}}} \left\{ \mathbf{U}_{ij,k}^H \right\} = \underset{i=1}{\overset{N}{\text{col}}} \left\{ \mathbf{U}_{ij,k} \right\} \underset{i=1}{\overset{N}{\text{row}}} \left\{ \mathbf{U}_{ji,k} \right\} = \mathbf{u}_k^* \mathbf{u}_{j,k}^T \mathbf{u}_{j,k}^* \mathbf{u}_k^T = \|\mathbf{u}_{j,k}\|^2 \mathbf{U}_k. \quad (\text{D.38})$$

Consequently, Lemma 4.2 does indeed apply and

$$(\Delta_k \boxtimes \mathbf{U}_k)^H (\Delta_k \boxtimes \mathbf{U}_k) = (\Delta_k^H \mathbf{D}_{\mathbf{u},k} \Delta_k) \boxtimes \mathbf{U}_k, \quad (\text{D.39})$$

with the diagonal matrix $\mathbf{D}_{\mathbf{u},k}$ from (4.88). Inserting (D.36) and (D.39) in (D.34) yields

$$\mathbf{B}_k^H \mathbf{B}_k = \mathbf{I} - \underbrace{(\Delta_k + \Delta_k^H - \Delta_k^H \mathbf{D}_{\mathbf{u},k} \Delta_k)}_{\mathbf{\Gamma}_k \text{ in (4.88)}} \boxtimes \mathbf{U}_k. \quad (\text{D.40})$$

Referring to Section 4.3, the matrix obtained by the Khatri-Rao product in (D.40) is Hermitian. As a consequence, it is easy to see that all eigenvalues of $\mathbf{B}_k^H \mathbf{B}_k$ are less or equal to one iff (4.87) is satisfied.

D.2.4 Proof of Lemma 4.4

According to Section 4.3, $\mathbf{\Gamma}_k \geq 0$ together with $\mathbf{U}_k \geq 0$ is sufficient for (4.87). Condition $\mathbf{U}_k \geq 0$ is always fulfilled since \mathbf{U}_k has rank one and the one eigenvalue that differs from zero is non-negative and given by $\|\mathbf{u}_k\|^2$. Consequently, (4.89) is sufficient for $\sigma_i(\mathbf{B}_k) \leq 1, \forall i \in \{1, \dots, M\}$.

It remains open to show that \mathbf{B}_k has at least $M - N$ unit singular values. From [HJ99, Theorem 4.2.15] and with the fact that \mathbf{U}_k has rank one, it follows that the null space of the Kronecker

product $\Delta_k \otimes \mathbf{U}_k$ has dimension $(M-1)N$. Moreover, note that due to (4.23),

$$\mathbf{B}_k = \mathbf{I} - \Delta_k \boxtimes \mathbf{U}_k = \mathbf{I}_N - \mathbf{S}^\top (\Delta_k \otimes \mathbf{U}_k) \mathbf{S} = \mathbf{S}^\top (\mathbf{I}_{MN} - \Delta_k \otimes \mathbf{U}_k) \mathbf{S}, \quad (\text{D.41})$$

is a submatrix of $\mathbf{I}_{MN} - \Delta_k \otimes \mathbf{U}_k$. It is obvious that the latter maps any vector contained in the null space of $\Delta_k \otimes \mathbf{U}_k$ to itself and thus, has (at least) $(M-1)N$ unit singular values. Finally, the interlacing property (C.9) for the singular values of a submatrix (with r given by (4.19)), ensures that \mathbf{B}_k cannot have more than N singular values that differ from one.

D.2.5 Proof of Lemma 4.5

With the eigenvalues and eigenvectors of Δ briefly denoted by λ_i and \mathbf{q}_i , respectively, and $i \in \mathcal{N}$,

$$\mathbf{q}_i^\text{H} \Gamma \mathbf{q}_i = \underbrace{\mathbf{q}_i^\text{H} \Delta \mathbf{q}_i}_{\lambda_i} + \underbrace{\mathbf{q}_i^\text{H} \Delta^\text{H} \mathbf{q}_i}_{\lambda_i^*} - \underbrace{\mathbf{q}_i^\text{H} \Delta^\text{H} \mathbf{D}_u \Delta \mathbf{q}_i}_{|\lambda_i|^2 (\mathbf{q}_i^\text{H} \mathbf{D}_u \mathbf{q}_i)} = 2\text{Re}\{\lambda_i\} - |\lambda_i|^2 \mathbf{q}_i^\text{H} \mathbf{D}_u \mathbf{q}_i. \quad (\text{D.42})$$

In order to satisfy (4.89), $\mathbf{x}^\text{H} \Gamma \mathbf{x} \geq 0$ has to hold for any vector $\mathbf{x} \in \mathbb{C}^M$. Thus, specifically $\mathbf{q}_i^\text{H} \Gamma \mathbf{q}_i \geq 0$ has to hold for all \mathbf{q}_i . With the constraint of non-vanishing excitation, i.e., $\mathbf{D}_u > \mathbf{0} \Leftrightarrow \mathbf{q}_i^\text{H} \mathbf{D}_u \mathbf{q}_i > 0$, it is easy to see that a violation of (4.90) causes (D.42) to become negative for at least one eigenvector of Δ , which entails $\Gamma \not\geq \mathbf{0}$. If Δ is nilpotent, all of its eigenvalues are zero causing the above argument to fail.

D.2.6 Proof of Lemma 4.6

Let the eigenvalues and eigenvectors of Δ briefly be denoted by λ_i and \mathbf{q}_i , respectively, with $i \in \mathcal{N}$. If Δ is normal, i.e., $\mathbf{q}_i^\text{H} \mathbf{q}_j = 0$, for all $i, j \in \mathcal{N}$, $i \neq j$, and Δ is diagonalised by unitary matrix $\mathbf{Q}_\Delta = [\mathbf{q}_1 \ \cdots \ \mathbf{q}_N]$, i.e., $\Delta = \mathbf{Q}_\Delta \Lambda_\Delta \mathbf{Q}_\Delta^\text{H}$, with $\Lambda_\Delta = \text{diag}_{i=1}^N \{\lambda_i\}$. Then, (4.89) is equivalent to

$$\text{Re}\{\Lambda_\Delta\} \geq \frac{1}{2} \Lambda_\Delta^* \mathbf{Q}_\Delta^\text{H} \mathbf{D}_u \mathbf{Q}_\Delta \Lambda_\Delta \geq \mathbf{0}, \quad (\text{D.43})$$

which is synonymous for $\text{Re}\{\lambda_i\} \geq 0$. The rightmost order relation is a consequence of Sylvester's law of inertia [HJ13, Theorem 4.5.8] which ensures $\mathbf{Q}_\Delta^\text{H} \mathbf{D}_u \mathbf{Q}_\Delta > \mathbf{0}$ and the fact [cmp. HJ13, Observation 7.1.8] that the matrix product in the middle of (D.43) leads to a positive semi-definite matrix with null space identical to that of $\mathbf{Q}_\Delta^\text{H} \mathbf{D}_u \mathbf{Q}_\Delta \Lambda_\Delta$.

D.2.7 Proof of Conjecture 4.1

This proof is considered incomplete as it does not cover certain special cases of non-normal matrices, e.g., nilpotent matrices, non-diagonalisable matrices. It may also fail for some non-normal matrices with an eigenspace that contains a subset of mutually orthogonal eigenvectors.

Assuming the existence of $m, n \in \mathcal{N}$, $m \neq n$, such that $\text{Re}\{\lambda_m\} > 0$, $\lambda_n = 0$, and $\mathbf{q}_m^\text{H} \mathbf{q}_n \neq 0$.

Then, it follows from (D.42), with some factor $a \in \mathbb{C} \setminus \{0\}$,

$$(\mathbf{q}_m + a\mathbf{q}_n)^H \mathbf{\Gamma} (\mathbf{q}_m + a\mathbf{q}_n) = \underbrace{\mathbf{q}_m^H \mathbf{\Gamma} \mathbf{q}_m}_{2\text{Re}\{\lambda_i\} - |\lambda_i|^2 \mathbf{q}_i^H \mathbf{D}_u \mathbf{q}_i} + |a|^2 \underbrace{\mathbf{q}_n^H \mathbf{\Gamma} \mathbf{q}_n}_0 + 2\text{Re} \left\{ \underbrace{a \mathbf{q}_m^H \mathbf{\Gamma} \mathbf{q}_n}_{a\lambda_m \mathbf{q}_m^H \mathbf{q}_n} \right\}. \quad (\text{D.44})$$

Choosing $a = -\frac{1}{\mathbf{q}_m^H \mathbf{q}_n}$, (4.89) is found to be violated, as (D.44) becomes

$$(\mathbf{q}_m + a\mathbf{q}_n)^H \mathbf{\Gamma} (\mathbf{q}_m + a\mathbf{q}_n) = -|\lambda_m|^2 \mathbf{q}_m^H \mathbf{D}_u \mathbf{q}_m < 0. \quad (\text{D.45})$$

D.3 Proofs for Chapter 5

D.3.1 Proof of Corollary 5.1

This proof follows the lines of [DR15]. Here, a slightly more general version is presented, which allows the coupling factors to be complex-valued. Moreover, it improves rigour with respect to [DR15].

As done in proof of Lemma 4.3, the singular values of mapping matrix \mathbf{B} in recursion (4.79) are analysed. With the partitioning vector in (4.86) given by $\mathbf{p}_u = [M_1 \ M_2]^T$, and the abbreviations

$$\Gamma_{11} \triangleq (\mathbf{\Gamma})_{11}, \quad \Gamma_{12} \triangleq (\mathbf{\Gamma})_{12} = (\mathbf{\Gamma})_{21}^*, \quad \Gamma_{22} \triangleq (\mathbf{\Gamma})_{22}. \quad (\text{D.46})$$

it follows from (D.40) for the Gramian matrix of \mathbf{B} ,

$$\mathbf{B}^H \mathbf{B} = \mathbf{I} - \mathbf{\Gamma} \boxtimes \mathbf{U} = \mathbf{I} - \begin{bmatrix} \Gamma_{11} & \Gamma_{12} \\ \Gamma_{12}^* & \Gamma_{22} \end{bmatrix} \boxtimes \begin{bmatrix} \mathbf{u}_1^* \mathbf{u}_1^T & \mathbf{u}_1^* \mathbf{u}_2^T \\ \mathbf{u}_2^* \mathbf{u}_1^T & \mathbf{u}_2^* \mathbf{u}_2^T \end{bmatrix} = \mathbf{I} - \begin{bmatrix} \Gamma_{11} \mathbf{u}_1^* \mathbf{u}_1^T & \Gamma_{12} \mathbf{u}_1^* \mathbf{u}_2^T \\ \Gamma_{12}^* \mathbf{u}_2^* \mathbf{u}_1^T & \Gamma_{22} \mathbf{u}_2^* \mathbf{u}_2^T \end{bmatrix}. \quad (\text{D.47})$$

The here conducted analysis bares strong similarities to Section 2.3.3. The right-sided singular vectors \mathbf{t}_j of \mathbf{B} , $j \in \{1, \dots, M\}$, coincide with the eigenvectors of the Gramian in (D.47). With domain $\mathcal{D}_1 = \mathbb{C}^{M_1}$ of \mathbf{u}_1 and domain $\mathcal{D}_2 = \mathbb{C}^{M_2}$ of \mathbf{u}_2 , the singular vectors are found to be contained in the direct sum of both, i.e., $\mathbf{t}_j \in \mathcal{D} = \mathcal{D}_1 \oplus \mathcal{D}_2 = \mathbb{C}^M$, with $M = M_1 + M_2$. Hence, the singular vectors can be decomposed into their projection $\mathbf{t}_j^{\mathcal{D}_1} \in \mathbb{C}^{M_1}$ onto \mathcal{D}_1 , and their projection $\mathbf{t}_j^{\mathcal{D}_2} \in \mathbb{C}^{M_2}$ onto \mathcal{D}_2 , such that

$$\mathbf{t}_j = \mathbf{t}_j^{\mathcal{D}_1} + \mathbf{t}_j^{\mathcal{D}_2}. \quad (\text{D.48})$$

Conversely, for excitation vectors \mathbf{u}_1 and \mathbf{u}_2 , an extension into \mathcal{D} can be defined as

$$\mathbf{u}_1^{\mathcal{D}} \triangleq \text{col} \{ \mathbf{u}_1, \mathbf{0}_{M_2} \} \in \mathbb{C}^M, \quad \mathbf{u}_2^{\mathcal{D}} \triangleq \text{col} \{ \mathbf{0}_{M_1}, \mathbf{u}_2 \} \in \mathbb{C}^M. \quad (\text{D.49})$$

With (D.49), (D.47) can be equivalently written as

$$\mathbf{B}^H \mathbf{B} = \mathbf{I} - \Gamma_{11} (\mathbf{u}_1^{\mathcal{D}})^* (\mathbf{u}_1^{\mathcal{D}})^T - \Gamma_{12} (\mathbf{u}_1^{\mathcal{D}})^* (\mathbf{u}_2^{\mathcal{D}})^T - \Gamma_{12}^* (\mathbf{u}_2^{\mathcal{D}})^* (\mathbf{u}_1^{\mathcal{D}})^T - \Gamma_{22} (\mathbf{u}_2^{\mathcal{D}})^* (\mathbf{u}_2^{\mathcal{D}})^T, \quad (\text{D.50})$$

which directly shows that any singular vector that is orthogonal to

$$\mathcal{S}_{1,2}^{\mathcal{D}} \triangleq \text{span} \{ \mathbf{u}_1^{\mathcal{D}}, \mathbf{u}_2^{\mathcal{D}} \}, \quad (\text{D.51})$$

corresponds to the unit singular value. As $\mathcal{S}_{1,2}^D$ defines a plane in \mathbb{C}^M , (D.51) also allows to conclude that $M - 2$ such (right-sided) singular vectors can be found, entailing that $\sigma_j = 1$, wo.l.o.g., with $j \in \{3, \dots, M\}$. As already pointed out in Section 3.3.2, the choice of indices may lead to a violation of the ordering assumed in Section 2.3.1. However, similarly to Section 3.3.2, here, the latter ordering is not of central importance, thus, confusion is hopefully kept on a tolerable level. The remaining two singular values can, e.g., be calculated by identifying the roots of (A.1), which is straightforward and therefore skipped here. The derivation results in

$$\sigma_i^2 = 1 - \frac{1}{2} \left(\Gamma_{11} \|\mathbf{u}_1\|^2 + \Gamma_{22} \|\mathbf{u}_2\|^2 \right) + (-1)^{i-1} \frac{1}{2} \sqrt{(\Gamma_{11} \|\mathbf{u}_1\|^2 - \Gamma_{22} \|\mathbf{u}_2\|^2)^2 + 4\Gamma_{12}^2 \|\mathbf{u}_1\|^2 \|\mathbf{u}_2\|^2} \quad (\text{D.52})$$

$$= 1 - \frac{1}{2} \left(\Gamma_{11} \|\mathbf{u}_1\|^2 + \Gamma_{22} \|\mathbf{u}_2\|^2 \right) \left(1 + (-1)^{i-1} \sqrt{1 + \frac{4(\Gamma_{12}^2 - \Gamma_{11}\Gamma_{22}) \|\mathbf{u}_1\|^2 \|\mathbf{u}_2\|^2}{(\Gamma_{11} \|\mathbf{u}_1\|^2 + \Gamma_{22} \|\mathbf{u}_2\|^2)^2}} \right), \quad (\text{D.53})$$

where, wo.l.o.g., $i \in \{1, 2\}$, thus, $\sigma_1 \geq \sigma_2$. Finally, notice that that in Corollary 5.1 the

1. non-increasing behaviour in Case 1 corresponds to $\sigma_1 \leq 1$,
2. the non-decreasing behaviour in Case 2 corresponds to $\sigma_2 \geq 1$,
3. the indefinite behaviour in Case 3 corresponds to $\sigma_1 > 1 > \sigma_2$, and
4. the length-preserving behaviour in Case 4 corresponds to $\sigma_1 = \sigma_2 = 1$.

With all this at hand, it remains open to show that the four above listed configurations of singular values correspond to the conditions given in Cases 1 to 4 of Corollary 5.1.

Case 1, i.e., $1 \geq \sigma_1 \geq \sigma_2$:

From (D.52), it is found that if Condition B is violated, $\sigma_1 \geq 1$. Hence, Condition B is necessary for Case 1. Then, it follows from (D.52), that $\sigma_1 \leq 1$ is equivalent to

$$\sqrt{(\Gamma_{11} \|\mathbf{u}_1\|^2 - \Gamma_{22} \|\mathbf{u}_2\|^2)^2 + 4\Gamma_{12}^2 \|\mathbf{u}_1\|^2 \|\mathbf{u}_2\|^2} \leq \Gamma_{11} \|\mathbf{u}_1\|^2 + \Gamma_{22} \|\mathbf{u}_2\|^2, \quad (\text{D.54})$$

which entails after squaring on both sides,

$$\Gamma_{12}^2 \leq \Gamma_{11}\Gamma_{22}. \quad (\text{D.55})$$

Accordingly, Condition A is sufficient for Case 1.

Case 2, i.e., $\sigma_1 \geq \sigma_2 \geq 1$:

Analogous to the above case, Condition C is found to be necessary for $\sigma_2 \geq 1$. Then, based on (D.52), the latter condition translates to

$$\sqrt{(\Gamma_{11} \|\mathbf{u}_1\|^2 - \Gamma_{22} \|\mathbf{u}_2\|^2)^2 + 4\Gamma_{12}^2 \|\mathbf{u}_1\|^2 \|\mathbf{u}_2\|^2} \leq - \left(\Gamma_{11} \|\mathbf{u}_1\|^2 + \Gamma_{22} \|\mathbf{u}_2\|^2 \right), \quad (\text{D.56})$$

which as before, entails (D.55). Consequently, Condition A is sufficient for Case 2.

Case 3, i.e., $\sigma_1 > 1 > \sigma_2$:

Together with the constraint that the excitation vectors \mathbf{u}_1 and \mathbf{u}_2 do not vanish, satisfying either Condition B or C ensures the left-hand bracket expression in (D.53) to be non-zero. Then, in the right-hand bracket expression, the square-root has to be larger than one, in order to obtain $\sigma_1 > 1 > \sigma_2$. This in turn can only be achieved if Condition A is violated.

Case 4, i.e., $\sigma_1 = \sigma_2 = 1$:

As already found before, fulfilling either Condition B or C is necessary for $\sigma_1 \neq 1$ and $\sigma_2 \neq 1$. Hence, if both are violated, i.e., $\Gamma_{11} \|\mathbf{u}_1\|^2 + \Gamma_{22} \|\mathbf{u}_2\|^2 = 0$, $\sigma_1 = \sigma_2 = 1$.

D.3.2 Proof of Lemma 5.1

From (5.64), it is found that

$$\|\tilde{\mathbf{w}}_k\|^2 = \left(\tilde{\mathbf{w}}_{k-1}^H - \tilde{\mathbf{e}}_k^H \mathbf{D}_k \mathbf{U}'^T \right) \left(\tilde{\mathbf{w}}_{k-1} - \mathbf{U}'^* \mathbf{D}_k \tilde{\mathbf{e}}_k \right) \quad (\text{D.57})$$

$$= \|\tilde{\mathbf{w}}_{k-1}\|^2 + \tilde{\mathbf{e}}_k^H \mathbf{D}_k \mathbf{U}'^T \mathbf{U}'^* \mathbf{D}_k \tilde{\mathbf{e}}_k - 2\text{Re} \left\{ \tilde{\mathbf{e}}_k^H \mathbf{D}_k \mathbf{e}_k + \mathbf{v}_k^H \mathbf{D}_k \mathbf{e}_k \right\}. \quad (\text{D.58})$$

Adding $\mathbf{v}_k^H \mathbf{D}_k \mathbf{v}_k - \mathbf{v}_k^H \mathbf{D}_k \mathbf{v}_k$ on the right-hand side, the latter expression modifies to

$$\|\tilde{\mathbf{w}}_k\|^2 = \|\tilde{\mathbf{w}}_{k-1}\|^2 + \mathbf{v}_k^H \mathbf{D}_k \mathbf{v}_k - \mathbf{e}_k^H \mathbf{D}_k \mathbf{e}_k - \tilde{\mathbf{e}}_k^H \mathbf{D}_k \left[\mathbf{D}_k^{-1} - \mathbf{U}'^T \mathbf{U}'^* \right] \mathbf{D}_k \tilde{\mathbf{e}}_k, \quad (\text{D.59})$$

which has the same structure as (2.56). Accordingly, the same line of arguments can be followed. Since $\mathbf{D}_k \geq \mathbf{0}$, $\tilde{\mathbf{e}}_k^H \mathbf{D}_k \left[\mathbf{D}_k^{-1} - \mathbf{U}'^T \mathbf{U}'^* \right] \mathbf{D}_k \tilde{\mathbf{e}}_k \geq 0$ is equivalent to,

$$\mathbf{D}_k^{-1} - \mathbf{U}'^T \mathbf{U}'^* \geq \mathbf{0} \quad \Leftrightarrow \quad \begin{bmatrix} \mathbf{I} & \mathbf{U}'^* \\ \mathbf{U}'^T & \mathbf{D}_k^{-1} \end{bmatrix} \geq \mathbf{0} \quad \Leftrightarrow \quad \mathbf{I} - \mathbf{U}'^T \mathbf{D}_k \mathbf{U}'^* \geq \mathbf{0}, \quad (\text{D.60})$$

where the equivalence of semi-definiteness of a Hermitian matrix and its Schur complement was used [HJ13, Theorem 7.7.9] twice. Then, summing (D.59) on both sides up, from initialisation, i.e., $k = -1$, to some iteration index K , and by applying the Minkowsky inequality, (5.65) is obtained.

D.3.3 Proof of Lemma 5.2

From (5.64), it follows that the homogeneous recursion of the form (2.17), corresponding to (5.58) has a mapping matrix

$$\mathbf{B}_k \triangleq \mathbf{I} - \mathbf{U}'^* \mathbf{D}_k \mathbf{U}'^T. \quad (\text{D.61})$$

As \mathbf{B}_k is Hermitian, its spectral radius is equivalent its maximum singular value, which in turn represents the maximum stretching that can occur when $\tilde{\mathbf{w}}_{k-1}$ is mapped to $\tilde{\mathbf{w}}_k$ by (2.17) with \mathbf{B}_k from (D.61). It is straight forward to see that the eigenvalues² λ_i of \mathbf{B}_k are given by

$$\lambda_i = 1 - \lambda_i \left(\mathbf{U}'^* \mathbf{D}_k \mathbf{U}'^T \right), \quad (\text{D.62})$$

and that $\lambda_i \leq 1$ since $\mathbf{D}_k \geq \mathbf{0}$. Thus, $|\lambda_i| \leq 1$ is ensured iff,

$$\lambda_i \left(\mathbf{U}'^* \mathbf{D}_k \mathbf{U}'^T \right) \leq 2, \quad \text{or equivalently,} \quad 2\mathbf{I} - \mathbf{U}'^* \mathbf{D}_k \mathbf{U}'^T \geq \mathbf{0}. \quad (\text{D.63})$$

Similarly to (D.60), the left-hand side of (5.68) commutes with the right-hand side.

² As pointed out in Section 1.4, the arguments for eigenvalues and singular values that refer to mapping matrix \mathbf{B}_k , are suppressed throughout this whole thesis.

D.3.4 Proof of Lemma 5.3

Since all coupling factors $\nu_i(k) = 1$, and the step-sizes are identical, the coupling matrix is given by $\mathbf{\Delta}_k = \mu(k)\mathbf{1}\mathbf{1}^\top$. Hence, $\mathbf{\Gamma}_k$ from (4.88) is obtained as

$$\mathbf{\Gamma}_k = \mathbf{\Delta}_k + \mathbf{\Delta}_k^H - \mathbf{\Delta}_k^H \mathbf{D}_{\mathbf{u}',k} \mathbf{\Delta}_k = \mu(k)\mathbf{1}\mathbf{1}^\top + \mu(k)^*\mathbf{1}\mathbf{1}^\top - |\mu(k)|^2 \mathbf{1}\mathbf{1}^\top \mathbf{D}_{\mathbf{u}',k} \mathbf{1}\mathbf{1}^\top \quad (\text{D.64})$$

$$= \left[2\text{Re}\{\mu(k)\} - |\mu(k)|^2 (\mathbf{1}^\top \mathbf{D}_{\mathbf{u}',k} \mathbf{1}) \right] \mathbf{1}\mathbf{1}^\top. \quad (\text{D.65})$$

Thus, (4.89) in Lemma 4.4 can only be satisfied if (5.75) holds.

Bibliography

- [Abr72] M. Abramowitz, *Handbook of Mathematical Functions*, 10th ed. Washington, DC, USA: National Bureau of Standards, 1972 (cit. on p. 16).
- [Abu82] S. Abu El Ata, “Asymptotic behavior of an adaptive estimation algorithm with application to M -dependent data,” *IEEE Transactions on Automatic Control*, vol. 27, no. 6, pp. 1255–1257, Dec. 1982 (cit. on p. 29).
- [AEF12] S. Afsardoost, T. Eriksson, and C. Fager, “Digital predistortion using a vector-switched model,” *IEEE Transactions on Microwave Theory and Techniques*, vol. 60, no. 4, pp. 1166–1174, Apr. 2012 (cit. on p. 2).
- [Aga92] R. P. Agarwal, *Difference Equations and Inequalities*. New York, NY, USA: Marcel Dekker, 1992 (cit. on p. 14).
- [ASSC02] I. F. Akyildiz, W. Su, Y. Sankarasubramaniam, and E. Cayirci, “A survey on sensor networks,” *IEEE Communications Magazine*, vol. 40, no. 8, pp. 102–114, Aug. 2002 (cit. on p. 69).
- [AHdR12] D. Alberer, H. Hjalmarsson, and L. del Re, “System identification for automotive systems: Opportunities and challenges,” in *Identification for Automotive Systems*, vol. 418, London, UK: Springer, 2012, pp. 1–10 (cit. on p. 1).
- [APT99] N. Ampazis, S. Perantonis, and J. Taylor, “Dynamics of multilayer networks in the vicinity of temporary minima,” *Neural Networks*, vol. 12, no. 1, pp. 43–58, 1999 (cit. on p. 117).
- [And82] B. D. O. Anderson, “Exponential convergence and persistent excitation,” in *Proceedings of the IEEE Conference on Decision and Control*, vol. 21, Dec. 1982, pp. 12–17 (cit. on p. 12).
- [AJ82] B. D. O. Anderson and C. R. Johnson Jr., “Exponential convergence of adaptive identification and control algorithms,” *Automatica*, vol. 18, no. 1, pp. 1–13, 1982 (cit. on p. 16).
- [Ant00] P. J. Antsaklis, “Special issue on hybrid systems: Theory and applications – A brief introduction to the theory and applications of hybrid systems,” *Proceedings of the IEEE*, vol. 88, no. 7, pp. 879–887, Jul. 2000 (cit. on p. 38).
- [Asc05] E. Aschbacher, “Digital pre-distortion of microwave power amplifiers,” Doctor’s Thesis, TU Wien, Sep. 2005 (cit. on pp. 2, 16).
- [AR03] E. Aschbacher and M. Rupp, “Robust identification of an L-N-L system,” in *Conference Record of the 37th Asilomar Conference on Circuits, Systems and Computers*, Monterey, CA, USA, Nov. 2003, pp. 1298–1302 (cit. on pp. 103, 105).
- [AR05] E. Aschbacher and M. Rupp, “Robustness analysis of a gradient identification method for a nonlinear Wiener system,” in *Proceedings of the 13th Statistical Signal Processing Workshop*, Bordeaux, France, Jul. 2005, pp. 103–108 (cit. on p. 2).
- [ÅW95] K. J. Åström and B. Wittenmark, *Adaptive Control*, 2nd ed. Reading, MA, USA: Addison-Wesley Company, 1995 (cit. on pp. 11, 21).

- [AZF+11] L. A. Azpicueta-Ruiz, M. Zeller, A. R. Figueiras-Vidal, J. Arenas-García, and W. Kellermann, “Adaptive combination of Volterra kernels and its application to nonlinear acoustic echo cancellation,” *IEEE Transactions on Audio, Speech, and Language Processing*, vol. 19, no. 1, pp. 97–110, Mar. 2011 (cit. on p. 16).
- [AZF+13] L. A. Azpicueta-Ruiz, M. Zeller, A. R. Figueiras-Vidal, W. Kellermann, and J. Arenas-García, “Enhanced adaptive Volterra filtering by automatic attenuation of memory regions and its application to acoustic echo cancellation,” *IEEE Transactions on Signal Processing*, vol. 61, no. 11, pp. 2745–2750, Mar. 2013 (cit. on p. 16).
- [BBC+94] R. Barrett, M. Berry, T. F. Chan, J. Demmel, J. Donato, J. Dongarra, V. Eijkhout, R. Pozo, C. Romine, and H. van der Vorst, *Templates for the Solution of Linear Systems: Building Blocks for Iterative Methods*, 2nd ed. Society for Industrial and Applied Mathematics (SIAM), 1994 (cit. on p. 19).
- [BLM04] J. R. Barry, E. A. Lee, and D. G. Messerschmitt, *Digital Communication*, 3rd ed. New York, NY, USA: Springer Science+Business Media, 2004 (cit. on pp. 66, 97, 98).
- [Bee12] R. A. Beezer, *A First Course in Linear Algebra*, 2.99. Tacoma, WA, USA: University of Puget Sound, Oct. 2012 (cit. on p. 19).
- [BG02] J. Benesty and S. L. Gay, “An improved PNLMS algorithm,” in *Proceedings of the IEEE International Conference on Acoustics, Speech and Signal Processing*, vol. 2, Orlando, FL, USA, May 2002, pp. 1881–1884 (cit. on pp. 27, 29, 50).
- [BP79] A. Berman and R. J. Plemmons, *Nonnegative Matrices in the Mathematical Sciences*. New York, NY, USA: Academic Press, 1979 (cit. on pp. 72, 74, 146).
- [Ber85] N. J. Bershad, “Comments on ‘Comparison of the convergence of two algorithms for adaptive FIR digital filters’,” *IEEE Transactions on Acoustics, Speech, and Signal Processing*, vol. 33, no. 6, pp. 1604–1606, Dec. 1985 (cit. on p. 38).
- [Ber86] N. J. Bershad, “Analysis of the normalized LMS algorithm with Gaussian inputs,” *IEEE Transactions on Signal Processing*, vol. 34, no. 4, pp. 793–806, Aug. 1986 (cit. on p. 29).
- [BCV00] N. J. Bershad, P. Celka, and J.-M. Vesin, “Analysis of stochastic gradient tracking of time-varying polynomial Wiener systems,” *IEEE Transactions on Signal Processing*, vol. 48, no. 6, pp. 1676–1686, Jun. 2000 (cit. on pp. 2, 103).
- [Bis92] C. Bishop, “Exact calculation of the Hessian matrix for the multilayer perceptron,” *Neural Computation*, vol. 4, no. 4, pp. 494–501, Jul. 1992 (cit. on p. 117).
- [Bit84] R. Bitmead, “Persistence of excitation conditions and the convergence of adaptive schemes,” *IEEE Transactions on Information Theory*, vol. 30, no. 2, pp. 183–191, Mar. 1984 (cit. on pp. 16, 20, 21, 41, 55).
- [BA80a] R. Bitmead and B. Anderson, “Lyapunov techniques for the exponential stability of linear difference equations with random coefficients,” *IEEE Transactions on Automatic Control*, vol. 25, no. 4, pp. 782–787, Aug. 1980 (cit. on pp. 11, 12, 29).
- [BA80b] R. Bitmead and B. Anderson, “Performance of adaptive estimation algorithms in dependent random environments,” *IEEE Transactions on Automatic Control*, vol. 25, no. 4, pp. 788–794, Aug. 1980 (cit. on p. 29).
- [Bja95] E. Bjarnason, “Analysis of the filtered-x LMS algorithm,” *IEEE Transactions on Speech and Audio Processing*, vol. 3, no. 6, pp. 504–514, Nov. 1995 (cit. on pp. 106, 110).

- [BSC99] F. Bouteille, P. Scalart, and M. Corazza, “Pseudo affine projection algorithm new solution for adaptive identification,” in *Proceedings of the European Conference on Speech Communication and Technology*, Budapest, Hungary, Sep. 1999, pp. 427–430 (cit. on p. 27).
- [BS83] S. Boyd and S. Sastry, “On parameter convergence in adaptive control,” *System and Control Letters*, vol. 3, no. 6, pp. 311–319, Dec. 1983 (cit. on p. 16).
- [BV09] S. Boyd and L. Vandenberghe, *Convex Optimization*, 7th printing. Cambridge, UK: Cambridge University Press, 2009 (cit. on p. 74).
- [BH69] A. E. Bryson and Y.-C. Ho, *Applied Optimal Control*. Waltham, MA, USA: Blaisdell Publishing Company, 1969 (cit. on p. 117).
- [BKS93] J. A. Bucklew, T. G. Kurtz, and W. A. Sethares, “Weak convergence and local stability properties of fixed step size recursive algorithms,” *IEEE Transactions on Information Theory*, vol. 39, no. 3, pp. 966–978, Aug. 1993 (cit. on pp. 12, 38).
- [Cah15] J. J. Cahir, *Weather forecasting*, Encyclopædia Britannica Online: <http://www.britannica.com/science/weather-forecasting>, Accessed: 16 August, 2015 (cit. on p. 1).
- [CZY02] C.-G. Cao, X. Zhang, and Z.-P. Yang, “Some inequalities for the Khatri-Rao product of matrices,” *Electronic Journal of Linear Algebra*, vol. 9, pp. 276–281, Oct. 2002 (cit. on p. 75).
- [CBV01] P. Celka, N. Bershad, and J.-M. Vesin, “Stochastic gradient identification of polynomial Wiener systems: Analysis and application,” *IEEE Transactions on Signal Processing*, vol. 49, no. 2, pp. 301–313, Feb. 2001 (cit. on pp. 2, 103).
- [CBV00] P. Celka, N. J. Bershad, and J.-M. a. Vesin, “Fluctuation analysis of stochastic gradient identification of polynomial Wiener systems,” *IEEE Transactions on Signal Processing*, vol. 48, no. 6, pp. 1820–1825, Jun. 2000 (cit. on pp. 2, 103).
- [Che14] M. Y. Cheong, “Development of digital predistorters for broadband power amplifiers in OFDM systems using the simplicial canonical piecewise linear function,” Doctor’s Thesis, Aalto University, Department of Signal Processing and Acoustics, Helsinki, Finland, Apr. 2014 (cit. on pp. 16, 27).
- [CWB+12] M. Y. Cheong, S. Werner, M. J. Bruno, J. L. Figueroa, J. E. Cousseau, and R. Wichman, “Adaptive piecewise linear predistorters for nonlinear power amplifiers with memory,” *IEEE Transactions on Circuits and Systems—Part I: Fundamental Theory and Applications*, vol. 59, no. 7, pp. 1519–1532, Jul. 2012 (cit. on pp. 16, 27).
- [Cio87] J. M. Cioffi, “Limited-precision effects in adaptive filtering,” *IEEE Transactions on Circuits and Systems*, vol. 34, no. 7, pp. 821–833, Jul. 1987 (cit. on p. 39).
- [CM81] T. A. C. M. Claasen and W. F. G. Mecklenbräuker, “Comparison of the convergence of two algorithms for adaptive FIR digital filters,” *IEEE Transactions on Circuits and Systems*, vol. 28, no. 6, pp. 510–518, Jun. 1981 (cit. on pp. 38, 55, 57, 127).
- [CCM+98] C. J. Clark, G. Chrisikos, M. S. Muha, A. A. Moulthrop, and C. P. Silva, “Time-domain envelope measurement technique with application to wideband power amplifier modeling,” *IEEE Transactions on Microwave Theory and Techniques*, vol. 46, no. 12, pp. 2531–2540, Dec. 1998 (cit. on p. 2).
- [TUW07] “Code of conduct – Rules to ensure good scientific practice,” *Bulletin of the TU Wien*, no. 26, Oct. 2007 (cit. on p. iv).

- [CM80] C. F. N. Cowan and J. Mavor, "Design and performance evaluation of a 256-point adaptive filter," *IEE Proceedings F (Communications, Radar and Signal Processing)*, vol. 127, no. 3, pp. 179–184, Jun. 1980 (cit. on p. 38).
- [Cri02] S. Cripps, *Advanced Techniques in RF Power Amplifier Design*. Boston, MA, USA: Artech House, 2002 (cit. on p. 2).
- [DLA03] J.-P. Da Costa, A. Lagrange, and A. Arliaud, "Acoustic echo cancellation using nonlinear cascade filters," in *Proceedings of the IEEE International Conference on Acoustics, Speech and Signal Processing*, vol. 5, Hong Kong, PRC, Apr. 2003, pp. 389–392 (cit. on p. 101).
- [Dal07] R. Dallinger, "Pre-distortion algorithms for power amplifiers," Master's Thesis, TU Wien, Vienna, Austria, Nov. 2007 (cit. on p. 16).
- [DRWR10] R. Dallinger, H. Ruotsalainen, R. Wichman, and M. Rupp, "Adaptive pre-distortion techniques based on orthogonal polynomials," in *Conference Record of the 44th Asilomar Conference on Circuits, Systems and Computers*, Pacific Grove, CA, USA, Nov. 2010, pp. 1945–1950 (cit. on pp. 4, 6, 16).
- [DR09a] R. Dallinger and M. Rupp, "A strict stability limit for adaptive gradient type algorithms," in *Conference Record of the 43rd Asilomar Conference on Circuits, Systems and Computers*, Pacific Grove, CA, USA, Nov. 2009, pp. 1370–1374 (cit. on pp. 4, 5, 20, 28, 41, 45).
- [DR09b] R. Dallinger and M. Rupp, "On robustness of coupled adaptive filters," in *Proceedings of the IEEE International Conference on Acoustics, Speech and Signal Processing*, Taipei, Taiwan, Apr. 2009, pp. 3085–3088 (cit. on pp. 4, 5, 93, 95, 97).
- [DR10] R. Dallinger and M. Rupp, "Stability analysis of an adaptive Wiener structure," in *Proceedings of the IEEE International Conference on Acoustics, Speech and Signal Processing*, Dallas, TX, USA, Mar. 2010, pp. 3718–3721 (cit. on pp. 4, 5, 103).
- [DR11] R. Dallinger and M. Rupp, *Adaptive digital pre-distortion based on two-block models*, IEEE Forum on Signal Processing for Radio Frequency Systems, Vienna, Austria, Mar. 2011 (cit. on pp. 5, 6).
- [DR12] R. Dallinger and M. Rupp, "Improved robustness and accelerated power amplifier identification with adaptive Wiener models in the complex domain," in *Conference Record of the 46th Asilomar Conference on Circuits, Systems and Computers*, Pacific Grove, CA, USA, Nov. 2012, pp. 787–791 (cit. on pp. 5, 6, 103).
- [DR13] R. Dallinger and M. Rupp, "On the robustness of LMS algorithms with time-variant diagonal matrix step-size," in *Proceedings of the IEEE International Conference on Acoustics, Speech and Signal Processing*, Vancouver, BC, Canada, May 2013, pp. 5691–5695 (cit. on pp. 4, 6, 52).
- [DR15] R. Dallinger and M. Rupp, "Stability of adaptive filters with linearly interfering update errors," in *Proceedings of the 23rd European Signal Processing Conference*, Nice, France, Sep. 2015, pp. 2731–2735 (cit. on pp. 4, 6, 93, 95, 157).
- [dBB09] S. J. M. de Almeida, J. C. M. Bermudez, and N. J. Bershad, "A stochastic model for a pseudo affine projection algorithm," *IEEE Transactions on Signal Processing*, vol. 57, no. 1, pp. 107–118, Jan. 2009 (cit. on p. 39).

- [dBBC05] S. J. M. de Almeida, J. C. M. Bermudez, N. J. Bershad, and M. H. Costa, “A statistical analysis of the affine projection algorithm for unity step size and autoregressive inputs,” *IEEE Transactions on Circuits and Systems—Part I: Fundamental Theory and Applications*, vol. 52, no. 7, pp. 1394–1405, Jul. 2005 (cit. on p. 39).
- [dSTSM09] F. d. C. de Souza, O. J. Tobias, R. Seara, and D. R. Morgan, “Alternative approach for computing the activation factor of the PNLMS algorithm,” in *Proceedings of the 17th European Signal Processing Conference*, Glasgow, Scotland, Aug. 2009, pp. 2633–2637 (cit. on pp. 27, 50).
- [dSTSM10] F. d. C. de Souza, O. J. Tobias, R. Seara, and D. R. Morgan, “A PNLMS algorithm with individual activation factors,” *IEEE Transactions on Signal Processing*, vol. 58, no. 4, pp. 2036–2047, Apr. 2010 (cit. on pp. 27, 50).
- [DV75] C. A. Desoer and M. Vidyasagar, *Feedback Systems: Input-Output Properties*. New York, NY, USA: Academic Press, 1975 (cit. on p. 23).
- [DP73] D. H. Douglas and T. K. Peucker, “Algorithms for the reduction of the number of points required to represent a digitized line or its caricature,” *Cartographica*, vol. 10, no. 2, pp. 112–122, Oct. 1973 (cit. on p. 9).
- [Dut00] D. L. Duttweiler, “Proportionate normalized least-mean-squares adaptation in echo cancelers,” *IEEE Transactions on Speech and Audio Processing*, vol. 8, no. 5, pp. 508–518, Sep. 2000 (cit. on pp. 27, 29, 39, 50).
- [Ela99] S. N. Elaydi, *An Introduction to Difference Equations*, 2nd ed. New York, NY, USA: Springer, 1999 (cit. on p. 14).
- [Eli00] S. J. Elliott, “Optimal controllers and adaptive controllers for multichannel feedforward control of stochastic disturbances,” *IEEE Transactions on Signal Processing*, vol. 48, no. 4, pp. 1053–1060, Apr. 2000 (cit. on p. 110).
- [EBN92] S. J. Elliott, C. C. Boucher, and P. A. Nelson, “The behavior of a multiple channel active control system,” *IEEE Transactions on Signal Processing*, vol. 40, no. 5, pp. 1041–1052, May 1992 (cit. on pp. 110, 112).
- [ESN87] S. J. Elliott, I. M. Stothers, and P. A. Nelson, “A multiple error LMS algorithm and its application to the active control of sound and vibration,” *IEEE Transactions on Acoustics, Speech, and Signal Processing*, vol. 35, no. 10, pp. 1423–1434, Oct. 1987 (cit. on pp. 108, 110).
- [EP97] C. Eun and E. J. Powers, “A new Volterra predistorter based on the indirect learning architecture,” *IEEE Transactions on Signal Processing*, vol. 45, no. 1, pp. 223–227, Jan. 1997 (cit. on pp. 2, 16).
- [FBL93] P. L. Feintuch, N. J. Bershad, and A. K. Lo, “A frequency domain model for ‘filtered’ LMS algorithms—Stability analysis, design, and elimination of the training mode,” *IEEE Transactions on Signal Processing*, vol. 41, no. 4, pp. 1518–1531, Apr. 1993 (cit. on pp. 106, 110).
- [FS12] G. Ferrari-Trecate and M. Sznaier, “System identification for biological systems,” *International Journal of Robust and Nonlinear Control*, vol. 22, no. 10, pp. 1063–1064, May 2012 (cit. on p. 1).
- [FW85] A. Feuer and E. Weinstein, “Convergence analysis of LMS filters with uncorrelated Gaussian data,” *IEEE Transactions on Acoustics, Speech, and Signal Processing*, vol. ASSP-33, no. 1, pp. 222–230, Feb. 1985 (cit. on p. 15).

- [FP62] M. Fiedler and V. Pták, “On matrices with non-positive off-diagonal elements and positive principal minors,” *Czechoslovak Mathematical Journal*, vol. 12, no. 3, pp. 382–400, 1962 (cit. on pp. 72, 74, 146).
- [Fra04] R. Fraanje, “Robust and fast schemes in broadband active noise and vibration control,” Doctor’s Thesis, University of Twente, Enschede, Netherlands, May 2004 (cit. on p. 110).
- [FEV07] R. Fraanje, S. J. Elliott, and M. Verhaegen, “Robustness of the filtered-x LMS algorithm—Part II: Robustness enhancement by minimal regularization for norm bounded uncertainty,” *IEEE Transactions on Signal Processing*, vol. 55, no. 8, pp. 4038–4047, Aug. 2007 (cit. on p. 110).
- [FVE07] R. Fraanje, M. Verhaegen, and S. J. Elliott, “Robustness of the filtered-x LMS algorithm—Part I: Necessary conditions for convergence and the asymptotic pseudo-spectrum of toeplitz matrices,” *IEEE Transactions on Signal Processing*, vol. 55, no. 8, pp. 4029–4037, Aug. 2007 (cit. on p. 110).
- [Gar84] W. A. Gardner, “Learning characteristics of stochastic-gradient-descent algorithms: A general study, analysis, and critique,” *Signal Processing*, vol. 6, no. 2, pp. 113–133, Apr. 1984 (cit. on p. 15).
- [Gay98] S. Gay, “An efficient, fast converging adaptive filter for network echo cancellation,” in *Conference Record of the 32nd Asilomar Conference on Circuits, Systems and Computers*, Pacific Grove, CA, USA, Nov. 1998, pp. 394–398 (cit. on pp. 27, 50).
- [GP13] N. V. George and G. Panda, “Advances in active noise control: A survey, with emphasis on recent nonlinear techniques,” *Signal Processing*, vol. 93, no. 2, pp. 363–377, Feb. 2013 (cit. on p. 106).
- [GH09] F. M. Ghannouchi and O. Hammi, “Behavioral modeling and predistortion,” *IEEE Microwave Magazine*, vol. 10, no. 7, pp. 52–64, Dec. 2009 (cit. on pp. 2, 101).
- [GS01] G. B. Giannakis and E. Serpedin, “A bibliography on nonlinear system identification,” *Signal Processing*, vol. 81, no. 3, pp. 533–580, Mar. 2001 (cit. on pp. 1, 101).
- [GMW82] R. Gitlin, H. Meadors, and S. Weinstein, “The tap leakage algorithm: An algorithm for the stable operation of a digitally implemented, fractionally spaced adaptive equalizer,” *Bell Systems Technical Journal*, vol. 61, no. 8, pp. 1817–1839, Oct. 1982 (cit. on pp. 39, 40).
- [Glo79] J. Glover, “High order algorithms for adaptive filters,” *IEEE Transactions on Communications*, vol. 27, no. 1, pp. 216–221, Jan. 1979 (cit. on p. 110).
- [GV96] G. Golub and C. Van Loan, *Matrix Computations*, 3rd ed. Baltimore, MD, USA: Johns Hopkins University Press, 1996 (cit. on pp. 18, 178).
- [GT92] M. Gori and A. Tesi, “On the problem of local minima in backpropagation,” *IEEE Transactions on Pattern Analysis and Machine Intelligence*, vol. 14, no. 1, pp. 76–86, Jan. 1992 (cit. on pp. 117, 118).
- [Gra13] C. R. Graham, “Linear analysis (math 554),” University of Washington, Seattle, WA, USA, Lecture notes, autumn 2013 (cit. on p. 19).
- [Gre92] W. Greblicki, “Nonparametric identification of Wiener systems,” *IEEE Transactions on Information Theory*, vol. 38, no. 5, pp. 1487–1493, Sep. 1992 (cit. on p. 103).

- [GZ11] L. Guan and A. Zhu, “Simplified dynamic deviation reduction-based Volterra model for Doherty power amplifiers,” in *Proceedings of the Workshop on Integrated Nonlinear Microwave and Millimetre-Wave Circuits*, Vienna, Austria, Apr. 2011, pp. 1–4 (cit. on p. 2).
- [GG91] H. Guo and S. B. Gelfand, “Analysis of gradient descent learning algorithms for multilayer feedforward neural networks,” *IEEE Transactions on Circuits and Systems*, vol. 38, no. 8, pp. 883–894, Aug. 1991 (cit. on p. 117).
- [Gus95] K. Gustafson, “Matrix trigonometry,” *Linear Algebra and its Applications*, vol. 217, pp. 117–140, Mar. 1995 (cit. on pp. 59, 154).
- [Gus00] K. Gustafson, “An extended operator trigonometry,” *Linear Algebra and its Applications*, vol. 319, pp. 117–135, Nov. 2000 (cit. on pp. 52, 59, 145, 146, 154).
- [GR97] K. E. Gustafson and D. K. M. Rao, *Numerical Range*. New York, NY, USA: Springer, 1997 (cit. on pp. 50, 52, 59, 146, 154).
- [HY81] L. A. Hageman and D. M. Young, *Applied Iterative Methods*. New York, NY, USA: Academic Press, 1981 (cit. on p. 18).
- [HV83] C. J. Harris and J. M. E. Valença, *The Stability of Input-Output Dynamical Systems*. London, UK: Academic Press, 1983 (cit. on pp. 74, 146).
- [HSK94] B. Hassibi, A. H. Sayed, and T. Kailath, “LMS and backpropagation are minimax filters,” in *Theoretical Advances in Neural Computation and Learning*, V. Roychowdhury, K. Siu, and A. Orlicsky, Eds., Norwell, MA, USA: Kluwer Academic Publishers, Nov. 1994, ch. 12, pp. 425–447 (cit. on pp. 104, 118, 121).
- [HSK99] B. Hassibi, A. H. Sayed, and T. Kailath, *Indefinite-Quadratic Estimation and Control: A unified approach to H^2 and H^∞ theories*. Philadelphia, PA, USA: Society for Industrial and Applied Mathematics (SIAM), 1999 (cit. on p. 22).
- [HC90] T. I. Haweel and P. M. Clarkson, “Analysis and generalization of a median adaptive filter,” in *Proceedings of the IEEE International Conference on Acoustics, Speech and Signal Processing*, vol. 3, Albuquerque, NM, USA, Apr. 1990, pp. 1269–1272 (cit. on p. 110).
- [Hay02] S. Haykin, *Adaptive Filter Theory*, 4th ed. Upper Saddle River, NJ, USA: Prentice-Hall, 2002 (cit. on pp. 1, 2, 11, 12, 15, 20, 21, 24, 29, 40, 55, 99, 101, 103).
- [Hay94] S. Haykin, *Neural Networks*. New York, NY, USA: Macmillan College Publishing Company, 1994 (cit. on pp. 15, 117, 118).
- [Hec89] R. Hecht-Nielsen, “Theory of the backpropagation neural network,” in *Proceedings of the International Joint Conference on Neural Networks*, vol. 1, Washington, DC, USA, Jun. 1989, pp. 593–605 (cit. on p. 117).
- [Hig02] N. J. Higham, *Accuracy and Stability of Numerical Algorithms*, 2nd ed. Philadelphia, PA, USA: Society for Industrial and Applied Mathematics (SIAM), 2002 (cit. on p. 18).
- [HT11] H. Holma and A. Toskala, *LTE for UMTS*, 2nd ed. Chichester, UK: John Wiley & Sons, 2011 (cit. on p. 2).
- [Hor54] A. Horn, “On the eigenvalues of a matrix with prescribed singular values,” *Proceedings of the American Mathematical Society*, vol. 5, no. 1, pp. 4–7, Feb. 1954 (cit. on p. 18).
- [HJ99] R. A. Horn and C. R. Johnson, *Topics in Matrix Analysis*. Cambridge, UK: Cambridge University Press, 1999 (cit. on pp. 75, 116, 146, 147, 155).

- [HJ13] R. A. Horn and C. R. Johnson, *Matrix Analysis*. Cambridge, NY, USA: Cambridge University Press, 2013 (cit. on pp. 17–19, 43, 47, 50–52, 77, 90, 94, 95, 123, 129, 130, 145, 147, 156, 159, 177).
- [HM92] R. A. Horn and R. Mathias, “Block-matrix generalizations of Schur’s basic theorems on Hadamard products,” *Linear Algebra and its Applications*, vol. 172, pp. 337–346, Jul. 1992 (cit. on pp. 75–77).
- [IK84] P. A. Ioannou and P. V. Kokotovic, “Instability analysis and improvement of robustness of adaptive control,” *Automatica*, vol. 20, no. 5, pp. 583–594, Sep. 1984 (cit. on p. 39).
- [IS96] P. A. Ioannou and J. Sun, *Robust Adaptive Control*. Upper Saddle River, NJ, USA: Prentice-Hall, 1996 (cit. on p. 110).
- [Kah13] W. M. Kahan, “Tutorial overview of vector and matrix norms,” University of California, Berkeley, CA, USA, Lecture notes, Jan. 2013, online (cit. on p. 19).
- [KKGK12] Y. Kajikawa, W.-S. Gan, and S. M. Kuo, “Recent advances on active noise control: Open issues and innovative applications,” *APSIPA Transactions on Signal and Information Processing*, vol. 1, no. e3, p. 21, Aug. 2012 (cit. on p. 106).
- [KAWC95] A. D. Kalafatis, N. Arifin, L. Wang, and W. R. Cluett, “A new approach to the identification of pH processes based on the Wiener model,” *Chemical Engineering Science*, vol. 50, no. 23, pp. 3693–3701, Dec. 1995 (cit. on p. 101).
- [Kal60] R. E. Kalman, “A new approach to linear filtering and prediction problems,” *Transactions of the ASME—Journal of Basic Engineering*, vol. 82, no. (Series D), pp. 35–45, 1960 (cit. on p. 128).
- [Kha02] H. K. Khalil, *Nonlinear Systems*, 3rd ed. Upper Saddle River, NJ, USA: Pearson Education, Jan. 2002 (cit. on pp. 21, 23, 24).
- [KR68] C. G. Khatri and C. R. Rao, “Solutions to some functional equations and their applications to characterization of probability distributions,” *Sankhyā: The Indian Journal of Statistics, Series A*, pp. 167–180, 1968 (cit. on p. 75).
- [KK01] J. Kim and K. Konstantinou, “Digital predistortion of wideband signals based on power amplifier model with memory,” *Electronics Letters*, vol. 37, no. 23, pp. 1417–1418, Nov. 2001 (cit. on p. 16).
- [KD75] J.-K. Kim and L. D. Davisson, “Adaptive linear estimation for stationary M-dependent processes,” *IEEE Transactions on Information Theory*, vol. 21, no. 1, pp. 23–31, Jan. 1975 (cit. on p. 110).
- [KM06] V. Klein and E. A. Morelli, *Aircraft System Identification: Theory and Practice*. Reston, VA, USA: American Institute of Aeronautics and Astronautics, 2006 (cit. on p. 1).
- [KNW91] R. H. Koning, H. Neudecker, and T. Wansbeek, “Block Kronecker products and the vecb operator,” *Linear Algebra and its Applications*, vol. 149, pp. 165–184, Apr. 1991 (cit. on p. 75).
- [KH86] M. J. Korenberg and I. W. Hunter, “The identification of nonlinear biological systems: LNL cascade models,” *Biological Cybernetics*, vol. 55, no. 2–3, pp. 125–134, Nov. 1986 (cit. on p. 101).
- [Kre09] K. Kreutz-Delgado, “The complex gradient operator and the CR-calculus,” University of California, San Diego, CA, USA, Tech. Rep. UCSD-ECE275CG-S2009v1.0, Jun. 2009 (cit. on pp. 12, 14).

- [KM99] S. M. Kuo and D. R. Morgan, "Active noise control: A tutorial review," *Proceedings of the IEEE*, vol. 87, no. 6, pp. 943–973, Jun. 1999 (cit. on p. 106).
- [KM08] S. M. Kuo and D. R. Morgan, "Active noise control," in *Springer Handbook of Speech Processing*, J. Benesty, M. M. Sondhi, and Y. A. Huang, Eds., Springer, 2008, pp. 1001–1018 (cit. on pp. 69, 106).
- [LLM98] I. D. Landau, R. Lozano, and M. M'Saad, *Adaptive Control*, ser. Communications and Control Engineering. Berlin, Germany: Springer, 1998 (cit. on pp. 21, 110).
- [LSR93] D. A. Lawrence, W. A. Sethares, and W. Ren, "Parameter drift instability in disturbance-free adaptive systems," *IEEE Transactions on Automatic Control*, vol. 38, no. 4, pp. 584–587, Apr. 1993 (cit. on pp. 39, 40).
- [LeC86] Y. LeCun, "Learning processes in an asymmetric threshold network," in *Disordered Systems and Biological Organization*, Springer, 1986, pp. 233–240 (cit. on p. 117).
- [LA05] H. Lin and P. J. Antsaklis, "Stability and persistent disturbance attenuation properties for a class of networked control systems: Switched system approach," *International Journal of Control*, vol. 78, no. 18, pp. 1447–1458, Feb. 2005 (cit. on p. 39).
- [LA09] H. Lin and P. J. Antsaklis, "Stability and stabilizability of switched linear systems: A survey of recent results," *IEEE Transactions on Automatic Control*, vol. 54, no. 2, pp. 308–322, Feb. 2009 (cit. on pp. 38, 39).
- [Lin13] M. Lin, "Angles, majorization, Wielandt inequality and applications," Doctor's Thesis, University of Waterloo, Waterloo, ON, Canada, May 2013 (cit. on p. 63).
- [LS12] M. Lin and G. Sinnamon, "The generalized Wielandt inequality in inner product spaces," *Eurasian Mathematical Journal*, vol. 3, no. 1, pp. 72–85, 2012 (cit. on p. 150).
- [Liu99] S. Liu, "Matrix results on the Khatri-Rao and Tracy-Singh products," *Linear Algebra and its Applications*, vol. 289, no. 1, pp. 267–277, Mar. 1999 (cit. on pp. 75, 76).
- [LT08] S. Liu and G. Trenkler, "Hadamard, Khatri-Rao, Kronecker and other matrix products," *International Journal of Information and Systems Sciences*, vol. 4, no. 1, pp. 160–177, 2008 (cit. on p. 75).
- [Lju99] L. Ljung, *System Identification*, 2nd ed., ser. Information and System Sciences. Upper Saddle River, NJ, USA: Prentice-Hall, 1999 (cit. on pp. 1, 11, 16, 110).
- [Lju77] L. Ljung, "Analysis of recursive stochastic algorithms," *IEEE Transactions on Automatic Control*, vol. 22, no. 4, pp. 551–575, Aug. 1977 (cit. on p. 110).
- [Lju10] L. Ljung, "Perspectives on system identification," *Annual Reviews in Control*, vol. 34, no. 1, pp. 1–12, Apr. 2010 (cit. on p. 1).
- [LS85] L. Ljung and T. Söderström, *Theory and Practice of Recursive Identification*, 2nd ed., ser. Series in Signal Processing, Optimization, and Control. Cambridge, MA, USA: MIT Press, Feb. 1985 (cit. on pp. 11, 12).
- [LLP89] G. Long, F. Ling, and J. G. Proakis, "The LMS algorithm with delayed coefficient adaptation," *IEEE Transactions on Acoustics, Speech, and Signal Processing*, vol. 37, no. 9, pp. 1397–1405, Sep. 1989 (cit. on pp. 106, 108).
- [LLP92] G. Long, F. Ling, and J. G. Proakis, "Correction to 'The LMS algorithm with delayed coefficient adaptation'," *IEEE Transactions on Signal Processing*, vol. 40, no. 1, pp. 230–232, Jan. 1992 (cit. on pp. 106, 108).

- [Luc65] R. W. Lucky, "Automatic equalization for digital communication," *Bell System Technical Journal*, vol. 44, no. 4, pp. 547–588, Apr. 1965 (cit. on pp. 27, 38).
- [MN79] J. R. Magnus and H. Neudecker, "The commutation matrix: Some properties and applications," *The Annals of Statistics*, vol. 7, no. 2, pp. 381–394, Mar. 1979 (cit. on p. 75).
- [MKK93] S. Makino, Y. Kaneda, and N. Koizumi, "Exponentially weighted stepsize NLMS adaptive filter based on the statistics of a room impulse response," *IEEE Transactions on Speech and Audio Processing*, vol. 1, no. 1, pp. 101–108, 1 Jan. 1993 (cit. on pp. 27, 29, 39, 50).
- [Mar06] M. Margaliot, "Stability analysis of switched systems using variational principles: An introduction," *Automatica*, vol. 42, no. 12, pp. 2059–2077, Dec. 2006 (cit. on pp. 38, 44).
- [MOA11] A. W. Marshall, I. Olkin, and B. C. Arnold, *Inequalities: Theory of Majorization and its Applications*, 2nd ed. New York, NY, USA: Springer, Feb. 2011 (cit. on p. 18).
- [MS00a] V. J. Mathews and G. L. Sicuranza, *Polynomial Signal Processing*. New York, NY, USA: John Wiley & Sons, 2000 (cit. on pp. 15, 16, 27).
- [McL65] R. M. McLeod, "Mean value theorems for vector valued functions," *Proceedings of the Edinburgh Mathematical Society (Series 2)*, vol. 14, no. 03, pp. 197–209, 1965 (cit. on p. 104).
- [Men73] J. M. Mendel, *Discrete Techniques of Parameter Estimation: The Equations Error Formulation*, ser. Control Theory. New York, NY, USA: Marcel Dekker, 1973 (cit. on pp. 12, 14, 18, 19, 22, 29, 32, 33).
- [Møl97] M. F. Møller, "Efficient training of feed-forward neural networks," Doctor's Thesis, Aarhus University, Århus, Denmark, Nov. 1997 (cit. on p. 118).
- [MS00b] T. Moon and W. Stirling, *Mathematical Methods and Algorithms for Signal Processing*. Upper Saddle River, NJ, USA: Prentice-Hall, 2000 (cit. on pp. 18, 21, 25, 29, 74, 79–81, 104, 121, 177).
- [Mor80] D. R. Morgan, "An analysis of multiple correlation cancellation loops with a filter in the auxiliary path," in *Proceedings of the IEEE International Conference on Acoustics, Speech and Signal Processing*, vol. 5, Denver, CO, USA, Apr. 1980, pp. 457–461 (cit. on p. 106).
- [Mos70] J. L. Moschner, "Adaptive filter with clipped input data," Doctor's Thesis, Department of Electrical Engineering, Stanford University, Stanford, CA, USA, 1970 (cit. on p. 38).
- [Moy77] P. J. Moylan, "Matrices with positive principal minors," *Linear Algebra and its Applications*, vol. 17, no. 1, pp. 53–58, 1977 (cit. on pp. 74, 146).
- [NN67] J.-I. Nagumo and A. Noda, "A learning method for system identification," *IEEE Transactions on Automatic Control*, vol. 12, no. 3, pp. 282–287, Jun. 1967 (cit. on pp. 29, 99, 101).
- [Nas99] V. H. Nascimento, "Stability and performance of adaptive filters without slow adaptation approximations," Doctor's Thesis, University of California, Los Angeles, CA, USA, Mar. 1999 (cit. on pp. 21, 39, 40, 127).
- [Nie14] M. A. Nielsen, *Neural Networks and Deep Learning*. Determination Press, 2014 (cit. on pp. 117, 118, 121).

- [Nik68] H. Nikaido, *Convex Structure and Economic Theory*. New York, NY, USA: Academic Press, 1968 (cit. on p. 74).
- [OCV14] *OpenCV (open source computer vision library)*, <http://opencv.org/>, Accessed: 17 February, 2014 (cit. on p. 9).
- [OWN97] A. Oppenheim, A. Willsky, and S. H. Nawab, *Signals & Systems*, 2nd ed., ser. Signal Processing. Upper Saddle River, NJ, USA: Prentice-Hall, 1997 (cit. on p. 75).
- [OU84] K. Ozeki and T. Umeda, “An adaptive filtering algorithm using orthogonal projection to an affine subspace and its properties,” *Electronics and Communications in Japan*, vol. 67-A, no. 5, pp. 19–27, 1984 (cit. on p. 27).
- [Par82] D. B. Parker, “Learning-logic,” Office of Technology Licensing, Stanford University, Stanford, CA, USA, Invention Report. S81-64, File 1, 1982 (cit. on p. 117).
- [PHW07] M. Pawlak, Z. Hasiewicz, and P. Wachel, “On nonparametric identification of Wiener systems,” *IEEE Transactions on Signal Processing*, vol. 55, no. 2, pp. 482–492, Feb. 2007 (cit. on p. 103).
- [Pro95] J. Proakis, *Digital Communications*, 3rd ed. New York, NY, USA: McGraw-Hill, 1995 (cit. on pp. 97, 98).
- [RQZ04] R. Raich, H. Qian, and G. T. Zhou, “Orthogonal polynomials for power amplifier modeling and predistorter design,” *IEEE Transactions on Vehicular Technology*, vol. 53, no. 5, pp. 1468–1479, Sep. 2004 (cit. on pp. 16, 27).
- [RZ04] R. Raich and G. T. Zhou, “Orthogonal polynomials for complex Gaussian processes,” *IEEE Transactions on Signal Processing*, vol. 52, no. 10, pp. 2788–2797, Oct. 2004 (cit. on pp. 16, 27).
- [RZV05] R. Raich, G. T. Zhou, and M. Viberg, “Subspace based approaches for Wiener system identification,” *IEEE Transactions on Automatic Control*, vol. 50, no. 10, pp. 1629–1634, Oct. 2005 (cit. on pp. 2, 101, 103).
- [Ram72] U. Ramer, “An iterative procedure for the polygonal approximation of plane curves,” *Computer Graphics and Image Processing*, vol. 1, no. 3, pp. 244–256, Nov. 1972 (cit. on p. 9).
- [Rao70] C. R. Rao, “Estimation of heteroscedastic variances in linear models,” *Journal of the American Statistical Association*, vol. 65, no. 329, pp. 161–172, Mar. 1970 (cit. on p. 75).
- [Rao05] C. R. Rao, “Antieigenvalues and antisingularvalues of a matrix and applications to problems in statistics,” *Research Letters in the Information and Mathematical Sciences*, vol. 8, pp. 53–76, 2005 (cit. on pp. 52, 63, 145, 146).
- [RKS10] V. G. Reju, S. N. Koh, and I. Y. Soon, “Underdetermined convolutive blind source separation via time-frequency masking,” *IEEE Transactions on Audio, Speech, and Language Processing*, vol. 18, no. 1, pp. 101–116, Jan. 2010 (cit. on p. 150).
- [RVAS81] C. E. Rohrs, L. Valavani, M. Athans, and G. Stein, “Analytical verification of undesirable properties of direct model reference adaptive control algorithms,” in *Proceedings of the 20th IEEE Conference on Decision and Control including the Symposium on Adaptive Processes*, San Diego, CA, USA, Dec. 1981, pp. 1272–1284 (cit. on p. 39).
- [Roj96] R. Rojas, *Neural Networks*. Berlin, Germany: Springer, 1996 (cit. on pp. 117, 118, 121, 124).

- [RS89] S. Roy and J. Shynk, "Analysis of the data-reusing LMS algorithm," in *Proceedings of the 32nd Midwest Symposium on Circuits and Systems*, vol. 2, Aug. 1989, pp. 1127–1130 (cit. on p. 111).
- [Rud09] W. Rudin, *Reelle und komplexe Analysis*, 2nd ed. Munich, Germany: Oldenbourg Wissenschaftsverlag, 2009 (cit. on p. 105).
- [RHW86a] D. E. Rumelhart, G. E. Hinton, and R. J. Williams, "Learning internal representations by error propagation," in *Parallel Distributed Processing: Foundations*, vol. 1, Cambridge, MA, USA: MIT Press, Jul. 1986, ch. 8 (cit. on p. 117).
- [RHW86b] D. E. Rumelhart, G. E. Hinton, and R. J. Williams, "Learning representations by back-propagating errors," *Nature*, vol. 323, pp. 533–536, Oct. 1986 (cit. on p. 117).
- [Rup98] M. Rupp, "A family of adaptive filter algorithm with decorrelating properties," *IEEE Transactions on Signal Processing*, vol. 46, no. 3, pp. 771–775, Mar. 1998 (cit. on p. 27).
- [Rup11a] M. Rupp, "On gradient type adaptive filters with non-symmetric matrix step-sizes," in *Proceedings of the IEEE International Conference on Acoustics, Speech and Signal Processing*, Prague, Czech Republic, May 2011, pp. 4136–4139 (cit. on pp. 20, 32).
- [Rup11b] M. Rupp, "Pseudo affine projection algorithms revisited: Robustness and stability analysis," *IEEE Transactions on Signal Processing*, vol. 59, no. 5, pp. 2017–2023, May 2011 (cit. on p. 39).
- [RC00] M. Rupp and J. Cezanne, "Robustness conditions of the LMS algorithm with time-variant matrix step-size," *Signal Processing*, vol. 80, no. 9, pp. 1787–1794, Sep. 2000 (cit. on pp. 14, 29, 31, 46, 50, 55, 56, 127).
- [RF94] M. Rupp and R. Frenzel, "Analysis of LMS and NLMS algorithms with delayed coefficient update in the presence of spherically invariant processes," *IEEE Transactions on Signal Processing*, vol. 42, no. 3, pp. 668–672, Mar. 1994 (cit. on p. 108).
- [RS95] M. Rupp and A. H. Sayed, "Local and global passivity relations for Gauss-Newton methods in adaptive filtering," in *Proceedings of the SPIE Conference on Advanced Signal Processing*, vol. 2563, San Diego (CA), USA, Jul. 1995, pp. 218–229 (cit. on pp. 27, 39).
- [RS96a] M. Rupp and A. H. Sayed, "A time-domain feedback analysis of filtered-error adaptive gradient algorithms," *IEEE Transactions on Signal Processing*, vol. 44, no. 6, pp. 1428–1439, Jun. 1996 (cit. on pp. 2, 22, 24, 78, 108, 111).
- [RS96b] M. Rupp and A. H. Sayed, "On the robustness of perceptron learning recurrent networks," in *Proceedings of the 13th IFAC World Congress*, vol. 1, San Francisco, CA, USA, Jun. 1996, pp. 243–248 (cit. on pp. 104, 118, 122).
- [RS96c] M. Rupp and A. H. Sayed, "Robustness of Gauss-Newton recursive methods: A deterministic feedback analysis," *Signal Processing*, vol. 50, no. 3, pp. 165–187, May 1996 (cit. on pp. 27, 39).
- [RS97] M. Rupp and A. H. Sayed, "Supervised learning of perceptron and output feedback dynamic networks: A feedback analysis via the small gain theorem," *IEEE Transactions on Neural Networks*, vol. 8, no. 3, pp. 612–622, May 1997 (cit. on pp. 104, 118, 122).
- [RS98] M. Rupp and A. H. Sayed, "Robust FxLMS algorithm with improved convergence performance," *IEEE Transactions on Speech and Audio Processing*, vol. 6, no. 1, pp. 78–85, Jan. 1998 (cit. on p. 108).

- [Say03] A. H. Sayed, *Fundamentals of Adaptive Filtering*. Hoboken, NJ, USA: John Wiley & Sons, 2003 (cit. on pp. 1, 2, 11–13, 15, 20, 21, 24, 27, 29, 39, 55, 99, 101, 103).
- [SR95a] A. H. Sayed and M. Rupp, “A feedback analysis of perceptron learning for neural networks,” in *Conference Record of the 29th Asilomar Conference on Circuits, Systems and Computers*, Pacific Grove, CA, USA, Oct. 1995, pp. 894–898 (cit. on pp. 104, 118, 121).
- [SR95b] A. H. Sayed and M. Rupp, “A time-domain feedback analysis of adaptive gradient algorithms via the small gain theorem,” in *Proceedings of the SPIE Conference on Advanced Signal Processing: Algorithms, Architectures, and Implementations*, vol. 2563, San Diego, CA, USA, Jul. 1995, pp. 458–469 (cit. on p. 24).
- [SR96] A. H. Sayed and M. Rupp, “Error-energy bounds for adaptive gradient algorithms,” *IEEE Transactions on Signal Processing*, vol. 44, no. 8, pp. 1982–1989, Aug. 1996 (cit. on pp. 2, 20, 24, 29, 32, 46, 50, 55, 78, 111).
- [Sch01] K. Scharnhorst, “Angles in complex vector spaces,” *Acta Applicandae Mathematica*, vol. 69, no. 1, pp. 95–103, Oct. 2001 (cit. on p. 150).
- [Sch80] M. Schetzen, *The Volterra and Wiener Theories of Nonlinear Systems*. New York, NY, USA: John Wiley & Sons, 1980 (cit. on p. 16).
- [SJ93] B. A. Schnaufer and W. K. Jenkins, “New data-reusing LMS algorithms for improved convergence,” in *Conference Record of the 27th Asilomar Conference on Circuits, Systems and Computers*, vol. 2, Pacific Grove, CA, USA, Nov. 1993, pp. 1584–1588 (cit. on p. 111).
- [SOGG09] D. Schreurs, M. O’Droma, A. Goacher, and M. Gadringer, Eds., *RF Power Amplifier Behavioural Modeling*. Cambridge, UK: Cambridge University Press, 2009 (cit. on p. 2).
- [Set92] W. A. Sethares, “Adaptive algorithms with nonlinear data and error functions,” *IEEE Transactions on Signal Processing*, vol. 40, no. 9, pp. 2199–2206, Sep. 1992 (cit. on pp. 12, 16, 21, 34, 40, 118, 127).
- [SAJ89] W. A. Sethares, B. D. O. Anderson, and C. R. Johnson Jr., “Adaptive algorithms with filtered regressor and filtered error,” *Mathematics of Control, Signals and Systems*, vol. 2, no. 4, pp. 381–403, Dec. 1989 (cit. on pp. 16, 34).
- [SLJB86] W. A. Sethares, D. A. Lawrence, C. Johnson, Jr., and R. R. Bitmead, “Parameter drift in LMS adaptive filters,” *IEEE Transactions on Acoustics, Speech, and Signal Processing*, vol. 34, no. 4, pp. 868–879, Aug. 1986 (cit. on pp. 21, 39, 40, 127).
- [SMA+88] W. A. Sethares, I. M. Y. Mareels, B. D. O. Anderson, C. R. Johnson, Jr., and R. R. Bitmead, “Excitation conditions for signed regressor least mean squares adaptation,” *IEEE Transactions on Circuits and Systems*, vol. 35, no. 6, pp. 613–624, Jun. 1988 (cit. on pp. 16, 38).
- [SW83] S. Shaffer and C. Williams, “Comparison of LMS, alpha LMS, and data reusing LMS algorithms,” in *Conference Record of the 17th Asilomar Conference on Circuits, Systems and Computers*, Pacific Grove (CA), USA, Nov. 1983, pp. 260–264 (cit. on p. 111).
- [She12] A. J. Shepherd, *Second-Order Methods for Neural Networks: Fast and Reliable Training Methods for Multi-Layer Perceptrons*. London, UK: Springer, 2012 (cit. on pp. 117, 118).

- [Sil07] D. D. Silveira, “Black-box modeling of microwave amplifiers for linearization,” Doctor’s Thesis, TU Wien, Vienna, Austria, Nov. 2007 (cit. on p. 2).
- [SS89a] T. Söderström and P. Stoica, *System Identification*. New York, NY, USA: Prentice-Hall, 1989 (cit. on p. 1).
- [SK95] V. Solo and X. Kong, *Adaptive Signal Processing Algorithms*, ser. Information and System Sciences. Englewood Cliffs, NJ, USA: Prentice-Hall, 1995 (cit. on pp. 16, 39).
- [SS89b] E. D. Sontag and H. J. Sussmann, “Backpropagation separates when perceptrons do,” in *Proceedings of the International Joint Conference on Neural Networks*, vol. 1, Washington, DC, USA, Jun. 1989, pp. 639–642 (cit. on p. 118).
- [Tab12] I. Tabatabaei Ardekani, “Stability analysis of adaptation process in FxLMS-based active noise control,” Doctor’s Thesis, University of Auckland, Auckland, New Zealand, Mar. 2012 (cit. on pp. 106, 108).
- [TA10] I. Tabatabaei Ardekani and W. H. Abdulla, “Theoretical convergence analysis of FxLMS algorithm,” *Signal Processing*, vol. 90, no. 12, pp. 3046–3055, Dec. 2010 (cit. on p. 106).
- [TA11] I. Tabatabaei Ardekani and W. H. Abdulla, “On the convergence of real-time active noise control systems,” *Signal Processing*, vol. 91, no. 5, pp. 1262–1274, May 2011 (cit. on p. 108).
- [TF88] M. Tarrab and A. Feuer, “Convergence and performance analysis of the normalized LMS algorithm with uncorrelated Gaussian data,” *IEEE Transactions on Information Theory*, vol. 34, no. 4, pp. 680–691, Jul. 1988 (cit. on pp. 15, 29).
- [Ung72] G. Ungerboeck, “Theory on the speed of convergence in adaptive equalizers for digital communication,” *IBM J. Res. Develop.*, vol. 16, no. 6, pp. 546–555, 1972 (cit. on p. 15).
- [vdS00] A. van der Schaft, *L_2 -Gain and Passivity Techniques in Nonlinear Control*, 2nd ed. London, UK: Springer, 2000 (cit. on p. 23).
- [Var62] R. S. Varga, *Matrix Iterative Analysis*. Englewood Cliffs, NJ, USA: Prentice-Hall, 1962 (cit. on p. 18).
- [VM06] L. Vicente and E. Masgrau, “Novel FxLMS convergence condition with deterministic reference,” *IEEE Transactions on Signal Processing*, vol. 54, no. 10, pp. 3768–3774, Oct. 2006 (cit. on p. 108).
- [Vid02] M. Vidyasagar, *Nonlinear Systems Analysis*, 2nd ed. Philadelphia, PA, USA: SIAM (unabridged republication of the work first published by Prentice-Hall, Englewood Cliffs (NJ), USA, 1993), 2002 (cit. on pp. 21–24).
- [VRM01] J. Vuolevi, T. Rahkonen, and J. Manninen, “Measurement technique for characterizing memory effects in RF power amplifiers,” *IEEE Transactions on Microwave Theory and Techniques*, vol. 49, no. 8, pp. 1383–1389, Aug. 2001 (cit. on p. 2).
- [Vuo01] J. Vuolevi, “Analysis, measurement and cancellation of the bandwidth and amplitude dependence of intermodulation distortion in RF power amplifiers,” Doctor’s Thesis, University of Oulu, Oulu, Finland, Nov. 2001 (cit. on p. 2).
- [WR99] A. K. Wang and W. Ren, “Convergence analysis of the multi-variable filtered-x LMS algorithm with application to active noise control,” *IEEE Transactions on Signal Processing*, vol. 47, no. 4, pp. 1166–1169, Apr. 1999 (cit. on p. 110).

- [WM79] A. Weiss and D. Mitra, "Digital adaptive filters: Conditions for convergence, rates of convergence, effects of noise and errors arising from the implementation," *IEEE Transactions on Information Theory*, vol. 25, no. 6, pp. 637–652, Nov. 1979 (cit. on p. 16).
- [Wer74] P. J. Werbos, "Beyond regression: New tools for prediction and analysis in the behavioral sciences," Doctor's Thesis, Harvard University, Cambridge, MA, USA, Nov. 1974 (cit. on p. 117).
- [Wer90] P. J. Werbos, "Backpropagation through time: What it does and how to do it," *Proceedings of the IEEE*, vol. 78, no. 10, pp. 1550–1560, Oct. 1990 (cit. on p. 117).
- [Wey49] H. Weyl, "Inequalities between the two kinds of eigenvalues of a linear transformation," *Proceedings of the National Academy of Sciences of the United States of America*, vol. 35, no. 7, p. 408, Jul. 1949 (cit. on p. 18).
- [WH60] B. Widrow and M. E. Hoff, "Adaptive switching circuits," in *IRE WESCON Convention Record*, vol. 4, Los Angeles, CA, USA, Aug. 1960, pp. 96–104 (cit. on pp. 13, 15, 128).
- [WL90] B. Widrow and M. A. Lehr, "30 years of adaptive neural networks: Perceptron, Madaline, and backpropagation," *Proceedings of the IEEE*, vol. 78, no. 9, pp. 1415–1442, Sep. 1990 (cit. on p. 15).
- [WSS81] B. Widrow, D. H. Shur, and S. Shaffer, "On adaptive inverse control," in *Conference Record of the 15th Asilomar Conference on Circuits, Systems and Computers*, Pacific Grove, CA, USA, Nov. 1981, pp. 185–189 (cit. on p. 106).
- [Wie58] N. Wiener, *Nonlinear Problems in Random Theory*. Cambridge, MA, USA: MIT Press, 1958 (cit. on p. 2).
- [Wig90] T. Wigren, "Recursive identification based on the nonlinear Wiener model," Doctor's Thesis, Uppsala University, Uppsala, Sweden, Dec. 1990 (cit. on p. 103).
- [Wig94] T. Wigren, "Convergence analysis of recursive identification algorithms based on the nonlinear Wiener model," *IEEE Transactions on Automatic Control*, vol. 39, no. 11, pp. 2191–2206, Nov. 1994 (cit. on p. 103).
- [Wig95] T. Wigren, "Approximate gradients, convergence and positive realness in recursive identification of a class of non-linear systems," *International Journal of Adaptive Control and Signal Processing*, vol. 9, no. 4, pp. 325–354, Jul. 1995 (cit. on p. 103).
- [Won53] Y. K. Wong, "An inequality for Minkowski matrices," *Proceedings of the American Mathematical Society*, vol. 4, no. 1, pp. 137–141, Feb. 1953 (cit. on p. 146).
- [Yam14] K. Yamaguchi, *mexopencv*, <http://www.cs.stonybrook.edu/~kyamagu/mexopencv>, Accessed: 17 February, 2014 (cit. on p. 9).
- [Zad56] L. Zadeh, "On the identification problem," *IRE Transactions on Circuit Theory*, vol. 3, no. 4, pp. 277–281, Dec. 1956 (cit. on p. 1).
- [Zam66] G. Zames, "On the input-output stability of time-varying nonlinear feedback systems Part I: Conditions derived using concepts of loop gain, conicity, and positivity," *IEEE Transactions on Automatic Control*, vol. 11, no. 2, pp. 228–238, Apr. 1966 (cit. on p. 22).
- [ZYC02] X. Zhang, Z.-P. Yang, and C.-G. Cao, "Inequalities involving Khatri-Rao products of positive semidefinite matrices," *Applied Mathematics E-Notes*, vol. 2, pp. 117–124, 2002 (cit. on p. 75).

- [ZD07] D. Zhou and V. DeBrunner, “Novel adaptive nonlinear predistorters based on the direct learning algorithm,” *IEEE Transactions on Signal Processing*, vol. 55, no. 1, pp. 120–133, Jan. 2007 (cit. on p. 2).
- [ZDG96] K. Zhou, J. C. Doyle, and K. Glover, *Robust and Optimal Control*. Upper Saddle River, NJ, USA: Prentice-Hall, 1996 (cit. on p. 21).
- [ZDH+08] A. Zhu, P. J. Draxler, C. Hsia, T. J. Brazil, D. F. Kimball, and P. M. Asbeck, “Digital predistortion for envelope-tracking power amplifiers using decomposed piecewise Volterra series,” *Microwave Theory and Techniques, IEEE Transactions on*, vol. 56, no. 10, pp. 2237–2247, Oct. 2008 (cit. on pp. 2, 16).
- [ZPB06] A. Zhu, J. C. Pedro, and T. J. Brazil, “Dynamic deviation reduction-based Volterra behavioral modeling of RF power amplifiers,” *IEEE Transactions on Microwave Theory and Techniques*, vol. 54, no. 12, pp. 4323–4332, Dec. 2006 (cit. on p. 16).
- [ZB98] A. M. Zoubir and B. Boashash, “The bootstrap and its application in signal processing,” *IEEE Signal Processing Magazine*, vol. 15, no. 1, pp. 56–76, Jan. 1998 (cit. on p. 9).
- [ZI07] A. M. Zoubir and D. R. Iskander, “Bootstrap methods and applications,” *IEEE Signal Processing Magazine*, vol. 24, no. 4, pp. 10–19, Jul. 2007 (cit. on p. 9).

Frequently used Symbols

Note that the following table contains only a subset of the most frequently used symbols. Additionally, it is complemented by Tables 4.1, 5.2, and 5.3, which summarise the symbols describing the coupled structure in Chapter 4, the MC-FXLMS in Section 5.3, and the multilayer perceptron in Section 5.4, respectively.

\mathbb{N}	set of natural numbers (excluding zero)
\mathbb{N}_0	set of non-negative integers
\mathbb{Z}	set of integers
\mathbb{R}	set of real numbers
\mathbb{R}_{0+}	set of non-negative real numbers
\mathbb{R}_+	set of positive real numbers
\mathbb{R}_-	set of negative real numbers
\mathbb{C}	set of complex numbers
$\mathcal{N}_{\text{field}}^{\text{dim}}(\cdot, \cdot)$	normal distribution, where the first argument specifies the mean, the second the variance; the subscript specifies the field of numbers, e.g., \mathbb{R} or \mathbb{C} ; an optional superscript indicates that a multivariate distribution of corresponding dimension is addressed, then, the second argument stands for the covariance matrix [MS00b]
$E\{.\}$	(probabilistic) expected value
d	differential
$\frac{\partial}{\partial}$	partial derivative
$\text{expr.} \Big _{\text{constr.}}$	evaluation of some expression under a given constraint
$\langle \cdot, \cdot \rangle$	constitutes a pair of its arguments
$\{.\}$	indicates a sequence of its argument
$ \cdot $	cardinality of a set; note that the absolute value is denoted by the same notation, the meaning should be clear from the context
\sup	supremum
\Leftrightarrow	logical equivalence
\triangleq	defined as
$>, \geq, <, \leq$	order relations; if operands are Hermitian matrices, they are understood in the sense of Löwner partial ordering [HJ13, Definition 7.7.1], e.g., with Hermitian matrices \mathbf{A} and \mathbf{B} , $\mathbf{A} > \mathbf{B}$ means that $\mathbf{A} - \mathbf{B}$ is positive definite
$\succ, \succcurlyeq, \prec, \preccurlyeq$	element by element order relations; the operands are required to have the same dimension

\Rightarrow	logical implication
$\cdot \mapsto \cdot$	“maps to”, i.e., left operand, the domain, is mapped to right operand, the image
$\cdot \rightarrow \cdot$	“towards”, i.e., left operand approaches right operand in the limit
\wedge	logical conjunction, i.e., binary logical operator “and”
\vee	logical inclusive disjunction, i.e., binary logical operator “or”
\forall	for all
j	$j \triangleq \sqrt{-1}$
\cdot^*	complex conjugate
\cdot^T	transpose of a vector or a matrix
\cdot^H	conjugate transpose of a vector or a matrix
\cdot^{-*}	matrix inverse of the complex conjugate of an invertible square matrix
\cdot^{-H}	matrix inverse of the conjugate transpose of an invertible square matrix
$\text{sign}(\cdot)$	returns (element by element) the sign of its argument
$\text{Re}\{\cdot\}$	(element by element) real part
$\text{Im}\{\cdot\}$	(element by element) imaginary part
$ \cdot $	(element by element) absolute value; note that the cardinality of a set is denoted by the same notation, the meaning should be clear from the context
$\text{arc}(\cdot)$	(element by element) complex argument
$\ \cdot\ $	Euclidean norm (2-norm)
$\ \cdot\ _p$	p -norm
$\ \cdot\ _{\mathbf{A}}$	weighted vector norm, with a positive definite weighting matrix \mathbf{A}
$\ \cdot\ _{\ell_p}$	ℓ_p -norm (cf. Section 2.4.2)
$\text{diag}_{i=i_{\text{start}}}^{i_{\text{stop}}}\{\cdot\}$	diagonal matrix obtained by placing its arguments along the main diagonal, top-left to bottom-right
$\text{col}\{\cdot\}$	The column operator stacks the elements of its argument list upon each other, where the first one is on top, the last at the bottom. The elements of the argument list are required to have the same number of columns. Hence, scalars and (column) vectors are allowed to occur in one single list, e.g., $\text{col}\{a, \mathbf{b}, \mathbf{c}\} = [a \ \mathbf{c}^T]^T$, with a being scalar and \mathbf{b} and \mathbf{c} (column) vectors of arbitrary size. Instead of an argument list, the operator may be written in the form of an indexed argument and a given index range.
$\text{row}\{\cdot\}$	The row operator generates a row from the elements of its argument list. It is analogous to the col-operator.
\oplus	the direct sum [GV96, p. 49]
$\bigoplus_{i=i_{\text{start}}}^{i_{\text{stop}}}$	operator version of the direct sum, it expands to a sequence of its arguments, joined together by $i_{\text{stop}} - i_{\text{start}}$ direct sums

\otimes	the Kronecker (tensor) product
\boxtimes	the Khatri-Rao product, a block-Kronecker product, (cf. Section 4.3)
$\prod_{i=i_{\text{start}}}^{\overleftarrow{i_{\text{stop}}}}$	product running from right to left, i.e., the element with index i_{start} is the right-most, the element with index i_{stop} the left-most
$\prod_{i=i_{\text{start}}}^{\overrightarrow{i_{\text{stop}}}}$	product running from left to right, i.e., the element with index i_{start} is the left-most, the element with index i_{stop} the right-most
\mathbf{I} or \mathbf{I}_M	identity matrix, i.e., all main diagonal entries are equal to one, all other elements are zero; the dimension of the matrix is either inherently given by the context or explicitly specified by a subscript M
$\mathbf{0}$ or $\mathbf{0}_{R \times C}$	all-zero matrix or column vector; its actual dimension is either inherently given by the context or explicitly specified by a subscript in the form $\mathbf{0}_{R \times C}$, where R represents the number of rows and C the number of columns
$\mathbf{1}$	all-ones column vector
$\text{span}\{.\}$	space spanned by its arguments
$. \parallel .$	left and right operand are in parallel
$. \perp .$	left and right operand are perpendicular; operands may be single vectors or whole vector spaces
$\text{tr}\{.\}$	trace of matrix
$\text{rank}\{.\}$	rank of matrix
$\lambda_i(.)$	i^{th} eigenvalue of matrix given as argument
$\mathbf{q}_i(.)$	i^{th} eigenvector of matrix given as argument
$S(.)$	spectral radius of the matrix given as argument; coincides with the maximum magnitude of its eigenvalues
$\mathcal{E}(.)$	the eigenspace corresponding to the eigenvalue given as argument
$\mathcal{M}(.)$	for an eigenvalue given as argument, this symbol represents the index set that contains the indices of all eigenvectors that span the eigenspace $\mathcal{E}(.)$ of the same eigenvalue (cf. proof of Lemma 3.9)
$\sigma_i(.)$	i^{th} singular value of matrix given as argument
k	iteration index, initialisation takes place at $k = -1$, calculations start at $k = 0$
\mathbf{B}_k	mapping matrix (cf. (2.16))
$\lambda_i(k)$	i^{th} eigenvalue of mapping matrix \mathbf{B}_k (cf. Section 3.3.1)
$\mathbf{q}_i(k)$	i^{th} eigenvector of mapping matrix \mathbf{B}_k (cf. Section 3.3.1)
$\sigma_i(k)$	i^{th} singular value of mapping matrix \mathbf{B}_k (cf. (2.28))
$\mathbf{r}_{i,k}$	left-sided singular vector of mapping matrix \mathbf{B}_k (cf. Section 2.3.1)
$\mathbf{t}_{i,k}$	right-sided singular vector of mapping matrix \mathbf{B}_k (cf. Section 2.3.1)

\mathbf{R}_k	unitary square matrix containing the left-sided singular vectors of mapping matrix \mathbf{B}_k (cf. (2.28))
\mathbf{T}_k	unitary square matrix containing the right-sided singular vectors of mapping matrix \mathbf{B}_k (cf. (2.28))
\mathbf{u}_k	excitation vector
$\mathbf{e}_{\mathbf{u}_k}$	unit vector pointing in direction of excitation vector \mathbf{u}_k
$\mathbf{U}_{\mathbf{M},k}^{(K)}$	excitation matrix considering the K preceding iteration steps (cf. (2.26))
\mathbf{x}_k	regression vector
$\mathbf{e}_{\mathbf{x}_k}$	unit vector pointing in direction of regression vector \mathbf{x}_k
w_i	one single parameter of the reference system
$\hat{w}_i(k)$	one single parameter of the system model
\mathbf{w}	parameter vector of the reference system, assumed to be constant throughout the work (cf. (2.1), Figure 2.1)
$\hat{\mathbf{w}}_k$	parameter vector of the system model (cf. (2.2), Figure 2.1)
$\tilde{\mathbf{w}}_k$	parameter error vector, defined as $\tilde{\mathbf{w}}_k \triangleq \mathbf{w} - \hat{\mathbf{w}}_k$ (cf. (2.10), Figure 2.1)
$\mathbf{e}_{\tilde{\mathbf{w}}_k}$	unit vector pointing in direction of parameter error vector $\tilde{\mathbf{w}}_k$
$\mathbf{e}_{\mathbf{D}_k \tilde{\mathbf{w}}_{k-1}}$	unit vector pointing in direction of $\mathbf{D}_k \tilde{\mathbf{w}}_{k-1}$
$\tilde{\mathbf{w}}$	in text parts with suppressed iteration index k , $\tilde{\mathbf{w}}$ is synonymous for $\tilde{\mathbf{w}}_{k-1}$
$\mathbf{e}_{\tilde{\mathbf{w}}}$	unit vector pointing in direction of parameter error vector $\tilde{\mathbf{w}}$, hence, it is equivalent to $\mathbf{e}_{\tilde{\mathbf{w}}_{k-1}}$
$\tilde{w}_i(k)$	one entry of parameter error vector $\tilde{\mathbf{w}}_k$
\tilde{w}_i	in text parts with suppressed iteration index k , \tilde{w}_i is synonymous for $\tilde{w}_i(k-1)$
$\mathcal{S}_{\mathbf{u}_k^*, \mathbf{x}_k^*}$	hyperplane spanned by \mathbf{u}_k^* and \mathbf{x}_k^* (cf. (3.18))
$\mathcal{S}_{\mathbf{u}_k^*, \mathbf{x}_k^*}^\perp$	space orthogonal to hyperplane $\mathcal{S}_{\mathbf{u}_k^*, \mathbf{x}_k^*}$ (cf. (3.20))
$\mathcal{S}_{\tilde{\mathbf{w}}_{k-1}^*, \mathbf{D}_k \tilde{\mathbf{w}}_{k-1}^*}$	hyperplane spanned by $\tilde{\mathbf{w}}_{k-1}^*$ and $\mathbf{D}_k \tilde{\mathbf{w}}_{k-1}^*$, with diagonal step-size matrix \mathbf{D}_k (cf. (3.74))
$\mathcal{S}_{\tilde{\mathbf{w}}_{k-1}^*, \mathbf{D}_k \tilde{\mathbf{w}}_{k-1}^*}^\perp$	space orthogonal to hyperplane $\mathcal{S}_{\tilde{\mathbf{w}}_{k-1}^*, \mathbf{D}_k \tilde{\mathbf{w}}_{k-1}^*}$ (cf. (3.75))
$J(\cdot)$	cost function (cf. Section 2.1)
$m(\cdot)$	parameter mismatch (cf. (2.19))
$W(k)$	parameter error increment $W(k) \triangleq \ \tilde{\mathbf{w}}_k\ ^2 - \ \tilde{\mathbf{w}}_{k-1}\ ^2$ (cf. (2.41))
$v(k)$	additive noise (cf. Figure 2.1)
$d(k)$	noiseless response of reference system, i.e., $d(k) \triangleq \mathbf{w}^\top \mathbf{u}_k$ (cf. (2.20), Figure 2.1)
$\tilde{d}(k)$	noisy response of reference system, i.e., $\tilde{d}(k) \triangleq d(k) + v(k)$ (cf. Figure 2.1)
$\hat{d}(k)$	response of system model, i.e., $\hat{d}(k) \triangleq \hat{\mathbf{w}}_{k-1}^\top \mathbf{u}_k$ (cf. (2.20), Figure 2.1)

$e(k)$	noiseless a priori error between the response of the reference system and the response of the system model, i.e., $e(k) \triangleq d(k) - \hat{d}(k) = \mathbf{w}^\top \mathbf{u}_k - \hat{\mathbf{w}}_{k-1}^\top \mathbf{u}_k = \tilde{\mathbf{w}}_{k-1}^\top \mathbf{u}_k$
$\tilde{e}(k)$	noisy error between the response of the reference system and the response of the system model, i.e., $\tilde{e}(k) \triangleq \tilde{d}(k) - \hat{d}(k) = e(k) + v(k)$ (cf. (2.3), Figure 2.1)
$\mu(k)$	scalar step-size
$\bar{\mu}$	normalised step-size (cf. (3.2))
\mathbf{M}_k	general step-size matrix
\mathbf{D}_k	diagonal step-size matrix (cf. (3.1))
$d_i(k)$	diagonal elements of step-size matrix \mathbf{D}_k
$\alpha(k)$	effective step-size (cf. (3.11) and (3.60))
$\rho(k)$	correlation coefficient (cf. (3.12) and (3.61))
$\varphi_{\alpha\rho^*}(k)$	complex argument among $\rho^*(k)$ and $\alpha(k)$ (cf. (3.13))
$\psi_i(\cdot)$	i^{th} non-linear basis function $\psi_i : \mathbb{R} \mapsto \mathbb{R}$ (cf. Sections 2.2.1.3 and 5.2)
$\boldsymbol{\psi}(\cdot)$	vector of non-linear basis functions, evaluated at given scalar argument (cf. (5.30))
$\Theta_{\mathbf{D}}(\mathbf{x})$	(acute) angle enclosed by some vector \mathbf{x} and its image $\mathbf{D}\mathbf{x}$, with $\mathbf{D} \geq \mathbf{0}$ (cf. (3.83))

Acronyms

ANC	active noise control
APA	affine projection algorithm
BSD	Berkeley Software Distribution
DPD	digital pre-distortion
FIR	finite impulse response
FXLMS	filtered- x LMS
I/O	input/output
iff	if and only if
IIR	infinite impulse response
LMS	least-mean-squares
LUT	look-up table
MC-FXLMS	multichannel filtered- x LMS
MIMO	multiple input multiple output
MISO	multiple input single output
NLMS	normalised least-mean-squares
OpenCV	Open Source Computer Vision Library
PAP	pseudo affine projection
pdf	probability density function
PE	persistent excitation
PNLMS	proportionate normalised LMS
QPSK	quadrature phase shift keying
RLS	recursive-least-squares
SIMO	single input multiple output
SISO	single input single output
SPR	strict positive realness
SR-LMS	signed regressor LMS
s.t.	subject to
SVD	singular value decomposition
w.c.	worst case
wo.l.o.g.	without loss of generality

Index

A

antieigenvalue 52, 53, 59, 145
activation function 117, 118, 120
activation level 118, 120, 121
second-order gradient algorithm 14, 32
asymmetric algorithm v, vii, 3–7, 14, 20–22, 27, 28, 32, 38–41, 44, 45, 50–52, 55, 56, 66, 69, 74, 86, 88, 93, 101, 105, 106, 111, 114, 115, 120, 125–128
generalised gradient descent algorithm 14
Gauß-Newton algorithm 27, 39, 102
symmetric algorithm v, vii, 3, 4, 14, 55, 69, 88, 90, 99, 105, 111, 114–116, 120, 126
averaged LMS 110, 112
accumulated matrix deviation 31, 32
active noise control (ANC) v, vii, 3, 5, 7, 69, 93, 106, 108, 128
affine projection algorithm (APA) 27
a priori error v, vii, 3, 4, 13, 25, 40, 69, 70, 72, 79–81, 84, 85, 104, 105, 108, 123, 180
uniform asymptotic stability in the large 22
autonomous 17, 18, 20, 34, 38

B

backpropagation algorithm v, vii, 3, 5, 7, 93, 117, 118, 120–123, 125
Berkeley Software Distribution (BSD) 9

C

correlation coefficient 40, 41, 43, 44, 47, 52, 129, 130, 132, 151, 180
cross-entropy cost function 118, 121
coupling factor 70, 72, 81, 82, 85, 86, 88–90, 93, 95, 96, 98, 99, 101, 105, 112, 113, 157, 159
Cholesky factorisation 50
confidence interval 9, 29, 32, 34, 38, 64, 99, 101
cancelling loudspeaker 93, 106, 108, 110, 112

D

direct sum 77, 90, 157
Douglas-Peucker 9
parameter error increment 20, 29, 45–48, 51, 53–55, 57, 179
digital pre-distortion (DPD) v, vii, 2, 125
data-reusing LMS 110

E

error microphone 93, 106, 108, 110, 112, 114, 115
eigenspace v, vii, 3, 4, 41, 51, 53–56, 126, 127, 151, 153, 154, 156, 178

effective step-size 40, 43, 44, 46, 47, 49, 52–54, 60, 129–131, 151, 180
envelope tracking 2
eigenvalue 8, 16–19, 28, 34, 38, 40, 41, 48, 50, 51, 53–56, 63, 75, 87, 106, 112, 127, 139, 145–147, 151, 154–156, 159, 177, 178
eigendecomposition 50
exponential stability 34, 38, 118

F

finite impulse response (FIR) ix, 3, 15, 64, 96, 98, 101–103
filtered- x LMS (FXLMS) 5, 106, 108, 110, 112

G

Gaussian elimination 72, 74
Gramian matrix 17, 41, 154, 157
gradient type algorithm v, vii, 1–6, 11–13, 15–17, 27, 31, 34, 40, 46–48, 50, 51, 69, 72, 90, 94–97, 99, 101, 103, 104, 120, 125, 126, 128

H

Hadamard product 4, 75
Hermitian matrix 18, 32, 41, 49, 50, 56, 75, 90, 114, 155, 159, 177
higher order LMS 110
homogeneous v, vii, 4, 11, 17, 20–22, 28, 49, 51, 85, 95, 111, 115, 118, 126, 127

I

independence assumptions 103
identical error 3, 20, 69, 88, 93, 105, 125, 126, 128
if and only if (iff) 18, 41, 47, 54, 86, 90, 95, 111, 133, 142, 155, 159
infinite impulse response (IIR) 39, 40, 102
input-output stability 22, 23, 69, 78, 85
iteration step 14, 34, 50, 51, 53, 78

K

Kantorovich inequality 53, 146
Khatri-Rao product v, vii, 4, 69, 74–77, 85, 86, 155, 177
Kronecker product 75, 76, 154, 155, 177

L

ℓ_2 -stability v, vii, 3–7, 20, 24, 25, 29, 32, 39, 69, 72, 74, 78, 80–82, 84, 85, 89, 93–95, 97, 99, 105, 106, 110–112, 114–116, 118, 123, 126, 127, 145
linear combiner 14, 15, 28, 101
Leontief's input-output analysis 72

- least-mean-squares (LMS) v, vii, 1–4, 12–14, 20, 21, 24, 25, 27–29, 31, 32, 39, 55, 69, 70, 72, 78, 79, 103, 106, 111, 112, 114, 125, 127
- law of cosines 150
- leading principal minor 74, 145–147
- ℓ_p -space 22, 23
- ℓ_p -stability 21, 23, 80
- look-up table (LUT) 101
- Lyapunov 22, 32
- ## M
- parameter mismatch 14, 29, 31, 64, 99, 101, 179
- positive definite 33, 45, 46, 49–51, 55, 56, 59, 116, 145, 146, 152
- mapping matrix v, 4, 7, 8, 13, 14, 17, 19, 28, 34, 38, 40, 41, 44, 45, 47, 48, 50–52, 66, 86, 87, 101, 114, 115, 118, 129, 130, 157, 159, 178
- Monte Carlo 9, 29, 33, 38, 98, 127, 128
- mixing condition 16
- main coupling factor 70, 78, 94
- multichannel filtered- x LMS (MC-FXLMS) v, vii, x, 3, 5, 7, 27, 69, 93, 106–116, 125, 128, 177
- excitation matrix 16, 34, 38, 116, 178
- multiple input multiple output (MIMO) x, 5, 106, 108, 110, 112, 114–116
- Minkowsky inequality 24, 79–81, 84, 127, 159
- minor 145, 147
- multiple input single output (MISO) x, 5, 110, 112–115
- multilayer perceptron v, 3, 5, 7, 93, 117, 118, 120–123, 125, 177
- M -matrix v, vii, 4, 7, 74, 126, 145–147
- system model 1, 2, 4, 8, 11, 12, 14, 28, 39, 40, 69, 72, 98, 101, 102, 118, 179, 180
- matrix step-size v, vii, 2–4, 6, 14, 27–29, 31, 32, 39, 45, 46, 49, 50, 53, 55, 66, 90, 101, 125, 127
- mean value theorem 104, 121
- ## N
- nonautonomous 13, 17, 19, 34, 85
- non-Hermitian matrix 18, 19, 56
- nonhomogeneous 11, 13, 20
- normalised least-mean-squares (NLMS) 29, 31, 99, 101
- neural network 7, 69, 93, 117, 118, 120, 124
- normal matrix 45, 50, 51, 56, 64, 66, 67, 88–90, 123, 128, 151, 156
- non-stalling adaptation 32, 47, 48, 54, 56
- parameter error distance 18, 21, 28, 29, 34, 40, 44–47, 49, 53–57, 62, 64, 69, 85, 86, 98, 101, 126, 153
- ## O
- Open Source Computer Vision Library (OpenCV) 9
- operator trigonometry 4, 7, 52, 59, 145
- ## P
- power amplifier v, vii, 2
- pseudo affine projection (PAP) 27, 39
- parameter drift 20, 21, 39, 40, 127
- pre-distorter 2
- probability density function (pdf) 15, 29, 38
- persistent excitation (PE) ix, 11, 14, 16, 20, 32, 34, 38, 40, 55, 118, 127
- principal minor 146, 147
- proportionate normalised LMS (PNLMS) 27, 39
- primary path 106, 108, 112
- principal submatrix 147
- piecewise linear 15
- ## Q
- quadrature phase shift keying (QPSK) 98, 99, 101
- ## R
- recursion 18, 19
- reference system 1, 2, 8, 11, 12, 14, 15, 39, 40, 69, 70, 72, 98, 101, 102, 105, 108, 118, 126, 127, 178–180
- recursive-least-squares (RLS) 27, 39
- reference microphone 93, 106, 108, 110, 112
- Rayleigh quotient 52, 145, 153
- ## S
- squared error cost function 121
- excitation sequence vii, 3, 4, 6, 11, 12, 14–16, 28, 34, 38, 39, 44, 56, 66, 96, 98, 99, 125, 127
- small gain theorem 39, 106
- system identification 1–3, 8, 11, 12, 15, 21, 27, 101, 102, 118, 127
- single input multiple output (SIMO) x, 5, 108, 110–112, 114
- single input single output (SISO) 15, 101, 106, 112
- stimulus level 118, 120, 124
- system of linear difference equations 13, 17, 111, 115, 145
- switched linear system 38
- submatrix 7, 75, 77, 145, 147, 156
- Sherman-Morrison-Woodbury formula 129
- secondary path 5, 106, 108, 110, 112, 128
- strict positive realness (SPR) 39
- spectral radius 18, 38, 41, 49, 101, 146, 159, 178
- sufficient richness condition 16
- signed regressor LMS (SR-LMS) 27, 38, 55, 57
- step-size 2, 4, 12, 24, 28, 29, 32–34, 38, 41, 49, 51, 53–56, 66, 72, 88, 90, 95, 98, 99, 101, 103–106, 108, 111–115, 118, 120, 150, 153, 159, 180
- step-size matrix v, vii, 3, 4, 12, 13, 24, 27, 29, 31–34, 39, 40, 45, 46, 49–57, 59, 60, 64, 66, 67, 70, 101, 106, 108, 111, 114–116, 120, 126, 127, 151–154, 179, 180
- subject to (s.t.) 141
- slow time variation lemma 34, 118
- singular value v, vii, 4, 7, 8, 17–20, 28, 40, 42–45, 47, 48, 50, 51, 66, 75, 86–88, 90, 116, 129, 130, 133–136, 147, 151, 154–159, 178
- singular value decomposition (SVD) ix, 17, 41, 43, 44, 48
- ## T
- triangle inequality 21, 79–81, 127

U

uniform stability 21, 22
 unitary invariance 47
 unitary matrix 48, 50, 51, 156, 178

V

antieigenvector 52, 53, 145, 146
 eigenvector 8, 17, 41, 51, 52, 63, 87, 140, 145, 151, 156, 157, 178
 excitation vector 3, 4, 12, 14–16, 27, 29, 31, 32, 34, 38, 40, 41, 45–49, 51–55, 57, 58, 62, 64, 66, 67, 69, 70, 72, 85, 86, 88, 90, 96, 98, 103, 108, 111, 115, 116, 127, 128, 153, 154, 157, 158, 178
 Vieta's formula 129, 130
 motion vector 22
 Volterra Series 16, 101
 parameter vector 3, 8, 11, 14–16, 21, 27, 28, 70, 72, 98, 104, 106, 108, 110, 115, 126, 127, 179
 parameter error vector 3–5, 7, 8, 13, 14, 19–21, 31–33, 38–41, 44–49, 51, 53–56, 60, 69, 70, 72, 74, 80, 82,

86, 88, 90, 93, 95, 99, 103, 106, 108, 110, 111, 113, 115, 116, 126, 127, 149, 152, 179
 regression vector vii, 3, 4, 13, 14, 27, 34, 38, 40, 41, 44–49, 51, 52, 54, 55, 57, 66, 88, 116, 128, 149, 178
 singular vector 8, 40, 42, 43, 45, 48, 66, 157
 left-sided singular vector 17, 42, 66, 178
 right-sided singular vector 17, 19, 42, 48, 66, 178
 state vector 38

W

worst case (w.c.) v, vii, ix, x, 3, 4, 6, 7, 20, 27–29, 31, 33, 34, 38, 44–48, 55–59, 61, 63–67, 98, 99, 101, 106, 125, 127, 128, 150
 Wielandt inequality 63, 146
 Wiener model v, vii, 2–4, 7, 27, 93, 101–103, 106, 123, 125, 128
 without loss of generality (wo.l.o.g.) 17, 19, 42, 43, 49, 63, 74, 88, 90, 157, 158

Z

Z-matrix 72, 74

Errata

In the sequel, important errors and typos are addressed, which occurred in the approved and printed version of this thesis.

Erratum 1 (p. 22)

In the explanation following Definition 2.2, the use of ε and $\delta(\varepsilon)$ is confused. The first sentence has to be reworded to

Thus, a uniformly stable equilibrium $\tilde{\mathbf{w}}_e$ ensures that for any sufficiently close initial state $\tilde{\mathbf{w}}_{-1}$, with a distance to $\tilde{\mathbf{w}}_e$ that is not larger than $\delta(\varepsilon)$, trajectory $\mathbf{s}_k(\tilde{\mathbf{w}}_{-1})$ remains bounded within an M -dimensional ball of finite radius ε .

Erratum 2 (p. 25)

The actual relation that is used to get from (2.58) to (2.59) is not the Minkowsky inequality, but instead, the fact that the 1-norm of a vector always upper bounds its 2-norm (cf. (E.8)).

Erratum 3 (p. 42)

It is not correct that the matrix in (3.17) is the Hermitian of (3.16). The sentence before (3.16) and (3.17) has to be modified to

The general structure of the mapping matrix for asymmetric algorithm in (2.16) leads to the following expressions for the Gramian of the columns, respectively the rows, of \mathbf{B} ...

Erratum 4 (p. 53)

The denominator of the right-hand side expression in (3.66) has to be corrected to $d_{\min}(k) + d_{\max}(k)$.

Erratum 5 (p. 55)

The claim of Theorem 3.2 goes too far, as its proof is not able to justify it up to its whole extent. The theorem has to be loosened to (changes are typeset in *italics*)

If (3.15) is satisfied, and the step-size matrix is positive definite and constant, i.e., $\mathbf{D}_k = \mathbf{D}$, with its minimum and maximum eigenvalue, d_{\min} and d_{\max} , defined by (3.67), then, under worst case (w.c.) excitation, parameter error vector $\tilde{\mathbf{w}}_k$ converges *asymptotically to the union of all eigenspaces* $\mathcal{E}(d_i)$, for which

$$\alpha(k) \leq 2 \frac{d_i}{d_{\max}}. \tag{E.2}$$

This page did not exist in the originally approved version of this thesis.

Erratum 6 (p. 59)

The order of terms in (3.83) is broken, the correct form is given by

$$0 < \bar{\lambda}_1(\mathbf{D}) \triangleq \frac{2\sqrt{d_1 d_M}}{d_1 + d_M} \leq \cos(\Theta_{\mathbf{D}}(\mathbf{e}_{\tilde{\mathbf{w}}})) \triangleq \frac{\|\mathbf{D}^{1/2} \mathbf{e}_{\tilde{\mathbf{w}}}\|^2}{\|\mathbf{D} \mathbf{e}_{\tilde{\mathbf{w}}}\|} \leq 1. \quad (\text{E.3})$$

Consequently, the two sentences following (3.83) have to be reformulated to

The bound on the left-hand side of the cosine corresponds to the first antieigenvalue $\bar{\lambda}_1(\mathbf{D})$ of step-size matrix \mathbf{D} . It is always positive since \mathbf{D} is assumed to be positive definite.

Moreover, (3.84) can be confined to

$$0 \leq |\Theta_{\mathbf{D}}(\mathbf{e}_{\tilde{\mathbf{w}}})| < \arccos(\bar{\lambda}_1(\mathbf{D})) < \frac{\pi}{2}. \quad (\text{E.4})$$

Erratum 7 (p. 80)

On page 80, it is said that (4.41) is obtained from (4.40) by combined application of the triangle and the Minkowsky inequality. As the latter just generalises the former to any p -norm [MS00b, p. 871], bellow, it is clarified that indeed only the triangle inequality in its basic form is required here. However, instead, an additional relation among the 1-norm and the 2-norm of a vector has to be applied. As a consequence, (4.41) has to be modified slightly.

Defining the two sequences for $k \geq 0$

$$a_i(k) \triangleq \sum_{j \in \mathcal{N} \setminus \{i\}} \frac{\nu_{ij}(k)}{\sqrt{\nu_{ii}(k)}} e_j(k), \quad b_i(k) \triangleq \sum_{j \in \mathcal{N}} \frac{\nu_{ij}(k)}{\sqrt{\nu_{ii}(k)}} v_j(k), \quad (\text{E.5})$$

(4.40) is equivalent to

$$\sqrt{\sum_{k=0}^K \nu_{ii}(k) |e_i(k)|^2} \leq \|\tilde{\mathbf{w}}_{i,-1}\| + \sqrt{\sum_{k=0}^K |a_i(k) + b_i(k)|^2}. \quad (\text{E.6})$$

Thus, due to the triangle inequality, an upper bound is given by

$$\sqrt{\sum_{k=0}^K \nu_{ii}(k) |e_i(k)|^2} \leq \|\tilde{\mathbf{w}}_{i,-1}\| + \sqrt{\sum_{k=0}^K |a_i(k)|^2} + \sqrt{\sum_{k=0}^K |b_i(k)|^2}. \quad (\text{E.7})$$

In order to end up at (4.41), property¹ [GV96, p. 53]

$$\|\mathbf{v}\| \leq \|\mathbf{v}\|_1 \leq \sqrt{N} \|\mathbf{v}\|, \quad (\text{E.8})$$

is consulted, which allows to bound the 1-norm of some N -dimensional vector $\mathbf{v} \in \mathbb{C}^N$ by its 2-norm,

¹ Note that in this thesis the symbol $\|\cdot\|$ without any subscript denotes the 2-norm.

leading to

$$|a_i(k)| = \left| \sum_{j \in \mathcal{N} \setminus \{i\}} \frac{\nu_{ij}(k)}{\sqrt{\nu_{ii}(k)}} e_j(k) \right| \leq \sum_{j \in \mathcal{N} \setminus \{i\}} \left| \frac{\nu_{ij}(k)}{\sqrt{\nu_{ii}(k)}} e_j(k) \right| \leq \sqrt{N-1} \sqrt{\sum_{j \in \mathcal{N} \setminus \{i\}} \left| \frac{\nu_{ij}(k)}{\sqrt{\nu_{ii}(k)}} e_j(k) \right|^2}, \quad (\text{E.9})$$

$$|b_i(k)| = \left| \sum_{j \in \mathcal{N}} \frac{\nu_{ij}(k)}{\sqrt{\nu_{ii}(k)}} v_j(k) \right| \leq \sum_{j \in \mathcal{N}} \left| \frac{\nu_{ij}(k)}{\sqrt{\nu_{ii}(k)}} v_j(k) \right| \leq \sqrt{N} \sqrt{\sum_{j \in \mathcal{N}} \left| \frac{\nu_{ij}(k)}{\sqrt{\nu_{ii}(k)}} v_j(k) \right|^2}. \quad (\text{E.10})$$

Inserting (E.9) and (E.10) in (E.7), results in

$$\begin{aligned} & \sqrt{\sum_{k=0}^K \nu_{ii}(k) |e_i(k)|^2} \\ & \leq \|\tilde{\mathbf{w}}_{i,-1}\| + \sqrt{N-1} \sqrt{\sum_{k=0}^K \sum_{j \in \mathcal{N} \setminus \{i\}} \frac{|\nu_{ij}(k)|^2}{\nu_{ii}(k)} |e_j(k)|^2} + \sqrt{N} \sqrt{\sum_{k=0}^K \sum_{j \in \mathcal{N}} \frac{|\nu_{ij}(k)|^2}{\nu_{ii}(k)} |v_j(k)|^2}, \quad (\text{E.11}) \end{aligned}$$

which corrects (4.41).

Erratum 8 (p. 81)

In (4.50), the right-hand side has to be multiplied by number N of coupled gradient type algorithms, in Eqs. (4.51) to (4.53) and (4.57) by \sqrt{N} . This can be seen, starting with the left-hand side of (4.9), i.e.,

$$\varepsilon_i(k) \triangleq \sum_{j \in \mathcal{N}} \nu_{ij}(k) e_j(k). \quad (\text{E.12})$$

Hence, the squared magnitude of update error $\varepsilon_i(k)$ can be bounded from above by

$$|\varepsilon_i(k)|^2 = \left| \sum_{j \in \mathcal{N}} \nu_{ij}(k) e_j(k) \right|^2 \leq \left(\sum_{j \in \mathcal{N}} |\nu_{ij}(k)| |e_j(k)| \right)^2 \leq N \sum_{j \in \mathcal{N}} |\nu_{ij}(k)|^2 |e_j(k)|^2, \quad (\text{E.13})$$

where validity of the final step can either be verified by Young's inequality² [Nas99, p. 257] or by property (E.8).

² G. H. Hardy, J. E. Littlewood, and G. Pólya, *Inequalities*, 2nd ed. Cambridge, UK: Cambridge University Press, 1997.

Erratum 9 (p. 82)

Errata 7 and 8 require a slight modification of Theorem 4.1. This is, as the changes of (4.41), introduced by Erratum 7, analogously apply to (4.47), i.e.,

$$\begin{aligned} & \sqrt{\sum_{k=0}^K |e_i(k)|^2} \\ & \leq \frac{\|\tilde{\mathbf{w}}_{i,-1}\|}{\sqrt{\tilde{\nu}_{ii}(K)}} + \sqrt{N-1} \sum_{j \in \mathcal{N} \setminus \{i\}} \frac{\hat{\eta}_{ij}(K)}{\sqrt{\tilde{\nu}_{ii}(K)}} \sqrt{\sum_{k=0}^K |e_j(k)|^2} + \sqrt{N} \sum_{j \in \mathcal{N}} \frac{\hat{\eta}_{ij}(K)}{\sqrt{\tilde{\nu}_{ii}(K)}} \sqrt{\sum_{k=0}^K |v_j(k)|^2}. \end{aligned} \quad (\text{E.14})$$

Modifying the definition of coupling matrix $\bar{\Delta}_K$ in (4.65), which establishes the relation among absolute energies, to

$$\bar{\Delta}_K \triangleq \begin{bmatrix} \frac{1}{\sqrt{N-1}} & -\frac{\hat{\eta}_{12}(K)}{\sqrt{\tilde{\nu}_{11}(K)}} & \cdots & -\frac{\hat{\eta}_{1N}(K)}{\sqrt{\tilde{\nu}_{11}(K)}} \\ -\frac{\hat{\eta}_{21}(K)}{\sqrt{\tilde{\nu}_{22}(K)}} & \frac{1}{\sqrt{N-1}} & \cdots & -\frac{\hat{\eta}_{2N}(K)}{\sqrt{\tilde{\nu}_{22}(K)}} \\ \vdots & \vdots & \ddots & \vdots \\ -\frac{\hat{\eta}_{N1}(K)}{\sqrt{\tilde{\nu}_{NN}(K)}} & -\frac{\hat{\eta}_{N2}(K)}{\sqrt{\tilde{\nu}_{NN}(K)}} & \cdots & \frac{1}{\sqrt{N-1}} \end{bmatrix}, \quad (\text{E.15})$$

for $N \geq 2$, the set of inequalities in (4.49) changes slightly to

$$\bar{\Delta}_K \mathbf{e}_K \preceq \frac{1}{\sqrt{N-1}} \check{\mathbf{D}}_{\nu,K}^{-1} \boldsymbol{\omega}_{-1} + \sqrt{\frac{N}{N-1}} \left(\check{\mathbf{D}}_{\nu,K}^{-1} \hat{\mathbf{D}}_{\nu,K} + \frac{1}{\sqrt{N-1}} \mathbf{I} - \bar{\Delta}_K \right) \mathbf{v}_K. \quad (\text{E.16})$$

Then, together with factor \sqrt{N} , introduced due to Erratum 8, and redefinition of the bounding matrix for absolute energies to

$$\hat{\Delta}_{\eta,K} \triangleq \sqrt{N-1} \hat{\mathbf{D}}_{\nu,K} + \check{\mathbf{D}}_{\nu,K} (\mathbf{I} - \bar{\Delta}_K), \quad (\text{E.17})$$

(4.56) and (4.57) become

$$\mathbf{e}_K \preceq \frac{1}{\sqrt{N-1}} \bar{\Delta}_K^{-1} \check{\mathbf{D}}_{\nu,K}^{-1} \left(\boldsymbol{\omega}_{-1} + \sqrt{\frac{N}{N-1}} \hat{\Delta}_{\eta,K} \mathbf{v}_K \right), \quad (\text{E.18})$$

and

$$\varepsilon_K \preceq \sqrt{\frac{N}{N-1}} \hat{\Delta}_{\nu,K} \bar{\Delta}_K^{-1} \check{\mathbf{D}}_{\nu,K}^{-1} \left(\boldsymbol{\omega}_{-1} + \sqrt{\frac{N}{N-1}} \hat{\Delta}_{\eta,K} \mathbf{v}_K \right). \quad (\text{E.19})$$

Erratum 10 (p. 84)

As a consequence of the missing factor addressed by Erratum 8, also the right-hand side of (4.72) has to be multiplied by N , the right-hand sides of (4.73), (4.74), and (4.78) by \sqrt{N} .

Erratum 11 (p. 85)

Analogous to the explanation in Erratum 7, (4.69) has to be modified to

$$\sqrt{\sum_{k=0}^K \nu_{ii}(k) |e_i(k)|^2} \leq \|\tilde{\mathbf{w}}_{i,-1}\| + \sqrt{N-1} \sqrt{\sum_{k=0}^K \sum_{j \in \mathcal{N} \setminus \{i\}} \frac{|\nu_{ij}(k)|^2}{\nu_{ii}(k)\nu_{jj}(k)} \nu_{jj}(k) |e_j(k)|^2} + \sqrt{N} \sqrt{\sum_{k=0}^K \sum_{j \in \mathcal{N}} \frac{|\nu_{ij}(k)|^2}{\nu_{ii}(k)\nu_{jj}(k)} \nu_{jj}(k) |v_j(k)|^2}, \quad (\text{E.20})$$

which turns (4.71) into

$$\bar{\Delta}'_K \mathbf{e}_K \preceq \frac{1}{\sqrt{N-1}} \boldsymbol{\omega}_{-1} + \sqrt{\frac{N}{N-1}} \left[\bar{\Delta}'_K + \left(1 - \frac{1}{\sqrt{N-1}}\right) \mathbf{I} \right] \mathbf{v}_K, \quad (\text{E.21})$$

where in a way similar to (E.15), matrix $\bar{\Delta}'_K$, which relates the weighted error energies, originally defined in (4.59), is redefined to

$$\bar{\Delta}'_K \triangleq \begin{bmatrix} \frac{1}{\sqrt{N-1}} & -\hat{\eta}'_{12}(K) & \cdots & -\hat{\eta}'_{1N}(K) \\ -\hat{\eta}'_{21}(K) & \frac{1}{\sqrt{N-1}} & \cdots & -\hat{\eta}'_{2N}(K) \\ \vdots & \vdots & \ddots & \vdots \\ -\hat{\eta}'_{N1}(K) & -\hat{\eta}'_{N2}(K) & \cdots & \frac{1}{\sqrt{N-1}} \end{bmatrix}. \quad (\text{E.22})$$

Introducing the bounding matrix for absolute energies, originally specified in (4.60), slightly different, as

$$\hat{\Delta}'_{\eta,K} \triangleq \sqrt{N} \left[\bar{\Delta}'_K + \left(1 - \frac{1}{\sqrt{N-1}}\right) \mathbf{I} \right], \quad (\text{E.23})$$

(4.77) modifies to

$$\mathbf{e}'_K \preceq \frac{1}{\sqrt{N-1}} \bar{\Delta}'_K^{-1} \left(\boldsymbol{\omega}_{-1} + \hat{\Delta}'_{\eta,K} \mathbf{v}'_K \right). \quad (\text{E.24})$$

Then, according to Erratum 10, taking the missing factor \sqrt{N} into account, (4.78) becomes

$$\boldsymbol{\varepsilon}_K \preceq \frac{1}{\sqrt{N-1}} \hat{\mathbf{D}}_{\nu,K} \hat{\Delta}'_{\eta,K} \bar{\Delta}'_K^{-1} \left(\boldsymbol{\omega}_{-1} + \hat{\Delta}'_{\eta,K} \mathbf{v}'_K \right). \quad (\text{E.25})$$

Erratum 12 (p. 87)

The proof of Lemma 4.5 in Appendix D.2.5 is correct. However, (4.90) and (4.91) do not agree with it. Equation (4.90) should have the form

$$0 \leq \frac{1}{2} |\lambda_i(\boldsymbol{\Delta}_k)|^2 \mathbf{q}_i^H(\boldsymbol{\Delta}_k) \mathbf{D}_{\mathbf{u}} \mathbf{q}_i(\boldsymbol{\Delta}_k) \leq \text{Re} \{ \lambda_i(\boldsymbol{\Delta}_k) \}, \quad (\text{E.26})$$

and (4.91) has to be modified to,

$$0 \leq \frac{1}{2} |\lambda_i(\mathbf{\Delta}_k)|^2 \max_{i \in \mathcal{N}} \{ \|\mathbf{u}_{i,k}\|^2 \} \leq \text{Re} \{ \lambda_i(\mathbf{\Delta}_k) \}. \quad (\text{E.27})$$

Note that the explanations following Lemma 4.5 are based on the correct forms of (4.90) and (4.91), and thus, remain valid without modification.

Erratum 13 (p. 146)

The term in the middle of (C.7) has to be squared, i.e.,

$$\frac{(\mathbf{x}^\top \mathbf{A} \mathbf{z})^2}{(\mathbf{x}^\top \mathbf{A} \mathbf{x})(\mathbf{z}^\top \mathbf{A} \mathbf{z})} \leq \left(\frac{\lambda_1(\mathbf{A}) - \lambda_M(\mathbf{A})}{\lambda_1(\mathbf{A}) + \lambda_M(\mathbf{A})} \right)^2 = 1 - \bar{\lambda}_1^2(\mathbf{A}) \leq 1. \quad (\text{E.28})$$

Erratum 14 (p. 150)

On the right-hand side of (D.5), a multiplicative factor is missing. It has to be modified to

$$|\tilde{\mathbf{w}}^H \mathbf{e}_u^*|^2 = \dots = |\tilde{\mathbf{w}}^H \mathbf{e}_u^*|^2 \left(1 + |\alpha\rho|^2 - 2|\alpha\rho| \cos(\varphi_{\alpha\rho^*}) \right). \quad (\text{E.29})$$

Erratum 15 (p. 151)

In the paragraph following (D.12), it is argued that the difference of the two square roots in (D.11) is never larger than zero. This is not true in general, as combinations of ρ_B and α exist, for which it becomes positive. Nevertheless, as shown in the sequel of this Erratum, the drawn conclusion that $\sigma_{\max, A}^2 \leq \sigma_{\max, B}^2$ still holds.

As a first step, from Lemma 3.2, or equivalently, (A.57), it can be seen that the two non unit singular values increase monotonously with growing magnitude of the complex argument $\varphi_{\alpha\rho^*}$. For the maximum singular value σ_1 , the same holds with respect to the magnitude of effective step-size α (cf. (A.21)). Moreover, due to (A.35), σ_1 *increases* with *falling* magnitude $|\rho|$ of the correlation coefficient, as long as $-\frac{\pi}{2} < \varphi_{\alpha\rho^*} < \frac{\pi}{2}$. Lets keep this in mind for a moment.

For the two cases, A and B, considered in the proof of Lemma 3.8, it is easy to verify that

$$|\rho_B| \leq |\rho_A|, \quad (\text{E.30})$$

and

$$\varphi_{\alpha\rho^*, A} \triangleq \arccos(\alpha\rho_A^*) \equiv 0, \quad (\text{E.31})$$

whereas

$$\varphi_{\alpha\rho^*, B} \triangleq \arccos(\alpha\rho_B^*) \quad (\text{E.32})$$

is typically different from zero. Thus, from (E.31) and (E.32), it is clear that

$$0 = |\varphi_{\alpha\rho^*, A}| \leq |\varphi_{\alpha\rho^*, B}|. \quad (\text{E.33})$$

As in both cases, the effective step-size is identical, the afore memorised dependency of the maximum singular value with the correlation coefficient, allows to conclude that for $-\frac{\pi}{2} < \varphi_{\alpha\rho^*,B} < \frac{\pi}{2}$, $\sigma_{\max,A} \leq \sigma_{\max,B}$ is ensured.

Finally, it has to be shown that latter condition, $\sigma_{\max,A} \leq \sigma_{\max,B}$, also holds for

$$\frac{\pi}{2} \leq |\varphi_{\alpha\rho^*,B}| \leq \pi. \quad (\text{E.34})$$

According to (D.11), as $\alpha \in \mathbb{R}_{0+}$, this is equivalent to requiring

$$\operatorname{Re}\{\rho_B\} - \rho_A + \sqrt{\frac{\alpha^2}{4} - \alpha\rho_A + 1} - \sqrt{\frac{\alpha^2}{4} - \alpha\operatorname{Re}\{\rho_B\} - \operatorname{Im}^2\{\rho_B\} + 1} \stackrel{!}{\leq} 0. \quad (\text{E.35})$$

From (E.30), (E.33), and (E.34), with the fact $\rho_A \in [0, 1]$, it follows that

$$\operatorname{Re}\{\rho_B\} = -\gamma\operatorname{Re}\{\rho_A\} = -\gamma\rho_A, \quad (\text{E.36})$$

with some real-valued factor $\gamma \in [0, 1]$. Inserting (E.36) in (E.35), multiplying the whole expression by -1 , and separating terms, this translates to requirement

$$\gamma\rho_A + \rho_A + \sqrt{\frac{\alpha^2}{4} + \alpha\gamma\rho_A - \operatorname{Im}^2\{\rho_B\} + 1} \stackrel{!}{\geq} \sqrt{\frac{\alpha^2}{4} - \alpha\rho_A + 1}. \quad (\text{E.37})$$

Squaring (E.37) on both sides, after basic rearrangement of terms, the following expression is obtained

$$\rho_A^2(1+\gamma)^2 + \alpha\rho_A(1+\gamma) - \operatorname{Im}^2\{\rho_B\} + 2\rho_A(1+\gamma)\sqrt{\frac{\alpha^2}{4} + \alpha\gamma\rho_A - \operatorname{Im}^2\{\rho_B\} + 1} \stackrel{!}{\geq} 0. \quad (\text{E.38})$$

As for the imaginary part of ρ_B , it holds that

$$\operatorname{Im}^2\{\rho_B\} = |\rho_B|^2 - \operatorname{Re}^2\{\rho_B\} = |\rho_B|^2 - \gamma^2\rho_A^2 \stackrel{(\text{E.30})}{\leq} \rho_A^2(1-\gamma^2), \quad (\text{E.39})$$

the left-hand side of (E.38) can be bounded from below, yielding

$$\begin{aligned} & \rho_A^2(1+\gamma)^2 + \alpha\rho_A(1+\gamma) - \operatorname{Im}^2\{\rho_B\} + 2\rho_A(1+\gamma)\sqrt{\frac{\alpha^2}{4} + \alpha\gamma\rho_A - \operatorname{Im}^2\{\rho_B\} + 1} \\ & \stackrel{(\text{E.39})}{\geq} (1+\gamma) \left(\rho_A^2(1+\gamma) + \alpha\rho_A - \rho_A^2(1-\gamma)\{\rho_B\} + 2\rho_A\sqrt{\frac{\alpha^2}{4} + \alpha\gamma\rho_A - \operatorname{Im}^2 + 1} \right). \end{aligned} \quad (\text{E.40})$$

The right-hand side of (E.40) can be further simplified to

$$\underbrace{\rho_A(1+\gamma)}_{\geq 0} \left(\underbrace{2\gamma\rho_A}_{\geq 0} + \underbrace{\alpha}_{\geq 0} + \underbrace{2\sqrt{\frac{\alpha^2}{4} + \alpha\gamma\rho_A - \operatorname{Im}^2\{\rho_B\} + 1}}_{\geq 0} \right) \geq 0, \quad (\text{E.41})$$

which shows that (E.38), and as a consequence (E.35) is satisfied. Hence, $\sigma_{\max,A} \leq \sigma_{\max,B}$ is ensured to hold also for (E.34), and is thus valid for any $\varphi \in (-\pi, \pi]$.

Erratum 16 (p. 157)

In (D.44), in the expression beneath the leftmost brace that specifies term $\mathbf{q}_m^H \mathbf{\Gamma} \mathbf{q}_m$ in more detail, index i has to be replaced by m , i.e.,

$$\mathbf{q}_m^H \mathbf{\Gamma} \mathbf{q}_m = 2\text{Re} \{ \lambda_m \} - |\lambda_m|^2 \mathbf{q}_m^H \mathbf{D}_u \mathbf{q}_m. \quad (\text{E.42})$$